UNED Escuela Internacional de Doctorado EIDUNED

TESIS DOCTORAL

AÑO 2019

SOLUCIONES PARA EL DESARROLLO E INTEGRACIÓN DE FUENTES DE ENERGÍA RENOVABLE PARA EL CUMPLIMIENTO DE LOS OBJETIVOS DE MITIGACIÓN DEL CAMBIO CLIMÁTICO

SEVERO CAMPÍÑEZ ROMERO

PROGRAMA DE DOCTORADO EN TECNOLOGÍAS INDUSTRIALES

DIRECTOR: D. ANTONIO COLMENAR SANTOS

CODIRECTORA: Dña. ÁFRICA LÓPEZ-REY GARCÍA-ROJAS

ÍNDICE

LISTA DE ILUSTRACIONES Y TABLAS

ILUSTRACIONES

<u>TABLAS</u>

1 PREÁMBULO

En los últimos ciento veinte años la Tierra ha experimentado un incremento en la temperatura media de su superficie en torno a 1 °C. Esta variación, aunque pueda parecer insignificante, ha producido cambios relevantes en las condiciones climáticas del planeta y, por extensión, en las condiciones de los seres vivos que habitamos en él.

Este cambio climático está motivado por la modificación de las condiciones del denominado efecto invernadero. Este es un proceso natural de interrelación entre la superficie terrestre y la atmósfera, cuyo funcionamiento depende de la capacidad de la atmósfera para absorber y emitir la radiación térmica recibida del sol y la proveniente de la superficie terrestre. Gracias a este efecto la temperatura del planeta se mantiene en niveles adecuados para los seres vivos.

La composición de la atmósfera determina su capacidad para absorber y emitir la radiación, por lo que la presencia de determinados compuestos modifica el balance energético del efecto invernadero y por tanto la temperatura media de la superficie terrestre. Estos compuestos, conocidos como Gases de Efecto Invernadero (GEIs) son fundamentalmente el vapor de agua (H_2O), el dióxido de carbono (CO_2), el metano (CH_4), el óxido nitroso (N_2O), el ozono (O_3), los clorofluorocarbonos (CFCs) y los hidrofluorocarbonos (HCFCs y HFCs).

Desde la época preindustrial (1880-1900) las emisiones de GEIs a la atmósfera se ha incrementado drásticamente. Este aumento en las emisiones tiene un origen antropogénico, es decir está provocado por la actividad del ser humano. Los cambios en la sociedad acaecidos desde la Revolución Industrial y la forma en que vivimos y usamos los recursos del planeta están detrás del incremento de las emisiones y, por tanto, del cambio climático producido por el aumento de la temperatura media.

La sociedad debe implementar medidas para adaptarse a las nuevas condiciones climáticas y sus efectos, pero además debe tomar medidas encaminadas a limitar, incluso reducir, el cambio climático y sus riesgos. La comunidad científica ha cuantificado que, para limitar los riesgos derivados del cambio climático a niveles asumibles para la vida y los ecosistemas del planeta, el incremento máximo de la temperatura media del planeta respecto de la era preindustrial debería limitarse a 2° C. Teniendo en cuenta que, a día de hoy, la temperatura ya se ha elevado 1 °C, para conseguir dicho objetivo deben tomarse con carácter urgente medidas drásticas y sostenidas en el tiempo encaminadas a la reducción de las emisiones de GEIs.

Diversas instituciones y organismos especializados, organizaciones gubernamentales y la comunidad científica han definido y diseñado estrategias y líneas maestras para la implementación de medidas encaminadas a la mitigación de las emisiones de GEIs. Estas estrategias abarcan todos los sectores de actividad de la sociedad; todos ellos responsables, en mayor o menor medida, del incremento de las emisiones.

No obstante, la traducción de estas estrategias y líneas maestras en medidas prácticas y realizables es una tarea muchas veces ardua, cuyo desarrollo se enfrenta a múltiples barreras técnicas, medioambientales, financieras y políticas. Esto hace que la implementación de las medidas de mitigación y la obtención de los resultados esperados no vayan al ritmo requerido.

2 INTRODUCCIÓN

2.1 Cambio climático. Emisiones de gases de efecto invernadero

El año 2018 fue el cuarto año más caluroso de la historia [1] y el mes de junio de 2019 ha sido el más caluroso en el continente europeo [2] desde que se tienen registros. El calentamiento global[1] de la Tierra ha sido ampliamente constatado con un alto grado de certidumbre por la comunidad científica internacional, liderada por el Panel Internacional para el Cambio Climático[2]. Fruto del trabajo de éste y otros organismos internacionales, se ha determinado que la temperatura media de la superficie de la Tierra se ha incrementado entre 1901 y 2012 hasta en 2,5 °C en algunas regiones del planeta (Ilustración 1).

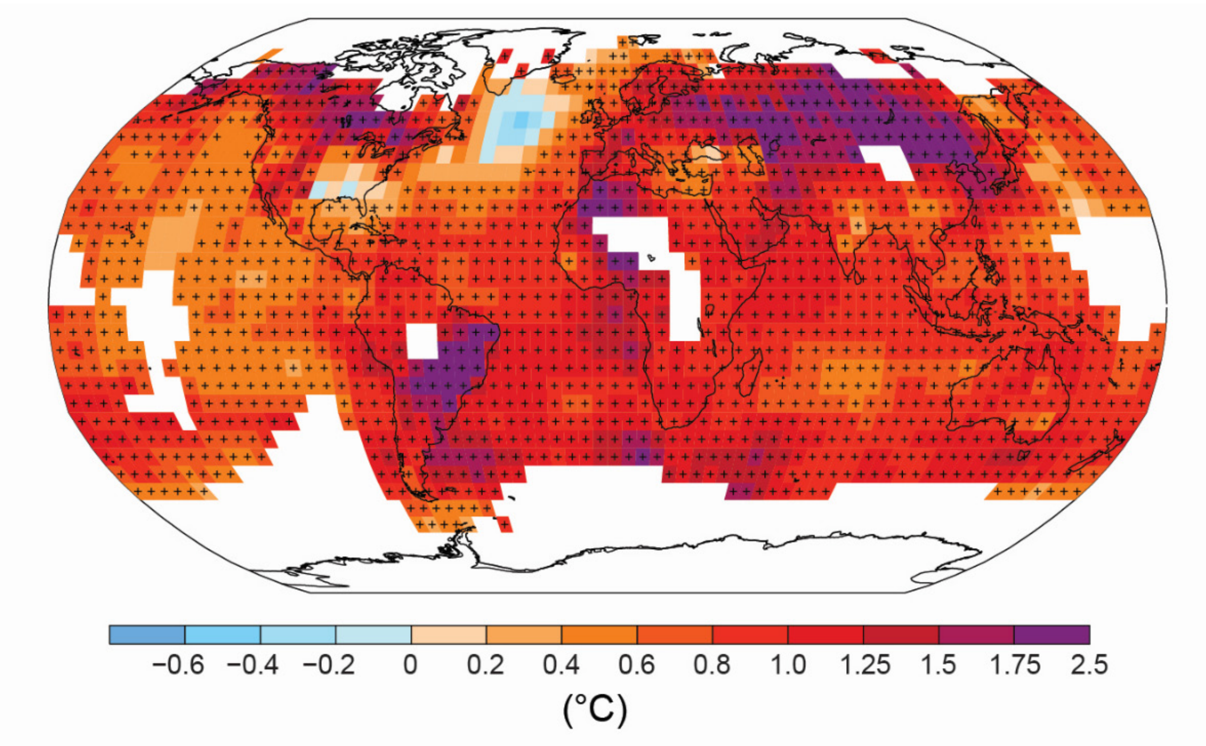

Ilustración 1: Cambios observados en la temperatura de la superficie de la tierra entre 1901 y 2012 [3]

---

[1] El Panel Intergubernamental para el Cambio Climático define el calentamiento global como el incremento en la temperatura media en la superficie terrestre y los océanos, ponderadas sobre un periodo de 30 años. Los indicadores sobre el calentamiento global, a no ser que indique lo contrario, se expresan en relación con el periodo temporal comprendido entre los años 1850 y 1900, periodo que se considera representativo de las temperaturas en la era preindustrial.

[2] El Panel Intergubernamental para el Cambio Climático (*Intergovernmental Panel on Climate Change*) es un organismo de las Naciones Unidas para el asesoramiento científico en lo relativo al cambio climático.

Entre 1880 y 2012 la temperatura global media en la superficie terrestre y los océanos se incrementó en torno a 0,85 °C, mientras que el incremento total observado en el periodo 2003-2012 respecto a la era preindustrial (1850-1900) se situó en torno a los 0,78 °C [3]. Según la Organización Meteorológica Mundial, en 2018 el incremento de la temperatura media del planeta respecto del periodo preindustrial se sitúa en 0,99 ± 0,13 ˚C, es decir, prácticamente en 1 ˚C [1].

El calentamiento se ha acelerado en las últimas décadas, en las que la temperatura media terrestre ha ido alcanzando incrementos decenales en torno a los 0,2 °C (Ilustración 2).

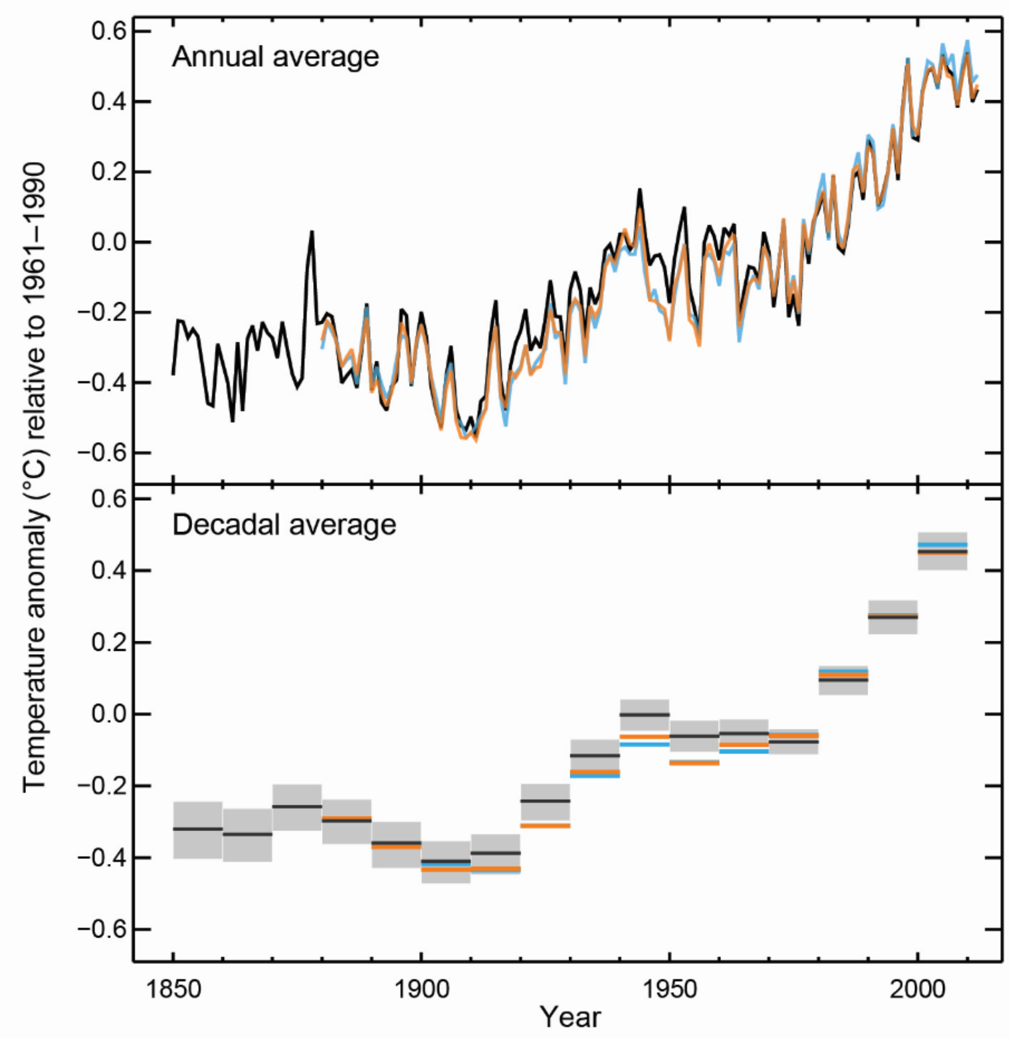

Ilustración 2: Anomalías observadas en la temperatura global media en la superficie terrestre y oceánica desde 1850 a 2012 referidas a la temperatura media del periodo 1961−1990. Gráfico superior: valores medios anuales. Gráfico inferior: valores medios decenales [3].

El cambio climático está directamente relacionado con la concentración de gases de efecto invernadero[3] en la atmósfera. Desde la época preindustrial, los niveles de concentración de dióxido de carbono (CO_2), metano (CH_4) y óxido nitroso (N_2O) no han parado de aumentar a ritmos cada vez más elevados (Ilustración 3).

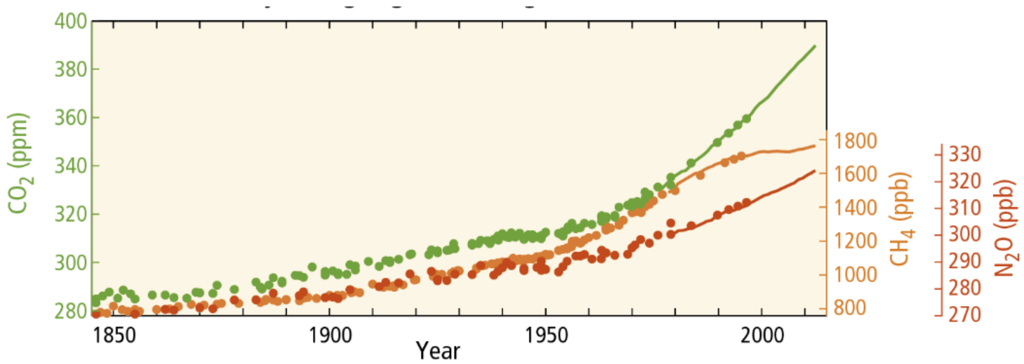

Ilustración 3: Concentraciones atmosféricas de los gases de efecto invernadero dióxido de carbono (CO_2), metano (CH_4) y óxido nitroso (N_2O) [4].

El incremento en las emisiones de gases de efecto invernadero tiene un origen antropogénico, es decir, está producido por la actividad del ser humano y proviene fundamentalmente del incremento en las emisiones de CO_2. En la Ilustración 4 se aprecia como las emisiones de CO_2 de origen antropogénico han crecido de forma sostenida desde la época preindustrial, basadas fundamentalmente en el uso creciente de combustibles fósiles.

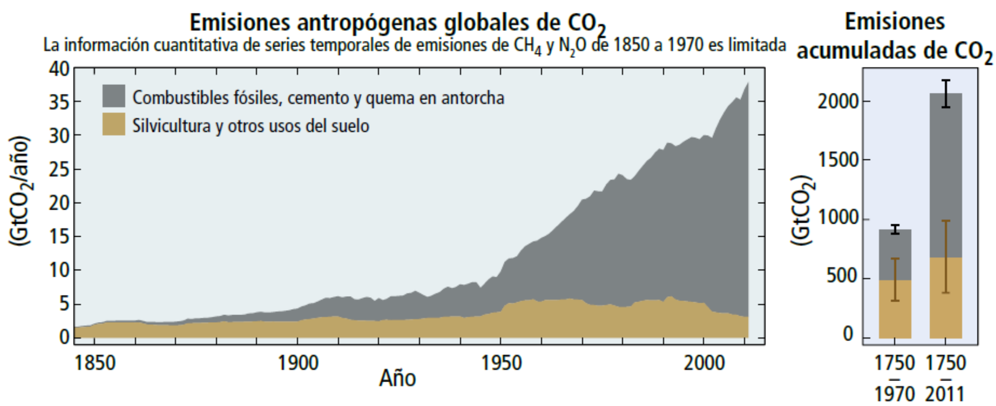

Ilustración 4: Evolución de las emisiones globales de CO_2 de origen antropogénico [4]

[3] Los gases de efecto invernadero son: vapor de agua (H_2O), dióxido de carbono (CO_2), metano (CH_4), óxido nitroso (N_2O), ozono (O_3), clorofluorocarbonos (CFCs), hidrofluorocarbonos (HCFCs y HFCs)

Durante el año 2010 las emisiones de gases de efecto invernadero de origen antropogénico a la atmosfera fueron de 49 GtCO2eq[4]. Las emisiones han ido creciendo en los últimos 50 años, debido fundamentalmente al incremento de las emisiones antropogénicas provenientes del uso de combustibles fósiles y los procesos industriales (Ilustración 5).

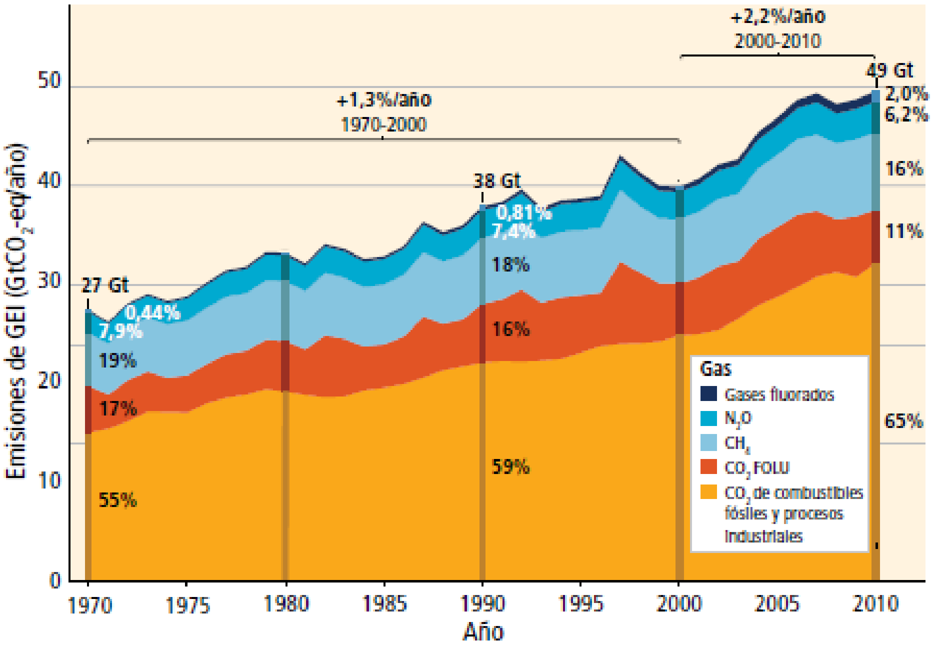

Ilustración 5: Evolución de las emisiones de gases de efecto invernadero de origen antropogénico en el periodo 1970 – 2010 [4]

Las emisiones de gases de efectos invernadero siguen creciendo y no hay señales de que hayan alcanzado aún sus niveles máximos. Así, las emisiones durante el año 2017 alcanzaron los 53,5 $GtCO_2e$, lo que representa un incremento de más del 9% respecto de los niveles de 2010 [5].

2.2 Efectos y riesgos del cambio climático. Adaptación y mitigación

El incremento en la temperatura media del planeta ha tenido efectos negativos tangibles en el medio ambiente como el calentamiento de los mares y océanos, modificaciones de las condiciones

[4] La unidad tCO_2eq se utiliza como unidad de medición para indicar el potencial de calentamiento global de cada uno de los gases de efecto invernadero, en comparación con el dióxido de carbono. Los gases de efecto invernadero distintos del dióxido de carbono son convertidos a su valor de dióxido de carbono equivalente (CO_2eq) multiplicando la masa del gas en cuestión por su potencial de calentamiento global.

meteorológicas (sequías, inundaciones), cambios en los niveles de los mares y una reducción notable de las masas polares y los glaciares.

Si no se reducen las emisiones de gases de efecto invernadero y sus niveles de concentración atmosférica por la vía de mecanismos de captura de CO_2, la temperatura seguirá creciendo y se incrementará el número y efecto de los riesgos asociados, lo que tendrá como consecuencia una mayor probabilidad de sufrir impactos graves e irreversibles para el medio ambiente y la vida en la Tierra.

La limitación de los riesgos derivados del cambio climático a niveles asumibles para la vida y los ecosistemas del planeta está condicionada por niveles moderados de riesgos compatibles con un incremento máximo de la temperatura media del planeta de 2 °C respecto de la era preindustrial (Ilustración 6).

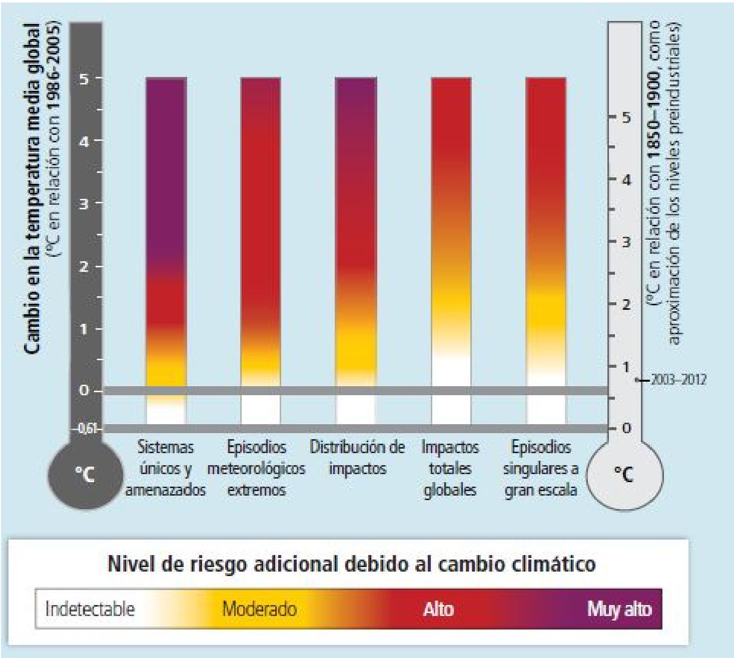

Ilustración 6: Niveles de riesgo asociados al incremento de la temperatura media del planeta [4]

Sin embargo, el nivel de emisiones ha seguido aumentando. Así, durante el año 2017, las emisiones anuales alcanzaron 53,5 $GtCO_2eq$, lo que representa un incremento de más del 9% respecto de los niveles de 2010 [5] y la concentración atmosférica de CO_2 alcanzó 405,5 ppm, lo que representa un 146% sobre los niveles preindustriales [1].

Los niveles de emisión y concentración atmosférica futuros dependerán de la evolución de múltiples variables como los cambios demográficos, el desarrollo económico, el uso de la energía, la intensidad energética, el uso del suelo y las estrategias de adaptación y mitigación[5] al cambio climático. La evolución de estas variables determinará distintos escenarios en los que los niveles de emisión de gases de efecto invernadero y las respectivas concentraciones atmosféricas presentarán valores diferenciados y llevarán a distintos niveles de calentamiento. Diversos organismos han desarrollado modelos para definir los posibles escenarios y evaluar, en qué forma diferentes trayectorias en la evolución de las emisiones pueden contribuir a la consecución del objetivo de mantener el calentamiento global por debajo de los 2 °C respecto de la era preindustrial[6].

En la mayoría de los escenarios en los que no se prevé la implantación de medidas adicionales de mitigación, se estima que las emisiones anuales de gases de efecto invernadero se situarán entre 75 y 140 $GtCO_2eq$ en 2100. En estos escenarios la concentración atmosférica superaría las 450 ppm CO_2eq en 2030, llegando a niveles de entre 750 y 1.300 ppm CO_2eq en 2100. En estas circunstancias se alcanzaría un calentamiento global entre 3,7 °C y 4,8 °C en 2100 respecto de los niveles preindustriales [6].

Solo aquellos escenarios en los que la concentración atmosférica de gases de efecto invernadero se situara en 2100, en niveles máximos en el entorno de los 450 ppm de CO_2eq, llevarían a la consecución, con un alto grado de probabilidad, de cumplir el objetivo de limitar el calentamiento global en el siglo XXI por debajo de los 2 °C respecto de los niveles preindustriales. Las trayectorias para conseguir este grado de concentración en 2100 suponen una reducción respecto de las emisiones anuales de 2010 de entre el 41 al 71 % en 2050 y entre el 78 y el 118% en 2100.

[5] Por adaptación se entiende el proceso de adecuación de las actividades humanas a las nuevas situaciones derivadas del cambio climático real o proyectado con el fin de minimizar los daños y aprovechar las oportunidades. El concepto de mitigación se utiliza en este contexto como la intervención humana encaminada a reducir las emisiones de gases de efecto invernadero o aumentar la captura de estos gases de la atmósfera.

[6] El grupo de trabajo del Panel Internacional para el Cambio Climático han determinado y clasificado alrededor de 300 escenarios de referencia (sin medidas de mitigación) y 900 escenarios de mitigación por concentración de CO_2eq para 2100. Otras organizaciones, como la Agencia Internacional de la Energía (IEA por sus siglas en inglés) ha determinado escenarios propios para evaluar y analizar el impacto de distintas estrategias de adaptación y reducción de las emisiones.

Por lo tanto, solo la implementación urgente de medidas de mitigación, enfocadas a conseguir un recorte drástico y continuado de las emisiones de gases de efecto invernadero durante las próximas décadas, podrá conducirnos al objetivo común e inaplazable de limitar el calentamiento global a 2° C respecto de los niveles preindustriales para evitar el grave impacto de los riesgos asociados a dicho calentamiento.

Con este objetivo, el 12 de diciembre de 2015 los 195 países participantes en la XXI Conferencia Internacional sobre Cambio Climático celebrada en París [7] organizada por la Convención Marco de las Naciones Unidas sobre el Cambio Climático [8], alcanzaron el Acuerdo de París [9] para reducir las emisiones de carbono lo antes posible y hacer todo lo posible para mantener el calentamiento global muy por debajo de 2 °C respecto a los niveles de la era preindustrial.

2.3 Contribución a las emisiones de origen antropogénico de gases de efecto invernadero y principales medidas de mitigación por sector económico

El reparto de las emisiones entre los distintos sectores económicos en 2010 se muestra en la Ilustración 7, donde puede verse que la producción de energía lidera las emisiones seguido del sector industrial.

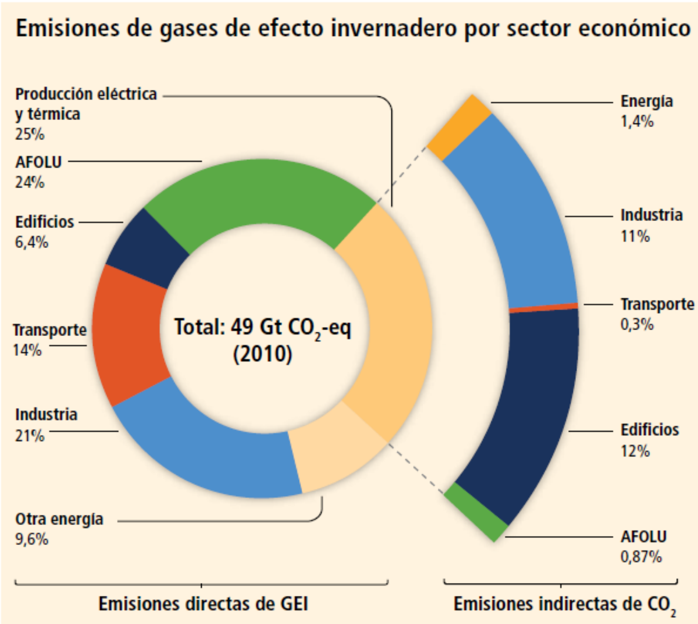

Ilustración 7: Emisiones de gases de efecto invernadero por sector económico en 2010 [4]

En la Ilustración 8 se muestran los niveles de reducción en las emisiones de CO_2 y otros gases de efecto invernadero que serían necesarios para mantener la concentración atmosférica en torno a los 450 ppm de CO_2eq y limitar el calentamiento global a 2 °C en 2100. Todos los sectores deben reducir sus emisiones de forma drástica y sostenida en el tiempo, pero son los sectores de la generación eléctrica, el transporte y el sector industrial, como principales emisores, los que deben hacer un esfuerzo mayor.

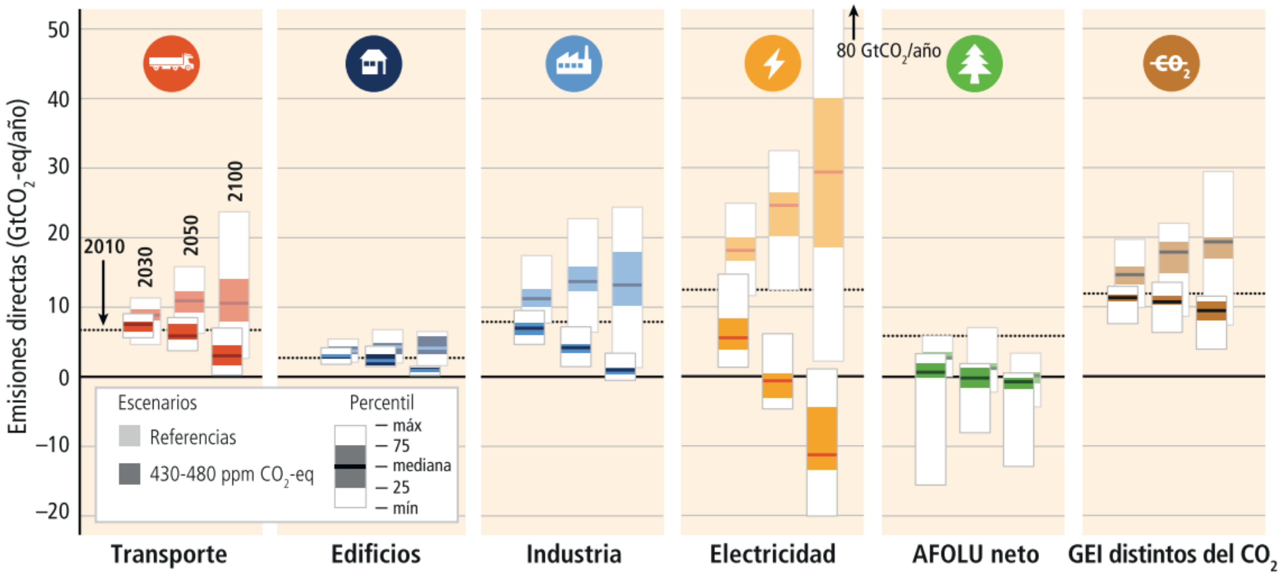

Ilustración 8: Emisiones de CO_2 y otros gases de efecto invernadero (GEI) por sector económico en los escenarios definidos por el Panel Intergubernamental para el Cambio Climático sin implementación de mitigación (escenarios de referencia) y en los escenarios de mitigación en los que se llega a concentraciones de aproximadamente 450 ppm CO_2eq en 2100 [4].

La comunidad internacional ha determinado las líneas generales de diferentes estrategias de mitigación que deben traducirse en soluciones concretas a implementar en cada sector económico para conseguir los objetivos de reducción de emisiones.

La Ilustración 9 muestra un resumen de las medidas de mitigación a implementar por cada uno de los sectores. Entre estas medidas se encuentra la integración masiva de fuentes de energía renovable y el uso de combustibles con pocas o ninguna emisión de gases de efecto invernadero, como, por ejemplo, el hidrógeno.

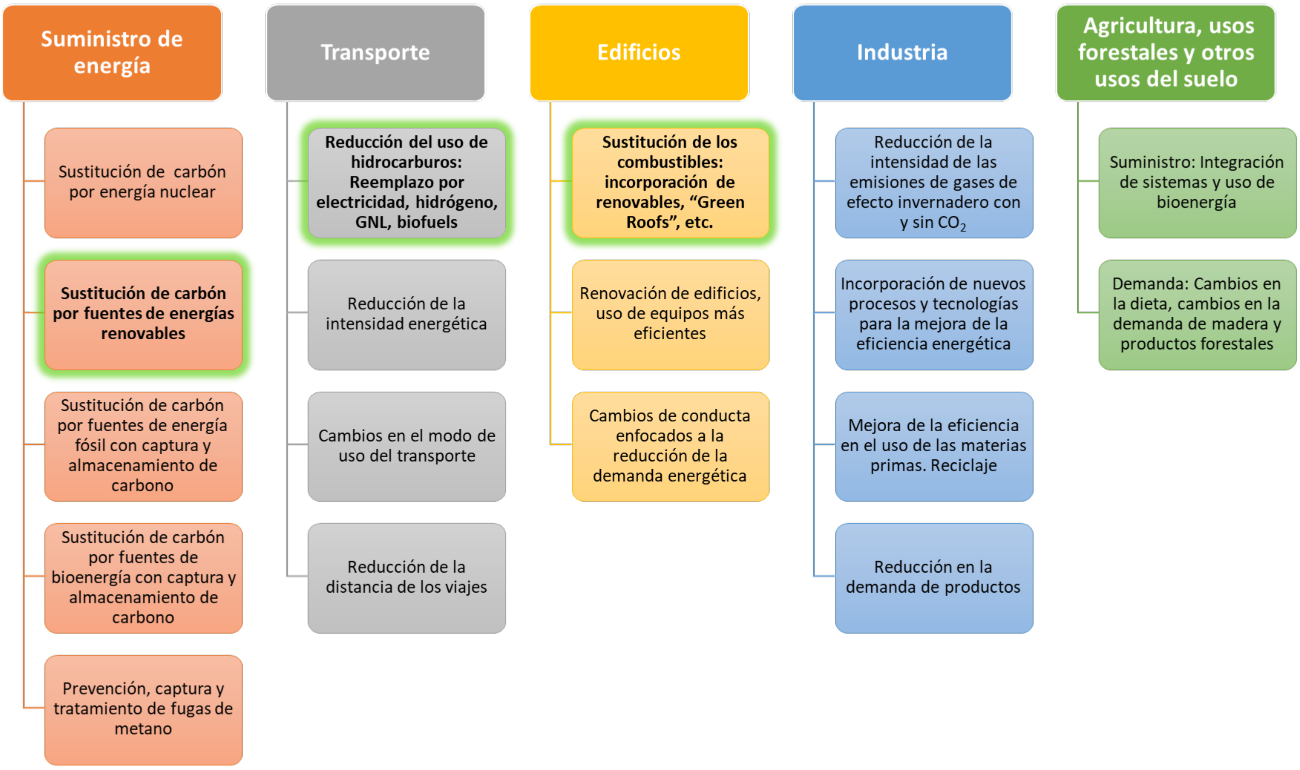

Ilustración 9: Medidas de mitigación para la reducción de emisiones de gases de efecto invernadero [4] y elaboración propia

3 OBJETIVO DE LA TESIS

La base argumental del trabajo de investigación de la presente tesis doctoral es la siguiente:

1. La **reducción** de las **emisiones de gases de efecto invernadero** es obligada para limitar el incremento en la temperatura de la Tierra.
2. Esta reducción requiere la **implementación de medidas a nivel global** en todos los sectores y ámbitos de la actividad humana. Dichas medidas han sido ampliamente debatidas y consensuadas en la comunidad internacional sobre la base de un desarrollo sostenible y sostenido en las próximas décadas. La mayor parte de los países del mundo se ha comprometido con objetivos tangibles de reducción de emisiones que requieren la implementación de medidas a corto, medio y largo plazo.
3. Una parte importante de las estrategias de mitigación del cambio climático se basan en la **integración de fuentes de energía renovable** en los distintos sectores productivos y actividades del ser humano.
4. No obstante, hay **barreras** de tipo técnico, político, regulatorio y económico que hace que, en determinados sectores, la implementación de las medidas no se esté realizando con el ritmo adecuado para cumplir los objetivos de emisiones.
5. Por lo tanto, hay una necesidad de encontrar **soluciones prácticas** que **aceleren la implementación de las medidas de mitigación**.

Basado en dichos argumentos, **el OBJETIVO DE LA TESIS DOCTORAL** ha sido el de **encontrar y aportar soluciones prácticas y realizables para favorecer la integración efectiva de una cantidad masiva de fuentes de energía de origen renovable en diversos sectores productivos y actividades del ser humano, ofreciendo soluciones viables al alcance de la ingeniería actual** para salvar las barreras que puedan limitar dicha integración.

La consecución de este objetivo se ha estructurado sobre las siguientes acciones:

1. Identificar alternativas tecnológicamente realizables para la integración de energías renovables en aquellos sectores económicos dentro de los más productores de emisiones de gases de efecto invernadero. Para favorecer su integración y asegurar que contribuirán

efectivamente al fin que se persigue, estas alternativas deberán presentar las siguientes características:

a. Estar alineadas con las estrategias de mitigación del cambio climático establecidas por los distintos organismos gubernamentales y la comunidad científica.
b. Introducir las energías renovables en cierto sector de actividad o favorecer aún más la integración de renovables en aquellos sectores en los que ya existe cierto nivel de integración.
c. Tener un ámbito global, con posibilidad de ser aplicados en múltiples territorios, países, sectores, etc.
d. Estar basadas en metodologías novedosas que consideren las circunstancias actuales y robustas, cuyos resultados sean válidos pese a cambios relevantes de las variables que participan.

2. Analizar las barreras técnicas, regulatorias y financieras que pudieran limitar la implementación de dichas alternativas.
3. Buscar soluciones prácticas y sostenibles para salvar dichas barreras.
4. Explorar las posibilidades de financiación y limitar el uso de subsidios.

3.1 Líneas de desarrollo del objetivo de la tesis y justificación con la unidad temática de la tesis

La unidad temática de la tesis, definida por su objetivo, es por tanto **encontrar y aportar soluciones prácticas y realizables para favorecer la integración efectiva de una cantidad masiva de fuentes de energía de origen renovable en diversos sectores productivos y actividades del ser humano**. Del análisis detallado de las distintas medidas de mitigación definidas por la comunidad científica internacional para cada uno de los sectores de actividad (ver Ilustración 9), se concluye que hay medidas y sectores específicos en los cuales la integración de fuentes de energía renovable es más determinante: el **suministro de energía**, los **edificios** y el **transporte**.

Por lo tanto, bajo una misma unidad temática y para lograr la consecución del objetivo de la tesis, el trabajo de investigación se ha acometido y acotado en tres líneas de desarrollo, cada una de las cuales se ha enfocado en la búsqueda de soluciones prácticas dirigidas a la integración de fuentes de energía renovable dentro de las medidas de mitigación definidas para los sectores de actividad más emisores de GEIs (resaltadas en verde en la Ilustración 9). Estas tres líneas de desarrollo son

- La integración de energías renovables en el sector del **suministro de energía**.
- La incorporación de fuentes de energía renovable en **edificios**.
- El reemplazo de hidrocarburos por combustibles con bajas o nulas emisiones de gases de efecto invernadero en el sector del **transporte**.

3.2 Sobre la modalidad de presentación de la tesis

La presente tesis doctoral se presenta bajo la modalidad de **Tesis por compendio de publicaciones**.

Esta modalidad de presentación de la tesis doctoral está regulada por el documento aprobado por el Comité de Dirección de la Escuela Internacional de Doctorado de la Universidad Nacional de Educación a Distancia (EIDUNED), en su reunión de 16 de enero de 2017, y por la Comisión de Investigación y Doctorado de la UNED, con fecha 21 de febrero de 2017.

Conforme lo determinado en dicha regulación, la tesis doctoral presentada por compendio de publicaciones deberá estar constituida por un conjunto de trabajos publicados y/o aceptados, justificados por su unidad temática, de acuerdo con la siguiente estructura:

- Introducción, en la que se justifique la unidad temática de la tesis.
- Hipótesis y objetivos a alcanzar, indicando en qué publicación o publicaciones se abordan.
- Marco teórico en el que se inscribe el tema de la tesis y herramientas metodológicas o remisión a las publicaciones.
- Copia completa de las publicaciones, ya sean publicadas o aceptadas para publicación, donde conste el nombre y adscripción de la autoría y coautoría, en su caso, así como la referencia completa de la revista o editorial en la que los trabajos hayan sido publicados o aceptados para su publicación, en cuyo caso se aportará justificante de la aceptación de la revista o editorial. En todos estos casos siempre deberá constar de forma explícita la filiación del doctorando o doctoranda a la UNED.

- Conclusiones, indicando de qué publicación o publicaciones se desprenden.
- Resúmenes en español y en inglés o, en su defecto, en el idioma habitual para la comunicación científica en su campo de conocimiento científico, técnico o artístico
- Otras aportaciones científicas derivadas directamente de la tesis doctoral.
- Informe con el factor de impacto y cuartil del *Journal Citation Reports* (SCI y/o SSCI), *SCOPUS*, Sello de Calidad FECYT o de toda base de datos selectiva y con factor de impacto de referencia del área en el que se encuentran las publicaciones presentadas.
- Fuentes y/o Bibliografía.

La regulación determina tres opciones para la clase y número de publicaciones que deben formar el compendio. Para la presentación de esta tesis doctoral se ha optado por la primera de las opciones, según la cual: *"..el compendio de publicaciones estará formado por un mínimo de 3 artículos (al menos, dos ya publicados y el tercero aceptado) en revistas de índices de impacto en los dos primeros cuartiles de la relación de revistas del ámbito de la especialidad del Programa en el que está inscrita dicha tesis y referenciadas en la última relación publicada por el Journal Citation Reports (SCI y/o SSCI) y de SCOPUS. Todos los artículos deben estar publicados con fecha posterior a la primera matrícula de tutela académica en la EIDUNED. El doctorando o doctoranda debe ser primer firmante o segundo, en este último caso, el primero debe ser el director o directora de la tesis".*

3.3 Hipótesis y objetivos de las líneas de desarrollo del trabajo de investigación. Publicaciones en que se abordan

Como se ha mencionado anteriormente, el trabajo de investigación se ha acometido y acotado en tres líneas de desarrollo, todas ellas bajo la misma unidad temática y con el objetivo común de la tesis de encontrar algunas de estas soluciones, enfocadas en la integración de fuentes de energía renovable en tres de los sectores que originan más emisiones de gases efecto invernadero: la generación de energía, el sector del transporte y los edificios.

El resultado de cada una de las líneas desarrollo llevadas a cabo para la consecución del objetivo de la tesis doctoral se ha plasmado en la elaboración de tres artículos científicos que han sido publicados en revistas del sector con alto factor de impacto. En cada uno de los subapartados siguientes se introducen las hipótesis y líneas de desarrollo del trabajo de investigación que han dado lugar a cada una de las publicaciones.

3.3.1 Sector del suministro de energía

La Ley 54/1997 del Sector Eléctrico [10], implantó un nuevo marco regulatorio para el sector eléctrico español, con el objetivo de garantizar el suministro eléctrico con la mayor calidad y al menor coste posible dentro un nuevo modelo de funcionamiento que, en lo relativo a la producción de energía, se basa en la libre competencia sin más intervención del estado que la propia regulación específica (la Ley 54/97 del Sector Eléctrico fue derogada y sustituida en el año 2013 por la Ley 24/2013, de 26 de diciembre del Sector Eléctrico [11], que mantiene la finalidad y los objetivos esenciales de la Ley 54/97).

Desde el punto de vista retributivo, la nueva regulación estableció un sistema de incentivos basado en *feed-in-tariff* (*FIT*) sin límite temporal, consistente en el cobro de una prima sobre el precio obtenido en el mercado diario de electricidad (spot). Como una segunda opción, se podía optar por el cobro de una cantidad fija [12-14]. Con esta base regulatoria estable y un desarrollo normativo adecuado para su autorización [15], en el mes de marzo de 2012 la energía eólica alcanzó un grado de abastecimiento superior al 25% de la demanda de energía eléctrica en el mercado español en barras de central [16]. Para España, con unos niveles de dependencia energética del 75,6% en 2011 [17], este hecho supuso la constatación del éxito obtenido en la implantación de las energías renovables en su conjunto y muy especialmente la energía eólica [18-20], en el mix energético.

El mes de enero de 2012, el Gobierno español suspendió los incentivos económicos para nuevas instalaciones de generación eléctrica a partir de fuentes renovables, incluyendo la energía eólica [21]. En este contexto energético, y sin haber alcanzado aún los objetivos establecidos por la Unión Europea y el Estado Español para cubrir la demanda energética con fuentes de energía renovable [22,23], son necesarias nuevas estrategias y políticas regulatorias para continuar con la integración de las fuentes renovables [24-26].

Los primeros aerogeneradores instalados presentaban, en la fecha de elaboración del trabajo

(2015) más de quince años en operación comercial y estaban llegando al último tramo de su vida útil [27]. Además, la repotenciación de parques eólicos tiene beneficios para el sistema eléctrico en su conjunto [28].

En la publicación correspondiente con esta línea de desarrollo del trabajo de investigación se examina cómo la energía eólica puede contribuir aún más a los objetivos de integración de renovables en el mix energético ya que, especialmente por su grado de madurez, se convierte en una posibilidad adecuada abriendo escenarios que impliquen los menores costes posibles para el sector eléctrico en su conjunto. Por ello, el objetivo de este trabajo ha consistido en analizar si la repotenciación de parques eólicos es rentable y en qué términos; si para ello es determinante mantener las *FIT* o es posible ofrecer rentabilidades atractivas para los inversores pagando la energía generada a precio del mercado diario (spot).

Con dicho objetivo se analizaron los parques eólicos instalados y se definió, cuantifico y caracterizó el mercado apto para su repotenciación. Se ha examinado el impacto de la repotenciación en el aprovechamiento del recurso eólico mediante el estudio de la producción esperada para el parque eólico repotenciado y su variación respecto a su situación anterior. Para evaluar los costes derivados de la repotenciación, se han definido y evaluado las instalaciones que forman un parque eólico y en qué medida estas instalaciones pueden reutilizarse durante la repotenciación para disminuir así los costes de construcción. También se realizó un análisis y estimación de los costes de desmontaje y valorización de recursos de los aerogeneradores antiguos.

Así mismo, se realizó un análisis de la rentabilidad económica financiera esperada para el parque eólico repotenciado. Se propuso una solución retributiva basada en el precio del mercado spot y un estudio comparativo respecto de la retribución mediante la *FIT* vigente en el momento del estudio. Para validar la robustez de la metodología empleada, se llevaron a cabo análisis de sensibilidad de la rentabilidad, respecto de las principales variables consideradas.

El artículo correspondiente con esta línea de desarrollo dentro del proceso de investigación fue publicado con el título "*Repowering: An actual possibility for wind energy in Spain in a new scenario without feed-in-tariffs*", en enero de 2015, en el número 41 de la revista *Renewable and Sustainable*

Energy Reviews. Todos los detalles del artículo se muestran en la Tabla 4 del apartado 5.

3.3.2 Edificios

Una de las mayores contribuciones a la emisión global de gases de efecto invernadero es la derivada de la generación de electricidad, por lo que desde este sector debe realizarse una importante contribución a la consecución de los objetivos de mitigación. Aunque ya se ha avanzado mucho en la implementación de fuentes de energía renovable, dentro de los objetivos para un nuevo mix eléctrico con un nivel reducido de emisiones, éstas deben tener un papel protagonista con una integración masiva, que contribuya destacadamente a la transición desde una generación eléctrica basada fundamentalmente en la utilización de hidrocarburos [29].

Dentro de las fuentes de energía renovable, la energía solar fotovoltaica tiene una característica esencial que facilita su integración masiva: su grado de dispersión: la radiación solar es recibida en prácticamente todo el planeta, en niveles que dependen de la latitud de la ubicación específica de la instalación, con una intensidad tal que es posible su utilización para la obtención de energía eléctrica. Además, las tecnologías para su utilización presentan en la actualidad un nivel de madurez técnico-económico que permite la generación con un alto grado de eficiencia y a costes reducidos, lo que ha conseguido que cada vez en más lugares sea posible la generación eléctrica a un precio comparable con los métodos térmicos convencionales [30-35].

Diversos estudios se han llevado a cabo para determinar el potencial fotovoltaico de edificios, algunos enfocados especialmente en el sector residencial [36-38] y la mayoría sin hacer distinción entre el tipo de uso de los edificios analizados y, por tanto, sin especificar el potencial de cada uno de ellos [39-45]. En general, la literatura existente ha considerado a todos los edificios de igual forma a la hora valorar los problemas de integración en la red eléctrica de la energía generada por las instalaciones fotovoltaicas que en ellos se pudieran instalar, independientemente del uso al que esté destinado el edificio.

Los centros comerciales presentan características constructivas que favorecen la instalación de paneles solares en sus tejados. El grado de aprovechamiento de los edificios residenciales es en general inferior al de los edificios comerciales. Según [46] el grado de aprovechamiento en edificios residenciales oscila entre el 22% y el 27% y algunos estudios sitúan este ratio entre el 25% y el 50% para ciudades de alta densidad de población en la que priman los edificios residenciales multifamiliares [36]. Sin embargo, el grado de aprovechamiento de los tejados de los edificios comerciales puede situarse entre el 60% y 65% [46]. Esto hace que, en igualdad de condiciones se pueda instalar entre 2 y 3 veces más potencia en tejados de centros comerciales que en edificios residenciales.

En términos de transporte y distribución de energía, el lugar más eficiente para la generación de energía eléctrica es junto al punto de consumo. En este sentido los centros comerciales presentan también importantes ventajas frente a otros tipos de edificios, ya que en cuanto a las posibilidades de autoconsumo, tiene un consumo elevado y algunos estudios apuntan que los perfiles de consumo de los centros comerciales se ajustarían más al perfil de generación de una instalación solar que cualquier otro tipo de edificio [47].

Las instalaciones solares fotovoltaicas situadas en el suelo cerca de puntos de gran consumo, fundamentalmente núcleos urbanos o industriales, presentan un inconveniente importante, ya que los terrenos próximos a este tipo de núcleos tienen un alto valor y los costes de alquiler pueden penalizar los costes de explotación. Sin embargo, los centros comerciales, para que sean accesibles por el consumidor, están ubicados dentro o en las inmediaciones de núcleos de población, a menudo en áreas industriales próximas a las ciudades, por lo que los excedentes de generación eléctrica pueden ser utilizados para abastecer, a través de la red de distribución, a otros consumos cercanos con pocas pérdidas de transporte.

No obstante, la integración a gran escala de fuentes de energía renovable dentro del sistema eléctrico presenta problemas técnicos derivados de su carácter no gestionable, es decir, no se puede controlar el nivel de generación para adaptarlo a la demanda. Para conseguir un alto grado de penetración, las instalaciones deben contar con sistemas específicos que favorezcan la integración de la energía generada e incluso con elementos para el almacenamiento de la electricidad excedente para su consumo en momentos de déficit de generación [48-50]. Esto es un inconveniente para instalaciones pequeñas ubicadas en edificios residenciales o en viviendas unifamiliares, incluso para pequeños edificios comerciales, en los que los usuarios no tendrán en general un perfil técnico adecuado para la explotación diaria de la instalación y, muy probablemente, deberán implementar en su vida diaria otra "*utility*" para gestionarla.

Algunas de estas medidas deben ser introducidas por las compañías distribuidoras de electricidad ya que sus redes, inicialmente diseñadas para el flujo de potencia en una sola dirección, deben permitir ahora la integración de la energía eléctrica desde los puntos de consumo [51]. Otras deben ser directamente implementadas en las instalaciones de generación, fundamentalmente los siguientes:

- Predicción de la generación de electricidad a corto plazo.
- Almacenamiento de la generación excedente para su consumo en periodos de déficit.
- Servicios complementarios para la regulación de tensión/energía reactiva en el punto de conexión.
- Gestión de la demanda para contribuir al equilibrio consumo – generación.
- Reducción de la generación

Algunas de estas medidas, como la regulación de tensión o energía reactiva podrán ser implementadas en los equipos de la instalación, como los inversores. Pero otras, como la predicción de la generación o la gestión de la demanda, van a requerir de atención técnica periódica y por tanto de personal especialista o la contratación del servicio por parte del *prosumer*[7].

En este sentido los centros comerciales también ofrecen ventajas frente a los edificios residenciales, ya que por sus características suelen disponer de importante equipamiento técnico de tipo industrial, como sistemas de alimentación de energía (eléctrica, vapor, combustibles), sistemas de refrigeración, seguridad, gestión energética, etc., y en algunas ocasiones de sistemas propios de generación de energía eléctrica. La existencia de estos sistemas conlleva que el centro disponga de un servicio de explotación y mantenimiento de las instalaciones y el equipamiento asociado, bien propio o contratado, que podría incluir entre sus actividades la gestión de la instalación fotovoltaica.

[7] Un *prosumer* es un consumidor de energía eléctrica que también tiene la capacidad de generarla.

Todas estas cualidades convierten a los centros comerciales en construcciones especialmente adecuadas para la instalación de instalaciones fotovoltaicas y por tanto deben ser objeto de un tratamiento individualizado a la hora de analizar su potencial.

En este caso, el objetivo buscado en esta línea de desarrollo dentro del trabajo de investigación ha sido analizar el potencial de los centros comerciales para la instalación de instalaciones solares fotovoltaicas.

El artículo correspondiente con esta línea de desarrollo del trabajo de investigación fue publicado con el título "*An assessment of photovoltaic potential in shopping centres*", en octubre de 2016 en el número 135 de la revista *Solar Energy*. Todos los detalles del artículo se muestran en la Tabla 5 del apartado 5.

3.3.3 Sector del transporte

En 2010 las emisiones de gases de efecto invernadero provenientes del sector transporte fueron de 7 $GtCO_2eq$, lo que representó el 14% del total. De ellas el 72% correspondieron al transporte por carretera [3]. Sin la implementación de las estrategias adecuadas de mitigación, las emisiones globales provenientes del transporte alcanzarían en 2050 las 12 $GtCO_2eq$. Sin embargo, en los escenarios encaminados a conseguir la limitación a 2 ˚C, el nivel de emisiones del transporte en el año 2050 debería situarse en torno a los 6 $GtCO_2eq$, es decir, a niveles inferiores a los registrados en 2010 [3].

Los países más contaminantes son aquellos más desarrollados [52]. Durante el año 2014, las emisiones del sector transporte alcanzaron al 26% del total en Estados Unidos [53]. Así mismo, en el conjunto de países de la EU-28 el sector del transporte contribuyó en 2014 con el 25,5% del total de emisiones, siendo el transporte por carretera responsable del 73% de estas emisiones y dentro de éstas, los vehículos de pasajeros el 44% [54].

Hay tres ejes fundamentales en los que se basan las estrategias de mitigación de las emisiones de gases de efecto invernadero en el sector transporte (descarbonización): el incremento de la eficiencia de los vehículos, el cambio en los hábitos de transporte y el uso de combustibles de bajas emisiones (*lower-carbon fuels*) [55].

En esta línea, los Estados Unidos de América a través de sus agencias *Environmental Protection Agency* (*EPA*) y *National Highway Traffic Safety Administration* (*NHTSA*) [56] han desarrollado planes y estándares para la fabricación de vehículos más eficientes y con menos niveles de emisión, con el objetivo de reducir las emisiones totales en más de 3,1 $GtCO_2$ hasta el año 2025 [57]. También, la *EPA* desarrolla el *Renewable Fuel Standard* [58] dirigido a asegurar el uso de un porcentaje mínimo de combustibles de origen renovable con el objetivo de reducir las emisiones en 138 $MtCO_2$ para 2022.

La Unión Europea desarrolló el *Roadmap* 2050 [59], para analizar y determinar las rutas encaminadas a conseguir el compromiso de la Unión Europea de que en el año 2050 el nivel de emisiones de gases de efecto invernadero sea inferior al 80% de los niveles de emisión del año 1990. Para alcanzar estos compromisos se han planteado escenarios en los que sería necesaria una total electrificación de los vehículos de baja y media carga y la sustitución de hasta el 90% de combustibles fósiles por biocombustibles e hidrógeno en vehículos pesados. Las estrategias para conseguir estos objetivos integran una gran cantidad de medidas transversales, soportadas con 39.000 millones de euros de fondos disponibles bajo el *European Structural and Investment Fund* 2014-2020 [60] para favorecer la movilidad con bajas emisiones, que incluyen 12.000 millones de euros exclusivamente para proyectos en zonas urbanas y con 6.400 millones de euros para el periodo 2014-2020 en el programa *Horizon* 2020 [61] desarrollado en el área de transportes para la investigación en proyectos enfocados en la mejora de la eficiencia y la reducción de los efectos climáticos y medioambientales, entre otros.

No obstante, todos estos planes no están teniendo el desarrollo esperado. Según la *International Energy Agency* en 2016 algunos países estarían en vías de conseguir, incluso superar, los objetivos de reducción relacionados con el sector energético (incluye el transporte) establecidos como consecuencia del Acuerdo de París, pero, aunque estos avances serían suficientes para ralentizar el incremento de emisiones relacionadas con el sector en su conjunto, no serían suficientes para conseguir el objetivo final de limitar el calentamiento global a 2 ˚C [62].

Una parte muy importante de las estrategias de mitigación para este sector del transporte se dirigen al ámbito de la sustitución de combustibles. Los combustibles mayoritariamente utilizados hoy en día son de origen fósil y presentan altas emisiones de gases de efecto invernadero. Dadas las características del transporte por carretera en cuanto a sus necesidades de autonomía y repostaje, los combustibles actuales pueden ser reemplazados principalmente por la energía eléctrica y el hidrógeno para su uso en vehículos eléctricos (*Electric Vehicles - EV*) y por biocombustibles en vehículos con motores de combustión interna (*Internal Combustion Engine - ICE*) adecuados para ello. Dentro de la categoría de vehículos eléctricos (EVs) se encuentran aquellos propulsados por pilas de hidrógeno (*Fuel cell electric vehicles* – FCEV), los propulsados únicamente por baterías eléctricas (*Battery Electric Vehicles* – BEV) y aquellos que disponen de un motor de combustión interna y de un motor eléctrico acompañado de baterías que pueden recargarse enchufando el vehículo a la red eléctrica (*Plug-in Hybrid Electric Vehicle* – PHEV). La Ilustración 10 muestra las principales características de funcionamiento de los *EVs* y los *ICEs*.

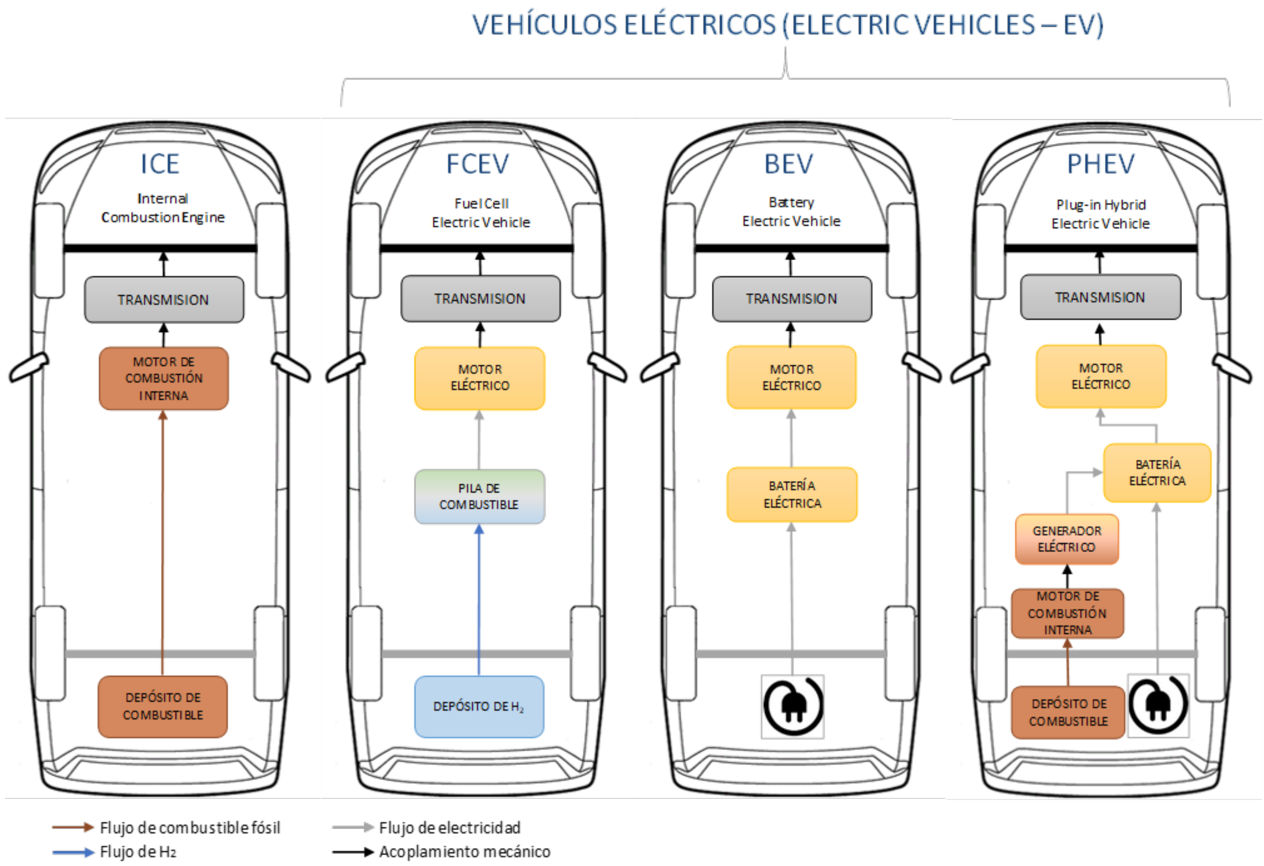

Ilustración 10: Principios de funcionamiento de los vehículos eléctricos y con motor de combustión interna

En cuanto al uso de biocombustibles, en el sector transporte se alcanzó en 2015 una cuota de mercado del 3% y se prevé un incremento muy marginal hasta alcanzar el 4% en 2021 [63].

Similares avances se han hecho en la integración de *PHEVs* y *BEVs*. En el año 2018 había alrededor de 5 millones de unidades, con un crecimiento de 2 millones de unidades respecto del año anterior. Noruega lideró nuevamente con una integración del 46% de la flota de vehículos [64].

El menor avance entre las posibilidades para la transición hacia combustibles menos contaminantes se ha producido en la integración del hidrógeno. El uso del hidrógeno en el transporte se realiza mediante vehículos equipados con motores de combustión interna de hidrógeno (*Hidrogen Internal Combustion Engine - HICE*) o *EVs* propulsados con pilas de hidrógeno (*FCEV*). En comparación con los otros tipos de *EVs*, los *FCEV*s ofrecen un menor nivel de emisiones que los *PHEV*s y un tiempo de recarga muy inferior y una autonomía mayor que los *BEV*s, con lo que ofrecen una movilidad muy similar a los vehículos convencionales con muy bajas emisiones [65].

Los principales métodos de producción de hidrógeno son: el reformado de metano con vapor de agua (*Steam Methane Reforming - SMR*), la electrolisis del agua (*Water Electrolysis - WE*) y la gasificación de carbón (*Coal Gasification - CG*) [65-68]. Tanto el *SMR* como la *WE* pueden realizarse de forma centralizada en grandes centrales o de forma distribuida cerca de los puntos de consumo. Los procesos de *CG* pueden incorporar sistemas de captura de carbono (*Carbon Capture Systems - CCS*) para disminuir las emisiones. La *WE* emplea energía eléctrica, que puede ser generada mediante fuentes renovables (solar, eólica, hidroeléctrica, etc.) aumentando así sus niveles de integración en el mix energético.

El nivel de emisiones *well-to-wheel*[8] de los *FCEV*s dependerá del mix de producción del hidrógeno y del porcentaje de fuentes renovables en la generación eléctrica de producción, pero en general se sitúa muy por debajo de los *ICEs* y *PHEVs* y en el entorno de los *BEVs* en función del mix de producción [65,67,69,70].

---

[8] El nivel de emisiones "*well to wheel*" indica las emisiones que produce un determinado vehículo que usa un determinado tipo de combustible considerando las emisiones generadas desde que el combustible es extraído (*from well*) hasta que se usa en el vehículo (*to wheel*).

En cuanto al coste de combustible, diversos análisis determinan que, aunque el coste por distancia recorrida de los *PHEVs* y los *BEs* son actualmente inferiores, en términos de coste total para el propietario[9] (*TCO – Total Cost of Ownership*), *FCEVs* y *BEVs* presentan valores comparables y levemente superiores a los *PHEVs* [65,69,71].

Gracias a estas características de eficiencia, coste y emisiones, todas las estrategias de reducción de gases de efecto invernadero incorporan en gran medida la integración de *FCEVs* en el parque automovilístico. En las estrategias diseñadas por la *International Energy Agency* para alcanzar el escenario 2DS [10], la integración de un 25% de *FCEVs* en el transporte por carretera para el año 2050 contribuiría a una reducción de hasta el 10% de todas las emisiones relacionadas con el transporte [65]. En el proyecto *HYWAYS* [72], desarrollado por la Unión Europea, se prevé la existencia de 2,5 millones de *FCEVs* para el año 2020. En el estado de California se proyectaba la existencia de 10.500 *FCEVs* para el año 2018 y más de 34.000 para finales de año 2021 [73] y un mínimo de 10 millones, pudiendo llegar a 40 millones en el mejor escenario, para los Estados Unidos en 2035 [74].

Son varios los fabricantes de automóviles que comercializan ya *FCEVs* y la mayoría de ellos tienen planes para su venta a corto y medio plazo [75-79], y la industria y la comunidad científica continúan trabajando en soluciones que mejoren técnicamente estos vehículos [80]. No obstante, aunque los *FCEVs* y los sistemas de producción y repostaje de H_2 presentan tecnologías maduras, que permiten una explotación de toda la cadena de suministro en niveles comerciales para el público en general [81,82], la situación actual está muy lejos de conseguir los objetivos.

En el año 2016 la flota mundial de *FCEVs* era inferior a las 2.000 unidades y su presencia se daba fundamentalmente en los Estados Unidos de América, principalmente en el estado de California, algunos países de Europa y Japón [75,83,84].

El desarrollo de las estaciones de repostaje (*Hydrogen Refuelling Stations – HRS*) es similar. En el año 2016 había en operación en torno a 200 estaciones. California, Japón y algunos países europeos

---

[9] El Coste Total para el Propietario o *TCO* por sus siglas in inglés (*Total Cost of Ownership*) considera todos los costes relacionados con la compra y el uso del vehículo, incluyendo el coste del combustible.

[10] El escenario IEA 2DS establece estrategias para limitar el incremento de la temperatura media del planeta a 2 °C en 2100.

dominan nuevamente el mercado [75,84,85].

El motivo fundamental que impide el despliegue de los *FCEVs* es la falta de una red de abastecimiento de H_2. La decisión de los usuarios de comprar un *FCEV*, además de estar motivada por aspectos técnicos y medioambientales, debe estar respaldada por la certeza de poder reponer el combustible de forma segura, cercana y sin restricciones, y no ver así reducido el nivel de confort que actualmente tiene usando los vehículos tradicionales. Por lo tanto, la integración de *FCEVs* necesita previamente de una infraestructura de *HRSs* adecuada. Sin embargo, para crear una infraestructura de *HRSs* que permita el suministro continuo y seguro de H_2 es necesario que su implementación sea económicamente sostenible o rentable y en gran medida, financiable. Esto significa que la venta de H_2 esté soportada por un mercado sostenido y preferiblemente creciente de *FCEVs* que genere los ingresos suficientes. Esta situación en un claro ejemplo de lo que se conoce como el dilema del "*huevo y la gallina*" [72,86,87].

Diversos investigadores han propuesto soluciones para el desarrollo de una infraestructura de suministro de hidrógeno a través de *HRSs*, desde métodos para la búsqueda de las mejores ubicaciones [88,89] hasta análisis de la mejor composición de métodos de producción, transporte y distribución del combustible para optimizar el coste de las infraestructuras [90,91], pero son difícilmente implementables sin un mercado suficiente de *FCEVs*. Para soslayar este dilema son necesarias medidas para una integración coordinada y sostenida de *FCEV*s y *HRSs*.

Una forma de conseguir un mercado importante de *FCEVs* puede ser su integración en flotas de vehículos. Las ciudades con gran población son grandes focos de contaminación por la gran concentración de vehículos. Una característica común de las ciudades, especialmente de las grandes, pero también en las de mediano tamaño, es la existencia de importantes flotas de taxis (ver Tabla 1).

Tabla 1: Población, tamaño de la flota de taxis y número de coches de pasajeros en algunas ciudades muy pobladas

Ciudad	Población (millones de habitantes)	Flota de taxis	Taxis /habitante	Coches de pasajeros (millones)	Taxis/Coches
Londres [92-94]	8,50	22.500	2,65	2,60	0,9%
Ciudad de Nueva York [95-97]	8,55	31.500 ª	3,68	2,10	1,5%

Ciudad	Población (millones de habitantes)	Flota de taxis	Taxis /habitante	Coches de pasajeros (millones)	Taxis/Coches
Madrid [98-101]	3,16	15.000	4,75	1,44	1,0%
ª El número incluye Yellow y Boro taxis y "coches negros" (black cars).					

Las flotas de taxis presentan características que pueden ser adecuadas para iniciar un despliegue de *FCEVs,* porque:

- Son una gran flota de vehículos y por lo tanto un gran mercado para las futuras *HRSs*. En ciudades con alta población pueden llegar a varias decenas de miles de unidades (ver Tabla 1).
- Su ámbito de actuación está básicamente restringido a la ciudad a la que pertenecen, con lo que sería suficiente una red local de *HRSs* para la provisión del combustible.
- Están generalmente sometidos a un procedimiento de autorización o licencia por las autoridades locales, por lo que se pueden incluir en los requisitos para la autorización, que los vehículos presenten determinadas características.
- Tienen un periodo corto de reemplazo, con lo que se puede cambiar toda la flota en el medio plazo.
- Recorren diariamente grandes distancias por lo que son los vehículos de pasajeros más contaminantes de las ciudades. Cualquier actuación sobre estos vehículos tendrá un mayor impacto que sobre los vehículos del público en general.
- Pagan sus impuestos en la ciudad a la que pertenecen por lo que es posible la subvención de los vehículos y el combustible vía exenciones de impuestos.

Con un desarrollo de taxis propulsados por pila de hidrógeno (*Fuel Cell Electric Taxis - FCETs*) controlado, el siguiente paso sería diseñar de forma coordinada una red de *HRSs* capaz de, en principio, atender las necesidades de combustible. Nuevamente un desarrollo coordinado por las autoridades locales puede presentar grandes ventajas, ya que:

- Las autoridades locales disponen de terrenos en la ciudad que pueden poner a disposición de las *HRSs* y disminuir los costes.

- Pueden disponer regulaciones que agilicen la construcción de las instalaciones.
- Pueden instrumentar subvenciones a la construcción, a la financiación e incluso a la explotación de las *HRSs*. Estas subvenciones pueden integrar fondos de otras autoridades nacionales o supranacionales. A modo de ejemplo, el estado de California, a través de la *California Energy Commission* ha distribuido ayudas de 20 millones de dólares anuales para el desarrollo de una red de suministro de hidrógeno que alcance 100 *HRSs*. Hasta el año 2015 más de 80 millones de dólares se han dispuesto para el desarrollo de 49 *HRSs*, más fondos adicionales de casi 10 millones de dólares para subvencionar los costes de operación y mantenimiento de las instalaciones [73].
- Las ciudades serán directamente beneficiarias de la reducción de la polución, con lo que conseguirán importantes ahorros derivados de la mejora en la calidad del aire.

En este caso, el objetivo ha sido determinar una solución realizable, rentable y financiable para iniciar, en ciudades de gran población, una red de *HRSs* para el suministro de hidrógeno que sirva como soporte a una integración masiva de *FCEVs* en el entorno urbano, utilizando como mercado estable la flota de taxis de la ciudad, y determinar las condiciones político–económicas adecuadas para la implementación de una infraestructura de repostaje adecuada. Para aplicar e ilustrar la metodología, se han utilizado datos reales de la ciudad de Madrid, capital de España, pero los resultados son extrapolables a ciudades similares que dispongan de flotas de taxis.

El artículo correspondiente a esta línea de desarrollo del trabajo de investigación fue publicado con el título "*A hydrogen refuelling stations infrastructure deployment for cities supported on fuel cell taxi roll-out*", en abril de 2018 en el número 148 de la revista *Energy*. Todos los detalles del artículo se muestran en la Tabla 6 del apartado 5.

4 MARCO TEÓRICO EN EL QUE SE INSCRIBE EL TEMA DE LA TESIS Y HERRAMIENTAS METODOLÓGICAS. REMISIÓN A LAS PUBLICACIONES

En cada uno de los resultados de las distintas líneas de desarrollo del trabajo de investigación se han definido metodologías novedosas y aplicadas al objetivo específico que se persigue en cada uno de ellos. No obstante, dado que el objetivo general de la investigación está enfocado en la búsqueda de soluciones reales y prácticas para el desarrollo e integración de fuentes de energías renovables, para asegurar que el objetivo general se mantiene en cada una de las líneas de desarrollo, ciertas líneas básicas se han mantenido en todas las metodologías utilizadas. Estas líneas básicas son las siguientes:

- Siempre que ha sido posible, se han utilizado datos reales obtenidos de bases de datos contrastadas o de informes sectoriales elaborados por entidades de reconocido prestigio en el ámbito correspondiente. Se ha evitado el uso de datos sintéticos calculados a partir de datos análogos para otras localizaciones, sectores, etc.
- En aquellos casos en los que se plantean soluciones cuya viabilidad no ha sido previamente contrastada desde un punto de vista financiero, la metodología ha incluido una evaluación de la viabilidad económica y las posibilidades de financiación mediante el estudio y cuantificación de las variables relativas a la rentabilidad de la solución planteada. Se ha realizado la determinación, en su caso, de subsidios requeridos para permitir la implantación real de las soluciones obtenidas desde un punto de vista de sostenibilidad financiera.
- Para comprobar la robustez de las metodologías propuestas, en todos los trabajos se han incluido múltiples análisis de sensibilidad de los resultados obtenidos respecto de las variables más importantes incluidas en los modelos.

La definición de las hipótesis y diseño de las metodologías se definen e ilustran en detalle en cada uno de los artículos publicados, no obstante, en los subapartados siguientes se mencionan los aspectos básicos.

4.1 Publicación 1: "*Repowering: An actual possibility for wind energy in Spain in a new scenario without feed-in-tariffs*"

La decisión de acometer la repotenciación de un parque eólico se tomará si el proyecto ofrece un nivel de rentabilidad adecuado. Este nivel dependerá del perfil del inversor, pero es razonable pensar que estará en el entorno de la rentabilidad ofrecida por los actuales parques eólicos.

Desde un punto de vista económico, la solución más ventajosa para el conjunto del sistema eléctrico será la de pagar la energía generada por los parques eólicos al precio del mercado eléctrico spot y ser capaces de suministrar energía en términos de paridad de red. Este modelo está siendo aplicado con éxito en la actualidad en muchos países, incluso con tecnologías menos eficientes que la eólica.

La propuesta retributiva analizada en este trabajo está basada en:

1. Mantener el derecho actual de los productores en de verter toda la producción de energía del parque en el sistema siempre que sea técnicamente posible (prioridad de despacho).
2. Recibir por la energía vertida en cada hora el precio horario del mercado spot.

Bajo este marco, el análisis se ha enfocado en dos aspectos: si un parque eólico repotenciado puede ofrecer rentabilidades interesantes para los inversores, siendo una alternativa mejor que la de la construcción de un nuevo parque eólico y por otro lado si la propuesta retributiva es suficiente para asegurar una rentabilidad razonable. Por lo tanto, se analizarán dos escenarios:

1. La repotenciación de un parque eólico existente.
2. La instalación de un parque eólico en un emplazamiento nuevo. Para que el análisis sea homogéneo se considerará la misma potencia que para el escenario anterior.

En ambos escenarios la rentabilidad para el inversor se ha estimado utilizando la Tasa Interna de Retorno (*Internal Rate of Return - IRR*) durante un periodo igual a la vida útil de los aerogeneradores considerando una fuente de financiación externa, lo que se conoce como *IRR* para el Accionista. Para obtener la *IRR* se calculan, en primer lugar, los flujos de caja de la inversión según el método indicado en la Tabla 2.

Tabla 2: Método para el cálculo de los flujos de caja

	Flujo de Caja para el Accionista
+	Ingresos por la venta de energía
-	Gastos de operación
=	**Margen bruto (EBITDA)**
-	Depreciación de activos
=	**Beneficios antes de intereses e impuestos (EBIT)**
-	Gastos financieros y devolución de principal
=	**Beneficios antes de impuestos**
-	Impuestos
=	**Beneficios después de impuestos**
+	Depreciación de activos
=	**Flujo de caja anual** ($\boldsymbol{CF_z}$)
+	Flujo de caja acumulado del año anterior
=	**Flujo de caja acumulado del año actual** ($\boldsymbol{CFA_z}$)

El Valor Actual Neto (*Net Present Value – NPV*) de la inversión se calcula a partir de los flujos de caja anuales obtenidos, trasladando todas las cantidades futuras al presente a una tasa de interés k, por lo tanto, será:

$$NPV = \sum_{z=1}^{n} \frac{CF_z}{(1+k)^z} - I_o \qquad [1]$$

Dónde I_o es la parte de los costes totales que debe aportar el accionista inversor y dependerá del grado de Apalancamiento Financiero (*Financial Leverage – FL*)[11]:

$$I_o = FL\ x\ Coste\ total \qquad [2]$$

La *IRR* se define como el valor de la tasa de interés k que hace cero el *NPV*, es decir:

$$0 = \sum_{z=1}^{n} \frac{CF_z}{(1+IRR)^z} - I_o \qquad [3]$$

[11] El grado de apalancamiento financiero (*Financial Leverage – FL*) es el porcentaje de la inversión total que se financiará con recurso ajeno o deuda.

4.2 Publicación 2: "*An assessment of photovoltaic potential in shopping centres*"

La metodología que se ha seguido para determinar el potencial fotovoltaico de los centros comerciales, tanto en potencia instalada como en generación, se muestra en la Ilustración 11

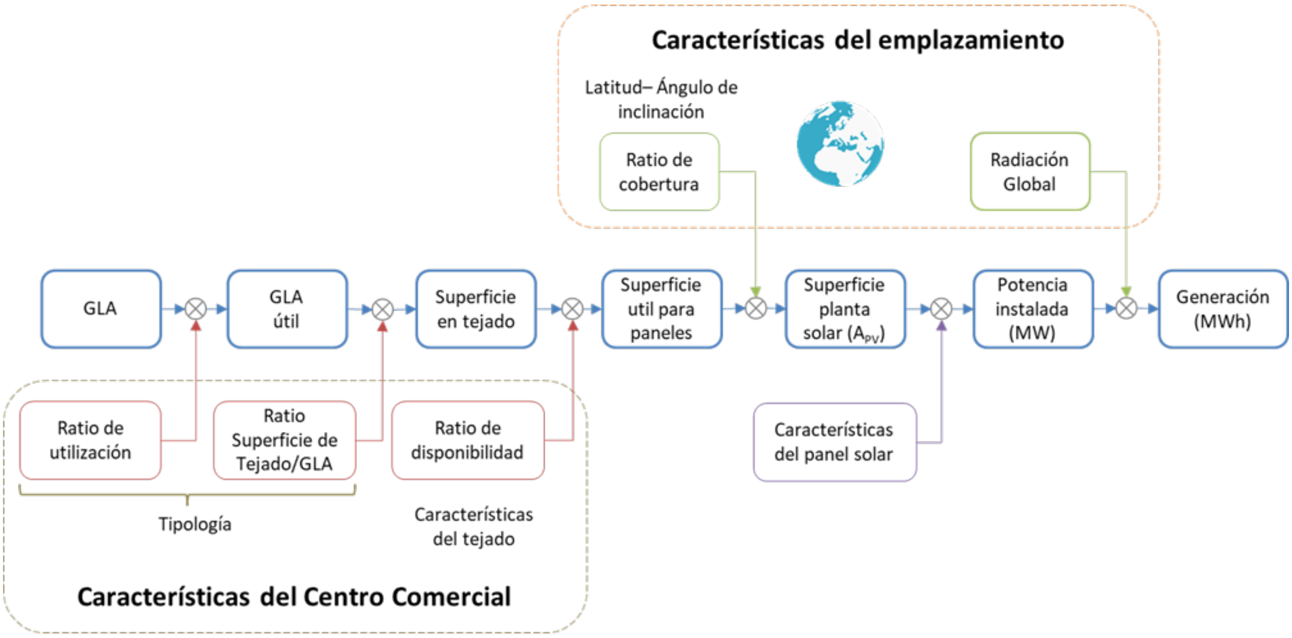

Ilustración 11: Metodología para la determinación del potencial fotovoltaico

El primer paso de la metodología es la cuantificación de la superficie disponible en centros comerciales. Para ello, recurriendo a información estadística, se obtuvo el valor de la superficie total disponible para alquilar (*Gross Leasable Area – GLA*) para múltiples localizaciones. Este parámetro *GLA* es utilizado en el sector inmobiliario para determinar la superficie útil en el centro comercial que es destinada a la venta de productos o servicios. Es un término utilizado para clasificar por tamaño los centros comerciales, ya que indica la cantidad de espacio disponible para alquilar.

No en todos los centros comerciales será factible la instalación de una instalación solar fotovoltaica ya que no dispondrán de tejado o este no estará accesible. En algunos casos en los tejados se ubican aparcamientos y en otros casos, principalmente aquellos centros comerciales ubicados dentro de los núcleos urbanos, los centros comerciales están en lugares subterráneos o integrados en edificios con otras funcionalidades, como hoteles o viviendas.

Para aquellos sin tejado o no accesible en su totalidad, al no existir datos estadísticos, es imposible hacer una estimación de su cantidad y volumen en términos de *GLA* basada en hechos objetivos. No obstante, hay que considerar que estos centros comerciales sin tejado, subterráneos o integrados estarán ubicados principalmente en el interior de núcleos urbanos y tendrán en general un tamaño reducido. En el ámbito de este estudio se incluyen únicamente aquellos centros comerciales con una superficie superior a los 5.000 metros cuadrados y, por tanto, aunque la mayoría de aquellos sin tejado están fuera del estudio, es posible que un cierto número reducido de los centros comerciales incluidos en el estudio presente una imposibilidad total para la instalación de una planta solar fotovoltaica. Para contemplar esta posibilidad se ha establecido un factor de reducción por nivel de adecuación conservador del 80% (ratio de utilización).

A partir del valor obtenido para la superficie en centros comerciales factibles, se ha estimado la superficie disponible en el tejado, para lo cual es necesario establecer una relación entre el *GLA* y la superficie de tejado del centro comercial. Este será un factor que dependerá de las características individuales de cada centro comercial, no obstante, para los objetivos de este artículo, una relación media entre el valor de *GLA* y la superficie disponible en tejado se ha obtenido mediante el análisis de una muestra de 500 centros comerciales repartidos por los países incluidos en este estudio. El análisis ha consistido en la identificación en la aplicación informática Google Earth™ de todos los centros comerciales de la muestra y la medición de las superficies de sus tejados

No todo el espacio en el tejado está libre de obstáculos y es posible la instalación de paneles solares. Hay elementos arquitectónicos, como tragaluces o superficies sin capacidad portante, elementos funcionales, como equipos de ventilación y refrigeración, y construcciones propias o cercanas que pueden dar sombra. Todos ellos hacen que disminuya la superficie utilizable del tejado, por tanto, habrá que considerar un factor de reducción, que denominaremos ratio de disponibilidad, para obtener la superficie de tejado disponible para la instalación de la planta solar fotovoltaica.

Resultado de la aplicación de todos los factores de reducción anteriormente explicados, se ha obtenido, a partir del *GLA*, una estimación de la superficie disponible en tejado para la instalación de los paneles solares.

Una vez determinada la superficie disponible en el tejado del centro comercial para la instalación de los paneles solares, se podrá determinar tanto la potencia instalable como la capacidad de generación. Dos aspectos son fundamentales para realizar este cálculo: por un lado, la localización del centro comercial, que determinará el recurso solar, el ángulo óptimo de inclinación de los paneles y la separación entre filas de paneles y por otro las características de los paneles y del resto de los equipos que formarán parte de la instalación solar

La evaluación de la potencia instalable y la capacidad de generación dará como resultado la estimación del potencial fotovoltaico de los centros comerciales.

4.3 Publicación 3: *"A hydrogen refuelling stations infrastructure deployment for cities supported on fuel cell taxi roll-out"*

La metodología tiene por objetivo determinar un *caso base* técnicamente viable y financieramente sostenible para la construcción y explotación de la red de estaciones de repostaje de hidrógeno (*HRSs*) necesarias para el suministro de H_2 a la flota de *FCETs* de una ciudad. El *caso base* se centró en las unidades que presenten el peor escenario, que serán aquellas que se pongan en operación el primer año porque tendrán los primeros años de explotación un ratio de utilización menor y por tanto menos ingresos, y unos costes de instalación y explotación mayores, al no verse beneficiadas por la reducción de coste derivado de la curva de aprendizaje y la economía de escala.

La definición técnica se realizó mediante el análisis de las tecnologías viables en el momento de elaboración del trabajo, seleccionando aquellas más adecuadas para la implantación en el medio urbano y de un tamaño acorde al despliegue de *FCETs* diseñado.

La evaluación de la rentabilidad y viabilidad financiera de las *HRSs* se realizó mediante la cuantificación de los indicadores financieros de la Tasa Interna de Retorno (*Internal Rate of Return - IRR*) y el Ratio de Anual Cobertura al Servicio de la Deuda (*Annual Debt Service Coverage Ratio – ADSCR*).

La *IRR* determina la tasa de interés o rentabilidad que ofrece la inversión. La inversión será tanto más rentable cuanto mayor sea el *IRR* obtenido. Se calculó durante un periodo de 25 años en dos escenarios: con y sin considerar una fuente de financiación externa, lo que se denomina *IRR* para el Accionista e *IRR* del Proyecto respectivamente.

Para obtener la *IRR* se han calculado, en primer lugar, los flujos de caja de la inversión para ambos escenarios según el método indicado en la Tabla 3.

Tabla 3: Cálculo de los flujos de caja

Flujo de caja del proyecto Sin fuente de financiación externa		**Flujo de caja para el accionista** Con Fuente de financiación externa	
+	Ingresos por la venta de H_2 Precio de compra del H_2 más margen de venta	+	Ingresos por la venta de H_2 Precio de compra del H_2 más margen de venta
-	Costes de construcción (CAPEX)	-	Costes de construcción (CAPEX)
-	Costes de operación O&M. OPEX. Precio de coste del H_2	-	Costes de operación O&M. OPEX. Precio de coste del H_2
=	**Margen bruto operativo (EBITDA)**	=	**Margen bruto operativo (EBITDA)**
-	Depreciación de activos	-	Depreciación de activos
=	**Beneficios antes de intereses e impuestos (EBIT)**	=	**Beneficios antes de intereses e impuestos (EBIT)**
		-	Repago de la deuda (capital + intereses)
=	**Beneficios antes de impuestos**	=	**Beneficios antes de impuestos**
-	Impuestos	-	Impuestos
=	**Beneficios después de impuestos**	=	**Beneficios después de impuestos**
+	Depreciación de activos	+	Depreciación de activos
=	**Flujo de caja anual (CF_z)**	=	**Flujo de caja anual (CF_z)**
+	Flujo de caja acumulado del año anterior	+	Flujo de caja acumulado del año anterior
=	**Flujo de caja acumulado del año actual (CFA_z)**	=	**Flujo de caja acumulado del año actual (CFA_z)**

El Valor Actual Neto (*Net Present Value* - NPV) de la inversión se calcula a partir de los flujos de caja anuales obtenidos, trasladando todas las cantidades futuras al presente a una tasa de interés k, por lo tanto será:

$$NPV = \sum_{z=1}^{n} \frac{CF_z}{(1+k)^z} - I_o \qquad [4]$$

Dónde I_o es la parte de los costes totales que debe aportar el inversor accionista y dependerá del grado de Apalancamiento Financiero (*Financial Leverage - FL*)[12]:

$$I_o = FL\ x\ CAPEX \qquad [5]$$

La *IRR* se define como el valor de la tasa de interés k que hace cero el *NPV*, es decir:

$$0 = \sum_{z=1}^{n} \frac{CF_z}{(1+IRR)^z} - I_o \qquad [6]$$

El *ADSCR* es un factor determinante para evaluar la inversión, ya que cuantifica la capacidad de la *HRS* para generar ingresos suficientes para repagar la deuda ajena utilizada para financiar la instalación. Cuanto mayor sea el *ADSCR* a 1 mejor será la inversión desde el punto de vista del retorno de la deuda. El *ADSCR* se ha calculado según la siguiente ecuación:

$$ADSCR_z = \frac{EBIT}{Repago\ de\ la\ deuda\ (capital+intereses)} \qquad [7]$$

Los pasos seguidos para determinar la solución del caso base fueron:

1. Caracterizar el despliegue de la flota de *FCETs*.
2. Establecer los parámetros técnicos y económicos que definen el número y el funcionamiento de las *HRS*.
3. Determinar las necesidades de subsidios y ayudas financieras para asegurar la viabilidad económica de las instalaciones. Estas necesidades determinarán el caso base para una *HRS* viable.
4. Realizar un análisis de sensibilidad para determinar la robustez del caso base.

[12] El grado de apalancamiento financiero (*Financial Leverage – FL*) es el porcentaje de la inversión total que se financiará con recurso ajeno o deuda.

5 TRABAJOS PUBLICADOS

Las publicaciones que integran la presente tesis cumplen con los requisitos establecidos en el Documento aprobado por el Comité de Dirección de la Escuela Internacional de Doctorado de la Universidad Nacional de Educación a Distancia (EIDUNED), en su reunión de 16 de enero de 2017, y por la Comisión de Investigación y Doctorado de la UNED, con fecha 21 de febrero de 2017 para ser considerados válidas en la tesis doctoral presentada por compendio de publicaciones. Dichos requisitos son los siguientes:

1. El compendio de publicaciones estará formado por un mínimo de 3 artículos. Al menos dos de ellos deben estar publicados y el tercero aceptado. En este caso, los tres artículos han sido publicados con anterioridad a la presentación de esta tesis.
2. Los artículos han de ser publicados en revistas de índices de impacto en los dos primeros cuartiles de la relación de revistas del ámbito de la especialidad del Programa en el que está inscrita dicha tesis y referenciadas en la última relación publicada por el *Journal Citation Reports* (SCI y/o SSCI) y de *SCOPUS*. Los tres artículos han sido publicados en revistas con índices de impacto en los dos primeros cuartiles.
3. Todos los artículos deben estar publicados con fecha posterior a la primera matrícula de tutela académica en la EIDUNED. En este caso la primera matrícula se produjo en el curso académico 2014/2015 (octubre 2014) y los artículos se han publicado entre enero de 2015 y abril de 2018.
4. El doctorando o doctoranda debe ser primer firmante o segundo, en este último caso, el primero debe ser el director o directora de la tesis. En todas las publicaciones que integran la tesis doctoral, el doctorando es primer o segundo firmante, siendo en este caso, el director de la tesis D. Antonio Colmenar Santos, el primer autor.

A continuación, en las tablas 4, 5 y 6 se muestran todos los datos correspondientes a cada una de las publicaciones incluidas en esta tesis por compendio.

Tabla 4: Datos del primer trabajo científico publicado: "*Repowering: An actual possibility for wind energy in Spain in a new scenario without feed-in-tariffs*".

Datos sobre la publicación del trabajo científico		
Título de la publicación	*Repowering: An actual possibility for wind energy in Spain in a new scenario without feed-in-tariffs*	
Autores	1. Antonio Colmenar Santos (Director de la tesis) 2. Severo Campíñez Romero (Doctorando) 3. Clara Pérez Molina 4. Francisco Mur Pérez	
Afiliación de los autores	Departamento de Ingeniería Eléctrica, Electrónica y de Control de la Escuela Técnica Superior de Ingenieros Industriales de la UNED	
Revista	*Renewable and Sustainable Energy Reviews*	
Estado de publicación	Publicado en enero de 2015 en el número 41 de la revista	
D.O.I.	10.1016/j.rser.2014.08.041	
Índices de impacto *Journal Citation Reports* de la revista en el año 2018 (último índice publicado)		
Categoría	*Energy&Fuels*	*Green & sustainable science technology*
Índice de impacto	10,556	
Quartil	Q1	Q1
Índices de impacto *Scopus* de la revista en el año 2018 (último índice publicado)		
CiteScore 2018 All publication types	12,21	
SCImago Journal Rank (SJR) 2018	3,288	
Source Normalized Impact per Paper (SNIP) 2018	3,694	
CiteScore rank and Percentile per category	***CiteScore rank***	***Percentile***
Energy: Renewable Energy, Sustainability and the Environment	7/153	95

En los anexos I, II y III se incluyen los siguientes documentos relativos a la publicación del primer trabajo científico:

- Anexo I: Copia de la publicación.
- Anexo II: Certificado de la publicación.
- Anexo III: Informes relativos con los índices de impacto.

Tabla 5: Datos del segundo trabajo científico publicado: "*An assessment of photovoltaic potential in shopping centres*".

Datos sobre la publicación del trabajo científico		
Título de la publicación	*An assessment of photovoltaic potential in shopping centres*	
Autores	1. Antonio Colmenar Santos (Director de la tesis) 2. Severo Campíñez Romero (Doctorando) 3. Clara Pérez Molina 4. Francisco Mur Pérez	
Afiliación de los autores	Departamento de Ingeniería Eléctrica, Electrónica y de Control de la Escuela Técnica Superior de Ingenieros Industriales de la UNED	
Revista	*Solar Energy*	
Estado de publicación	Publicado en octubre de 2016 en el volumen 135 de la revista.	
D.O.I.	10.1016/j.solener.2016.06.049	
Índices de impacto *Journal Citation Reports* de la revista en el año 2018 (último índice publicado)		
Categoría	*Energy&Fuels*	
Índice de impacto	4,674	
Quartil	Q1	
Índices de impacto *Scopus* de la revista en el año 2018 (último índice publicado)		
CiteScore 2018 (All publication types):	5,24	
SCImago Journal Rank (SJR)	1,593	
Source Normalized Impact per Paper (SNIP)	1,622	
CiteScore rank and Percentile per category	***CiteScore rank***	***Percentile***
Energy: Renewable Energy, Sustainability and the Environment	24/153	84
Materials Science: General Materials Science	49/439	88

En los anexos IV, V y VI se incluyen los siguientes documentos relativos a la publicación del primer trabajo científico publicado:

- Anexo IV: Copia de la publicación.
- Anexo V: Certificado de la publicación.
- Anexo VI: Informes relativos con los índices de impacto.

Tabla 6: Datos del tercer trabajo científico publicado: *"A hydrogen refuelling stations infrastructure deployment for cities supported on fuel cell taxi roll-out"*.

Datos sobre la publicación del trabajo científico		
Título de la publicación	*A hydrogen refuelling stations infrastructure deployment for cities supported on fuel cell taxi roll-out*	
Autores	1. Severo Campíñez Romero (Doctorando) 2. Antonio Colmenar Santos (Director de la tesis) 3. Clara Pérez Molina 4. Francisco Mur Pérez	
Afiliación de los autores	Departamento de Ingeniería Eléctrica, Electrónica y de Control de la Escuela Técnica Superior de Ingenieros Industriales de la UNED	
Revista	*Energy*	
Estado de publicación	Publicado en abril de 2018 en el volumen 148 de la revista	
D.O.I.	10.1016/j.energy.2018.02.009	
Índices de impacto *Journal Citation Reports* de la revista en el año 2018 (último índice publicado)		
Categoría	*Energy&Fuels*	*Thermodynamics*
Índice de impacto	5,537	
Quartil	Q1	Q1
Índices de impacto *Scopus* de la revista en el año 2018 (último índice publicado)		
CiteScore 2018 All publication types	6,2	
SCImago Journal Rank (SJR)	2,048	
Source Normalized Impact per Paper (SNIP)	1,822	
CiteScore rank and Percentile per category	***CiteScore rank***	***Percentile***
Engineering: Civil and Structural Engineering	3/288	99
Engineering: Building and Construction	5/168	97
Engineering: Mechanical Engineering	20/579	96
Engineering: Industrial and Manufacturing Engineering	15/323	95
Environmental Science: Pollution	7/109	94
Engineering: Electrical and Electronic Engineering	45/661	93

En los anexos VII, VIII y IX se incluyen los siguientes documentos relativos a la publicación del primer trabajo científico publicado:

- Anexo VII: Copia de la publicación.

- Anexo VIII: Certificado de la publicación.
- Anexo IX: Informes relativos con los índices de impacto.

5.1 Publicación 1: "*Repowering: An actual possibility for wind energy in Spain in a new scenario without feed-in-tariffs*"

5.1.1 Resumen de la publicación

Resumen en español

El pasado mes de enero de 2012, el Gobierno español suspendió los incentivos económicos para nuevas instalaciones de generación eléctrica a partir de fuentes renovables, incluyendo la energía eólica.

No obstante, España sigue teniendo un grado de dependencia energética muy elevado que solo puede resolverse mediante la aplicación de medidas de ahorro energético y utilización masiva de fuentes de energía renovables. Además, aún no está cumplido el objetivo marcado por la Unión Europea y asumido por el Estado español, que el porcentaje de energía primaria generada a partir de fuentes renovables alcance el 20% en el año 2020.

En España hay parques eólicos con más de 15 años en operación comercial, ofreciendo un mercado amplio para la repotenciación. El uso de nuevos aerogeneradores más eficientes mediante la repotenciación conlleva beneficios para la totalidad del sector eléctrico optimizando el uso de los recursos naturales y facilitando la integración en red de la energía que hasta entonces era generada por los antiguos parques.

Este artículo analiza el parque actual de generación eólica y cuantifica el mercado apto para la repotenciación. Así mismo se analiza si la repotenciación es una alternativa válida y rentable para continuar con la integración de la energía eólica en el mix energético español y si esta rentabilidad es suficiente cuando la venta de la energía generada es retribuida al precio del mercado diario de electricidad. Los resultados muestran que la repotenciación es una alternativa rentable, en algunas ocasiones y bajo ciertas condiciones ofreciendo mejores rentabilidades que la construcción de nuevos parques eólicos.

Resumen en inglés

At the end January 2012, the Spanish government suspended the economic incentives for electricity generation facilities using renewable energy sources, including wind energy plants.

Spain maintains a high level of energy dependence that can only be reduced by applying measures to increase energy efficiency and using massive amounts of renewable sources. In addition, the target assumed by Spain, i.e., to have at least 20% of the primary energy to be supplied by renewable sources by 2020, has not yet been reached.

In Spain, wind farms, a number of which have been in commercial operation for over 15 years, offer a broad market appropriate for repowering. The use of more efficient wind turbines by means of repowering provides benefits to the electricity sector as a whole by optimizing the use of natural resources and facilitating the grid integration of the energy generated.

This paper analyses existing wind farms to quantify and characterize the market suitable for repowering. We discuss whether repowering is a valid alternative from the point of view of feasibility to enable the continuation of the integration of wind energy in the Spanish energy mix and whether this feasibility is sufficient when the energy generated is charged at the electricity market price in terms of grid parity. The results support that repowering is a profitable alternative and is often even better than the construction of new wind farms under certain conditions.

5.1.2 Conclusiones de la publicación

A la vista de los resultados del artículo, la inversión en la repotenciación de parques eólicos puede ser más rentable que la construcción de un nuevo parque eólico si los aerogeneradores son adecuadamente seleccionados de acuerdo con las características particulares del recurso eólico del emplazamiento y si las instalaciones de evacuación de energía son reutilizadas.

Los costes de desarrollo y construcción en su conjunto serán sensiblemente inferiores para el parque eólico repotenciado, aun teniendo en cuenta los costes de desmantelamiento de los antiguos aerogeneradores e instalaciones, ya que estos costes se verán reducidos de forma importante por los ingresos obtenidos en la valorización de los residuos del desmantelamiento.

Partiendo de parques eólicos con un recurso eólico superior a los recientemente construidos o a los emplazamientos disponibles actualmente, la repotenciación con nuevos aerogeneradores, más eficientes y tecnológicamente avanzados, ofrece aprovechamiento del recurso eólico con un alto grado de capacidad. Este hecho hace que un parque eólico repotenciado vendiendo su energía al precio del mercado spot ofrezca una rentabilidad similar, incluso mejor, que un parque eólico nuevo, con un factor de capacidad muy inferior, bajo el anterior sistema retributivo basado en *feed-in-tariff*.

La repotenciación dispone de un mercado actual (en el momento de elaboración del artículo) en torno a los 2,3 GW de potencia instalada con un periodo de operación igual o superior a 13 años. Este volumen se verá incrementado en los próximos años – a un ritmo en torno a 1 GW/año – a medida que el parque de generación vaya envejeciendo.

La rentabilidad está fuertemente condicionada por el precio de la energía, así que la estabilidad o posibilidad de predicción de la evolución de los precios spot puede condicionar la decisión de acometer la repotenciación. No obstante, existen soluciones que podrían ayudar a otorgar seguridad a los inversores en este aspecto: contratos bilaterales de venta de energía a consumidores o agentes comercializadores y productos ofrecidos por entidades aseguradoras para asegurar un suelo para el precio spot. Estas soluciones están siendo aplicadas con éxito en mercados emergentes para la financiación de plantas de energías renovables.

La repotenciación requiere de marcos regulatorios específicos, tanto técnicos como retributivos que podrían considerarse en futura legislación sectorial. Además, pueden tomarse medidas adicionales encaminadas a mejorar la rentabilidad sin que supongan un sobrecoste para el sistema eléctrico en su conjunto, facilitando el acceso al crédito financiero al inversor. Las medidas deberán estar enfocadas a proporcionar estabilidad a los ingresos y dar seguridad jurídica a largo plazo a la inversión, de esta forma las entidades financiadoras estarán más dispuestas a asumir deuda en acometer proyectos de repotenciación.

En resumen, la repotenciación se demuestra como una opción real y rentable para fomentar la integración de energías renovables en el mercado español. En la situación actual, debido a la falta de una regulación específica, un adecuado marco regulatorio habilitaría el desarrollo de un importante mercado con importantes expectativas de crecimiento a corto plazo.

Además, la electricidad producida por los parques eólicos repotenciados sería aportada al sistema eléctrico a precios de mercado spot, lo que implicará importantes ahorros para el sistema en su globalidad con respecto a los sistemas basados en *feed-in-tariff*, que en gran parte son aún aplicados a los parques eólicos actuales que serían aptos para su repotenciación.

5.2 Publicación 2: "*An assessment of photovoltaic potential in shopping centres*"

5.2.1 Resumen de la publicación

Resumen en español

La energía solar fotovoltaica es una fuente de energía renovable con un grado de madurez técnico-económico, que permite en muchos lugares la generación eléctrica a un precio comparable con los métodos térmicos convencionales. Aun así, aunque a finales de 2014 había 177 GW de potencia instalada en el mundo, el nivel de integración en el mix de generación eléctrica está aún lejos de los objetivos establecidos para esta tecnología en las estrategias de mitigación contra el calentamiento global.

Limitaciones técnicas, financieras y regulatorias impiden una penetración masiva de instalaciones fotovoltaicas, por lo que son necesarias medidas prácticas e innovadoras para facilitar su integración.

La integración de instalaciones fotovoltaicas en edificios es una solución eficiente, ya que la generación se produce cerca del punto de consumo y da un valor a los tejados y fachadas que antes no tenía.

En esta publicación se presenta una metodología, de aplicación científica para evaluar el potencial fotovoltaico de los centros comerciales, mediante la cual se puede afirmar que estos lugares ofrecen importantes ventajas para las instalaciones fotovoltaicas frente a otro tipo de edificaciones.

El potencial obtenido en los países considerados es de 16,8 GW, un 10% de la potencia instalada en 2014, con una generación anual de 22,7 TWh, un 14% de lo generado en 2014 mediante instalaciones fotovoltaicas.

Resumen en inglés

The solar photovoltaic is a renewable energy source which allows nowadays, in many places, the generation of electricity at a cost comparable with the conventional thermal generation methods. However, ending 2014, with a worldwide power capacity installed of 177 GW, the integration level in the electricity generation mix was still far from the targets set up for this technology in the global warming mitigation strategies.

Technical, financial and regulatory barriers slow down a massive penetration of photovoltaic generation facilities, hence practical and innovative measures are necessary to facilitate a wider deployment.

The building integration of solar photovoltaic facilities offers an efficient solution because the electricity is generated near the consumption point and gives a new economic value to roofs and facades. In this paper we develop a scientist methodology for determining the potential in shopping centres, to establish that, in terms of photovoltaic integration, these present important competitive advantages over other alternatives, i.e. the residential buildings. The power capacity potential obtained making use of this methodology in the countries selected is 16.8 GW, that means 10% of the worldwide capacity installed at the end of 2014, with a yearly electricity generation of 22.7 TW h equivalent to 14% of the worldwide generation in 2014.

5.2.2 Conclusiones de la publicación

La integración de instalaciones fotovoltaicas está aún muy lejos del cumplimiento de los objetivos determinados para esta tecnología para contribuir a la mitigación de las emisiones de gases de efecto invernadero responsables del cambio climático.

La implementación de energía solar fotovoltaica en edificios proporciona la posibilidad de instalar generación cerca de los consumos. En términos de integración en edificios, los centros comerciales son una de las mejores alternativas para la construcción de instalaciones solares fotovoltaicas en sus tejados ya que sus características constructivas hacen que, en igualdad de condiciones se pueda instalar hasta tres veces más potencia en centros comerciales que en edificios residenciales. No obstante, edificios destinados a otros usos, como colegios, hospitales o edificios industriales deberían ser objetivo de futura investigación enfocada a determinar su potencial.

Las instalaciones fotovoltaicas en centros comerciales pueden contribuir de forma relevante al cumplimiento de dichos objetivos, ya que el potencial fotovoltaico en términos de potencia instalada en los países considerados en este estudio es de 16,8 GW, equivalente al 10% de la potencia fotovoltaica total instalada en ellos a finales de 2014. Solo en US, donde en la actualidad hay instalados en torno a 325 MW en este tipo de edificios, se podrían instalar unos 11,8 GW, el 65% del total de potencia acumulada en ese país en 2014. Estas instalaciones supondrían la generación de 22,7 TWh al año, un 0,16 % de la generación total de dichos países y un 14% de la generación obtenida en 2014 mediante instalaciones fotovoltaicas.

Si se emplean para el autoconsumo, estas instalaciones fotovoltaicas podrían proporcionar una media del 7% de las necesidades de energía eléctrica, aunque en algunos países se podría alcanzar un grado de cobertura medio del 11%.

Por su ubicación territorial son también una buena elección para verter sus excedentes de energía a la red, ya que, al estar cerca de puntos de gran consumo, como ciudades o centros industriales, son lugares en los que la generación de energía eléctrica llegaría al consumo con menos pérdidas y, por tanto, de forma más eficiente.

La instalación del potencial fotovoltaico obtenido en el presente estudio evitaría el uso de más de 23.000 Ha de suelo (más que el área ocupada por las ciudades de Nueva York y Washington DC juntas).

5.3 Publicación 3: *"A hydrogen refuelling stations infrastructure deployment for cities supported on fuel cell taxi roll-out"*

5.3.1 Resumen de la publicación

Resumen en español

Un cambio hacia combustibles menos contaminantes y con baja huella de carbono es necesario para alcanzar la descarbonización del sector transporte que es responsable del 14% del total de emisiones.

Pese a ser vehículos con cero emisiones el uso de vehículos eléctricos propulsados por pilas de combustible de hidrógeno (*fuel cell electric vehicle – FCEV*) es actualmente residual con menos de 2.000 unidades en todo el mundo. Una integración masiva se enfrenta a un dilema del tipo "el huevo o la gallina": los vehículos necesitan de infraestructuras de repostaje que permitan el suministro continuo y seguro de hidrógeno, pero la implantación y puesta en operación de estas infraestructuras necesita el soporte de un mercado mínimo de vehículos para que su desarrollo sea rentable.

En el artículo correspondiente a esta publicación se determina una solución realizable para salvar el dilema e iniciar, en ciudades de gran población, una red de para el suministro de hidrógeno utilizando como mercado estable de vehículos la flota de taxis de la ciudad. El diseño de la red de estaciones de repostaje se basa en tres objetivos fundamentales: asegurar el suministro de hidrógeno, disponer en toda la ciudad alternativas cercanas para el repostaje y maximizar el uso de las infraestructuras.

Los resultados, aplicados a la ciudad de Madrid, determinan que con una asignación de fondos públicos de 415 millones de dólares a lo largo de 25 años sería posible disponer en seis años de una red de 112 estaciones de repostaje de hidrógeno capaz atender las necesidades de 15.000 nuevos vehículos propulsados por hidrógeno, evitando la emisión del entorno de 300 kt CO_2 al año.

<u>Resumen en inglés</u>

A shift towards lower-carbon fuels is mandatory to achieve the decarbonisation of the transport sector, which is responsible of 14% of world greenhouse gas emissions. Despite to the fact that fuel cell electric vehicles are zero tail-pipe emissions vehicles, their use is presently residual. A massive integration of fuel cell vehicles faces a "chicken-egg dilemma": vehicles need a proper refuelling infrastructure to provide a safe and continuous hydrogen supply, but a viable deployment of the refuelling infrastructure needs the support of an initial market of vehicles.

In this article, we design a feasible strategy for overcoming the dilemma, using the local taxi fleet as a stable market of hydrogen consumers to start up a retail hydrogen supply infrastructure in high populated cities. The design is based on three objectives: ensuring hydrogen supply, having throughout the city a nearby alternative for refuelling and maximizing the infrastructure utilisation rate.

The strategy applied to the city of Madrid show that $415 million of public funds allocated along 25 years would provide in six years a network of 112 hydrogen refuelling stations, able to supply the hydrogen needs of 15,000 new fuel cell electric taxis what would cut the emissions of 300 ktCO_2 yearly.

5.3.2 Conclusiones de la publicación

El objetivo esencial del artículo ha sido contribuir, con soluciones prácticas, a la implementación de estrategias de mitigación diseñadas para reducir de forma drástica las emisiones de gases de efecto invernadero para limitar el incremento de la temperatura media del planeta a 2 ˚C respecto de los niveles de la época preindustrial.

En este artículo se ha analizado si el desarrollo de una red de estaciones de repostaje de hidrógeno puede ser económicamente soportada en términos de rentabilidad por la sustitución de la flota de taxis de ciudades altamente pobladas por vehículos eléctricos propulsados por pila de hidrógeno., Como ejemplo para ilustrar los resultados obtenidos en el estudio se ha utilizado la ciudad de Madrid (España) que cuenta con unos 15.000 taxis

Esta línea del trabajo de investigación muestra que el desarrollo de una red de estaciones de repostaje de hidrógeno es técnica y económicamente viable con el apoyo de las autoridades gubernamentales de todos los niveles mediante la aplicación de políticas encaminadas a la promoción y el subsidio de las instalaciones.

En base a las hipótesis consideradas, el desarrollo de la red de estaciones de repostaje de hidrógeno solo sería posible con la asignación de fondos de forma prolongada en el tiempo en forma de subsidios aplicados (i) al coste de construcción, (ii) a los gastos de operación y (iii) a la exención de los impuestos. Dentro de las posibilidades de distribución de los fondos entre estos tres conceptos, se propone como solución óptima dedicar un porcentaje de subvención del 50% a los costes de construcción en el momento de iniciar la inversión y un 50% de los costes de operación y una exención del 50% de los impuestos a los beneficios durante 25 años. Este paquete de subsidios aseguraría una rentabilidad razonable del 10% anual durante los primeros 25 años de funcionamiento y permite el ajuste de los fondos asignados anualmente para compensar posibles variaciones de los parámetros que determinan la rentabilidad dentro de amplios límites de variación.

El importe total neto de los fondos dedicados al subsidio de las estaciones de repostaje de hidrógeno se estima en un total de $415 millones de valor actual a distribuir a lo largo de 25 años. Esta cantidad es fácilmente abarcable por los fondos destinados por organismos nacionales y supranacionales como el Gobierno Federal de los Estados Unidos o la Unión Europea. A título comparativo, el presupuesto para un solo año (2017) de la ciudad de Madrid es de cinco mil millones de euros.

La aplicación del modelo expuesto en el artículo a la ciudad de Madrid (España) permitiría disponer en seis años de una red de más 100 estaciones de repostaje de hidrógeno repartidas por toda la ciudad, en un radio máximo de 4 km desde cualquier punto. Esta infraestructura podría suministrar más de 15 Mkg de H_2 y atender las necesidades de 15.000 vehículos con un grado de utilización próximo al 75%, lo que permitiría atender las necesidades de hasta un 25% más de combustible con la misma infraestructura.

Para una ciudad altamente poblada, como la ciudad de Madrid, la sustitución de la flota de taxis, que representa alrededor del 1% de todos los vehículos de pasajeros de la ciudad, por vehículos eléctricos propulsados por pila hidrógeno, podría evitar la emisión en torno a 300 kt CO_2 al año, lo que supone más del 3% de las emisiones relacionadas con el transporte por carretera.

6 OTRAS APORTACIONES CIENTÍFICAS DERIVADAS DIRECTAMENTE DE LA TESIS DOCTORAL

Dentro del del trabajo de investigación de esta tesis doctoral se han abordado otras líneas de desarrollo encaminadas al objetivo fundamental de la investigación de encontrar soluciones para el desarrollo e integración de energía renovable que ayuden a materializar el cumplimiento de los objetivos de mitigación del cambio climático. El resultado de estas líneas de desarrollo se ha plasmado en la publicación en revistas científicas de dos artículos de investigación.

Un resumen de cada una de las publicaciones y los datos correspondientes a cada una de ellas se incluyen en los apartados siguientes.

6.1 Artículo "*Simplified Analysis of the Electric Power Losses for On-Shore Wind Farms Considering Weibull Distribution Parameters*"

6.1.1 Datos de la publicación

Los datos correspondientes a la publicación del artículo y la revista donde se ha publicado se detallan en la Tabla 7.

Tabla 7: Datos del artículo "*Simplified Analysis of the Electric Power Losses for On-Shore Wind Farms Considering Weibull Distribution Parameters*"

Datos sobre la publicación del trabajo científico	
Título de la publicación	*Simplified Analysis of the Electric Power Losses for On-Shore Wind Farms Considering Weibull Distribution Parameters*
Autores	1. Antonio Colmenar Santos (Director de la tesis). Afiliación (1) 2. Severo Campíñez Romero (Doctorando). Afiliación (1) 3. Lorenzo Alfredo Enríquez García. Afiliación (2) 4. Clara Pérez Molina. Afiliación (1)
Afiliación de los autores	(1) Departamento de Ingeniería Eléctrica, Electrónica y de Control de la Escuela Técnica Superior de Ingenieros Industriales de la UNED (2) Escuela Superior Politécnica de Chimborazo, Riobamba – Chimborazo, Ecuador
Revista	*Energies*
Estado de publicación	Publicado el 28 de octubre de 2014

D.O.I.	10.3390/en7116856	
Índices de impacto *Journal Citation Reports* de la revista en el año 2018 (último índice publicado)		
Categoría	*Energy&Fuels*	
Índice de impacto	2,707	
Quartil	Q3	
Índices de impacto *Scopus* de la revista en el año 2018 (último índice publicado)		
CiteScore 2018 All publication types	3,18	
SCImago Journal Rank (SJR)	0,612	
Source Normalized Impact per Paper (SNIP)	1,156	
CiteScore rank and Percentile per category	***CiteScore rank***	***Percentile***
Energy: Energy (miscellaneous)	4/19	81
Energy: Energy Engineering and Power Technology	42/197	78
Energy: Renewable Energy, Sustainability and the Environment	56/153	63
Engineering: Electrical and Electronic Engineering	122/661	81

6.1.2 Resumen de la publicación

Las pérdidas eléctricas están presentes constantemente durante toda la vida útil de un parque eólico y deben considerarse en el cálculo de los ingresos por venta de energía. Para su estimación se ha venido utilizando el valor calculado para el funcionamiento a plena potencia. Durante la fase de operación es necesario establecer algún método para comprobar que efectivamente el nivel de pérdidas reales está dentro del funcionamiento requerido. En el presente estudio se demuestra que no se puede utilizar el valor de las pérdidas a plena potencia como referencia para comprobar el funcionamiento del parque, y se determinará un método simplificado para analizar y predecir las pérdidas reales en función de las características de las infraestructuras eléctricas y el potencial eólico en el periodo considerado caracterizado según la distribución de Weibull. Esta metodología facilita un método sencillo para determinar a priori y comprobar posteriormente el nivel real de pérdidas.

Copia de la publicación se adjunta como Anexo X.

6.2 Artículo *"Evaluation of Supply–Demand Adaptation of Photovoltaic–Wind Hybrid Plants Integrated into an Urban Environment"*

6.2.1 Datos de la publicación

Los datos correspondientes a la publicación del artículo y la revista dónde se ha publicado se detallan en la Tabla 8.

Tabla 8: Datos del artículo *"Evaluation of Supply–Demand Adaptation of Photovoltaic–Wind Hybrid Plants Integrated into an Urban Environment"*

Datos sobre la publicación del trabajo científico		
Título de la publicación	*Evaluation of Supply–Demand Adaptation of Photovoltaic–Wind Hybrid Plants Integrated into an Urban Environment*	
Autores	1. África Lopez Rey (Co-Directora de la tesis) 2. Severo Campíñez Romero (Doctorando) 3. Rosario Gil Ortego 4. Antonio Colmenar Santos (Director de la tesis)	
Afiliación de los autores	Departamento de Ingeniería Eléctrica, Electrónica y de Control de la Escuela Técnica Superior de Ingenieros Industriales de la UNED	
Revista	*Energies*	
Estado de publicación	Publicado el 10 de mayo de 2019	
D.O.I.	10.3390/en12091780	
Índices de impacto *Journal Citation Reports* de la revista en el año 2017 (último índice publicado)		
Categoría	*Energy&Fuels*	
Índice de impacto	2,707	
Quartil	Q3	
Índices de impacto *Scopus* de la revista en el año 2018 (último índice publicado)		
CiteScore 2018 All publication types	3,18	
SCImago Journal Rank (SJR)	0,612	
Source Normalized Impact per Paper (SNIP)	1,156	
CiteScore rank and Percentile per category	***CiteScore rank***	***Percentile***
Energy: Energy (miscellaneous)	4/19	81
Energy: Energy Engineering and Power Technology	42/197	78
Energy: Renewable Energy, Sustainability and the Environment	56/153	63

CiteScore rank and Percentile per category	***CiteScore rank***	***Percentile***
Engineering: Electrical and Electronic Engineering	122/661	81

6.2.2 Resumen de la publicación

La integración masiva de fuentes de energía renovable es imperativa para cumplir los objetivos de reducción de las emisiones de gases de efecto invernadero establecidos para conseguir la limitación del calentamiento global.

No obstante, los niveles de integración actuales de estas tecnologías están muy lejos de los objetivos siendo una de las razones fundamentales las barreras técnicas derivadas de su carácter no gestionable. Las tecnologías fotovoltaica y eólica son las más extendidas y su grado de madurez permite la generación con un alto grado de eficiencia. Conocer en detalle las pautas de funcionamiento de las instalaciones y, especialmente, su grado de aportación a la demanda, es necesario para reducir los costes de integración y extender los límites técnicos y favorecer su integración.

En el artículo correspondiente a esta línea de investigación se presenta una metodología para analizar en qué medida las instalaciones híbridas fotovoltaicas – eólicas en el entorno urbano, presentan pautas de generación que se adaptan mejor a los perfiles de consumo que si las instalaciones se consideran de forma individual.

La metodología se ha aplicado a un gran número de localizaciones repartidas por todo el planeta. Los resultados indican que, con un alto grado de homogeneidad en todo el planeta en relación con las condiciones climáticas de la localización de las instalaciones, la adaptación de las instalaciones híbridas mejora hasta en un 15% la de las instalaciones fotovoltaicas y hasta un 35% la de las instalaciones eólicas.

Copia de la publicación se adjunta como Anexo XI.

7 CONCLUSIONES

El objetivo de la tesis doctoral ha sido el de encontrar alternativas prácticas y realizables para favorecer la integración efectiva de una cantidad masiva de fuentes de energía de origen renovable en diversos sectores productivos y actividades del ser humano, ofreciendo soluciones viables para salvar las barreras que puedan limitar dicha integración. Del resultado obtenido en cada una de las líneas de desarrollo del trabajo de investigación, puede afirmarse que el objetivo fundamental de la tesis doctoral se ha conseguido porque:

1. Se han encontrado soluciones prácticas y realizables para favorecer la integración efectiva de una cantidad masiva de fuentes de energía renovable en el consumo energético (cada una de las cuales se corresponde con una de las tres publicaciones que forman el compendio de esta tesis).
2. Las soluciones encontradas están totalmente alineadas con las estrategias de mitigación del cambio climático establecidas por los distintos organismos gubernamentales y la comunidad científica.
3. Están enfocadas en la integración de las energías renovables en tres sectores o ámbitos de actividad humana que son grandes productores de emisiones de gases de efecto invernadero.
4. Las soluciones propuestas afectan a varios sectores y tienen un ámbito global y son susceptibles de ser aplicadas en múltiples territorios, países, etc.
5. Las propuestas de implementación de energías renovables, basadas en los resultados de las distintas líneas de desarrollo acometidas dentro del trabajo de investigación, son novedosas y robustas, por tanto, su aplicación es viable en un amplio espectro de las hipótesis y variables involucradas.
6. Se han identificado las barreras técnicas, regulatorias y financieras que pudieran limitar la implementación de dichas alternativas y se han dado soluciones para salvar dichas barreras.
7. Se han analizado las posibilidades de financiación de cada una de las soluciones propuestas y, cuando se ha demostrado su necesidad como única alternativa para soportar su implementación, se han definido subsidios para favorecer su integración.

Si se analiza cada una de las soluciones resultantes del trabajo de investigación:

1. En el sector de la generación de energía eléctrica, responsable en 2010 del 25% de las emisiones de gases de efecto invernadero, la investigación se ha centrado en la repotenciación de parques eólicos. Así, se ha concluido que, en determinadas condiciones, la inversión en la repotenciación de parques eólicos puede ser más rentable que la construcción de uno nuevo. Solo en España, en el momento del estudio, existía un mercado para la repotenciación en torno a los 2,3 GW con estimaciones de crecimiento anual en torno a 1 GW/año. La repotenciación se demuestra como una opción real y rentable, de aplicación a un mercado amplio, para fomentar la integración de energías renovables en un sistema eléctrico con altas tasas de integración, como el español.
2. En el ámbito de los edificios, que en 2010 aportaban el 6,4% de las emisiones, se ha determinado que los centros comerciales presentan un potencial fotovoltaico en términos de potencia instalada, en los países considerados en el estudio, es de 16,8 GW, equivalente al 10% de la potencia fotovoltaica total instalada en dichos países a finales de 2014. Estas instalaciones aportarían en torno 22,7 TWh y podrían cubrir una parte importante del consumo propio de los centros comerciales, contribuyendo de esta manera a la integración de renovables en estas edificaciones, haciéndolas más eficientes.
3. Por último, en el sector del transporte, con unas emisiones que en 2010 suponían el 14% del total, se ha diseñado una solución práctica para sostener el desarrollo de una red de estaciones de repostaje de hidrógeno en grandes ciudades, basada en el uso de la flota de taxis de la ciudad. Para que esta solución sea financieramente realizable y sostenible, se han diseñado un paquete de subsidios gubernamentales con un bajo coste para los presupuestos públicos. Además de fomentar la integración de renovables en el sector del transporte, esta medida conllevaría una reducción importante en la emisión de otros tipos de contaminantes al cambiar el uso de combustibles fósiles por hidrógeno.

La implementación de todas estas medidas contribuiría en gran medida a la reducción de las emisiones de gases de efecto invernadero y, por tanto, al cumplimiento del objetivo último de limitar el calentamiento global del planeta, origen del cambio climático que vivimos, y mitigar los riesgos derivados de dicho cambio.

No obstante, aún se está lejos de cumplir con los objetivos que se han marcado encaminados a limitar el incremento de la temperatura media del planeta a 2 °C respecto de la era preindustrial, por lo que la sociedad en su conjunto debe continuar en la implementación de las estrategias de mitigación del cambio climático. En este trabajo, y en línea con las diversas soluciones propuestas en la presente tesis, se pueden proponer **nuevas líneas de investigación** enfocadas a:

- Conseguir una descarbonización total del sector eléctrico, mediante la implantación de un mix de generación eléctrica compuesto únicamente por fuentes de energía renovable con sistemas de bombeo y almacenamiento y adecuados sistemas de gestión que permitan garantizar la calidad y seguridad en el suministro eléctrico
- La transición del sector del transporte al uso de combustibles no contaminantes, como el hidrógeno, extendiendo su uso a los transportes pesados y la aviación, donde hasta ahora no ha habido avances en este sentido.
- La implantación de soluciones técnicas y de regulación específica que aporte seguridad jurídica para facilitar que los consumidores puedan generar su propia energía y ceder los excedentes a la red eléctrica. Esta regulación tendría un papel determinante en el ámbito de la integración de renovables en edificios de todo uso (residencia, terciario, servicios, etc.) porque son lugares que presentan posibilidades de instalación de renovables, especialmente solar térmica y fotovoltaica, en fachadas, tejados, etc., y su proximidad al punto de consumo les proporciona una localización óptima desde el punto de vista de la eficiencia.

8 REFERENCIAS

1. Organización Meteorologica Mundial. *WMO Statement on the State of the Global Climate in 2018*; WMO-No. 1233; Geneva, Switzerland, 2019.
2. Organización Meteorologica Mundial. European heatwave sets new temperature records. Availabe online: https://public.wmo.int/en/media/news/european-heatwave-sets-new-temperature-records (accessed on 06/07/2019).
3. *Climate Change 2013: The Physical Science Basis. Contribution of Working Group I to the Fifth Assessment Report of the Intergovernmental Panel on Climate Change*; United Kingdom and New York, NY, USA, 2013; p 1552.
4. *Climate Change 2014: Synthesis Report. Contribution of Working Groups I, II and III to the Fifth Assessment Report of the Intergovernmental Panel on Climate Change*; Geneva, Switzerland, 2014; p 151.
5. United Nations Environment Programme. *Emissions Gap Report 2018*; Nairobi, 2018; p 112.
6. *Climate Change 2014: Mitigation of Climate Change. Contribution of Working Group III to the Fifth Assessment Report of the Intergovernmental Panel on Climate Change*; United Kingdom and New York, NY, USA, 2013; p 1454.
7. United Nations. UN Climate Change Conference Paris 2015. Availabe online: http://www.un.org/sustainabledevelopment/cop21/ (accessed on 9/7/2016).
8. United Nations Framework Convention on Climate Change. . Availabe online: http://unfccc.int/2860.php (accessed on 5/7/2016).
9. United Nations Treaty Collection. Paris Agreement. Availabe online: https://treaties.un.org/pages/ViewDetails.aspx?src=TREATY&mtdsg_no=XXVII-7-d&chapter=27&lang=en (accessed on 9/7/2016).
10. Jefatura del Estado. Gobierno de España. Ley 54/1997, de 27 de noviembre, del Sector Eléctrico. 1997.
11. Jefatura del Estado. Gobierno de España. Ley 24/2013, de 26 de diciembre, del Sector Eléctrico. 2013.
12. del Río, P.; Gual, M.A. An integrated assessment of the feed-in tariff system in Spain. *Energy Policy* **2007**, *35*, 994-1012, doi:10.1016/j.enpol.2006.01.014.
13. Ciarreta, A.; Gutiérrez-Hita, C.; Nasirov, S. Renewable energy sources in the Spanish electricity market: Instruments and effects. *Renewable and Sustainable Energy Reviews* **2011**, *15*, 2510-2519, doi:10.1016/j.rser.2011.01.023.
14. Schallenberg-Rodriguez, J.; Haas, R. Fixed feed-in tariff versus premium: A review of the current Spanish system. *Renewable and Sustainable Energy Reviews* **2012**, *16*, 293-305, doi:10.1016/j.rser.2011.07.155.
15. Iglesias, G.; del Río, P.; Dopico, J.Á. Policy analysis of authorisation procedures for wind

energy deployment in Spain. *Special Section: Renewable energy policy and development* **2011**, *39*, 4067-4076, doi:10.1016/j.enpol.2011.03.033.

16. Red Eléctrica de España S.A. *El mercado eléctrico español en 2012*; 2013.
17. Ministerio de Industria Energía y Turismo. Gobierno de España. *La energía en España 2011*; 2012.
18. Burgos-Payán, M.; Roldán-Fernández, J.M.; Trigo-García, Á.L.; Bermúdez-Ríos, J.M.; Riquelme-Santos, J.M. Costs and benefits of the renewable production of electricity in Spain. *Energy Policy* **2013**, *56*, 259-270, doi:10.1016/j.enpol.2012.12.047.
19. Gil, H.A.; Gomez-Quiles, C.; Riquelme, J. Large-scale wind power integration and wholesale electricity trading benefits: Estimation via an ex post approach. *Modeling Transport (Energy) Demand and Policies* **2012**, *41*, 849-859, doi:10.1016/j.enpol.2011.11.067.
20. Rivier Abbad, J. Electricity market participation of wind farms: the success story of the Spanish pragmatism. *Large-scale wind power in electricity markets with Regular Papers* **2010**, *38*, 3174-3179, doi:10.1016/j.enpol.2009.07.032.
21. Jefatura del Estado. Gobierno de España. Real Decreto-Ley 1/2012 de 27 de enero, por el que se procede a la suspensión de los procedimientos de preasignación de retribución y a la supresión de los incentivos económicos para nuevas instalaciones de producción de energía eléctrica. 2012.
22. Idae. Ministerio de Industria Turismo y Comercio. Gobierno de España. *Plan de Energías Renovables 2011-2020*; 2011.
23. Ruiz Romero, S.; Colmenar Santos, A.; Castro Gil, M.A. EU plans for renewable energy. An application to the Spanish case. *Renewable Energy* **2012**, *43*, 322-330, doi:10.1016/j.renene.2011.11.033.
24. Colmenar-Santos, A.; Campíñez-Romero, S.; Pérez-Molina, C.; Castro-Gil, M. Profitability analysis of grid-connected photovoltaic facilities for household electricity self-sufficiency. *Renewable Energy in China* **2012**, *51*, 749-764, doi:10.1016/j.enpol.2012.09.023.
25. Ruiz-Romero, S.; Colmenar-Santos, A.; Gil-Ortego, R.; Molina-Bonilla, A. Distributed generation: The definitive boost for renewable energy in Spain. *Renewable Energy* **2013**, *53*, 354-364, doi:10.1016/j.renene.2012.12.010.
26. Toja-Silva, F.; Colmenar-Santos, A.; Castro-Gil, M. Urban wind energy exploitation systems: Behaviour under multidirectional flow conditions—Opportunities and challenges. *Renewable and Sustainable Energy Reviews* **2013**, *24*, 364-378, doi:10.1016/j.rser.2013.03.052.
27. Ortegon, K.; Nies, L.F.; Sutherland, J.W. Preparing for end of service life of wind turbines. *Journal of Cleaner Production* **2013**, *39*, 191-199, doi:10.1016/j.jclepro.2012.08.022.
28. del Río, P.; Calvo Silvosa, A.; Iglesias Gómez, G. Policies and design elements for the repowering of wind farms: A qualitative analysis of different options. *Energy Policy* **2011**, *39*, 1897-1908, doi:10.1016/j.enpol.2010.12.035.

29. Intergovernmental Panel on Climate Change. *Special Report on Renewable Energy Sources and Climate Change Mitigation*; Cambridge University Press: United Kingdom and New York, NY, USA, 2011.

30. Hernández-Moro, J.; Martínez-Duart, J.M. Analytical model for solar PV and CSP electricity costs: Present LCOE values and their future evolution. *Renewable and Sustainable Energy Reviews* **2013**, *20*, 119-132, doi:10.1016/j.rser.2012.11.082.

31. Ossenbrink, H.; Huld, T.; Jäger Waldau, A.; Taylor, N. *Photovoltaic Electricity Cost Maps*; JRC 83366; 2013.

32. Philipps, S.P.; Kost, C.; Schlegl, S. *Up-to-date levelised cost of electricity of photovoltaics*; Fraunhofer Institute for Solar Energy Systems ISE: 2014.

33. Ondraczek, J.; Komendantova, N.; Patt, A. WACC the dog: The effect of financing costs on the levelized cost of solar PV power. *Renewable Energy* **2015**, *75*, 888-898, doi:10.1016/j.renene.2014.10.053.

34. Feldman, D.; Margolis, R.; Boff, D. *Q2/Q3 '14 Solar Industry Update*; U.S. Department of Energy: 2014.

35. Lazard. *Levelized Cost of Energy v11*; 2017; p 22.

36. Karteris, M.; Slini, T.; Papadopoulos, A.M. Urban solar energy potential in Greece: A statistical calculation model of suitable built roof areas for photovoltaics. *Energy and Buildings* **2013**, *62*, 459-468, doi:10.1016/j.enbuild.2013.03.033.

37. Li, D.; Liu, G.; Liao, S. Solar potential in urban residential buildings. *Solar Energy* **2015**, *111*, 225-235, doi:10.1016/j.solener.2014.10.045.

38. Ordóñez, J.; Jadraque, E.; Alegre, J.; Martínez, G. Analysis of the photovoltaic solar energy capacity of residential rooftops in Andalusia (Spain). *Renewable and Sustainable Energy Reviews* **2010**, *14*, 2122-2130, doi:10.1016/j.rser.2010.01.001.

39. Defaix, P.R.; van Sark, W.G.J.H.M.; Worrell, E.; de Visser, E. Technical potential for photovoltaics on buildings in the EU-27. *Solar Energy* **2012**, *86*, 2644-2653, doi:10.1016/j.solener.2012.06.007.

40. Izquierdo, S.; Rodrigues, M.; Fueyo, N. A method for estimating the geographical distribution of the available roof surface area for large-scale photovoltaic energy-potential evaluations. *Solar Energy* **2008**, *82*, 929-939, doi:10.1016/j.solener.2008.03.007.

41. Peng, J.; Lu, L. Investigation on the development potential of rooftop PV system in Hong Kong and its environmental benefits. *Renewable and Sustainable Energy Reviews* **2013**, *27*, 149-162, doi:10.1016/j.rser.2013.06.030.

42. Pillai, I.R.; Banerjee, R. Methodology for estimation of potential for solar water heating in a target area. *Solar Energy* **2007**, *81*, 162-172, doi:10.1016/j.solener.2006.04.009.

43. Schallenberg-Rodriguez, J. Photovoltaic techno-economical potential on roofs in regions and

islands: The case of the Canary Islands. Methodological review and methodology proposal. *Renewable and Sustainable Energy Reviews* **2013**, *20*, 219-239, doi:10.1016/j.rser.2012.11.078.

44. Singh, R.; Banerjee, R. Estimation of rooftop solar photovoltaic potential of a city. *Solar Energy* **2015**, *115*, 589-602, doi:10.1016/j.solener.2015.03.016.

45. Wiginton, L.K.; Nguyen, H.T.; Pearce, J.M. Quantifying rooftop solar photovoltaic potential for regional renewable energy policy. *Computers, Environment and Urban Systems* **2010**, *34*, 345-357, doi:10.1016/j.compenvurbsys.2010.01.001.

46. Denholm, P.M., Robert. *Supply Curves for Rooftop Solar PV-Generated Electricity for the United States*; NREL/TP-6A0-44073; National Renewable Energy Laboratory: 2008.

47. International Energy Agency. *Technology Roadmap Solar Photovoltaic Energy. 2014 Edition*; Paris, France, 2014; p 20.

48. Luthander, R.; Widén, J.; Nilsson, D.; Palm, J. Photovoltaic self-consumption in buildings: A review. *Appl. Energy* **2015**, *142*, 80-94, doi:10.1016/j.apenergy.2014.12.028.

49. Barth, B.; Concas, G.; Binda Zane, E.; Franz, O.; Frías, P.; Hermes, R.; Lama, R.; Loew, H.; Mateo, C.; Rekinger, M., et al. *PV GRID. Final project report*; August 2014, 2014; p 52.

50. Mai, T.; Wiser, R.; Sandor, D.; Brinkman, G.; Heath, G.; Denholm, P.; Hostick, D.J.; Darghouth, N.; Schlosser, A.; Strzepek, K. *Exploration of High-Penetration Renewable Electricity Futures*; NREL/TP-6A20-52409-1; Golden, CO, 2012.

51. Stetz, T.; Rekinger, M.; Theologitis, I. *Transition from uni directional to bi directional distribution grids. Management summary of IEA Task 14 Subtask 2 - Recommendations based on Golbal Experience*; IEA PVPS Task 14:03-2014; September, 2014, 2014.

52. International Energy Agency. *Energy, Climate Change and Environment 2016 Insights*; Paris, France, 2016; p 133.

53. The United States Environmental Protection Agency. Greenhouse Gas Inventory Data Explorer,. Availabe online: https://www3.epa.gov/climatechange/ghgemissions/inventoryexplorer/ (accessed on 02/02/2017).

54. European Environmental Agency. Greenhouse gas emissions from transport. Availabe online: http://www.eea.europa.eu/data-and-maps/indicators/transport-emissions-of-greenhouse-gases/transport-emissions-of-greenhouse-gases-6 (accessed on 15/01/2017).

55. Sims, R.; Schaeffer, R.; Creutzig, F.; Cruz-Núñez, X.; D'Agosto, M.; Dimitriu, D.; Figueroa Meza, M.J.; Fulton, L.; Kobayashi, S.; Lah, O., et al. *Transport. In: Climate Change 2014: Mitigation of Climate Change. Contribution of Working Group III to the Fifth Assessment Report of the Intergovernmental Panel on Climate Change*; Cambridge United Kingdom and New York, NY, USA, 2014; p 72.

56. United States Department of Transportation. National Highway Traffic Safety Administration. Availabe online: https://www.nhtsa.gov/ (accessed on 28/01/2017).

57. The United States Environmental Protection Agency. Vehicles and Engines. Availabe online: https://www.epa.gov/vehicles-and-engines (accessed on 28/10/2017).

58. The United States Environmental Protection Agency. Renewable Fuel Standard Program. Availabe online: https://www.epa.gov/renewable-fuel-standard-program (accessed on 05/02/2017).

59. European Climate Foundation. *Roadmap 2050: a practical guide to a prosperous, low carbon Europe*; The Hague, The Netherlands, 2010.

60. European Comission. European Commission. European Structural & Investment Funds. Data. Availabe online: https://cohesiondata.ec.europa.eu/themes/4 (accessed on 28/12/2017).

61. European Commission. Directorate-General for Research and Innovation. HORIZON 2020. The EU Framework Programme for Research and Innovation. Smart, Green and Integrated Transport. Availabe online: https://ec.europa.eu/programmes/horizon2020/en/h2020-section/smart-green-and-integrated-transport (accessed on 08/02/2017).

62. International Energy Agency. *World Energy Outlook 2016. Executive Summary*; Paris, France, 2016; p 13.

63. International Energy Agency. *Key World Energy Statistics 2016*; Paris, France, 2016; p 80.

64. International Energy Agency. *Global EV Outlook 2019*; Paris, France, 2019.

65. International Energy Agency. *Technology Roadmap Hydrogen and Fuel Cells. 2013 Edition*; Paris, France, 2013; p 81.

66. Alazemi, J.; Andrews, J. Automotive hydrogen fuelling stations: An international review. *Renewable and Sustainable Energy Reviews* **2015**, *48*, 483-499, doi:10.1016/j.rser.2015.03.085.

67. Ramsden, T.; Ruth, M.; Diakov, V.; Laffen, M.; Timbario, T.A. *Hydrogen Pathways: Updated Cost, Well-to-Wheels Energy Use, and Emissions for the Current Technology Status of Ten Hydrogen Production, Delivery, and Distribution Scenarios*; NREL/TP-6A10-60528 United States 10.2172/1107463 NREL English; ; National Renewable Energy Laboratory (NREL), Golden, CO.: 2013; p Medium: ED; Size: 268 pp.

68. Sgobbi, A.; Nijs, W.; De Miglio, R.; Chiodi, A.; Gargiulo, M.; Thiel, C. How far away is hydrogen? Its role in the medium and long-term decarbonisation of the European energy system. *International Journal of Hydrogen Energy* **2016**, *41*, 19-35, doi:10.1016/j.ijhydene.2015.09.004.

69. Fuel Cells and Hydrogen Joint Undertaking. *A portfolio of power-trains for Europe: a fact-based analysis. The role of Battery Electric Vehicles, Plug-in Hybrids and Fuel Cell Electric Vehicles*; 2010.

70. The US Department of Energy. Office of Energy Efficiency & Renewable Energy. *Hydrogen and Fuel Cells Program Plan*; 2011.

71. Melaina, M.; Sun, Y.; Bush, B. *Retail Infrastructure Costs Comparison for Hydrogen and Electricity for Light-Duty Vehicles: Preprint*; ; National Renewable Energy Laboratory (NREL), Golden,

CO.: 2014; pp. Medium: ED; Size: 14 pp.

72. European Commission. Directorate-General for Research and Innovation. *HyWays. The European hydrogen roadmap*; EUR 23123; Luxembourg, 2008.

73. McKinney, J.; Bond, É.; Crowell, M.; Odufuwa, E. *Joint Agency Staff Report on Assembly Bill 8: Assessment of Time and Cost Needed to Attain 100 Hydrogen Refueling Stations in California*; CEC-600-2015-016.; California Energy Commission: 2015.

74. Bush, B.; Melaina, M. *National FCEV and Hydrogen Fueling Station Scenarios*; ; NREL (National Renewable Energy Laboratory (NREL), Golden, CO (United States)): 2016; pp. Medium: ED; Size: 2.3 MB.

75. European Alternative Fuels Observatory. Availabe online: http://www.eafo.eu/ (accessed on 05/07/2019).

76. Office of Transportation and Air Quality. U.S. Environmental Protection Agency. Compare Fuel Cell Vehicles. Availabe online: http://www.fueleconomy.gov/feg/fcv_sbs.shtml (accessed on 01/07/2019).

77. The United States Environmental Protection Agency. *Model Year 2018 Fuel Economy Guide: EPA Fuel Economy Estimates*; DOE/EE-1653; Other: 7798 United States Other: 7798 EE-LIBRARY English; ; U. S. Department of Energy, Washington, D.C.; U.S. Environmental Protection Agency, Washington, D.C.: 2017; p Medium: ED; Size: 49.

78. Curtin, S.; Gangi, J. *Fuel Cell Technologies Market Report 2015*; DOE/EE1485; ; NREL (National Renewable Energy Laboratory (NREL), Golden, CO (United States)): 2016.

79. Davis, S.C.; Williams, S.E.; Boundy, R.G.; Moore, S. *2015 Vehicle Technologies Market Report*; ORNL/TM--2016/142; Other: VT0505000; VT1202000; CEVT001 United States 10.2172/1255689 Other: VT0505000; VT1202000; CEVT001 ORNL English; ; Oak Ridge National Lab. (ORNL), Oak Ridge, TN (United States): 2016; p Medium: ED; Size: 216 p.

80. Colmenar-Santos, A.; Alberdi-Jiménez, L.; Nasarre-Cortés, L.; Mora-Larramona, J. Residual heat use generated by a 12 kW fuel cell in an electric vehicle heating system. *Energy* **2014**, *68*, 182-190, doi:10.1016/j.energy.2014.02.092.

81. Parks, G.; Boyd, R.; Cornish, J.; Remick, R. *Hydrogen Station Compression, Storage, and Dispensing Technical Status and Costs: Systems Integration*; NREL/BK-6A10-58564 United States 10.2172/1130621 NREL English; ; National Renewable Energy Laboratory (NREL), Golden, CO.: 2014; p Medium: ED; Size: 74 pp.

82. Sprik, S.; Kurtz, J.; Ainscough, C.; Jeffers, M.; Saur, G.; Peters, M. *Hydrogen Station Data Collection and Analysis*; Project ID TV017; ; NREL (National Renewable Energy Laboratory (NREL), Golden, CO (United States)): 2016.

83. National Renewable Energy Laboratory. Fuel Cell and Hydrogen Technology Validation. Availabe online: http://www.nrel.gov/hydrogen/proj_tech_validation.html (accessed on 01/12/2016).

84. International Partnership for Hydrogen and Fuel Cells in the Economy. IPHE Partners. Japan. Availabe online: http://www.iphe.net/partners/japan.html (accessed on 09/02/2017).

85. netinform. Hydrogen Filling Stations Worldwide. Availabe online: http://www.netinform.net/h2/H2Stations/Default.aspx (accessed on 01-02-2017).

86. Ogden, J.M.; Yang, C.; A. Nicholas, M.; Lewis, F. *NextSTEPS White Paper: The Hydrogen Transition*; UCD-ITS-RR-14-11; Institute of Transportation Studies, University of California, Davis,: 2014; p 57.

87. Roland Berger Strategy Consultants GmbH. *A roadmap for financing hydrogen refueling networks – Creating prerequisites for H2-based mobility*; Fuel Cells and Hydrogen Joint Undertaking,: 2013; p 102.

88. Dagdougui, H.; Ouammi, A.; Sacile, R. Modelling and control of hydrogen and energy flows in a network of green hydrogen refuelling stations powered by mixed renewable energy systems. *International Journal of Hydrogen Energy* **2012**, *37*, 5360-5371, doi:10.1016/j.ijhydene.2011.07.096.

89. Kim, J.-G.; Kuby, M. The deviation-flow refueling location model for optimizing a network of refueling stations. *International Journal of Hydrogen Energy* **2012**, *37*, 5406-5420, doi:10.1016/j.ijhydene.2011.08.108.

90. Agnolucci, P. Hydrogen infrastructure for the transport sector. *International Journal of Hydrogen Energy* **2007**, *32*, 3526-3544, doi:10.1016/j.ijhydene.2007.02.016.

91. Melaina, M.W. Initiating hydrogen infrastructures: preliminary analysis of a sufficient number of initial hydrogen stations in the US. *International Journal of Hydrogen Energy* **2003**, *28*, 743-755, doi:10.1016/S0360-3199(02)00240-9.

92. Government of the United Kingdom. Office for National Statistics. Overview of the UK population: February 2016. Availabe online: https://www.ons.gov.uk/peoplepopulationandcommunity/populationandmigration/populationestimates/articles/overviewoftheukpopulation/february2016 (accessed on 05/02/2017).

93. Kingdom., G.o.t.U. National Statistics. Vehicle licensing statistics: 2015. Availabe online: https://www.gov.uk/government/statistics/vehicle-licensing-statistics-2015 (accessed on 05/02/2017).

94. Kingdom., G.o.t.U. National Statistics. Taxi and private hire vehicles statistics, England: 2015. Availabe online: https://www.gov.uk/government/statistics/taxi-and-private-hire-vehicles-statistics-england-2015 (accessed on 05/02/2017).

95. City of New York. Department of City Planning. NYC population. Availabe online: https://www1.nyc.gov/site/planning/data-maps/nyc-population/current-future-populations.page (accessed on 09/02/2017).

96. New York City. Taxi & Limousine Comission. *2014 Taxicab Fact Book,*; 2014.

97. New York State. Department of Motor Vehicles. Statistical Summaries. Availabe online:

https://dmv.ny.gov/about-dmv/statistical-summaries (accessed on 02/01/2017).

98. Ayuntamiento de Madrid. Portal de datos abiertos. Taxi: Situación y Gestión,. Availabe online: http://datos.madrid.es/portal/site/egob/menuitem.c05c1f754a33a9fbe4b2e4b284f1a5a0/?vgnextoid=4f16216612d39410VgnVCM2000000c205a0aRCRD&vgnextchannel=374512b9ace9f310VgnVCM100000171f5a0aRCRD (accessed on 01/02/2017).

99. Instituto de Estadística de la Comunidad de Madrid. Anuario Estadístico de la Comunidad de Madrid. 1985-2017. Transportes y comunicaciones. Availabe online: http://www.madrid.org/iestadis/fijas/estructu/general/anuario/ianucap09.htm (accessed on 01/02/2017).

100. Instituto de Estadística de la Comunidad de Madrid. Población oficial por Comunidades Autónomas, provincias, capitales y municipios de la Comunidad de Madrid. Availabe online: (accessed on 01/02/2017).

101. Dirección General de Trafico. Ministerio del Interior del Gobierno de España. Seguridad vial. Estadísticas e indicadores. Parque de vehículos. Availabe online: http://www.dgt.es/es/seguridad-vial/estadisticas-e-indicadores/parque-vehiculos/ (accessed on 01/02/2017).

9 CURRICULUM VITAE DEL DOCTORANDO

Formación académica

- MÁSTER UNIVERSITARIO EN INVESTIGACIÓN en Ingeniería Eléctrica, Electrónica y de Control Industrial en la Universidad de Educación a Distancia (UNED) (2014).
- INGENIERO INDUSTRIAL en la Universidad de Educación a Distancia (UNED) en las especialidades de Electrónica y Automática e Ingeniería Eléctrica (2006-2011).
- INGENIERO TÉCNICO INDUSTRIAL en la especialidad de Electrónica Industrial en el Instituto Católico de Artes e Industrias (ICAI) de la Universidad Pontificia Comillas (1989-1992).

Experiencia profesional

- Octubre 2017 – Actualidad. Director de Desarrollo de Negocio de Alfanar Energía España.
- Septiembre 2011– octubre 2017: Jefe del Departamento de Energía Eólica. Isolux Ingeniería, S.A.
- Abril 2009 – septiembre 2011: Director de Ingeniería y Desarrollo de Negocio Cobián tecnología electromecánica y de control, S.L.
- Marzo 2005 – marzo 2009: Director del Área Eólica en Instituto de Energías Renovables, S.L.
- Julio 2000 - febrero 2005: Jefe del Área de Gestión de Proyectos y Puesta en Servicio en Made Tecnologías Renovables, S.A. (Grupo Endesa/Gamesa)
- Abril 1993 – julio 2000: Jefe de Proyecto en Unión Fenosa Ingeniería, S.A.

Experiencia docente.

- Profesor Asociado en la E.U.I.T. de Obras Públicas de la Universidad Politécnica de Madrid en el Área de Ingeniería Eléctrica en el Departamento de Ingeniería Civil: Tecnología Hidráulica y Energética. Curso 2011/2012.
- Profesor en el 1er Curso de Especialista en Gestión y Planificación de proyectos de Parques Eólicos impartido por el Instituto Postgrado y Formación Continua de la Universidad Pontificia Comillas en el año 2004.

- Director del curso de Operador de Subestaciones para el Servicio de Empleo de Extremadura (SEXPE) a través de la Agencia Extremeña de la Energía de Extremadura. Duración de 800 horas lectivas en 2010.
- Director del curso de Operador de Parques Eólicos para el Servicio de Empleo de Extremadura (SEXPE) a través de la Agencia Extremeña de la Energía de Extremadura. Duración de 160 horas en 2010.

Publicaciones.

- Lopez-Rey, A.; Campíñez-Romero, S.; Gil-Ortego, R.; Colmenar-Santos, A. Evaluation of Supply–Demand Adaptation of Photovoltaic–Wind Hybrid Plants Integrated into an Urban Environment. *Energies* **2019**, *12*, doi:10.3390/en12091780.
- Campíñez-Romero, S.; Colmenar-Santos, A.; Pérez-Molina, C.; Mur-Pérez, F. A hydrogen refuelling stations infrastructure deployment for cities supported on fuel cell taxi roll-out. *Energy* **2018**, *148*, 1018-1031, doi: 10.1016/j.energy.2018.02.009.
- Colmenar-Santos, A.; Campíñez-Romero, S.; Pérez-Molina, C.; Mur-Pérez, F. An assessment of photovoltaic potential in shopping centres. *Solar Energy* **2016**, *135*, 662-673, doi:10.1016/j.solener.2016.06.049.
- Colmenar-Santos, A.; Campíñez-Romero, S.; Pérez-Molina, C.; Mur-Pérez, F. Repowering: An actual possibility for wind energy in Spain in a new scenario without feed-in-tariffs. *Renewable and Sustainable Energy Reviews* **2015**, *41*, 319-337, doi: 10.1016/j.rser.2014.08.041.
- Colmenar-Santos, A.; Campíñez-Romero, S.; Enríquez-Garcia, A.L.; Pérez-Molina, C. Simplified Analysis of the Electric Power Losses for On-Shore Wind Farms Considering Weibull Distribution Parameters. *Energies* **2014**, *7*, doi:10.3390/en7116856.
- Colmenar-Santos, A.; Campíñez-Romero, S.; Pérez-Molina, C.; Castro-Gil, M. Profitability analysis of grid-connected photovoltaic facilities for household electricity self-sufficiency. *Energy Policy* **2012**, *51*, 749-764, doi: 10.1016/j.enpol.2012.09.023.

ANEXO I: "*REPOWERING: AN ACTUAL POSSIBILITY FOR WIND ENERGY IN SPAIN IN A NEW SCENARIO WITHOUT FEED-IN-TARIFFS*". COPIA DE LA PUBLICACIÓN.

Renewable and Sustainable Energy Reviews 41 (2015) 319–337

Contents lists available at ScienceDirect

Renewable and Sustainable Energy Reviews

journal homepage: www.elsevier.com/locate/rser

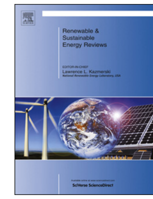

Repowering: An actual possibility for wind energy in Spain in a new scenario without feed-in-tariffs

Antonio Colmenar-Santos *, Severo Campíñez-Romero [1], Clara Pérez-Molina [1], Francisco Mur-Pérez [1]

Departamento de Ingeniería Eléctrica, Electrónica y de Control, UNED Juan del Rosal, 12 – Ciudad Universitaria, 28040 Madrid, Spain

A R T I C L E I N F O

Article history:
Received 23 April 2014
Received in revised form
24 July 2014
Accepted 16 August 2014

Keywords:
Wind energy repowering
Profitability
Grid parity

A B S T R A C T

At the end of January 2012, the Spanish government suspended the economic incentives for electricity generation facilities using renewable energy sources, including wind energy plants.

Spain maintains a high level of energy dependence that can only be reduced by applying measures to increase energy efficiency and using massive amounts of renewable sources. In addition, the target assumed by Spain, i.e., to have at least 20% of the primary energy to be supplied by renewable sources by 2020, has not yet been reached.

In Spain, wind farms, a number of which have been in commercial operation for over 15 years, offer a broad market appropriate for repowering. The use of more efficient wind turbines by means of repowering provides benefits to the electricity sector as a whole by optimizing the use of natural resources and facilitating the grid integration of the energy generated.

This paper analyses existing wind farms to quantify and characterize the market suitable for repowering. We discuss whether repowering is a valid alternative from the point of view of feasibility to enable the continuation of the integration of wind energy in the Spanish energy mix and whether this feasibility is sufficient when the energy generated is charged at the electricity market price in terms of grid parity. The results support that repowering is a profitable alternative and is often even better than the construction of new wind farms under certain conditions.

Contents

* Corresponding author. Tel.: +34 913 987 788.
E-mail address: acolmenar@ieec.uned.es (A. Colmenar-Santos).
[1] Tel.: +34 913 986 476; fax: +34 913 986 028.

http://dx.doi.org/10.1016/j.rser.2014.08.041
1364-0321/

1. Introduction

Law 54/1997 of the electricity sector [1] established a new regulatory framework, with the aim of guaranteeing the electricity supply with the highest quality standards and the lowest costs. This new framework was designed based on free competition with only the intervention of the administration to create the specific regulation.

From a retributive perspective, for the power plants under the special regime set up in the Law 54/1997,[2] the regulation established a system supported by a feed-in-tariff (FIT hereinafter) without time limits, which essentially consists of charging a bonus for renewable electricity fed into the grid over the price matched in the daily electricity market. As a second option, it was possible to choose a fixed tariff [2–4].

Under this stable regulatory framework and supported by an adequate legislation to facilitate the administrative authorization of the plants [5], at the end of March 2012, wind energy reached a degree of supply higher than 25% of the electricity demand in the Spanish market central bus-bars[3] [6].

Considering the significant level of primary energy dependence of Spain (75.6% in 2011), which is well above the average for the 27 countries in the European Union, the reduction to a value of approximately 55% at the end of March 2012 [7,8] indicates the success achieved in the implementation of the energetic mix of renewable energy sources (RES hereinafter), especially for wind energy [9–11], which exceeded a participation rate of 18% in the demand supply in 2012 [12].

In January 2012, the Spanish Government suspended the economic incentives for new-generation facilities based on RES, including wind energy [13]. Accounting for the fact that the targets established by the European Union (EU hereinafter) and the Spanish Government to cover 20.8% of the energy demand with renewable energy sources by 2020 have not yet been achieved [8,14], new strategies and regulatory policies are required to continue with the integration of RESs [15–17]. In this work, we examine wind energy as an important step toward attaining such a global objective; because of its degree of maturity, wind energy constitutes an actual possibility in a new setting without a FIT, thereby enabling scenarios that imply the lowest costs for the entire electricity sector [18].

The first wind turbine generators (WTG hereinafter) have been in commercial operation for more than 15 years and can be considered that they are entering the last stage of their nominal lifetime [19]. The repowering of wind farms (WF hereinafter) provides benefits to the electricity system as a whole [20], can improve the social and environmental impact [21,22] and may represent a reasonable option for the Spanish wind industrial sector to address the current critical situation [23].

This work is aimed at determining whether and under what conditions the repowering of a WF is a profitable alternative. We considered the feasibility of two possible alternatives to achieve a reasonable profitability for investors: maintaining the retributive system based on a FIT or charging the price determined in the daily electricity market (spot price hereinafter) for the electricity generated. The volume and the characteristics of the WFs that are suitable to be repowered are also determined.

Below, in Section 2, we analyze existing WFs to define, quantify and characterize the market formed by those suitable for repowering. Afterward, in Section 3, we estimate the expected production of a repowered wind farm (Rep-WF hereinafter) and the changes with respect to an old WF.

In Section 4, we define and estimate the costs of the facilities that form a WF and how these facilities could be reused in a Rep-WF to reduce the construction costs. In addition, the works for dismantling, waste treatment and valorization of the old WTG are also analyzed and considered.

In Section 5, we perform an analysis of the expected profitability of a Rep-WF, introducing a retributive proposal for the electricity generated based on the spot price and comparing the results with those obtained in case of retribution under the present scheme supported by FIT. Sensitivity analyses in relation to the most important parameters are included to consider the effect of their variations in the results.

Finally, Section 6 presents the conclusions of the study.

2. Determination of the market volume and its characteristics

2.1. Lifetime and financing

According to the standard IEC 61400 [24], a WTG should be designed for a lifetime of at least 20 years. During this period, with proper Operation and Maintenance (O&M hereinafter), the WTG will offer a level of mechanical availability[4] of nearly 100% during the first 5–10 years – presently, the typical values guaranteed by the manufacturers are approximately 97% – and over 90% for the remainder of its lifetime.

For most WFs, Project Finance was the method chosen by investors. With this method, the recourse to investor from the lenders is limited or even eliminated. The project itself, the WF in

[2] The article 27 of the Law 54/1997 defines the production of electricity in a special regime, such as that implemented in facilities up to 50 MW of installed power with the following characteristics. (a) The facility uses cogeneration or other electricity production methods associated to non-electric activities, and they suppose a high degree of energetic efficiency. (b) The facility uses as primary energy one of the renewable energies sources (RESs), biomass, or other type of biofuel, and the owner does not develop the production of electricity under the ordinary regime. (c) The facility uses non-renewable waste as primary energy.

[3] Energy fed into the grid from generators and international exchanges deducting the consumption required for generation and pumped storage.

[4] Mechanical availability is defined typically in a yearly period, as the percentage of time (year) in which the WTG is ready to produce electricity.

Nomenclature

General

C_P	coefficient of performance
FIT	feed-in-tariff
N-WF	new wind farm
O&M	operation and maintenance
P&C&G Grid	power, communications and grounding grid in the WF
Rep-WF	repowered wind farm
RES	renewable energy source
SCADA	supervisory control and data acquisition
Spot price	daily electricity market price
WTG	wind turbine generator or generators
WF	wind farm/wind farms

Generation and losses

CF	capacity factor (%)
E_L	electrical losses (%)
F_{AV}	mechanical availability factor (%)
W_L	wake effect losses (%)

Financial

IRR	internal rate of return
NPV	net present value
K	discount rate for NPV calculation
TDEP	depreciation period of the WF (years)
RPI	retail price index (%)
CF_z	cash flow for year z
CFA_z	cumulative cash flow for year z
NPV	net present value (€)
z	ordinal indicating the number of years the WF has been in commercial operation, which is used in the IRR calculation
FL	financial leverage
VAT	value added tax (%)
TAX	incomes taxes (%)

this case, will exclusively respond for repaying the debt. The incomes for selling the energy are the main guarantee, so these incomes must be predictable and sufficient [25,26].

For WFs, incomes can be estimated with a high level of confidence. Such an estimate is based on an adequate measurement campaign of the wind resources at the selected site, the retributive stability given by the regulatory framework during the entire commercial operation period and, finally, selecting an efficient and mature technology to ensure good functionality in the long term.

In the project finance method, the debt repayment period will depend on the cash flows generated by the WF. Therefore, to estimate this period, it is necessary to consider the special features of the project itself (its wind resource, the WTG, the costs, etc.). In general, periods in the range of 13–15 years are obtained [25].

From a financial approach, a suitable WF for repowering should have achieved a stage in which the investors had been able to repay the loan taken to finance the construction. However, from a technical point of view, the WTGs (of that generation) arriving to the end of their lifetimes will exhibit high failure rates, will require more maintenance and likely will suffer from a lack of relevant spare parts (generator, gearbox, blades, etc.).

Due to the evolution in the capital cost, the WFs first implemented in commercial operation were slightly more expensive to build [27]. This high capital cost considered separately could imply a negative impact on the repayment period; however, other factors also come into play. As will be demonstrated below, these WFs are located in regions of higher wind resources than the ones built later; in addition, the legislative evolution has allowed them to change to new frameworks, which are more advantageous in terms of retribution. Both of these facts imply a positive impact regarding incomes in the long term. For this reason, it is realistic to expect a lower repayment period that can be estimated in approximately 10 years,[5] which is shorter than the previously mentioned period. Thus, to characterize the repowering market, the considered WF must have an operation period equal to or longer than 13 years because during this period, it can be hoped that the incomes have allowed the investor to repay the debt incurred to finance the construction and have produced a positive cash flow for 3 years. In addition, the WTGs will not have arrived at the end of their lifetime but it is expected that a probable increase in the failure rates and the costs for O&M will occur to maintain a high level of mechanical availability [28].

2.2. Power of WFs

At the end of 2012, the WFs in Spain that were in commercial operation represented an installed power capacity of 22.6 GW [12]. The installation of the first units started in 1992, but the most significant growth has occurred since 1998 due to the stability provided by Law 54/97 [1] and subsequent regulations. This growth was also possible due to the evolution of WTG technology and the technical measures established to maximize their integration. For example, consider the forecasting of wind power generation [29,30] or the affiliation at control centers [31].

Fig. 1 shows the evolution of installed power in the period of 1998–2012 [12], which includes the years in operation. The first units, commissioned before 1999, were found to have a history of over 15 years in commercial operation.

The market volume of installed power for an operation period equal to or greater than 13 years (i.e., WFs installed up to the year 2000), would currently be approximately 2.3 GW. In addition, as shown in Fig. 1, the evolution of the yearly installed power will make this volume increase at a rate of approximately 1 GW per year.

2.3. Characterization of the power of WFs and WTGs

During the considered period of 1998–2012, approximately 1300 WFs were installed in the Spanish territory [12].

[5] In order to minimize the financial costs it is important to reduce the repayment period in which the investor must pay an interest rate for the borrowed money. This period is very sensitive with the electricity generated because more energy implies bigger incomes and the possibility for the investor to choose a smaller repayment period or reduce it during the commercial operation. By means of simulations carried out according with the cash-flows calculation method of

(*footnote continued*)
Table 9, an increase of around 10% in the yearly electricity generation can reduce the payback period between three and five years depending on other variables (i.e. the capital costs).

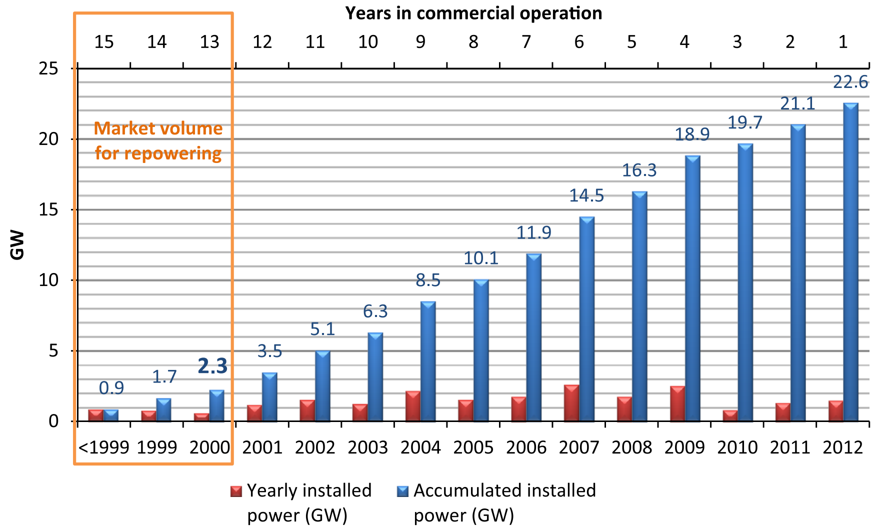

Fig. 1. Yearly and accumulated installed power in WFs and the number of years in commercial operation.
Source: National Energy Commission of Spain (CNE) [12]

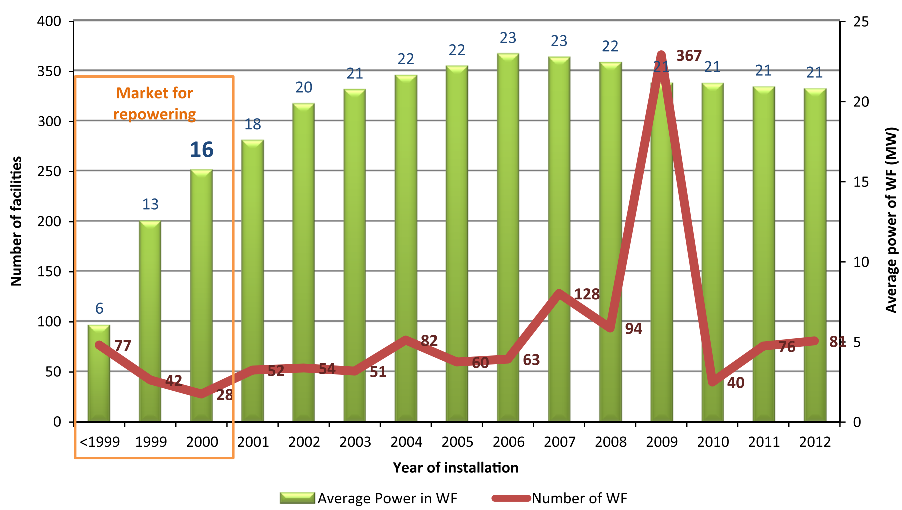

Fig. 2. Average power installed in WFs per year of installation.
Source: National Energy Commission of Spain (CNE) [12]

Fig. 2 shows the yearly evolution of the number of WFs installed and their average installed power. Note that the growth was regular and sustained, achieving a maximum in 2009 when 2.5 GW were installed in 367 WFs [12].

According to Law 54/97 [1], the capacity of the facilities under the special regime, including WF, cannot exceed 50 MW. Nevertheless, this maximum has yet to be approached; as Fig. 2 shows, the average installed power of WFs increased in the first years to become stabilized at approximately 20 MW.

Since the beginning of the deployment of wind energy, WTG technology has progressed to units that are more efficient and have a higher unitary rated power. This progress has encouraged the possibility to take more advantage of wind energy by both selecting the best places in the site – with a higher mean wind speed – and reductions in the construction and O&M costs, which is strongly influenced by the number of WTGs in the WF and by the use of these new WTGs [32].

Thus, WTGs have passed from the first units with a capacity of several hundred kilowatts to the current ones offered by the manufacturers with a rated power above 3 MW. Fig. 3 shows the evolution of the average rated power of a WTG installed up to 2012.

According to Fig. 2, for those WFs installed up to the year 2000, the value for the average installed power would be 16 MW. Nevertheless, for the purpose of characterizing a WF for repowering, an output of 18 MW was selected because it is the closest value to 16 MW which is a multiple of 2 and 3 MW and therefore facilitates the simulation with WTG of 2 and 3 MW.

Regarding the unitary rated power of a WTG, as shown in Fig. 3, for a WF that is 13 or more years in commercial operation, the typical value for the unitary rated power can be set between 559 and 651 kW.

2.4. Generation of electricity

Fig. 4 shows the annual evolution of the net WF capacity factor (CF hereinafter)[6] in the period of 1999–2012 differentiated by the

[6] The CF is defined, in a yearly period, as the percentage of the year during which the WF should have been working at nominal power to generate the entire production obtained in the year. The gross value (Gross CF) does not include the wake losses (W_L), the electric losses (E_L) up to the point where the electricity fed into the grid is measured, and the production losses due to the mechanical availability of the WTG (F_{AV}). The net value (Net CF) includes the effect of all the

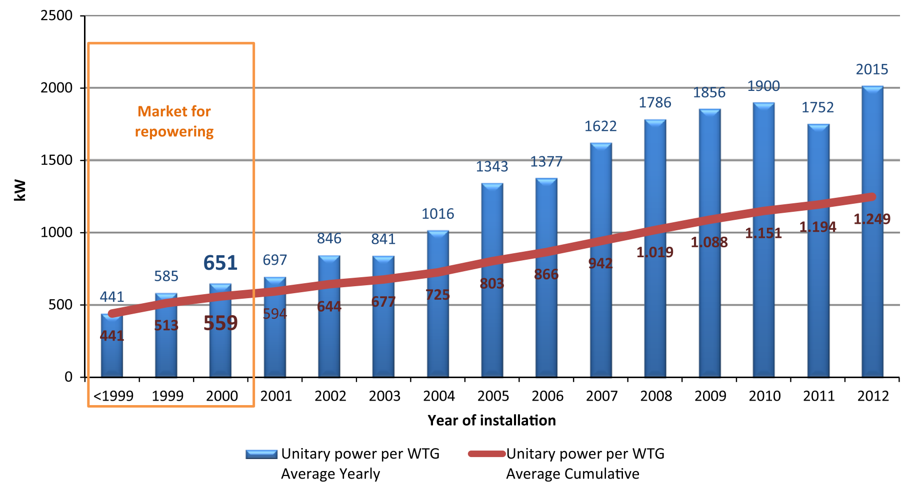

Fig. 3. Unitary rated power per WTG in a WF.
Source: Spanish Wind Energy Association (AEE) [23,33,34]

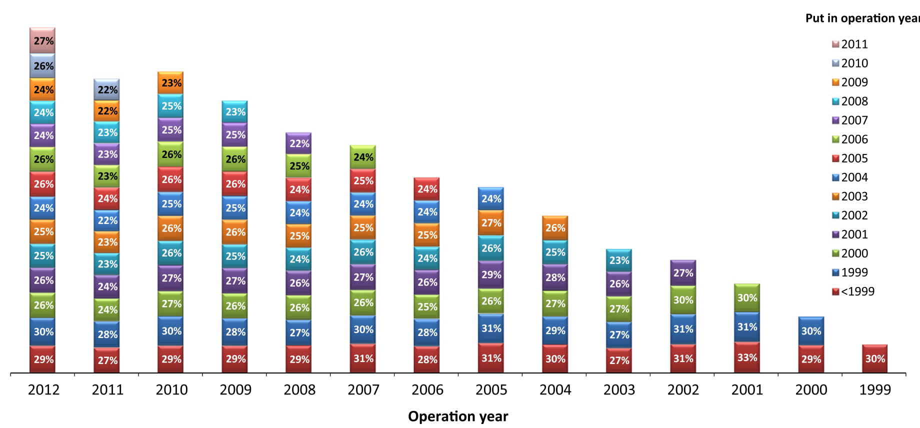

Fig. 4. Yearly capacity factor of WFs deployed during the year they were placed in operation.
Source: CNE [12]

year the WF was placed in commercial operation. Note that the WFs installed during the initial years continually offer the highest CF during the entire period.

In addition, Fig. 5 shows the temporary evolution of the yearly average net CF and its accumulated value for a WF in Spain, differentiated by the year they were placed in operation. The WTGs used in the first WFs were less efficient and less technologically advanced, besides considering that it is expected a relevant decline in their performance with age [28], one may conclude that the wind energy potential of the sites where the first WFs were built is substantially better than those of the later WFs.

By characterizing the WFs suitable for repowering, the average net CF considered for a WF with a minimum commercial operation period of 13 years is calculated and shown to be approximately 28% in Fig. 5.

2.5. Characterization of WFs suitable for repowering

Table 1 summarizes the results obtained from the characterization of WFs suitable for repowering that were described in the previous sections.

(*footnote continued*)
aforementioned losses (expressed as a percentage); therefore the relation between the Net CF and the Gross CF is the following:

$$\text{Net CF} = \text{Gross CF} \times W_L \times E_L \times (1 - F_{AV}).$$

3. Analysis of the electricity production of repowered WFs

The mechanical power, P_{wind}, represents the kinetic energy of the wind going through the rotor of a WTG, which depends on the non-disturbed wind speed (v), the air density (ρ) and the area swept by the rotor (S) according to the following expression:

$$P_{wind} = \tfrac{1}{2}\rho S v^3 \tag{1}$$

A WTG is able to extract only a portion of this kinetic energy to transform it into electricity. The limit of this transformation is $(16/27)\% \approx 59.25\%$, which is calculated according to Betz's law [36].

The formula for the mechanical power extractable from the wind stream by a WTG is

$$P_{util} = C_p \times P_{wind} = C_p \tfrac{1}{2}\rho S v^3 \tag{2}$$

where C_p is the coefficient of performance and determines how efficiently the WTG takes advantage of the wind stream going through the rotor. The value of C_p varies according to the wind speed and depends on the characteristics of the blades.

In addition, the increase of the wind speed with the height must be taken into consideration [37]. This increase depends on the particularities of the site. With the appropriate wind measurement campaign, the choice of the most convenient hub height can be determined.

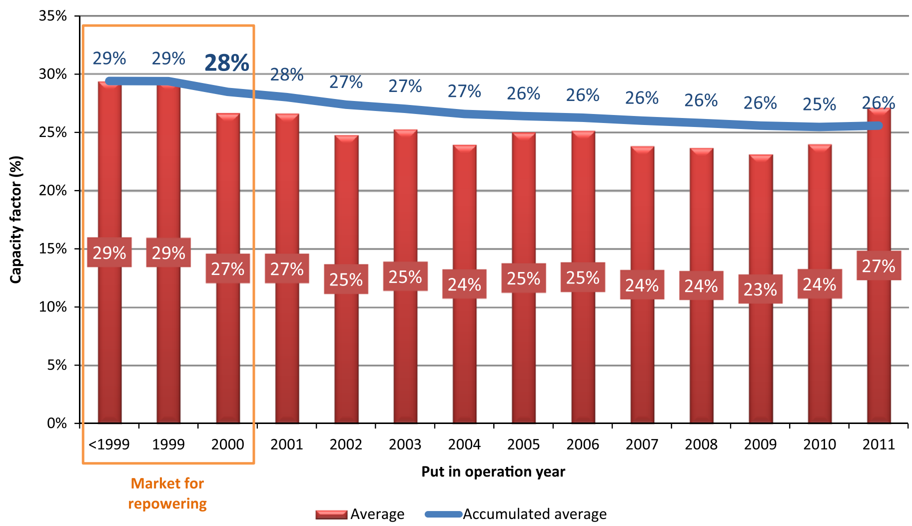

Fig. 5. Net average CF of WF's in the period 1998–2012 deployed for the year of entry in operation.
Source: CNE [12]

Table 1
Market volume and characteristics.

Year placed in operation	< 2000
Total installed power	2.3 GW
WTG average size	559–651 kW
WF average power size	18 MW
Average net CF	28%

Therefore, on the basis of (2), the possibilities for an improved use of wind resources in a specified location are the following:

(1) Increase the diameter of the rotor by increasing the length of the blades.
(2) Increase the wind speed through the rotor by installing the WTG hub higher – with a higher tower.

Increase C_p by installing the WTG with more efficient rotors.

In fact, the repowering of a WF takes advantage of these three possibilities when the older WTGs are replaced by those that are more technologically advanced and efficient, with larger blades and higher towers. In addition, new WTGs will have a larger rated power, making it possible to install more power in the best positions, i.e., those with more wind speed.

To quantify the effect of the replacement of a WTG, we performed a simulation of the expected production from wind measurements obtained over the last three years from an actual site located in the province of Lugo (Spain). As shown in Fig. 6, there are many other sites in the Spanish territory with similar wind conditions in terms of the average speed, so that the analysis performed in this section is valid for all of these sites.

The data were collected using a meteorological mast equipped with anemometers and wind vanes at heights of 45, 60 and 90 m and also equipped with pressure and temperature sensors. In addition, the mast provides a system to log, store and upload the raw data.

To characterize the wind resources in the site, the raw data were filtered and processed statistically. The characterization was performed using a probability Weibull distribution. The results, for the wind speed at heights of 45 m and 90 m are shown in Fig. 7.

The results classify the site in class I at a height of 90 m and in class II at a height of 45 m according to the classification established in IEC 61400-1 [24].

Two different types of WTGs were considered in the simulation:

(1) A representation of a WTG currently installed in a WF suitable for repowering and valid for the analyzed site (class II). As shown in Table 1, the rated power for a single unit is between 559 and 651 kW. In this range of power, the manufactures with more units installed (Vestas, Neg-Micon, Ecotecnia, Gamesa, and Made) had WTGs with 660 and 750 kW of rated power per unit [35], which were included in the representation. The hub height considered for these WTGs was 45 m, typical for the range of power.
(2) A representation of the WTGs currently offered by manufacturers and suitable for the analyzed site (class I). The rated power is between 2 and 3 MW because these are more frequently used [23], and among the possible hub heights, 90 m was chosen because we have actual measurements at that height.

Table 2 shows the main data and characteristics of the WTG used in the simulation.

Fig. 8 shows the power curves[7] of the WTGs included in the simulation as well as the Weibull distribution functions obtained for the analyzed site (shown in Fig. 7). It can be observed how the most modern WTGs exhibit a higher rated power and how they are able to more efficiently take advantage of the wind resource at low wind speeds between 5 and 10 m/s (lower than the speed at which nominal power is reached), which correspond to the more frequent range measured at the site.

The simulation to calculate the expected energy production was performed for each one of the WTGs using the software Windographer [42] considering one isolated WTG without including the weak losses [43].

The results of the simulation are shown in Fig. 9, where a large increase in the expected energy production given by the repowering or replacement of the old WTGs for the new ones is observed. Considering the average net CF obtained in the simulations for the WTGs that are representative of those currently installed (25.2% for NM48, 25.4% for AE46 and 29.1% for V47) over the average net CF for the new ones (45.3% for ECO100, 42.2% for G80 and 37.5% for

[7] The WTG power curve relates the speed of the wind running into the rotor with the power generated by the WTG. Usually, the power curve is verified and certified by an independent organization and is typically guaranteed by the WTG manufacturers, at least during the warranty period.

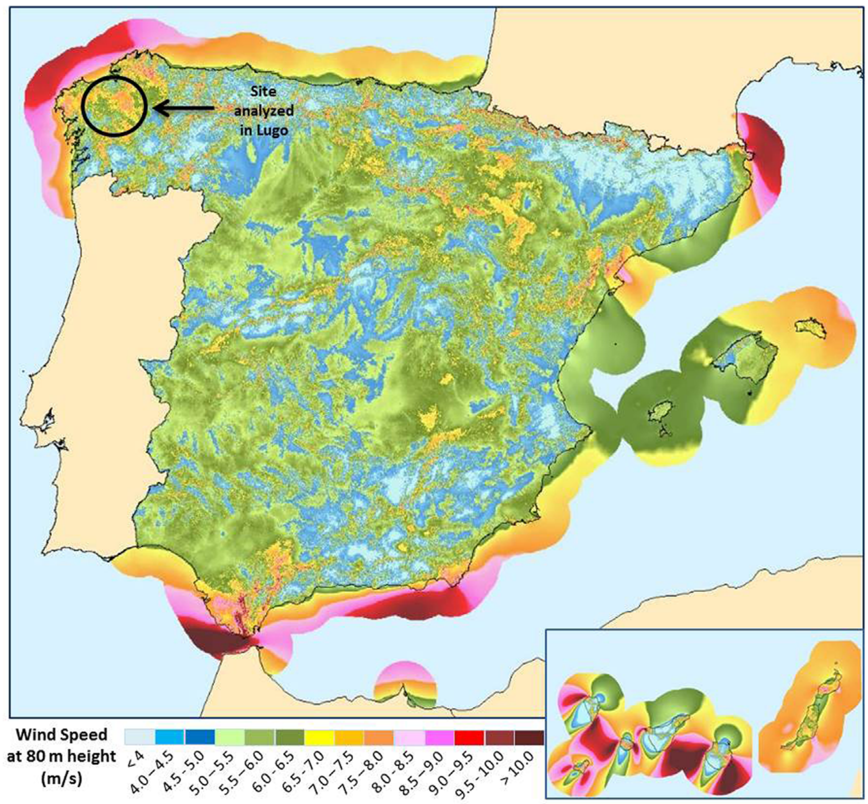

Fig. 6. Spanish wind map. Yearly average wind speed at 80-m height.
Source: IDAE [38]

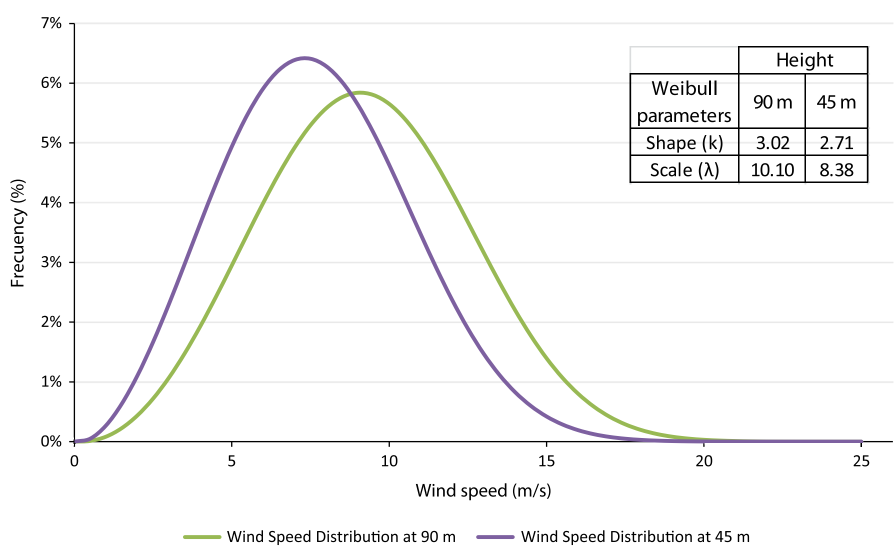

Fig. 7. Weibull curves and parameters for the wind speed distribution in the site.

Table 2
Characteristics of the WTGs included in the simulation.

Manufacturer	Type	Nameplate power	Class according IEC 61400-12	Rotor diameter (m)	Hub height (m)
MADE[a] [39]	AE-46	660 kW	II	46	45
NEG MICON[b] [40]	NM-48	750 kW	II	48	45
VESTAS [40]	V47	660 kW	II	47	45
ALSTOM [41]	ECO 100	3 MW	I	100	90
VESTAS	V90	3 MW	I	90	90
GAMESA [39]	G 80	2 MW	I	80	90

[a] The MADE Company was merged with Gamesa in 1999.
[b] The Neg Micon Company was merged with Vestas in 2004.

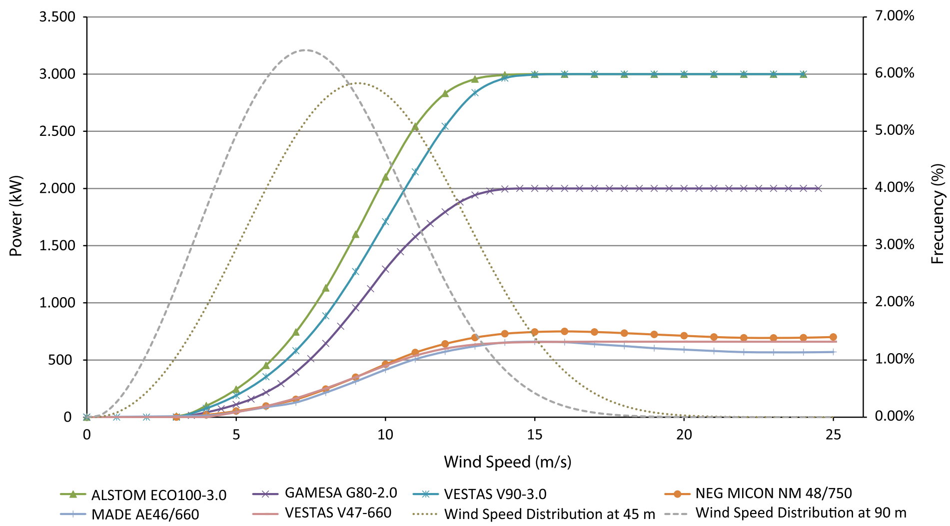

Fig. 8. Power curves of the WTG included in the simulation.

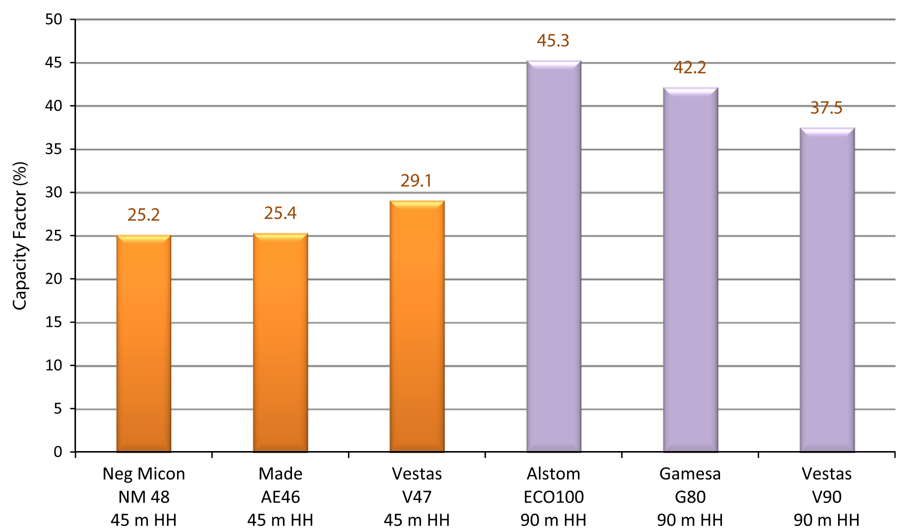

Fig. 9. CF estimated for the WTGs included in the simulation.

V90), the estimated increase of the net CF is approximately 57%. Moreover, in the best case scenario, the substitution of a Neg Micon NM48 (net CF of 25.2%) with an Alstom ECO100 (net CF of 45.3%) leads to an increase in the expected energy production with a net CF reaching a value of 79.8%.

Applying these results, the increase in the net CF was determined to be close to the previously obtained average value of 57%. Therefore, taking into consideration the characterization of a WF suitable for repowering that establishes the net CF of approximately 28% (see Table 1) in the remaining calculations, the average and representative value for the net CF for a Rep-WF was estimated to be 40% (a value lower than the result obtained from applying the 57% increase to the 28% characterization result; $28\% \times 1.57 = 43.96\% > 40\%$).

4. Definition of the scope of the works and the analysis of associated costs

The objective at this stage of the study was to define in detail the work required to develop, construct and operate a WF, estimate its cost according to the current market prices and differentiate the scope of works in two different cases: for a new WF (N-WF hereinafter) and for a Rep-WF. This study enables us to perform a comparative analysis of the feasibility for each case.

The scope of work for the development, construction and operation of a WF and its associated costs are different for a N-WF than for a Rep-WF. Among others factors, it is important to take into account that for a Rep-WF, some of the existing facilities can be reused and that before the repowering, it will be necessary to dismantle the old WTG.

The utilization of WTGs with higher unit power may enable an increase in the power of the WF after repowering. For an example, we have considered a distance between WTGs, measured perpendicular to the predominant wind direction, of three times the diameter of the rotor (a typical value for the design to reduce wake losses [44]). With this assumption, for WTGs with 46 m of rotor diameter and 660 kW of unit power, it is possible to install up to 2.4 MW/km, while for WTGs with 90 m of rotor diameter and 3 MW of unit power, it is possible to install up to 5.5 MW/km.

However, in the repowering process, it is very important to make an effort to maintain the validity and applicability of the permits, licenses and authorizations already obtained for the old WF. This will avoid additional work (and their associated costs) that could extend the development process.

This issue has a special relevance in relation to installed power because its variation can substantially modify the affected area of

Table 3
Comparison of capital and O&M costs between several sources and the estimate considered in the simulations.

Source	Range	WTG cost[a] (€/kW)	WF cost (€/kW)	WTG O&M cost (€/kWh)
[45] **(Valid for 2010)**	min		1501	0.011
	typ	1176		
	max		1704	0.020
[46] **(Valid for 2012)**	min	752		
	typ		1592	
	max	1069		
[47] **(Valid for 2014)**	min	560	800	
	typ			
	max	770	1100	
[7,8] **(Valid for 2010)**	min	744	1000	0.090
	typ			
	max	992	1300	0.120
Calculation based in the survey carried out for this paper. See Appendix A	typ for a Rep-WF	850	983	0.004
	Typ for a N-WF		1108	0.006

[a] When the data source was in USD, data were converted to € using the following USD/€ exchange rates: 1.233 in 2010 (value in 2010/06/15), 1.263 in 2012 (value in 2012/06/15) and (1.349 in 2014) (value in 2014/02/10).

the WF and the permits and contracts subscribed for access to the electric grid. The little good in terms of RES integration is the installed power. In the process of sectorial regulation, as well as to fix domestic targets established in the development plans [8], the installed power was largely used to delimit the integration limits. In addition, an increase in WF power will involve important modifications in evacuation facilities (substations and line) with the associated costs.

In contrast, unless there were physical constraints in the site that could limit the installation of the required number of new WTGs to achieve the old WF capacity, it is convenient not to reduce it, thus maximizing the use of the affected area and the potential of the site.

Therefore, for the aim of this paper, the installed power in a Rep-WF was considered to not vary with respect to the authorized power for the old WF.

4.1. Capital costs

The capital costs vary widely depending on multiple factors. Among others, the following factors can be pointed as the most important: the market status (supply and demand), the site (country and local characteristics), the characteristics of the connection point to the electric grid, the existence of nearby WTG factories and the local presence of experienced sub-contractors.

With the aim of counting on a solid base for the calculation of the capital costs and considering the possible variations we did the following:

A survey among several international companies with a large experience in the Spanish market, including engineering, WTG manufacturers, civil works and electric infrastructure subcontractors. The detailed definition of the scope of works included in the survey and the prices obtained can be found in the Appendix A.

Include sensitivity analysis for the results in relation with the main capital cost corresponding with the WTG.

Table 3 shows a comparative for the main costs between several sources and the result of the survey we carried out for this paper applied to the characteristics for both the Rep-WF and the N-WF. As shown, the results are consistent with the other sources but with a focus in the market.

Table 4
Summary of the development costs.
Source: Self-elaboration based on Table A1

Item	New WF			Rep-WF		
	€/kW	€	%	€/kW	€	%
Engineering	***2.2***	***40,000***	***12%***	***2.2***	***40,000***	***15%***
Wind resource assessment	***4.8***	***87,000***	***25%***	***0.4***	***7000***	***3%***
Meteo tower rent	4.4	80,000		0.0	0	
Final report	0.4	7000		0.4	7,000	
Personnel	***12.2***	***220,000***	***63%***	***12.2***	***220,000***	***82%***
Hourly average cost	6.7	120,000		6.7	120,000	
Other personnel costs	5.6	100,000		5.6	100,000	
Total development costs	**19.3**	**347,000**	**100%**	**14.8**	**267,000**	**100%**

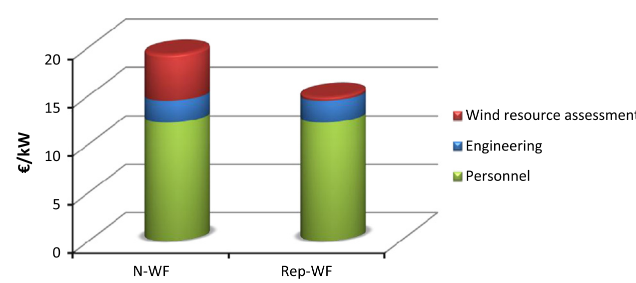

Fig. 10. Deployment of the development costs per kW.

4.1.1. Development

Development is performed prior to the construction of the WF and consist mainly of the study of the wind resource, the technical definition of the project and the management of the permits, licenses and authorizations necessary for the construction and the commercial operation.

Table 4 and Fig. 10 present a summary of the development costs to take into consideration in a N-WF or in the repowering of an existing one. The only difference is the wind resource assessment required to make an appropriate choice for the new WTG as well as a good production estimate. In the case of a Rep-WF, it will not be necessary to perform a new measurement campaign of wind resources because the data were obtained during the commercial operational period of the old WF.

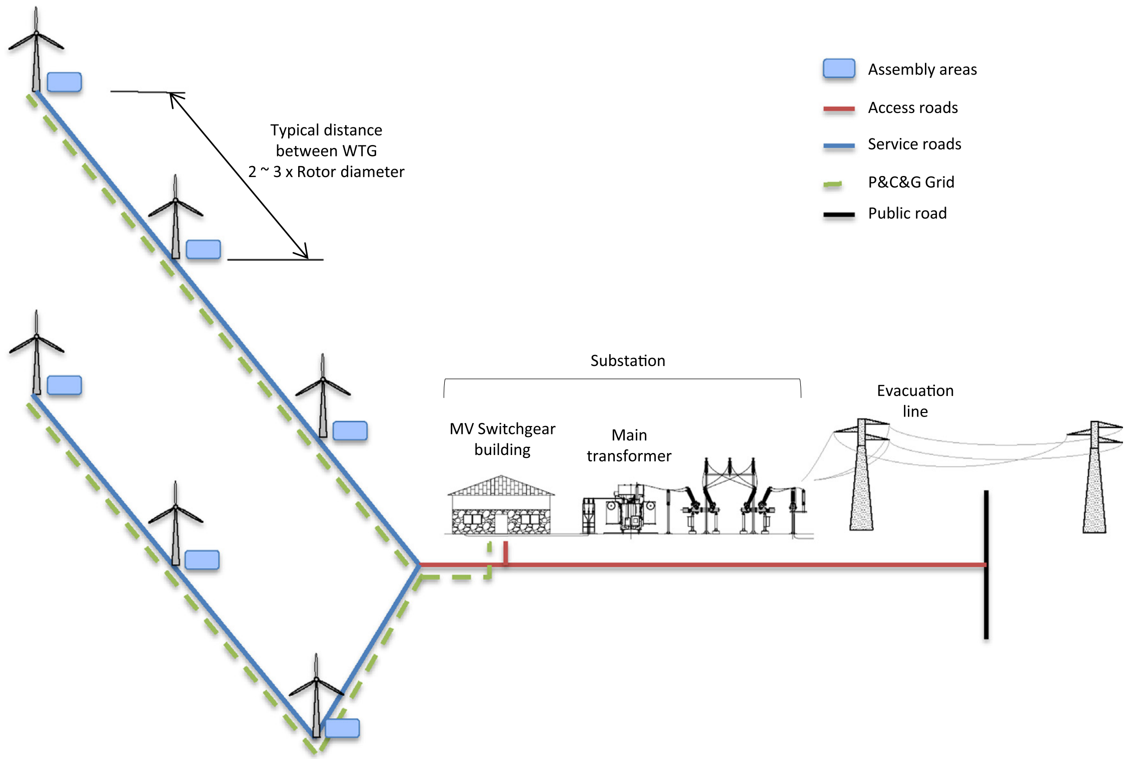

Fig. 11. Facilities in a WF.

Table 5
Summary of the construction costs.
Source: Self-elaboration based on Table A2

Item	New WF			Rep WF		
	€/kW	€	%	€/kW	€	%
Main equipment	***853.9***	***15,370,000***	***78***	***853.9***	***15,370,000***	***88***
WTG	850.0	15,300,000		850.0	15,300,000	
Meteorological mast	3.9	70,000		3.9	70,000	
Foundations and assembly areas	***56.1***	***1,010,000***	***5***	***56.1***	***1,010,000***	***6***
Foundations	53.3	960,000		53.3	960,000	
Assembly areas	2.8	50,000		2.8	50,000	
Roads	***26.0***	***468,000***	***2***	***17.3***	***312,000***	***2***
Access road length	12.5	225,000		8.3	150,000	
Services road length	13.5	243,000		9.0	162,000	
P&C&G grid	***15.3***	***275,400***	***1***	***15.3***	***275,400***	***2***
Civil works	11.3	202,500		11.3	202,500	
Supply and installation	4.1	72,900		4.1	72,900	
Substation	***55.6***	***1,000,000***	***5***	***0.0***	***0***	***0***
High voltage level	30.6	550,000		0.0	0	
Medium voltage level	8.3	150,000		0.0	0	
Main transformer power	16.7	300,000		0.0	0	
Evacuation line	***34.7***	***625,000***	***3***	***0.0***	***0***	***0***
Construction Permits	***47.2***	***849,957***	***4***	***25.9***	***466,825***	***3***
County Construction license	2.2	40,110		1.7	30,490	
Urban license	26.0	468,710		23.6	424,185	
Land owners permits	19.0	341,137		0.7	12,150	
Total construction costs	**1088.8**	**19,598,357**	**100**	**968.6**	**17,434,225**	**100**

4.1.2. Construction

For a given WTG, the facilities of a WF will depend on its geographical location (distance to the public road network, soil characteristics, rainfall, etc.) and the way to connect it to the electric grid (voltage level, evacuation line, specifications for the connection point, etc.). However, several basic elements allow us to estimate the costs of construction with an appropriate accuracy for the objectives of this paper.

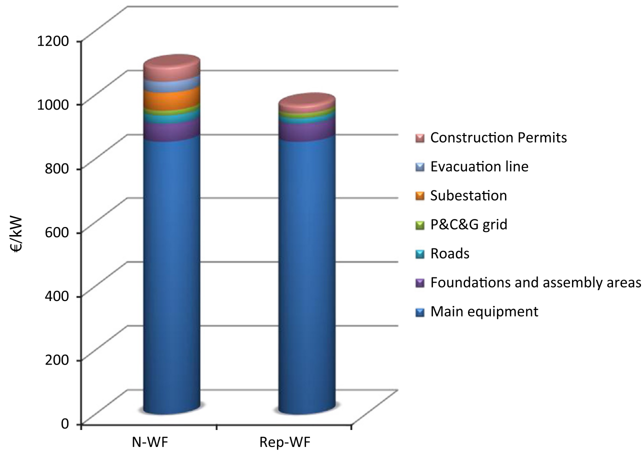

Fig. 12. Deployment of the construction costs per kW.

A basic scheme of the facilities, which is considered for the definition of the scope of the construction and the estimation of their associated costs, is shown in Fig. 11. These facilities are as follows:

The foundations of the WTG and the assembly areas to support the cranes and heavy transport vehicles during the assembly and maintenance of the WF.

The roads to allow access to all the facilities from the public transport network. These roads should be suitable for the transit of large-dimension transport vehicles and cranes.

The power, communications and grounding grid (P&C&G grid hereinafter). The P&C&G is composed of high-voltage cables and accessories to take the power generated in each WTG to the substation, communications cables (usually optical fiber) to provide communications between the WTGs, a meteorological tower, a supervisory control and data acquisition system (SCADA hereinafter) and ground network cables (usually bare copper wire). The associated civil works are also included.

The electric substation, in which the electricity generated by the WTG is collected, typically at a voltage level between 15 and 33 kV, and transformed to the voltage level of the electric grid where the WF connects.

The evacuation line to carry the electricity from the substation up to the connection point with the electric grid.

The extent of the roads and the P&C&G grid is directly conditioned by the distance between the WTGs. Obviously, the best positions, in terms of wind resource, should be selected. With the objective to maximize generation with the minimum cost, several methods have been suggested to optimize WF layouts [48], however, very often, especially in sites where wind resources are homogenous over all the area available and for the purpose of minimizing losses caused by the wake effect [43] the WTGs should be located with a distance in the range of two or three times the length of the WTG rotor diameter in the line perpendicular to the prevailing wind direction. At the same time, the typical distance between two WTG lines – both perpendicular to the prevailing wind direction – is approximately 10 times the length of the WTG rotor diameter [44].

Table 5 and Fig. 12 detail the construction costs considered for a N-WF and for a Rep-WF. As one might expect, the construction of a Rep-WF is less expensive for the following reasons:

(1) The roads must be constructed for a N-WF, while they only require renovation and adaption to the requirements of the new WTGs (dimensions and weights) for a Rep-WF.

Table 6
Dismantling and waste disposal costs and valorization incomes.
Source: Self-elaboration. Prices for dismantling and waste disposal are based on offers received in 2013 from companies that are specialized in the assembly and transportation of WTGs.

Item	€/kW	€
Dismantling of WTG's and waste disposal	*67.5*	*1,215,000*
Valorization of valuable scrap materials	*−25.9*	*−465,973*
Net effect	**41.6**	**749,027**

Table 7
Deployment and prices for valuable waste.
Source: Self-elaboration. Steel and copper mass per WTG from manufacturers information.Prices for valuable waste from [51,52]

Item	Average valuable waste per WTG	
	Steel (kg)	Copper (kg)
Blades (3#)	698	
Hub	2320	
Anchorage	3000	
Tower	30,000	
Main frame	6000	
Shaft (including bearing)	3100	
Gearbox	8000	
Coupling	160	Irrelevant
Yaw gear motor	500	Irrelevant
Yaw ring	620	
Hydraulic unit	60	
Generator		1000
Cables		866
Quantity per WTG	**54,458**	**1866**
Unitary price (€/kg)	0.280	1.077
Total price (€/WTG)	**15,248**	**2010**

(2) According to the assumption previously mentioned in this section, the installed power will not change; therefore, there is no work required in the substation and the evacuation line for a Rep-WF.
(3) The cost of the permits, which is calculated over the construction costs, will be higher for a N-WF.
(4) For a Rep-WF, the only land permits required are for new roads and P&C&G grid facilities.

4.2. Dismantling works and valorization of the valuable waste

For a market that is able to install more than 22 GW, the dismantling of an old WTG, which are much lighter and smaller than the new ones, is not a barrier for repowering. The services offered by specialized companies and the technical resources for the elevation and transport of heavy loads exceeds the necessities to perform these tasks.

The dismantling works and valorization of valuable waste will include

(1) The dismantling of the WTGs into manageable parts.
(2) Ensuring the adequacy of the transportation.
(3) The classification and transport of non-valuable waste and the delivery to authorized agents for their treatment.
(4) The transport of valuable waste to the delivery point.

For the dismantling and restoration of the rest of the facilities not reused in a Rep-WF the following assumptions have been taken into consideration:

Foundations: The dismantling is limited to eliminate protruding parts from the soil surface, usually consisting of the upper anchorage or anchor bolts and the structural concrete. After that, the surface is levelled and refilled with appropriate material; finally, environmental restoration will be performed.

Assembly areas: Due to environmental requirements, the assembly areas were normally restored at the end of the construction of the old WF; thus, no dismantling work is required.

Roads: Restoration is not required because they will be largely reused, and for the parts that are not reused, their removal is not advised because they provide an important service to the community by facilitating access or acting as firebreaks.

P&C&G grid: Reuse is not feasible because the positions of the WTGs will not be the same. In addition, restoration is not necessary because common practice is to bury the cables deeply enough to allow others soil uses (e.g., agriculture) and, according to environmental requirements, trenches must be restored upon completion of the old WF.

The appropriate time for the completion of the aforementioned works of dismantling and restoration is during the construction of new facilities for a Rep-WF. In this case, the cost of all of these construction projects can be considered to be a residual value and should be included in the construction scope for the Rep-WF (Table 5)

Regarding waste management, there are two different cases, depending on whether the waste is valuable, i.e., whether it is possible to obtain income with their disposal for recycling.

In the case of non-valuable waste (oil, plastic, etc.), the waste items should have their origins classified and be moved directly to qualified organizations authorized for their treatment and recycling. The costs of these tasks are included in the dismantling costs listed in Table 6, which were obtained by means of a request for a proposal issued to 10 companies that are specialized in the assembly and transport of WTGs.

In the case of valuable waste, currently, there are stable markets in which these waste items can be traded, thereby obtaining economic incomes [49,50]. Among all the valuable waste found in a WTG, the most important because of their quantity and price are copper and steel. Table 7 details the amount of copper and steel waste and their origin from a WTG. The amounts indicated are the average value for the three class II WTGs included in Table 2, the individual values were obtained from manufacturer's technical information.

The net effect of the dismantling works and the management and valorization of waste, shown in Table 6, was considered in the costs associated with repowering.

4.3. Operation works

The operation works are those necessary to keep the WF that is in commercial operation in optimal technical and safety conditions.

Among the operation works, the most important and expensive corresponds with the WTG O&M. This task is normally provided by the manufacturer of the WTGs and usually includes a mechanical availability guarantee.

A request for an updated WTG O&M price was included in the survey carried out among WTG manufactures for this paper. The result is included in Table 8, as well as the scope and the unitary costs for the operation works. The operation works, and therefore, the associated costs, are equal in both cases, for a N-WF and for a Rep-WF because the number of WTGs installed and the balance of plant infrastructures will be the same.

5. Profitability analysis

The substitution of old WTGs will bring environmental benefits [55]. Repowering would also bring important benefits for the entire electricity system, which would be mainly derived from the improved use of energetic sources by means of more efficient WTGs.

According to [56] a reduction in the spot price is expected with the increase of wind energy integration in the Iberian market (Spain and Portugal), while [57] predicts a very small impact in household electricity prices in EU countries. Integration could be favored by repowering due to the change of the old WTGs for ones more adapted to the new technical regulations.

Nevertheless, in a liberalized market, as that which exists in Span, the main decision factor for a possible investor to participate in it is the expected profitability, which is assured by regulatory stability.

Currently, the retributive system based on a FIT is suspended both for new plants and for the repowering of WFs in commercial operations [13]. Thus, as the main objective of this study, it is necessary to search for alternatives to ensure sufficient incomes to make repowering projects profitable.

Table 9
Cash flow calculation method.

	Shareholder cash flow
+	Incomes from electricity remuneration
−	Operating expenses
=	**Gross operating margin (EBITDA)**
−	Depreciation
=	**Earnings before interests and taxes (EBIT)**
−	Financial expenses
=	**Earnings before taxes**
−	Taxes
=	**Earnings after taxes**
+	Depreciation
=	**Yearly cash flow** (CF_z)
+	Cumulative previous year cash flow
=	**Cumulative present year cash flow** (CFA_z)

Table 8
Operation works scope and unitary prices.
Source: Prices for O&M are based on offers received in 2013 from WTG manufacturers and companies that are specialized in the balance of plant O&M services.

Item	Scope, prices and characteristics		Comment
O&M	*WTG*	*50.000€/(WTG × year)*	
	Balance of plant	*125.000€/year*	Roads, substation and evacuation line
Land easements	*WTG*	*3.000€/(MW × year)*	Including assembly areas
Insurance and administration	*Insurance*	*0.50% Incomes*	All risk and Civil Liability. Typically calculated over incomes
	Administration	*0.15*	Typically calculated over incomes
Cost update	*Annual increase of operation costs*	*2*	Estimate based on the trend in the inflation forecast [53,54]

Table 10
Common assumptions in IRR calculation for both scenarios.

Item	Name	Value	Unit	Comment
General	WF power	18	MW	According to Table 1
	Number of WTG	6		Corresponding with 3 MW nameplate power WTG
	Commercial operation year	2015		One year of construction period starting in 2014
Tariff	Average spot price 2013	50.49	€/MWh	Average price from 2013. Source: OMIE [60]
	Annual increase of spot price	2	%	Typically indexed to inflation. Estimate based on the trend in the inflation forecast [53,54]
Electricity generation and losses	Wake losses (W_L)	5	%	Typical
	Electric losses (E_L)	3	%	Estimate. It includes from WTG transformers up to grid connection point
	WTG mechanical availability (F_{AV})	95	%	Current market value. Source: WTG Manufacturers
Taxes	Profit taxes	30	%	
	Income taxes	2	%	The final value depends on council and incomes level. Mean value has been taken into consideration
	VAT	21	%	
Financial terms	Financial leverage (FL)	70	%	Over total costs. Estimate from [61]
	Interest rate	5	%	Annual estimate from [61]
	Loan repayment period	10	years	Typical
	T_{DEP}	10	years	Typical

From an economic point of view, the most favorable solution for the entire electric system would be to pay the spot price for the electricity generated by a WF, being able to provide energy in terms of grid parity. This model is currently being successfully applied in countries with emergent economies (e.g., Chile) even to support projects based in photovoltaic and concentrated solar thermal technologies, which are less efficient than wind energy [58,59].

The retributive system proposed and analyzed in this study is based on the following assumptions:

(1) Maintain the right to export the entire electricity surplus to the electric grid when it is technically feasible.
(2) Participate in the daily electricity market and charge the hourly spot price for the electricity fed into grid.

Under these assumptions, the analysis focused in two aspects: first, if a Rep-WF can provide an interesting profitability opportunity for the investors, being a similar or even better choice than constructing a N-WF, and second, if the retributive proposal is sufficient to ensure profitability.

To achieve this objective, two scenarios were analyzed and compared:

(1) The repowering of an existing WF with the characteristics indicated in Table 1.
(2) The construction of a WF in a new site, taking into consideration the development, construction and operation costs calculated in Section 4. To obtain homogeneous results, the installed power considered in this case has been the same as that considered in scenario 1 but the results are applicable to WFs in the same range of installed power.[8]

In both scenarios, the profitability for the investor was estimated using the internal rate of return (IRR hereinafter) calculated for a period equal to the WTG lifetime – 20 years – considering an external financing source. This return is known as the Shareholder IRR.

Before obtaining the IRR, the cash flows of the investment are calculated following the method described in Table 9.

The net present value (NPV, hereafter) of the investment is calculated from each of the yearly cash flows, discounting back to its present value at the discount rate k, that is

$$\mathrm{NPV} = \sum_{z=1}^{n} \frac{CF_z}{(1+k)^z} - I_o \quad (3)$$

where I_o is the portion of the total cost assumed by the investor, with its value depending on the Financial Leverage (FL hereinafter)[9]:

$$I_o = \mathrm{FL} \times \text{Total Cost} = \mathrm{FL} \times (\text{Development cost} + \text{Construction cost}) \quad (4)$$

IRR is defined as the interest rate k at which the NPV is zero, that is

$$0 = \sum_{z=1}^{n} \frac{CF_z}{(1+\mathrm{IRR})^z} - I_o \quad (5)$$

The common assumptions in the IRR calculations for both scenarios are detailed in Table 10.

The particular assumptions in the IRR calculations for each scenario are detailed and distinguished in Table 11.

Fig. 13 shows the variation of IRR as a function of CF in both scenarios analyzed. It can be observed that

(1) The IRR for a Rep-WF is independent of the CF and higher than the IRR for a N-WF because the total costs for the development and construction are lower, mainly due to the reuse of the electric infrastructure – substation and evacuation line.
(2) The IRR for a Rep-WF, with the increase of the CF after the repowering calculated in Section 3 (approximately 46% of the gross value or 40% of the net value), is greater than the IRR for a N-WF with the current expected value of CF (approximately 31% of the gross value or 27% of the net value).
(3) The IRR for a Rep-WF, with the increase of the CF and charging the spot price for the electricity generated, is even better than the IRR for the construction of a N-WF with the current expected value of CF (approximately 31% of the gross value or 27% of the net value).

[8] According with the Spanish regulation there is a limit for the installed power of RES facilities. For WFs this limit is of 50 MW.

[9] The financial leverage (FL) is the percentage of the investment financed with an external resource or debt.

Table 11
Particular assumptions in IRR calculations.

Item	Name	New WF		Rep WF		Comment
		Value	Unit	Value	Unit	
Costs	Development – total	19.28	€/kW	14.83	€/kW	According to calculations in Section 4
	Construction – total	1088.80	€/kW	968.57	€/kW	
	Dismantling and valorizations – net effect	0.00	€/kW	41.61	€/kW	
Electricity generation and losses	Gross CF	31	%	46	%	According to Section 3
	Net CF	27	%	40	%	

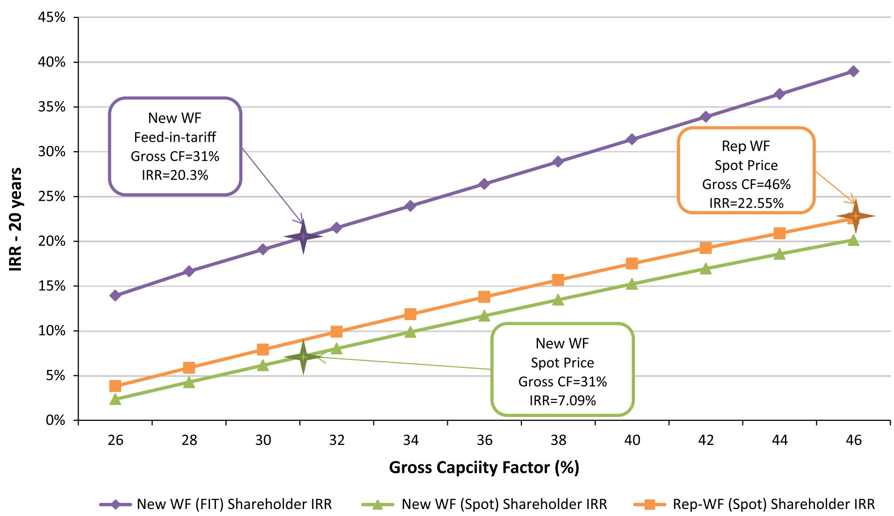

Fig. 13. IRR as a function of the gross CF.

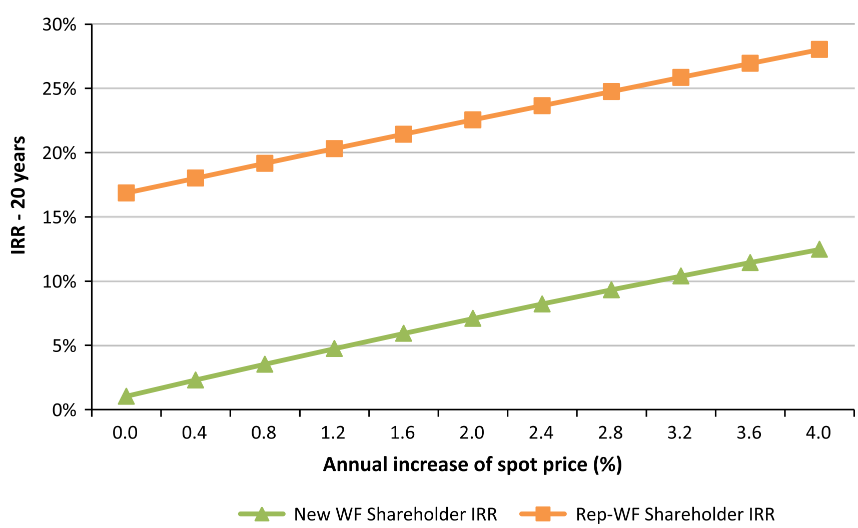

Fig. 14. IRR as a function of the annual increase of the spot price.

5.1. Sensitivity of the IRR results

5.1.1. Sensitivity in relation to incomes

Naturally, the variation of incomes has an important impact on the expected profitability because they are produced recurrently during the entire WF lifetime and provide the support to repay the debt. The path of growth estimated in the IRR calculations for the spot price, and thus for incomes, was 2% (annual increase of the spot price in Table 10 but the estimates made by the European Union exceed this value, foreseeing yearly increases of up to 15% [62]).

Fig. 14 shows the sensitivity of the expected IRR in relation to the variation of the trajectory of growth for the spot price. The sensitivity curve was obtained by varying the “Annual increase of spot price” value (Table 10) between 0% and 4%, keeping the rest of the assumptions fixed.

5.1.2. Sensitivity in relation to the costs

The WTG represents the most important cost in the construction of the WF, hence the sensitivity of the IRR in relation to the costs was focused in the variation of the WTG cost.

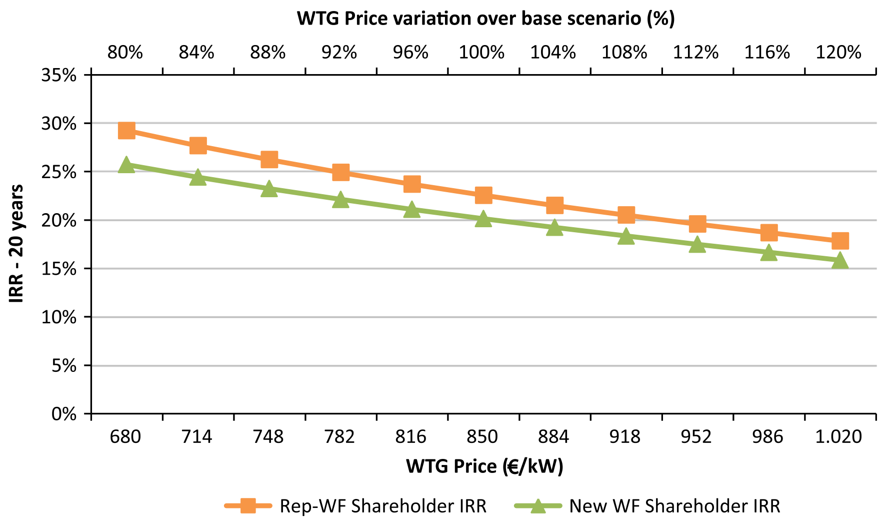

Fig. 15. IRR as a function of the WTG price.

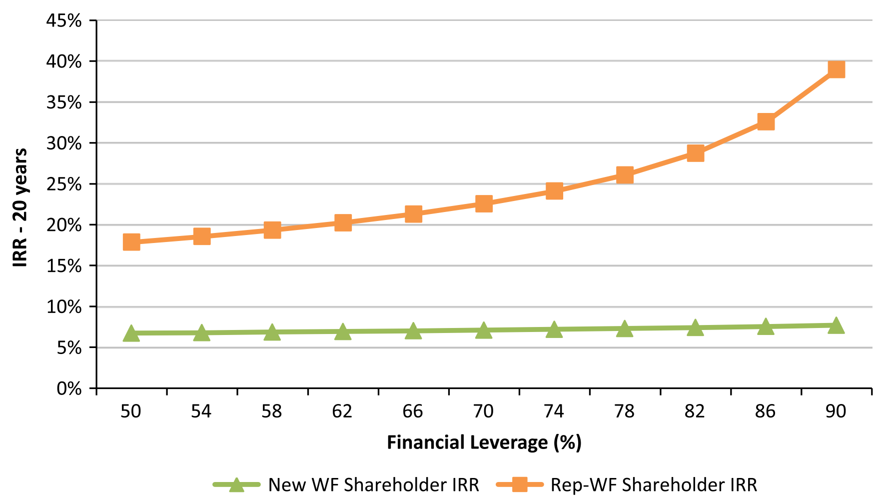

Fig. 16. IRR as a function of the FL for both scenarios.

Fig. 15 shows the IRR as a function of the WTG cost. The curve was obtained by varying the price for the WTG in the base scenario (Table A2) while keeping the other costs and assumptions fixed.

5.1.3. *Sensitivity in relation to the FL*

A way to improve the Shareholder IRR consists of obtaining better conditions in the Project Finance. This solution would not result in extra costs for the electric system due to an increase of the price for the electricity generated by means of a FIT or bonus over the spot price. Among these conditions, the variation of FL has the greatest effect.

Fig. 16 shows the IRR as a function of the FL. The curve was obtained by varying the value for FL (Table 10) between 50% and 90% while keeping other assumptions fixed. A low sensitivity of the IRR for the N-WF was indicated because the IRR is too low in the base case and the variation of FL does not have a perceptible effect. However, for the Rep-WF, the figure indicates how important growth can be obtained by improving the financial conditions without increasing the price for the energy fed into the grid.

5.1.4. *Sensitivity in relation to taxes*

Among the taxes applied to the activity of the generation of electricity during commercial operation, the most important, due to its value, is the profit tax.

Fig. 17 shows the IRR as a function of the profit tax that was obtained by varying its value (Table 10 over the range of 10% and 30% and keeping the rest of assumptions fixed). It can be observed that the sensitivity of the IRR is not significant in this case; therefore, the reduction of the tax burden will not have a relevant effect in the decision to go ahead with repowering.

6. Conclusions

In light of all that has been accomplished in this work, the investment in the repowering of a WF can be more profitable than investing in a N-WF if the new WTGs are properly selected according to the wind resources at the site and if the facilities for the extraction of the electricity generated are reused.

The total cost is lower for a Rep-WF, even when considering the costs for dismantling the older WTGs because these dismantling costs are considerably reduced by the incomes obtained from the valorization of the valuable waste.

For an old WF with wind resources greater than those recently made or than the sites currently available, the repowering with new WTGs, which are more efficient and technologically advanced, enables a better use of the wind. This fact allows a Rep-WF to sell the energy produced at the spot price, offering a

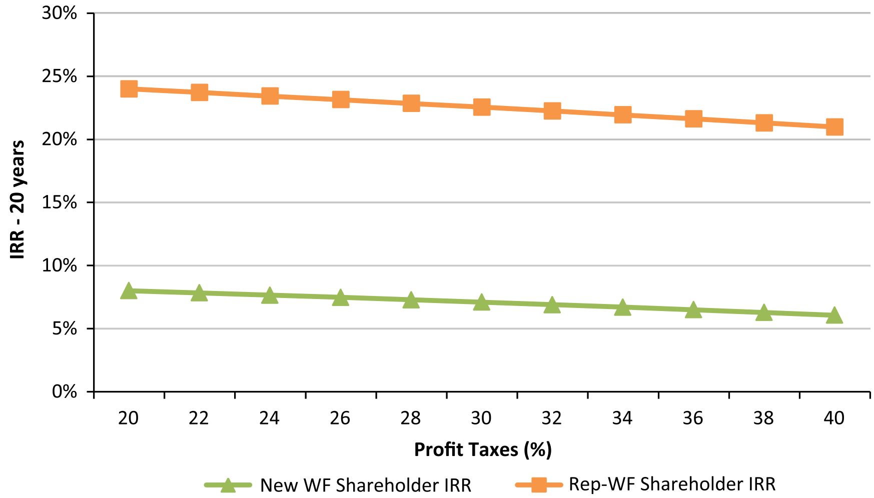

Fig. 17. IRR as a function of the profit taxes for both scenarios.

similar or even better profitability than a N-WF, with a CF that is much lower than that with a retributive system based on a FIT.

Currently, there is a market for repowering of approximately 2.3 GW of installed power in the entire Spanish territory with a period in commercial operation equal to or greater than 13 years. This volume will increase in the next few years – at a rate of approximately 1 GW per year – as electricity generation plants age.

Profitability is strongly subject to the electricity price; thus, the mid-term stability of the price or the possibility to forecast its evolution could make an important contribution in the decision to implement repowering. Nevertheless, there are solutions capable of providing security to investors: bilateral contracts for selling energy to consumers or traders and new products offered for insurance companies to ensure a minimum value in case the spot price decreases below the minimum value. These solutions are successfully being used in emerging markets to finance RES power plants.

Repowering requires a specific framework that is both technical and retributive, which should be taken into consideration in the next Spanish regulation implemented to allow participation in the daily market and to fit the characteristics of the technology. In addition, legal measurements can be established to improve profitability without an extra cost for the entire electric system by facilitating the access to financial credits for the investors. These measurements should be aimed at providing stability to the incomes and legal security in the long-term for the investment. In this way, investors will be more willing to commit funds to develop Rep-WF projects.

In summary, the repowering approach appears to be a real and feasible option for relaunching the integration of RESs into the Spanish energy mix. In the current situation, due to the lack of specific regulation, an adequate policy framework would enable the development of a large-sized market with sustainable growth in the short term. In addition, the electricity produced by Rep-WFs would be included in the electric market in the condition of grid parity, implying important savings for the entire system with respect to the retributive system based on a FIT applied to the WFs suitable for repowering to date.

Acknowledgments

The authors especially thank the following people for their contributions: Mr. Sergio Robles (Indra), Mr. José Carlos Bustos (Gamesa), Mr. David Gómez de Lucas and Mr. José Carlos García Sánchez (Isolux Ingeniería), Mr. Claudio Cortina (Aguado Wind), Mr. José Luis del Cerro Rico (Vestas Mediterranean) and Mr. Josep-María Borrell (Alstom Wind).

Appendix A. Detailed calculation of the development and construction costs

For the purposes of this paper, during the year 2013 a survey was carried out among several international companies specializing in the different procedures necessary for the construction and operation of a WF.

To make the estimations, technical requirements and bills of quantities were delivered to all the requested companies. All of this documentation was performed considering the WF characteristics determined by simulations (Table 1) and the scope of works established in Section 4.

The results of the survey for development and construction costs are included in the following tables for a WF of 20 MW. Nevertheless, the figures are applicable to WFs in the same installed power range.

Table A1 details the scope of the development and their associated costs.

Table A2 shows in detail the scope of the construction and the average costs associated.

Table A1
Development scope and unitary prices.
Source: Self-elaboration based on the survey carried out among specialized companies in engineering and wind resource measurement and assessment. Prices valid for H2 2013

Item	Scope, prices and characteristics			Comment
Engineering	*Technical project*		*30,000€*	The price includes the definition of the installations (WTG lay-out, power, communication and grounding grid, substation, evacuation line) and the technical specifications, drawings and supplements for informing the institutions and the other services affected.
	Environmental report		*10,000€*	
Wind resource assessment	*Meteo tower rent*		*40,000 €/year*	Includes the logger and the calibrated sensors.
	Height	90 m		
	Measurement heights	60/75/90 m		Includes periodic downloads of the raw data.
	Final report		*7000€*	
Personnel	*Hourly average cost*		*200€/h*	
	Hours of labor	600 h		
	Other personnel costs		*100,000 €*	Travel, etc.

Table A2
Construction scope and unitary prices.
Source: Self-elaboration based on the survey carried out with WTG manufacturers, electric materials suppliers, civil works and electric contractors and specialized companies for permits management. Prices valid for H2 2013

Item	Scope, prices and characteristics			Comment
WTG	*WTG*		*850*	The price includes:
	WTG unitary power	3 MW		Assembly and commissioning
	Number of WTGs	6 units		SCADA
	Hub height (HH)	90 m		Systems for controlling reactive power and generation
	Rotor diameter	90 m		
Meteorological mast	*Meteo mast*		*70,000*	Includes logger and calibrated sensors
	Height	90 m		
	Measurement heights	60/75/90 m		
Foundations and assembly areas	*Foundation*		*160,000*	Structural concrete: 430 m^3
	Foundation dimensions	$15 \times 15 \times 2$ m^3		Steel bars: 25 t
	Assembly area		*25*	Includes clearance, excavation, levelling and refilling with the appropriate material
	Dimensions	40×50 m^2		
Roads	*Construction of new roads*		*150*	Includes clearance, excavation, levelling and refilling with the appropriate material
	Average distance between WTG (three times rotor diameter)	270 m		
	Access road length	1500 m		Includes storm water trenches
	Services road length	1620 m		
	Adaptation of existing roads		*100*	
P&C&G grid	*Civil works*		*100*	Includes excavation, signalisation and refilling with the appropriate material
	Trenches length	2025 m		
	MV power cables		*15€/m*	Includes terminations, junctions and connections
	Maximum current per sub-circuit	630 A		
	Circuits number	2		
	Length	2430		
	Optical fiber cables		*6€/m*	Includes terminations, junctions and connections
	Type	Single-mode		
	Length	2025 m		
	Grounding cables		*12€/m*	Includes terminations, junctions and connections
	Section	50 m		
	Length	2025 m		
Substation	*High voltage EPC price*		*550,000 €*	The price includes an outdoor bay for line and transformer protection fully equipped and a control building
	High voltage level	132 kV		
	Medium voltage EPC price		*150,000 €*	Includes the following MV switchgears: bars measurement, transformer protection, line from WTG protection and auxiliary services transformer protection
	Medium voltage level	33 kV		
	Transformer price		*300,000 €*	ONAN/OFAF refrigeration
	Main transformer power	20 MVA		Equipped with on-load tap changer
Evacuation line	*EPC price*		*125,000 €/km*	Overhead line single circuit
	Voltage level	132 kV		Includes a fiber optic cable for communications installed in the earth

Table A2 (*continued*)

Item	Scope, prices and characteristics			Comment
	Length	5 km		
Construction and land owners permits	*County construction license*		*2%*	Percentage to be applied over labor and construction costs
	Urban license		*2.5%*	Percentage to be applied over the total cost
	Land owners permits			
	Road and trenches		6€/m^2	
	Typical roads width	6 m		
	Typical trenches width	1 m		
	Evacuation line – overhead cables		1€/m^2	
	Typical width	40 m		
	Evacuation line – pylon		5€/m^2	
	Used area per pylon	100 m^2		
	Number of pylons	33 units		One pylon every 150 m

References

[1] Jefatura del Estado. Gobierno de España. Ley 54/1997, de 27 de noviembre, del Sector Eléctrico; 1997.
[2] del Río P, Gual MA. An integrated assessment of the feed-in tariff system in Spain. Energy Policy 2007;35:994–1012.
[3] Ciarreta A, Gutiérrez-Hita C, Nasirov S. Renewable energy sources in the Spanish electricity market: Instruments and effects. Renew Sustain Energy Rev 2011;15:2510–9.
[4] Schallenberg-Rodriguez J, Haas R. Fixed feed-in tariff versus premium: a review of the current Spanish system. Renew Sustain Energy Rev 2012;16:293–305.
[5] Iglesias G, del Río P, Dopico JÁ. Policy analysis of authorisation procedures for wind energy deployment in Spain. Energy Policy 2011;39:4067–76.
[6] Red Eléctrica de España. El mercado eléctrico español en 2012; 2013.
[7] Ministerio de Industria, Energía y Turismo. Gobierno de España. La energía en España 2011; 2012.
[8] IDAE. Ministerio de Industria, Turismo y Comercio. Gobierno de España. Plan de Energías Renovables 2011–2020; 2011.
[9] Rivier Abbad J. Electricity market participation of wind farms: the success story of the Spanish pragmatism. Energy Policy 2010;38:3174–9.
[10] Burgos-Payán M, Roldán-Fernández JM, Trigo-García ÁL, Bermúdez-Ríos JM, Riquelme-Santos JM. Costs and benefits of the renewable production of electricity in Spain. Energy Policy 2013;56:259–70.
[11] Gil HA, Gomez-Quiles C, Riquelme J. Large-scale wind power integration and wholesale electricity trading benefits: estimation via an ex post approach. Energy Policy 2012;41:849–59.
[12] Comisión Nacional de la Energía 2013; 2013.
[13] Jefatura del Estado. Gobierno de España. Real Decreto-Ley 1/2012 de 27 de enero, por el que se procede a la suspensión de los procedimientos de preasignación de retribución y a la supresión de los incentivos económicos para nuevas instalaciones de producción de energía eléctrica; 2012.
[14] Ruiz Romero S, Colmenar Santos A, Castro Gil MA. EU plans for renewable energy. An application to the Spanish case. Renew Energy 2012;43:322–30.
[15] Toja-Silva F, Colmenar-Santos A, Castro-Gil M. Urban wind energy exploitation systems: Behaviour under multidirectional flow conditions – opportunities and challenges. Renew Sustain Energy Rev 2013;24:364–78.
[16] Ruiz-Romero S, Colmenar-Santos A, Gil-Ortego R, Molina-Bonilla A. Distributed generation: the definitive boost for renewable energy in Spain. Renew Energy 2013;53:354–64.
[17] Colmenar-Santos A, Campíñez-Romero S, Pérez-Molina C, Castro-Gil M. Profitability analysis of grid-connected photovoltaic facilities for household electricity self-sufficiency. Energy Policy 2012;51:749–64.
[18] Gómez A, Zubizarreta J, Dopazo C, Fueyo N. Spanish energy roadmap to 2020: socioeconomic implications of renewable targets. Energy 2011;36:1973–85.
[19] Ortegon K, Nies LF, Sutherland JW. Preparing for end of service life of wind turbines. J Clean Prod 2013;39:191–9.
[20] del Río P, Calvo Silvosa A, Iglesias Gómez G. Policies and design elements for the repowering of wind farms: a qualitative analysis of different options. Energy Policy 2011;39:1897–908.
[21] Joselin Herbert GM, Iniyan S, Amutha D. A review of technical issues on the development of wind farms. Renew Sustain Energy Rev 2014;32:619–41.
[22] Tabassum-Abbasi, Premalatha M, Abbasi T, Abbasi SA. Wind energy: increasing deployment, rising environmental concerns. Renew Sustain Energy Rev 2014;31:270–88.
[23] Asociación Empresarial Eólica. Eólica 2013; 2013.
[24] International Electrotechnical Commission. IEC 61400-1. Wind Turbines. Part 1: Design requirements; 2005.
[25] García López MJ, López Quero M, Avilés Palacios C. La Articulación De UnProject Finance Como Instrumento De Financiación De Parques Eólicos. In: Anonymous Estableciendo puentes en una economía global, Escuela Superior de Gestión Comercial y Marketing, ESIC; 2008.
[26] Pollio G. Project finance and international energy development. Energy Policy 1998;26:687–97.
[27] European Wind Energy Association. Pure Power. Wind energy targets for 2020 and 2030; 2011.
[28] Staffell I, Green R. How does wind farm performance decline with age? Renew Energy 2014;66:775–86.
[29] Foley AM, Leahy PG, Marvuglia A, McKeogh EJ. Current methods and advances in forecasting of wind power generation. Renew Energy 2012;37:1–8.
[30] Kusiak A, Zhang Z, Verma A. Prediction, operations, and condition monitoring in wind energy. Energy 2013;60:1–12.
[31] Gallardo-Calles J, Colmenar-Santos A, Ontañon-Ruiz J, Castro-Gil M. Wind control centres: state of the art. Renew Energy 2013;51:93–100.
[32] Blanco MI. The economics of wind energy. Renew Sustain Energy Rev 2009;13:1372–82.
[33] Asociación Empresarial Eólica. Eólica 2011; 2011.
[34] Asociación Empresarial Eólica. Eólica 2012; 2012.
[35] Asociación Empresarial Eólica. Eólica 2004; 2004.
[36] Betz A. Introduction to the theory of flow machines. Karlsruhe: G. Braun GmbH; .
[37] Carta González JA, Calero Pérez R, Colmenar Santos A, Castro Gil M. Centrales De Energías Renovables: Generación Eléctrica Con Energía Renovables Pearson Educación, S.A.: Madrid; 2009.
[38] IDAE. Ministerio de Industria, Turismo y Comercio. Gobierno de España. Spanish Wind Maps; 2013.
[39] Gamesa; 2014.
[40] Vestas; 2014.
[41] Alstom; 2014.
[42] Windographer. Windographer; 2013.
[43] González-Longatt F, Wall P, Terzija V. Wake effect in wind farm performance: steady-state and dynamic behavior. Renew Energy 2012;39:329–38.
[44] Amenedo Rodríguez JL, Burgos Díaz JC, Arnalte Gómez S. Sistemas Eólicos De Producción De Energía Eléctrica Rueda; 2003.
[45] International Renewable Energy Agency (IRENA). Renewable Energy Technologies: Cost Analysis Series. Volume 1: Power Sector. Issue 5/5. Wind Power; 2012. p. 1.
[46] Wiser R, Bolinger M. 2012 Wind Technologies Market Report; 2013.
[47] Serrano González J, Burgos Payán M, Santos JMR, González-Longatt F. A review and recent developments in the optimal wind-turbine micro-siting problem. Renew Sustain Energy Rev 2014;30:133–44.
[48] Turner SDO, Romero DA, Zhang PY, Amon CH, Chan TCY. A new mathematical programming approach to optimize wind farm layouts. Renew Energy 2014;63:674–80.
[49] European Ferrous Recovery and Recycling Federation. EU-27 Steel Scrap Statistics; 2013.
[50] Observatorio Industrial del Sector del Metal. El sector de reciclaje de metales en España; 2013.
[51] Eurofer. The European Steel Association. Scrap Price Index; 2013.
[52] Scrapmonster. European Scrap Prices; 2013.
[53] PWC. Economic Projections; 2014.
[54] European Commission. Economic and financial affairs. Econ Forecast 2014;2: 35–54.
[55] Iribarren D, Martín-Gamboa M, Dufour J. Environmental benchmarking of wind farms according to their operational performance. Energy 2013;61: 589–97.
[56] Pereira AJC, Saraiva JT. Long term impact of wind power generation in the Iberian day-ahead electricity market price. Energy 2013;55:1159–71.

[57] Moreno B, López AJ, García-Álvarez MT. The electricity prices in the European Union. The role of renewable energies and regulatory electric market reforms. Energy 2012;48:307–13.
[58] Entrevista a Carlos Barriá del Ministerio de Energía de Chile. CSP Today; 2013.
[59] La banca local de Chile se abre con cautela a la financiación de proyectos fotovoltaicos. Energías Renovables; 2013.
[60] OMIE. Operador del Mercado Eléctrico. Polo Español. Resultados del Mercado 2013; 2013.
[61] Kalamova M, Kaminker C, Johnstone N. Source of finance, investment policies and plant entry in the renewable energy sector. OECD Enviroment Working Papers; 2011. p. 37.
[62] European Commission. Directorate General for Energy. EU Energy Trends to 2030; 2009.

ANEXO II: "*REPOWERING: AN ACTUAL POSSIBILITY FOR WIND ENERGY IN SPAIN IN A NEW SCENARIO WITHOUT FEED-IN-TARIFFS*". CERTIFICADO DE PUBLICACIÓN.

ELSEVIER

Renewable & Sustainable Energy Reviews

Certificate of publication for the article titled:

"Repowering: An actual possibility for wind energy in Spain in a new scenario without feed-in-tariffs"

Authored by:

Antonio Colmenar-Santos, Severo Campíñez-Romero
Clara Pérez-Molina, Francisco Mur-Pérez

Published in:

Volume 41C, 2015, Pages 319-337

ANEXO III: "*REPOWERING: AN ACTUAL POSSIBILITY FOR WIND ENERGY IN SPAIN IN A NEW SCENARIO WITHOUT FEED-IN-TARIFFS*". FACTOR DE IMPACTO.

2018 Journal Performance Data for: RENEWABLE & SUSTAINABLE ENERGY REVIEWS

ISSN: 1364-0321
PERGAMON-ELSEVIER SCIENCE LTD
THE BOULEVARD, LANGFORD LANE, KIDLINGTON, OXFORD OX5 1GB, ENGLAND
USA

TITLES
ISO: Renew. Sust. Energ. Rev.
JCR Abbrev: RENEW SUST ENERG REV

LANGUAGES
English

CATEGORIES
GREEN & SUSTAINABLE SCIENCE & TECHNOLOGY - SCIE

ENERGY & FUELS - SCIE

PUBLICATION FREQUENCY
9 issues/year

The data in the two graphs below and in the Journal Impact Factor calculation panels represent citation activity in 2018 to items published in the journal in the prior two years. They detail the components of the Journal Impact Factor. Use the "All Years" tab to access key metrics and additional data for the current year and all prior years for this journal.

2018 Journal Impact Factor & percentile rank in category for: RENEWABLE & SUSTAINABLE ENERGY REVIEWS

10.556
2018 Journal Impact Factor

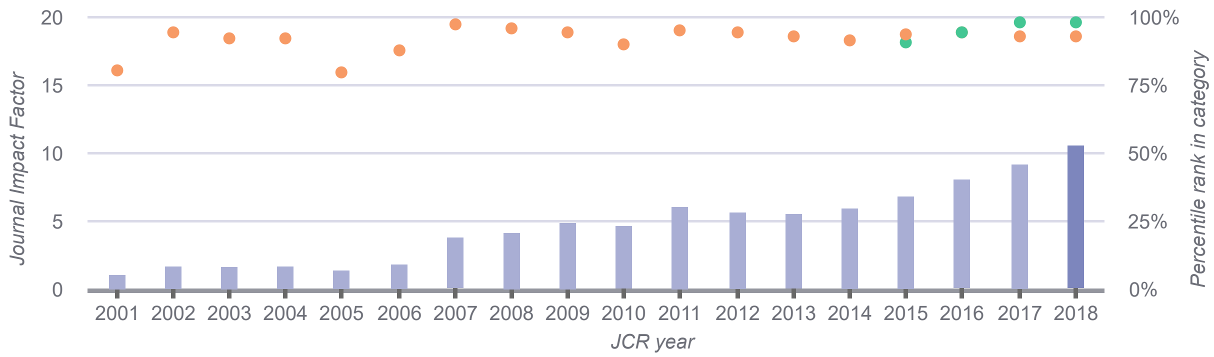

2018 JIF Citation Distribution for: RENEWABLE & SUSTAINABLE ENERGY REVIEWS

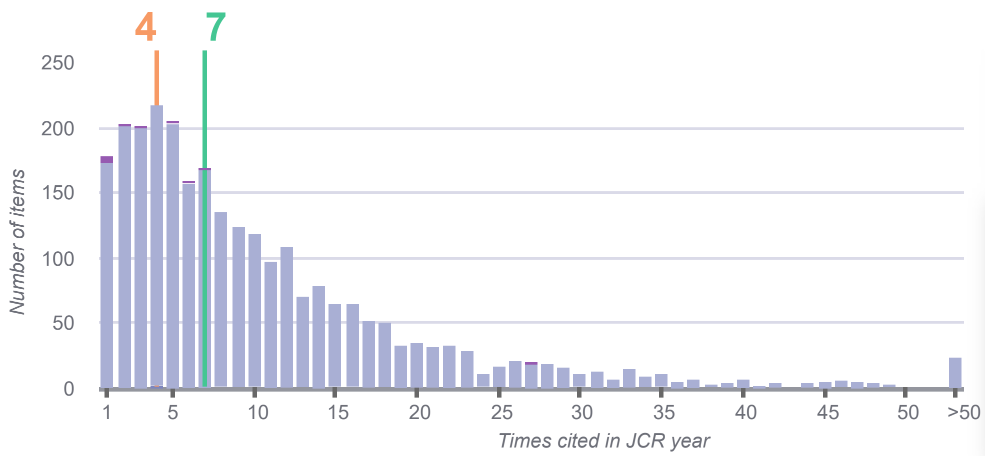

801
Unlinked citations

0
Times Cited

- **0** articles
- **83** reviews
- **21** other

Journal Impact Factor Calculation

$$\text{2018 Journal Impact Factor} = \frac{28{,}986}{2{,}746} = 10.556$$

How is Journal Impact Factor Calculated?

$$\text{JIF} = \frac{\text{Citations in 2018 to items published in } \mathbf{2016\ (15{,}254) + 2017\ (13{,}732)}}{\text{Number of citable items in } \mathbf{2016\ (1{,}321) + 2017\ (1{,}425)}} = \frac{28{,}986}{2{,}746}$$

Journal Impact Factor contributing items

Citable items in 2017 and 2016 (2,746)

TITLE	CITATIONS COUNTED TOWARDS JIF
Review on supercapacitors: Technologies and materials By: Gonzalez, Ander; Goikolea, Eider; Andoni Barrena, Jon; Mysyk, Roman **Volume: 58 Page: 1189-1206 Accession number: WOS:000371948100100** **Document Type: Review**	188
Lignocellulosic biomass pyrolysis: A review of product properties and effects of pyrolysis parameters By: Kan, Tao; Strezov, Vladimir; Evans, Tim J. **Volume: 57 Page: 1126-1140 Accession number: WOS:000370456000082** **Document Type: Review**	134
Hydrogen production from renewable and sustainable energy resources: Promising green energy carrier for clean development By: Hosseini, Seyed Ehsan; Wahid, Mazlan Abdul **Volume: 57 Page: 850-866 Accession number: WOS:000370456000063** **Document Type: Review**	102
Review on dye-sensitized solar cells (DSSCs): Advanced techniques and research trends By: Gong, Jiawei; Sumathy, K.; Qiao, Qiquan; Zhou, Zhengping **Volume: 68 Page: 234-246 Accession number: WOS:000391899200020** **Document Type: Review**	97
A comparative overview of hydrogen production processes By: Nikolaidis, Pavlos; Poullikkas, Andreas **Volume: 67 Page: 597-611 Accession number: WOS:000389088900045** **Document Type: Review**	90
Energy harvesting in wireless sensor networks: A comprehensive review By: Shaikh, Faisal Karim; Zeadally, Sherali **Volume: 55 Page: 1041-1054 Accession number: WOS:000368959200073** **Document Type: Review**	82
A review of lithium-ion battery state of charge estimation and management system in electric vehicle applications: Challenges and recommendations By: Hannan, M. A.; Lipu, M. S. H.; Hussain, A.; Mohamed, A. **Volume: 78 Page: 834-854 Accession number: WOS:000407185900061** **Document Type: Review**	78

Citations in 2018 (28,986)

TITLE	CITATIONS COUNTED TOWARDS JIF
RENEWABLE & SUSTAINABLE ENERGY REVIEWS	2999
ENERGIES	1233
JOURNAL OF CLEANER PRODUCTION	1179
ENERGY	1165
APPLIED ENERGY	1062
ENERGY CONVERSION AND MANAGEMENT	884
SUSTAINABILITY	714
RENEWABLE ENERGY	540
SOLAR ENERGY	493
BIORESOURCE TECHNOLOGY	378

Key Indicators 2018

IMPACT METRICS		
Total Cites	88,430	✓Trend
Journal Impact Factor	10.556	Trend
5 Year Impact Factor	11.239	Trend
Immediacy Index	3.361	Trend
Impact Factor Without Journal Self Cites	9.463	Trend

INFLUENCE METRICS		
Eigenfactor Score	0.13361	Trend
Article Influence Score	1.877	Trend
Normalized Eigenfactor	15.89438	Trend

SOURCE METRICS		
Citable Items	1,118	Trend
% Articles in Citable Items	1.79	Trend
Average JIF Percentile	96.130	Trend
Cited Half-Life	3.9	Trend
Citing Half-Life	6.3	Trend

Metric Trend

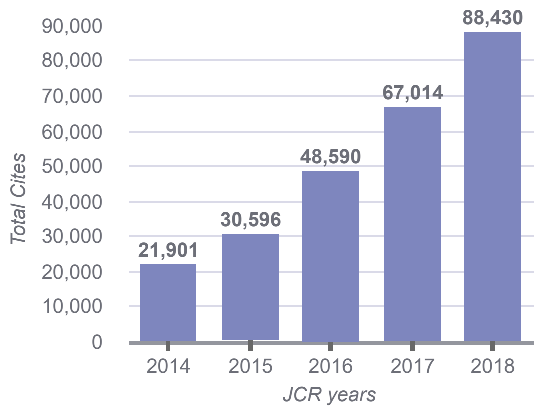

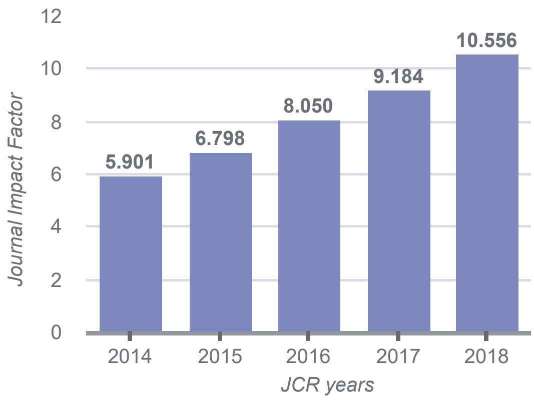

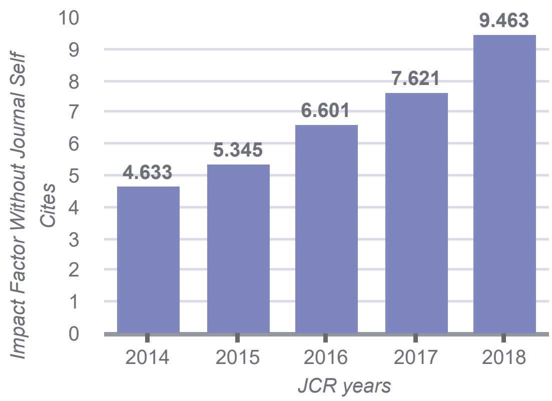

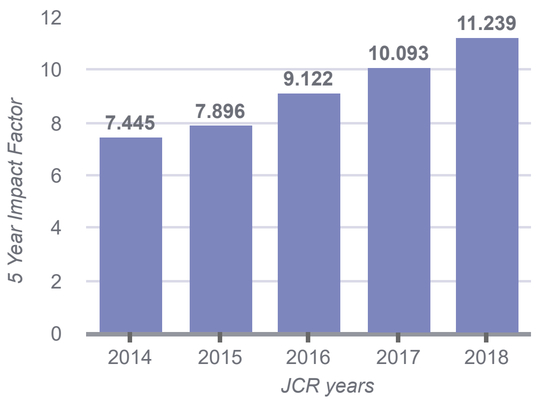

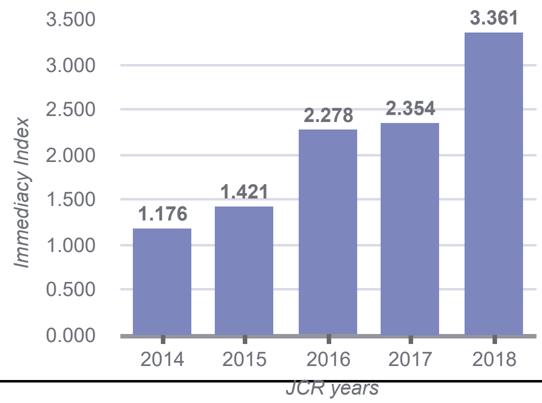

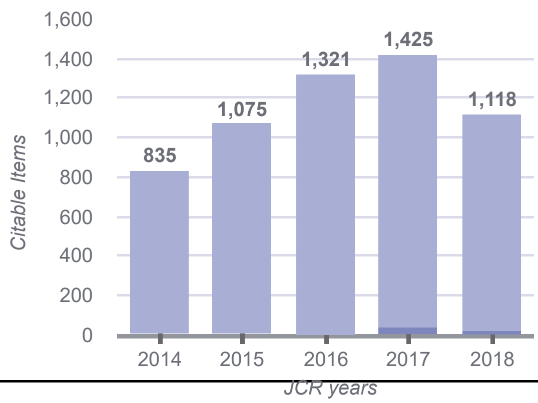

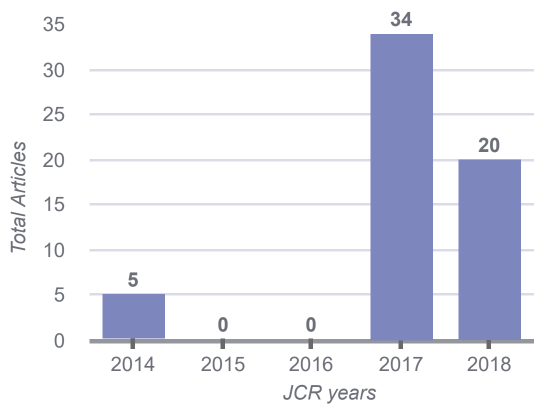
Total Articles
35
30
25
20
15
10
5
0
5
0
0
34
20
2014
2015
2016
2017
2018
JCR years

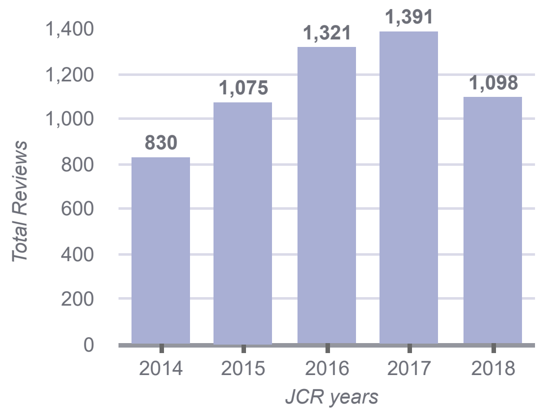
Total Reviews
1,400
1,200
1,000
800
600
400
200
0
830
1,075
1,321
1,391
1,098
2014
2015
2016
2017
2018
JCR years

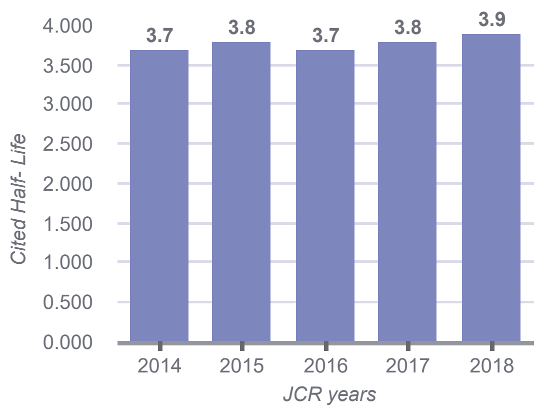
Cited Half- Life
4.000
3.500
3.000
2.500
2.000
1.500
1.000
0.500
0.000
3.7
3.8
3.7
3.8
3.9
2014
2015
2016
2017
2018
JCR years

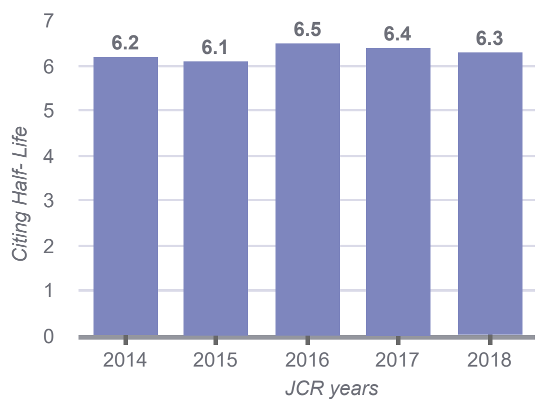
Citing Half- Life
7
6
5
4
3
2
1
0
6.2
6.1
6.5
6.4
6.3
2014
2015
2016
2017
2018
JCR years

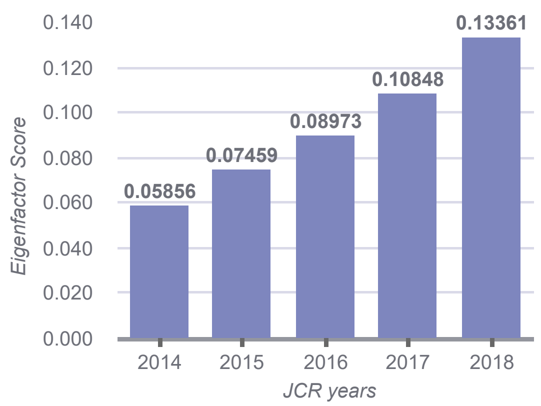
Eigenfactor Score
0.140
0.120
0.100
0.080
0.060
0.040
0.020
0.000
0.05856
0.07459
0.08973
0.10848
0.13361
2014
2015
2016
2017
2018
JCR years

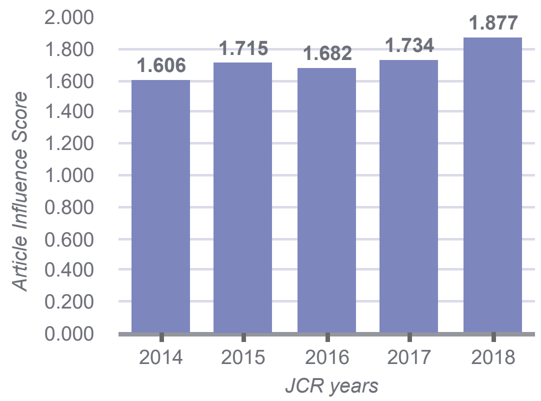
Article Influence Score
2.000
1.800
1.600
1.400
1.200
1.000
0.800
0.600
0.400
0.200
0.000
1.606
1.715
1.682
1.734
1.877
2014
2015
2016
2017
2018
JCR years

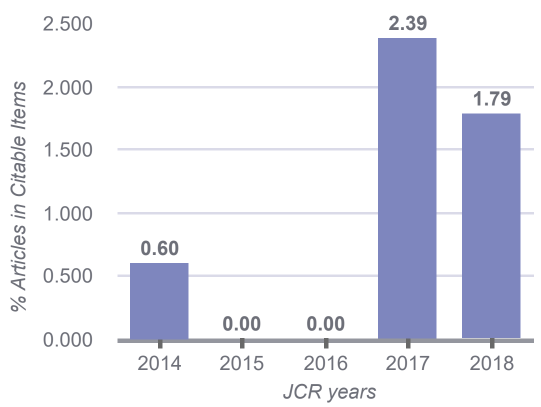
% Articles in Citable Items
2.500
2.000
1.500
1.000
0.500
0.000
0.60
0.00
0.00
2.39
1.79
2014
2015
2016
2017
2018
JCR years

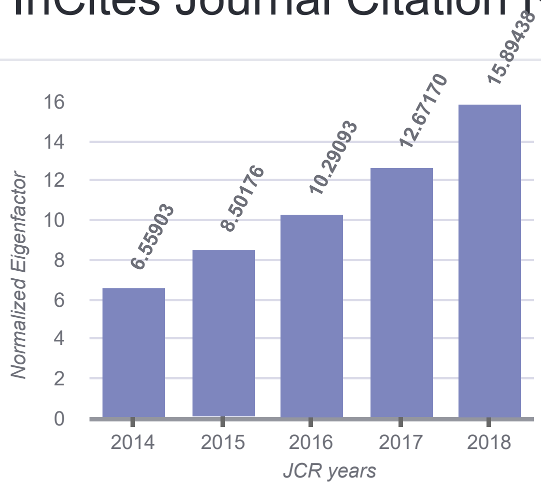
16
14
12
10
8
6
4
2
0
Normalized Eigenfactor
6.55903
8.50176
10.29093
12.67170
15.89438
2014
2015
2016
2017
2018
JCR years

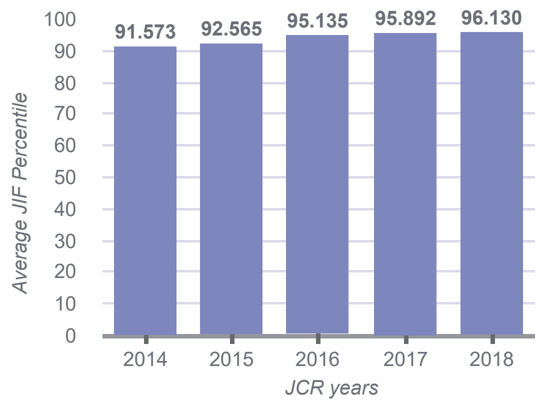
100
90
80
70
60
50
40
30
20
10
0
Average JIF Percentile
91.573
92.565
95.135
95.892
96.130
2014
2015
2016
2017
2018
JCR years

Source data

Journal source data 2018

	Articles	Reviews	Combined(C)	Other(O)	Percentage(C/(C+O))
Number in JCR Year 2018 (A)	20	1,098	1,118	27	97%
Number of References (B)	1,203	114,869	116,072	183	99%
Ratio (B/A)	60.2	104.6	103.8	6.8	

Box plot

Category Box Plot 2018

Category Box Plot

The category box plot depicts the distribution of Impact Factors for all journals in the category. The horizontal line that forms the top of the box is the 75th percentile (Q1). The horizontal line that forms the bottom is the 25th percentile (Q3). The horizontal line that intersects the box is the median Impact Factor for the category.
Horizontal lines above and below the box, called whiskers, represent maximum and minimum values.
The top whisker is the smaller of the following two values:
the maximum Impact Factor (IF)
Q1 IF + 3.5(Q1 IF - Q3 IF)
The bottom whisker is the larger of the following two values:
the minimum Impact Factor (IF)
Q1 IF - 3.5(Q1 IF - Q3 IF)
Box Plots are provided for the current JCR year for each of the categories in which the journal is indexed.

RENEW SUST ENERG REV, IF: 10.556

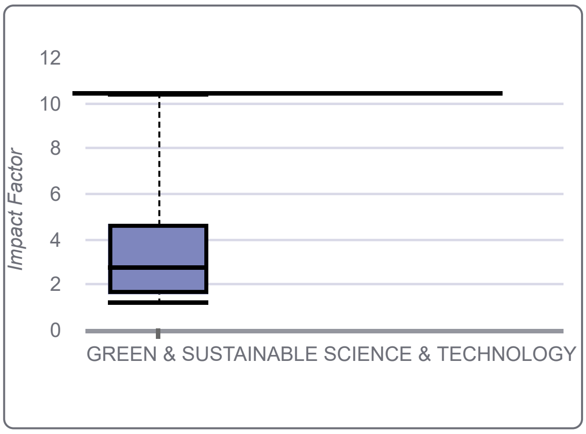

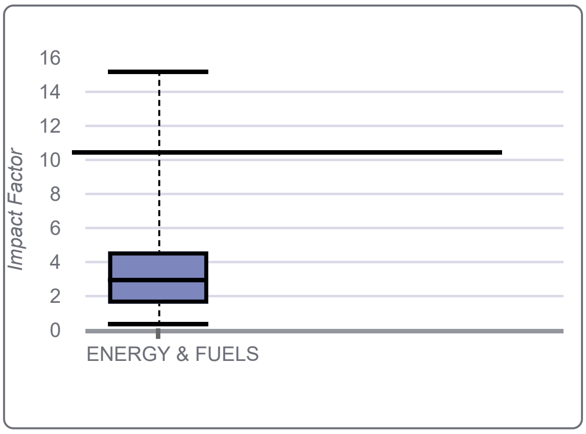

Rank

Rank

JCR Impact Factor

JCR Year	GREEN & SUSTAINABLE SCIENCE & TECHNOLOGY			ENERGY & FUELS		
	Rank	Quartile	JIF Percentile	Rank	Quartile	JIF Percentile
2018	1/35	Q1	98.571	7/103	Q1	93.689
2017	1/33	Q1	98.485	7/97	Q1	93.299
2016	2/31	Q1	95.161	5/92	Q1	95.109
2015	3/29	Q1	91.379	6/88	Q1	93.750
2014	N/A	N/A	N/A	8/89	Q1	91.573
2013	N/A	N/A	N/A	6/83	Q1	93.373
2012	N/A	N/A	N/A	5/81	Q1	94.444
2011	N/A	N/A	N/A	4/81	Q1	95.679
2010	N/A	N/A	N/A	8/79	Q1	90.506
2009	N/A	N/A	N/A	4/71	Q1	95.070
2008	N/A	N/A	N/A	3/67	Q1	96.269
2007	N/A	N/A	N/A	2/64	Q1	97.656
2006	N/A	N/A	N/A	8/62	Q1	87.903
2005	N/A	N/A	N/A	13/63	Q1	80.159
2004	N/A	N/A	N/A	5/61	Q1	92.623
2003	N/A	N/A	N/A	5/62	Q1	92.742
2002	N/A	N/A	N/A	4/63	Q1	94.444
2001	N/A	N/A	N/A	13/66	Q1	81.061

ESI Total Citations

Rank

JCR Year	ENGINEERING	ENVIRONMENT/ECOLOGY
2018	3/893-Q1	n/a
2017	5/867-Q1	n/a
2016	6/861-Q1	n/a
2015	12/850-Q1	12/338-Q1
2014	n/a	18/324-Q1
2013	n/a	26/312-Q1

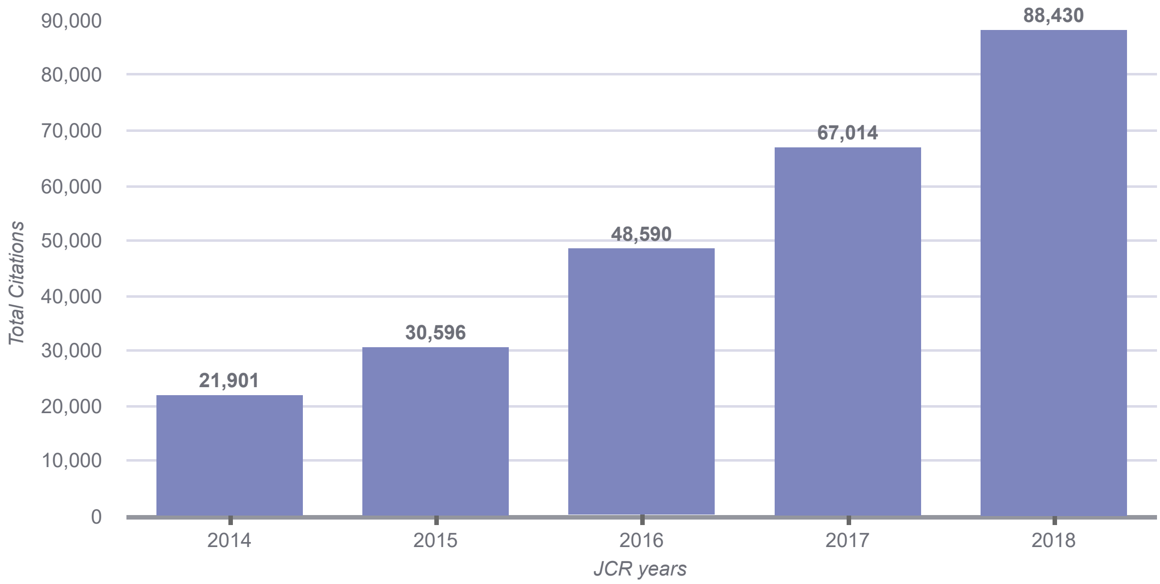

Cited Journal Data

Cited Half-Life Data

Cited Year	2018	2017	2016	2015	2014	2013	2012	2011	2010	2009	2008-All
#Cites from 2018	3,758	13,732	15,254	12,983	10,460	8,169	6,152	5,481	4,269	3,259	4,913
Cumulative %	4.25%	19.78%	37.03%	51.71%	63.54%	72.78%	79.73%	85.93%	90.76%	94.44%	100.00%

Cited Journal Graph 2018

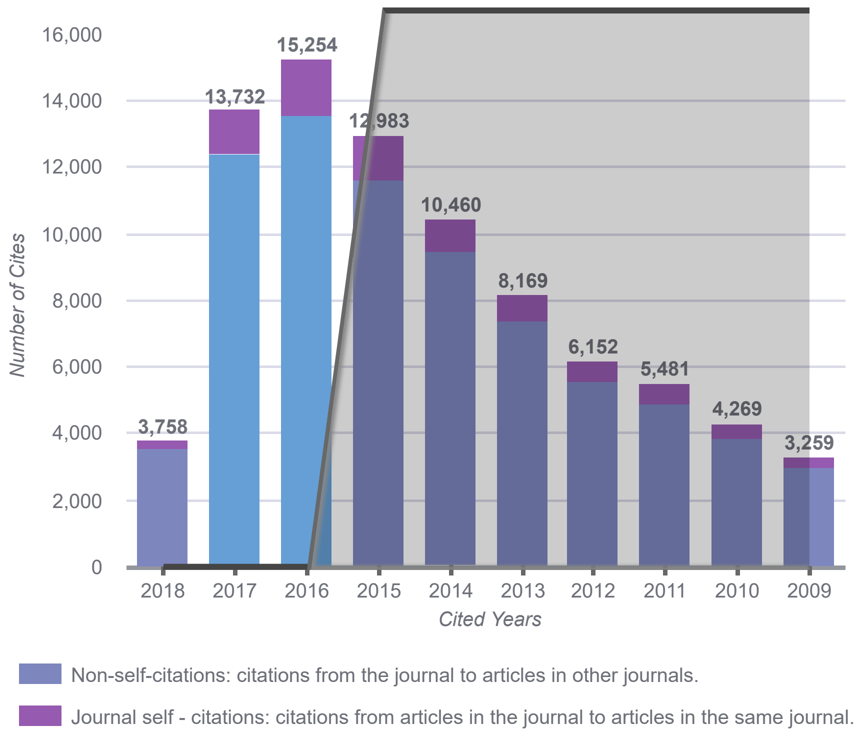

CITED JOURNAL GRAPH

The Cited Journal Graph shows the distribution (by cited year) of citations published in journals during the JCR year to items published in the Journal during the last 10 years.

The white/grey division indicates the cited half-life (if < 10.0). Half of the citations are to items that were published more recently than the cited half-life.

The two light-blue columns indicate citations used to calculate the Impact Factor (always the 2nd and 3rd columns).

Cited Journal Data 2018

	Impact	Citing Journal	All Yrs	2018	2017	2016	2015	2014	2013	2012	2011	2010	2009	Rest
		ALL Journals	88,430	3,758	13,732	15,254	12,983	10,460	8,169	6,152	5,481	4,269	3,259	4,913
		ALL OTHERS (1216)	1,216	39	160	212	173	181	106	93	62	69	51	70
1	10.556	RENEW SUST ENERG REV	8,594	212	1,322	1,677	1,314	955	794	598	584	393	301	444
2	2.707	ENERGIES	3,600	292	626	607	515	399	292	228	188	155	139	159
3	5.537	ENERGY	3,292	156	583	582	478	365	268	251	173	129	125	182
4	6.395	J CLEAN PROD	3,272	135	607	572	537	387	341	208	175	106	92	112
5	8.426	APPL ENERG	3,047	180	525	537	440	405	267	195	149	126	103	120
6	7.181	ENERG CONVERS MANAGE	2,323	169	487	397	300	235	201	148	133	102	57	94
7	5.439	RENEW ENERG	2,054	25	202	338	322	246	221	179	151	133	105	132
8	2.592	SUSTAINABILITY-BASEL	1,994	152	358	356	309	240	156	118	116	62	57	70
9	4.674	SOL ENERGY	1,414	93	253	240	210	133	162	78	73	83	44	45
10	4.026	APPL THERM ENG	1,212	41	170	206	157	138	119	72	102	66	63	78
11	4.084	INT J HYDROGEN ENERG	1,123	79	206	159	199	130	71	74	38	30	27	110
12	6.669	BIORESOURCE TECHNOL	1,097	49	194	184	168	154	103	60	65	76	20	24
13	4.880	ENERG POLICY	1,025	28	152	182	168	155	93	62	63	35	32	55
14	4.495	ENERG BUILDINGS	1,018	40	184	171	109	138	106	90	58	26	60	36
15	2.914	ENVIRON SCI POLLUT R	897	34	198	177	171	75	100	46	30	33	10	23
16	5.128	FUEL	828	21	140	139	96	91	91	76	75	38	23	38
17	4.624	SUSTAIN CITIES SOC	609	20	108	115	106	64	55	36	36	21	23	25
18	4.098	IEEE ACCESS	535	41	129	126	74	59	29	24	12	14	14	13
19	4.346	INT J HEAT MASS TRAN	493	13	77	83	60	52	38	30	42	34	26	38
20		GREEN ENERGY TECHNOL	455	5	77	57	65	64	36	39	25	37	19	31
21	1.511	J RENEW SUSTAIN ENER	449	20	73	72	66	46	30	48	25	26	17	26
22	3.021	ENERG FUEL	424	27	72	57	63	60	36	21	36	13	10	29
23	2.217	APPL SCI-BASEL	410	41	69	71	49	40	25	32	29	14	20	20
24	5.431	WASTE MANAGE	409	16	57	73	61	71	31	35	26	15	7	17
25	3.343	INT J ENERG RES	401	8	47	86	50	44	36	28	27	20	23	32
26	4.820	BUILD ENVIRON	395	32	71	68	45	59	34	17	27	15	16	11

Showing 1 - 28 rows of 2,713 total

Citing Journal Data

Citing Half-Life Data

Citing Year	2018	2017	2016	2015	2014	2013	2012	2011	2010	2009	2008-All
#Cites from 2018	1,049	7,088	12,713	12,790	11,464	10,097	8,375	7,968	6,388	5,376	32,947
Cumulative %	0.90%	7.00%	17.93%	28.94%	38.80%	47.48%	54.69%	61.54%	67.04%	71.66%	100.00%

Citing Journal Graph 2018

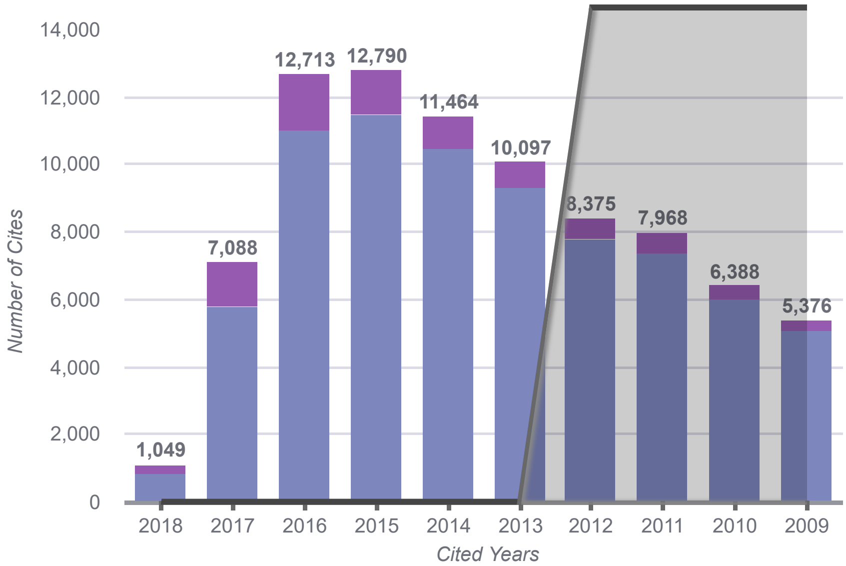

Non-self-citations: citations from the journal to articles in other journals.

Journal self - citations: citations from articles in the journal to articles in the same journal.

CITING JOURNAL GRAPH

The Citing Journal Graph shows the distribution (by cited year) of citations published in the Journal during the JCR year to items published in journals during the last 10 years.

The white/grey division indicates the citing half-life (if < 10.0). Half of the citations are to items that were published more recently than the citing half-life.

Citing Journal Data 2018

	Impact	Cited Journal	All Yrs	2018	2017	2016	2015	2014	2013	2012	2011	2010	2009	Rest
		ALL Journals	116,255	1,049	7,088	12,713	12,790	11,464	10,097	8,375	7,968	6,388	5,376	32,947
		ALL OTHERS (22870)	22,870	162	1,029	2,225	2,254	1,958	1,741	1,624	1,422	1,194	941	8,320
1	10.556	RENEW SUST ENERG REV	8,594	212	1,322	1,677	1,314	955	794	598	584	393	301	444
2	8.426	APPL ENERG	3,082	40	286	482	465	432	335	224	254	217	137	210
3	4.880	ENERG POLICY	2,909	19	104	183	139	238	368	332	281	310	188	747
4	5.537	ENERGY	2,678	34	199	345	382	369	252	257	216	167	71	386
5	5.439	RENEW ENERG	2,625	59	230	411	272	215	201	144	156	119	165	653
6	6.669	BIORESOURCE TECHNOL	2,537	38	154	268	256	278	318	232	308	205	103	377
7	4.674	SOL ENERGY	2,388	19	155	279	198	173	138	137	146	79	94	970
8	7.181	ENERG CONVERS MANAGE	2,196	13	172	314	372	315	150	59	96	63	104	538
9	4.084	INT J HYDROGEN ENERG	1,841	3	123	166	171	174	169	188	138	144	147	418
10	4.495	ENERG BUILDINGS	1,682	15	68	223	210	203	183	139	117	107	51	366
11	4.026	APPL THERM ENG	1,263	12	158	213	133	108	121	39	71	58	47	303
12	5.128	FUEL	995	7	44	116	120	138	117	66	62	77	27	221
13		ENRGY PROCED	868	0	82	76	200	269	81	86	51	0	23	0
14	3.537	BIOMASS BIOENERG	849	5	15	55	41	63	80	92	112	49	46	291
15	6.395	J CLEAN PROD	817	44	167	182	118	84	54	30	31	20	24	63
16	6.807	IEEE T POWER SYST	771	4	26	58	49	52	79	48	35	26	41	353
17	7.467	J POWER SOURCES	712	0	21	30	69	72	50	36	71	42	44	277
18	4.346	INT J HEAT MASS TRAN	674	6	51	53	74	45	46	31	39	34	46	249
19	7.224	IEEE T POWER ELECTR	590	6	28	64	68	67	66	51	47	19	31	143
20	6.019	SOL ENERG MAT SOL C	571	4	37	71	46	41	27	35	64	30	23	193
21		THESIS	571	1	12	41	43	51	43	61	48	36	36	199
22	4.820	BUILD ENVIRON	561	0	29	42	61	51	40	46	45	39	32	176
23		ENERG ECON	539	2	18	44	52	42	64	51	49	38	27	152
24	7.503	IEEE T IND ELECTRON	507	3	24	35	49	46	61	19	52	50	48	120

Showing 1 - 26 rows of 5,569 total

These data summarize the characteristics of the journal's published content for the most recent three years, that is, 2018 and the two prior years, combined. This information is based on all listed authors and addresses. It is meant to be descriptive rather than comparative.

Contributions by country/region

country		count
1.	CHINA MAINLAND	661
2.	India	490
3.	Malaysia	412
4.	USA	350
5.	England	253
6.	Spain	217
7.	Iran	209
8.	Australia	202
9.	Turkey	160
10.	Brazil	149

Contributions by organizations

organization		count
1.	UNIVERSITI MALAYA	117
2.	INDIAN INSTITUTE OF TECHNOLOGY SYSTEM (IIT SYSTEM)	114
3.	UNIVERSITI TEKNOLOGI MALAYSIA	100
4.	CHINESE ACADEMY OF SCIENCES	69
5.	TSINGHUA UNIVERSITY	67
6.	UNIVERSITI KEBANGSAAN MALAYSIA	58
7.	NORTH CHINA ELECTRIC POWER UNIVERSITY	50
8.	KING FAHD UNIVERSITY OF PETROLEUM & MINERALS	48
9.	ISLAMIC AZAD UNIVERSITY	43
10.	COMSATS INSTITUTE OF INFORMATION TECHNOLOGY (CIIT)	41

Scopus

Source details

Renewable and Sustainable Energy Reviews

Scopus coverage years: from 1997 to Present

Publisher: Elsevier

ISSN: 1364-0321

Subject area: Energy: Renewable Energy, Sustainability and the Environment

View all documents > Set document alert Save to source list Journal Homepage

CiteScore 2018
12.21

SJR 2018
3.288

SNIP 2018
3.694

CiteScore CiteScore rank & trend CiteScore presets Scopus content coverage

CiteScore 2018

Calculated using data from 30 April, 2019

12.21 = Citation Count 2018 / Documents 2015 - 2017* = 48.016 Citations > / 3933 Documents >

*CiteScore includes all available document types

View CiteScore methodology > CiteScore FAQ >

CiteScoreTracker 2019

Last updated on *14 October, 2019*
Updated monthly

11.40 = Citation Count 2019 / Documents 2016 - 2018 = 44.710 Citations to date > / 3921 Documents to date>

Metrics displaying this icon are compiled according to Snowball Metrics, a collaboration between industry and academia.

CiteScore rank

Category	Rank	Percentile
Energy — Renewable Energy, Sustainability and the Environment	#7/153	95th

View CiteScore trends > Add CiteScore to your site

Scopus

Compare sources

Select up to 10 sources to compare

Selected sources: ☐ Renewable and Sustainable Energy Reviews ×

Remove all selections

CiteScore publication by year

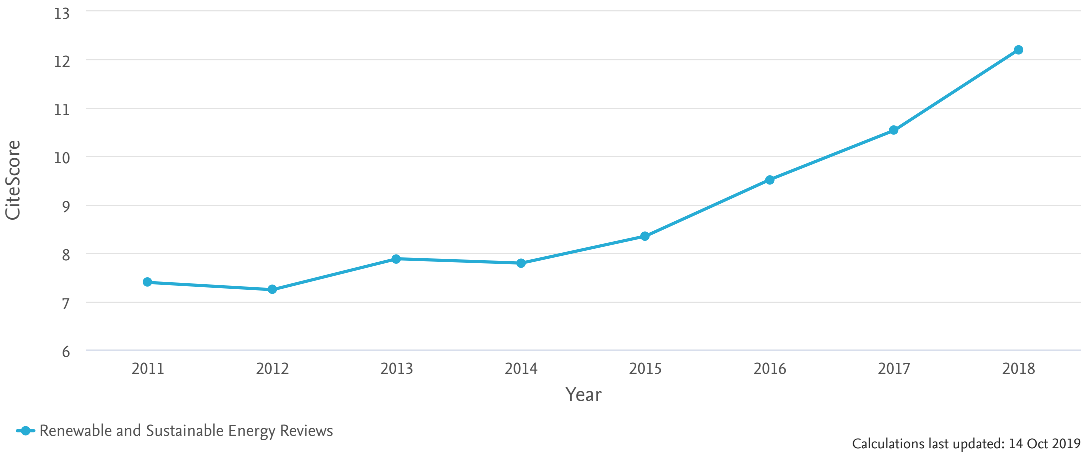

Calculations last updated: 14 Oct 2019

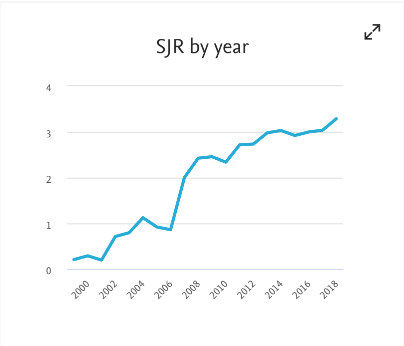

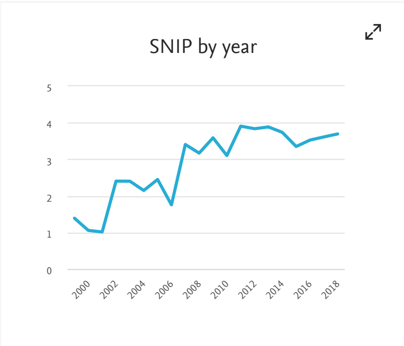

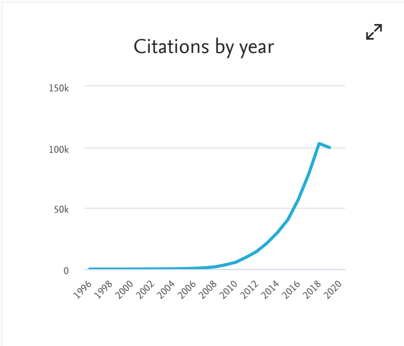

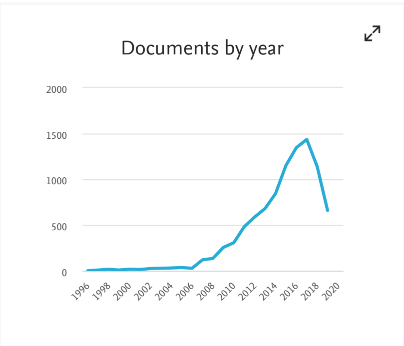

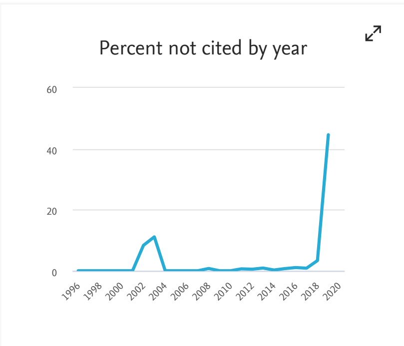

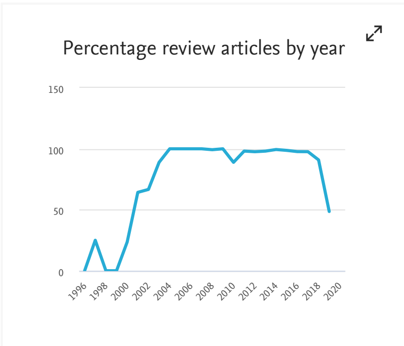

Renewable and Sustainable Energy Reviews

Country Netherlands - SIR Ranking of Netherlands

Subject Area and Category Energy
Renewable Energy, Sustainability and the Environment

Publisher Elsevier BV

Publication type Journals

ISSN 13640321

Coverage 1997-ongoing

Scope Renewable & Sustainable Energy Reviews publishes specially commissioned review articles designed to bring together under one cover, current advances in the ever broadening field of renewable and sustainable energy.

222

H Index

Homepage

How to publish in this journal

Contact

Join the conversation about this journal

Quartiles

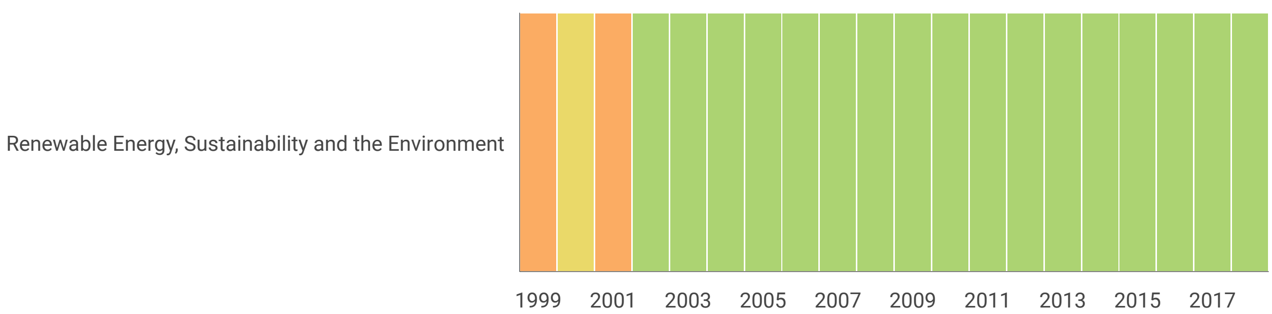

SJR

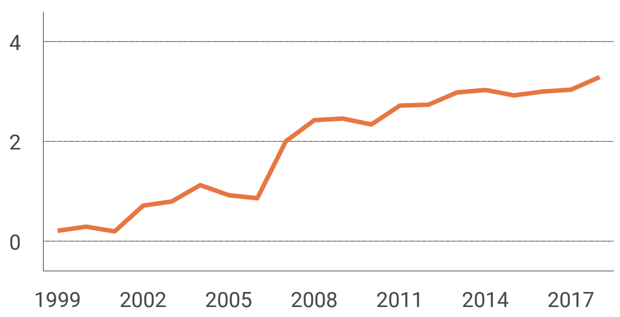

Citations per document

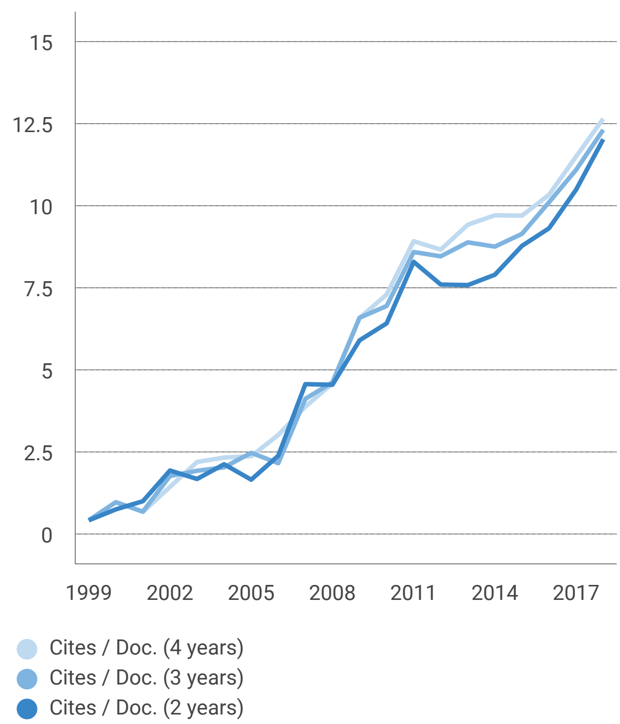

Total Cites Self-Cites

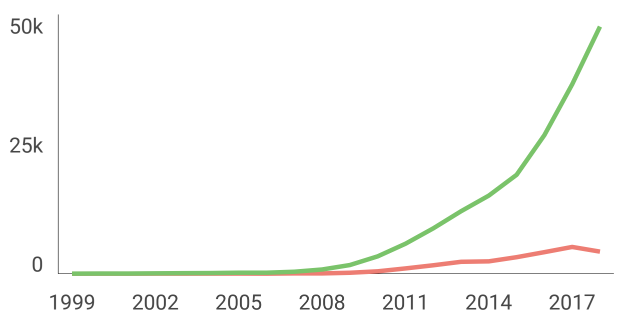

External Cites per Doc Cites per Doc

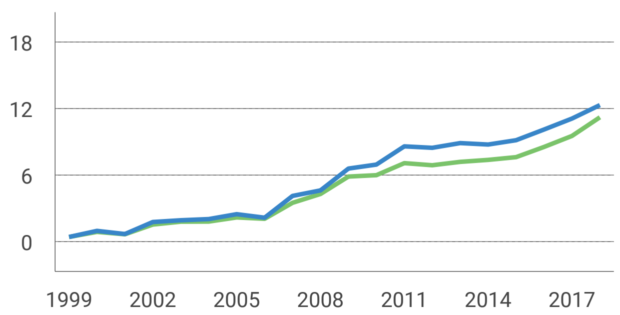

% International Collaboration

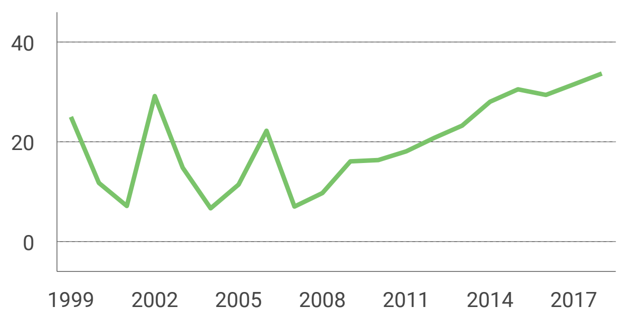

Citable documents Non-citable documents

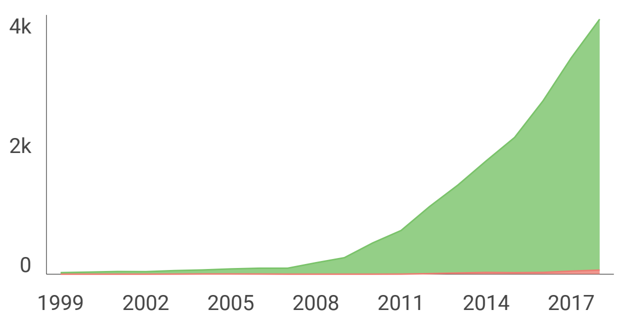

Cited documents Uncited documents

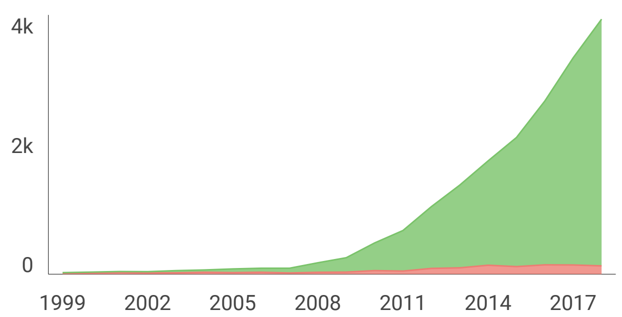

Show this widget in your own website

ANEXO IV: "*AN ASSESSMENT OF PHOTOVOLTAIC POTENTIAL IN SHOPPING CENTRES*". COPIA DE LA PUBLICACIÓN.

Solar Energy 135 (2016) 662–673

Contents lists available at ScienceDirect

Solar Energy

journal homepage: www.elsevier.com/locate/solener

An assessment of photovoltaic potential in shopping centres

Antonio Colmenar-Santos *, Severo Campíñez-Romero, Clara Pérez-Molina, Francisco Mur-Pérez

Departamento de Ingeniería Eléctrica, Electrónica y de Control, Universidad Nacional de Educación a Distancia, UNED, Juan del Rosal, 12 – Ciudad Universitaria, 28040 Madrid, Spain

ARTICLE INFO

Article history:
Received 13 December 2015
Received in revised form 23 May 2016
Accepted 20 June 2016
Available online 25 June 2016

Keywords:
Solar energy
Building integration
Grid integration
Shopping centres

ABSTRACT

The solar photovoltaic is a renewable energy source which allows nowadays, in many places, the generation of electricity at a cost comparable with the conventional thermal generation methods. However, ending 2014, with a worldwide power capacity installed of 177 GW, the integration level in the electricity generation mix was still far from the targets set up for this technology in the global warming mitigation strategies.

Technical, financial and regulatory barriers slow down a massive penetration of photovoltaic generation facilities, hence practical and innovative measures are necessary to facilitate a wider deployment.

The building integration of solar photovoltaic facilities offers an efficient solution because the electricity is generated near the consumption point and gives a new economic value to roofs and facades. In this paper we develop a scientist methodology for determining the potential in shopping centres, to establish that, in terms of photovoltaic integration, these present important competitive advantages over other alternatives, i.e. the residential buildings. The power capacity potential obtained making use of this methodology in the countries selected is 16,8 GW, that means 10% of the worldwide capacity installed at the end of 2014, with a yearly electricity generation of 22,7 TW h equivalent to 14% of the worldwide generation in 2014.

1. Introduction

Global warming experienced in the earth in the last decades is a reality with proved grave consequences. With a high degree of probability, the key reason behind this global warming is the anthropogenic greenhouse gasses (GHG hereinafter) emissions, fundamentally caused by the global population growth rate and the economic development since the beginning of the industrial era (Intergovernmental Panel on Climate Change, 2014).

To face this situation, the international community has adopted the commitment to limit the earth global warming to 2 °C above pre-industrial levels (European Climate Foundation, 2010; The White House. President of the US, 2013). The fulfilment of this commitment requires of global and important measures sustained over time to achieve a significant reduction of the GHG emissions. Many governments and international institutions have established future scenarios and designed strategies to reach this achievement that include necessarily interventions to mitigate the present emission levels.

According to the majority of the analysis carried out in this field, one of the main sources of GHG emissions is the power sector; therefore, important efforts should be done here to contribute as it should be, towards the achievement of the mitigation targets. The use of renewable energy sources (RES hereinafter) in the electricity generation is the base to support this contribution. Presently it has been reached a significant share of penetration of RES in the electric generation mix; but this rate should be increased massively to attain the transition from the present electricity generation scheme, fundamentally based on the use of hydrocarbons (Intergovernmental Panel on Climate Change, 2011), to a near-zero emissions power sector.

Among the RES, the solar photovoltaic source (PV hereinafter) has an essential characteristic that favours its massive penetration: the dispersion degree. The solar radiation is received worldwide with an intensity level that, depending on the specific location latitude, makes possible the production of electricity almost everywhere. Besides, the PV technology presents nowadays a technical and economical maturity that allows high efficiency generation at such a low cost comparable with the traditional generation based on conventional thermal methods (Colmenar-Santos et al., 2012; Feldman et al., 2014; Hernández-Moro and Martínez-Duart, 2013; Lazard, 2014; Ondraczek et al., 2015; Ossenbrink et al., 2013; Philipps et al., 2014).

The integration of a massive share of RES in the electric power grid implies technical barriers and problems with an impact on the operation and stability of the whole system. The facilities must

* Corresponding author.
E-mail address: acolmenar@ieec.uned.es (A. Colmenar-Santos).

http://dx.doi.org/10.1016/j.solener.2016.06.049
0038-092X/

Nomenclature

General		Greeks	
A_{SP}	area of the solar panel	α_s	solar altitude angle
A_{PV}	PV area	β	panel slope. It is the angle between the solar panel surface and the horizontal
CR	covering ratio	P_P	PV peak power
DOE	US Department of Energy	P_{SP}	maximum power of the solar panel at STC conditions
DSO	distribution system operator	PR	performance ratio of the PV facility
EU28	European Union 28 countries	PV	photovoltaic electricity source or facility
GLA	gross leverage area	RES	renewable energy source
GHG	greenhouse gases	SC	shopping centre
G_T	yearly solar irradiation (insolation) in kW h/m^2/year incident on an optimally-tilted solar panel	US	United States of America
		γ_s	Azimuth solar angle
		ε	solar panel efficiency
		φ	latitude angle

implement specific systems to favour the integration of the electricity generated, including eventually elements to storage the surplus generation to be used in deficit times (Barth et al., 2014; Luthander et al., 2015; Mai et al., 2012). This is a handicap for small facilities in residential buildings or single family houses, even for small commercial buildings, because all of these auxiliary systems can turn the facility more complex and with needs of professional assistance and likely their users will not have an adequate technical profile and will have to contract a utility company to do it.

In the previous technical literature, several studies have been carried out to determine roof area availability or solar PV potential in buildings. Most of them are focused only on residential buildings: (Karteris et al., 2013) analysed the suitable roof areas in multifamily buildings in cities based on statistical calculation obtaining that the solar roof factor of utilization in this type of residential buildings is only between 25% and 50%. (Li et al., 2015) investigated the annual solar yield per floor space in urban residential buildings at different levels of site density. (Ordóñez et al., 2010) developed a methodology to determine the solar PV generation potential on residential rooftops using statistical data to characterize the building stock.

Other previous research did not differentiate the use of the buildings under analysis and, therefore or do not detail the PV potential of every of them: (Defaix et al., 2012) estimated the technical potential in integrated PV for residential and non-residential buildings in the EU-27 countries, (Izquierdo et al., 2008) defined a methodology, based on statistics available data and GIS maps, for estimating roof surface area for large-scale PV potential evaluations in all type of existing buildings and applied this methodology to Spain to obtain an estimate of energy generation, (Peng and Lu, 2013) carried out an investigation about the PV potential of hotels and commercial buildings in the city of Hong Kong. (Pillai and Banerjee, 2007) developed a methodology to for potential estimation of solar water heating that applied to a synthetic area of 2 sq. km in India considering residential houses, hospital, nursing homes and hotels. (Schallenberg-Rodriguez, 2013) investigated about the solar PV potential on roofs for several type of buildings in regions and islands and applied their research for obtaining an estimate of the PV potential in the Canary Islands, (Singh and Banerjee, 2015) carried out a methodology for estimating solar photovoltaic potential in a city for all type of buildings and (Wiginton et al., 2010) defined a method to estimate total rooftop PV potential based in GIS and object-specific image recognition city of Ontario (Canada).

Generally, the pre-existing literature has considered any type of buildings with similar features to host PV facilities independently of its use. However, from a constructive point of view, the availability of residential building roofs is generally lower to commercial building ones.

All of the aforementioned features, as well as other analysed in more detail below, point to shopping centres as best-fitting buildings for the purpose of installing PV facilities and therefore they should be the target of a detailed assessment about their PV potential.

As a consequence, the likelihood of taking advantage more efficiently of the roof space and the better technical adaptability for the integration of PV generation contributes to maximize the effect in the building energy performance because it is possible to achieve a larger level of self-generation.

This paper is aimed firstly at analysing the particular advantages of shopping centre buildings to install PV facilities, including technical comparatives versus the residential buildings that represent the predominant type widely used to estimate the PV potential. Secondly, the article focuses the research on determining the shopping centres potential in terms of power capacity and electricity generation as well as the possible contribution to achieve the penetration targets set up for this technology. The research has been developed for a large area including all the countries in the 2014 PV power capacity top ten list.

Below in Section 2 we review the world present situation in terms of photovoltaic penetration and will be determined the reference targets used in this article. In Section 3, we specify the reasons for considering shopping centres as buildings with important advantages for PV facilities. In Section 4 we define the methodology developed to obtain the power capacity and generation potential in shopping centres located in different countries and in we carry out the determination of this potential. In Section 5 the methodology is applied to a real shopping centre located in Madrid (Spain) to obtain the capacity and share potential. Finally, in Section 6 the conclusions of the results obtained in the study are presented.

2. Present situation and targets

2.1. Present world situation

Ending 2014, the world PV power capacity installed was 177 GW. As shown in Fig. 1 the distribution of the capacity presents a high concentration degree, so that the top ten countries host 149 GW, what means 84% of total (Fig. 2).

The countries included in this article are those in the top ten list: the 28 countries members of the European Union (EU28

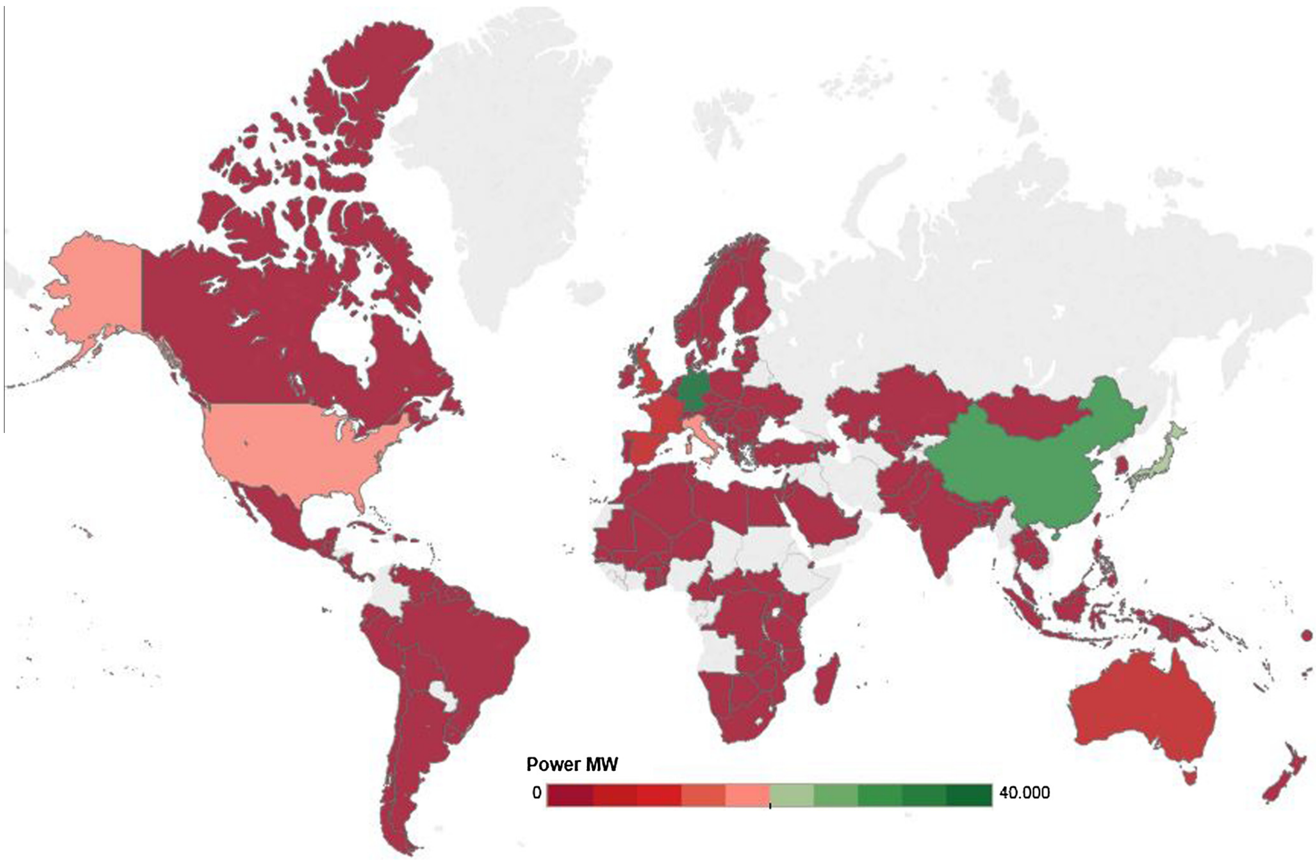

Fig. 1. Distribution of the PV installed power per country at the end of 2014. *Source:* International Renewable Energy Agency (2015).

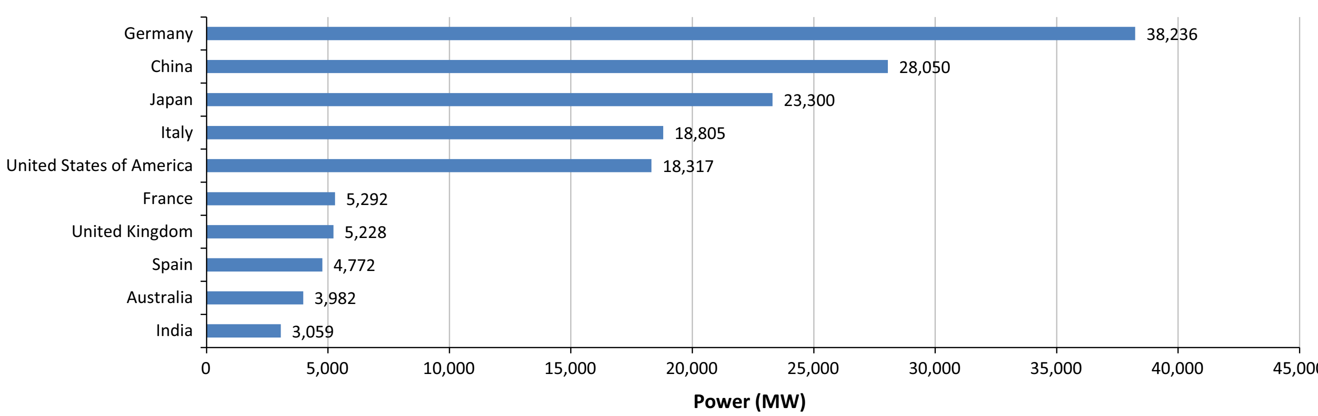

Fig. 2. Top ten countries by PV installed power. *Source:* International Renewable Energy Agency (2015).

hereinafter) including Germany, Italy, France, the United Kingdom and Spain; China, Japan, the United States of America (US hereinafter), Australia and India.

2.2. Photovoltaic integration targets

Several international governmental and non-governmental organizations have set up scenarios and paths focused on the power sector aimed to reduce its GHG emissions. Among all of that, those considered in this article, with a deployment period up to 2050, are the following:

– In the US, the targets set up in the SunShot Vision Study (National Renewable Energy Laboratory, 2012), which was developed under the US Department of Energy (DOE) (The US Department of Energy, 2015) SunShot Initiative. It is focused on the solar photovoltaic renewable source to be competitive with the traditional generations forms before 2020, favouring its integration and contributing to the achievement of the GHG emissions mitigation and reduction plans adopted by the Obama Administration in 2009 and 2013 (The White House. President of the US, 2013) and to the Clean Power Plan (U.S. Environmental Protection Agency, 2015), which has been recently implemented in 2015 to reduce the carbon emissions in the electricity generation facilities.
– In the 28 countries members of the EU28, the targets established in the Roadmap 2050 (European Climate Foundation, 2010), that analyses and sets up the paths to achieve the

European commitment to reach in 2050 GHG emissions below 80% of 1990 levels.

– In the rest of countries included in this article: Australia, China and India, the targets are those set up by the International Energy Agency in the high-renewables (IEA hi-Ren) scenario of the Energy Technology Perspectives 2014 report (ETP2014) (International Energy Agency, 2014a), where is stablished the limitation for the global warming in 2 °C above pre-industrial levels with a high share of RES penetration.

Figs. 3 and 4 illustrate a comparative between the capacity and share figures of PV ending 2014 and the targets foreseen for 2050 for the countries included in the study. It is noticeable that in all the cases, the increase necessary for both the capacity and the share to fulfil the targets. According to the IEA hi-Ren, the worldwide power capacity must go from the present 177–4674 GW, what means a sustained yearly increasing of 10% up to 2050; the share will go approximately from 1% to 16%. The region presently closest to achieve its targets is EU28, with 86.8 GW of power capacity, mainly in Germany (38.2 GW or 44% of total) and a share of 3.1%. EU28 will need a sustained yearly growing of 6% for power capacity and 5% for share to reach the Roadmap 2050 targets. To achieve the objectives set up in the SunShot Vision Study, US will need a sustained annually increasing for both the capacity power and the share of 10%, to go from the present 18.3 MW up to 632 MW and from 0.6% to 19% respectively. Finally, in China and India the yearly growth should be of 12% and 16% respectively to get the targets established in the IEA hi-Ren and 11% and 12% to achieve the share estimates.

2.3. Present integration in shopping centres

Nowadays, the PV capacity integrated in shopping centres worldwide is irrelevant. In example, in the US, ending 2014, there was 325 MW (Solar Energy Industries Association, 2014), barely 1,5% of total country PV capacity.

3. Why the shopping centres?

There are diverse types of buildings, as schools, hospitals or industrial and commercial buildings, that present particularities and different characteristics that advices to analyse each of them with different approaches in order to estimate their PV potential. In this article we have focused the research in developing a new

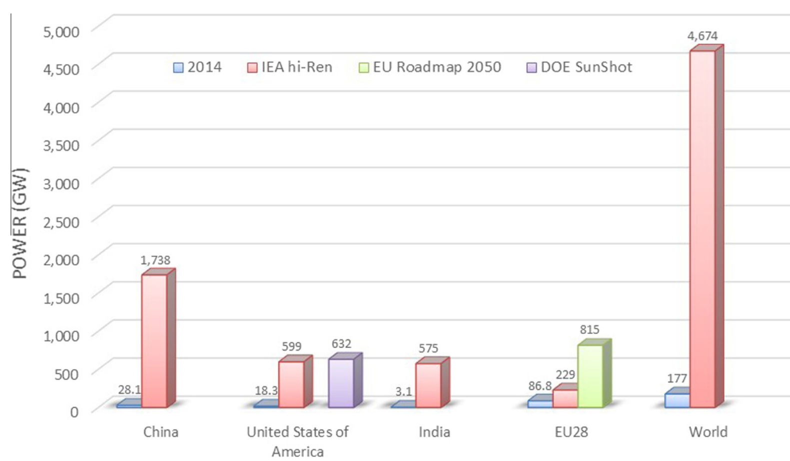

Fig. 3. Present PV power installed and targets for 2050. *Sources:* European Climate Foundation (2010), Feldman et al. (2015), International Energy Agency (2014a), International Renewable Energy Agency (2015), Johnston et al. (2015), National Renewable Energy Laboratory (2012), REN21 (2015), RTE Réseau de transport d'électricité (2015), Yamada and Ikki (2015).

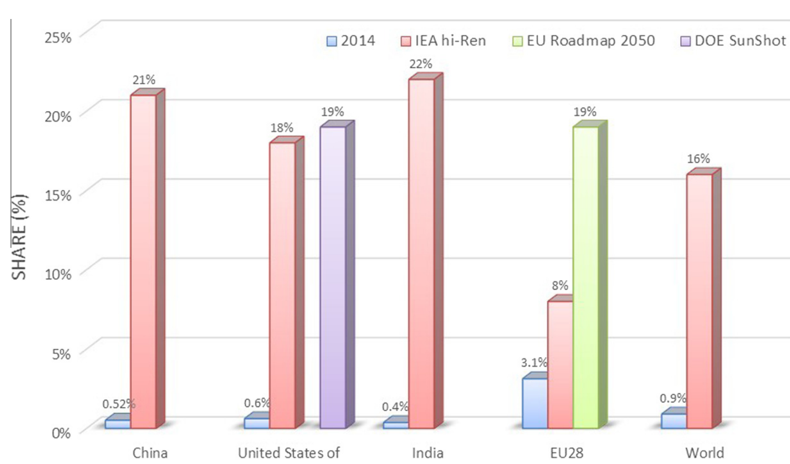

Fig. 4. Present PV share and targets for 2050. *Sources:* Arbeitsgemeinschaft Energiebilanzen (2014), Australian Energy Regulator (2014), British Petroleum (2015), European Climate Foundation (2010), Feldman et al. (2015), International Energy Agency (2014a), International Renewable Energy Agency (2015), Johnston et al. (2015), National Renewable Energy Laboratory (2012), Red Eléctrica de España S.A. (2015), RTE Réseau de transport d'électricité (2015), U.S. Energy Information Administration (2015), UK Government. Department of Energy and Climate Change (2015), Yamada and Ikki (2015).

methodology applicable to the shopping centres, using the residential buildings as a benchmark for highlighting the advantages for the implementation of PV integrated facilities versus the predominant building type.

These advantages of shopping centres are detailed, justified and compared along this chapter.

3.1. Construction characteristics

Shopping centres present construction features that favour the installation of PV in the roofs. As it is shown in (Denholm and Robert, 2008) the availability rate for residential buildings is between 22% and 27% and some other studies set up this rate in the 25–50% range for high population density cities where predominate multifamily buildings (Karteris et al., 2013). On the other hand, the availability rate for commercial buildings can be placed between 60% and 65% (Denholm and Robert, 2008). This means that, in similar conditions, it will be possible the installation of double or triple capacity in shopping centres roofs than in residential buildings.

3.2. Self-consumption and consumption profile

In terms of transport and distribution of energy, the most efficient place to generate electricity is nearest the consumption point. In this matter, the shopping centres offer also relevant advantages over other building types. On one hand because shopping centres are major electricity consumers and the generation can be mostly used for self-consumption, and on the other hand because some studies show that their consumption patterns match the PV generation profile better than any other type of buildings (International Energy Agency, 2014b).

Grounded PV facilities sited near high-consumption points present an important handicap, because with the purpose of being near the consumer they will have to be located in urban or industrial areas where the land is highly valued and the rent will penalize the PV operation costs. However, the shopping centres, by nature, are usually located near o inside cities or populated and industrial areas and the electricity surplus could be used to supply the local consumption through the distribution networks with few electric losses.

Last but not less important is the fact that, the self-generation of electricity will reduce the energy dependency of the building, contributing to increase the performance of the shopping centres in terms of efficiency.

3.3. Integration challenges

The electricity generated in PV facilities has a non-manageable character; it means that it is not possible to control instantaneously the generation level except to reduce it. This characteristic makes difficult a massive penetration therefore the implementation of specific systems and technical measures are necessary for an adequate management (Barth et al., 2014).

Some of these measures must be implemented by the distributor system operators (DSO) because their distribution networks were initially designed for a single direction energy flow, and now they must allow the feeding of energy from the consumption points (Stetz et al., 2014). Others will have to be implemented directly in the generation facilities, mainly the following ones:

– Short-term generation forecast.
– Storage of surplus generation to be used in deficit periods.
– Ancillary services for voltage and reactive energy control.
– Demand response.
– Generation curtailment.

Part of them may be implemented in the facility equipment; in example to carry out the voltage and reactive energy control. However, others, as the short-term generation forecast or the demand response will require of regular attention and professional management by the prosumer.[1]

In this aspect, shopping centres also present advantages over residential buildings, because they usually have on site industrial technical equipment, as energy supply (electricity, vacuum, fuel), heating and air conditioning systems, security, energy management, etc., and even electricity generation facilities for self-consumption. These systems already need a professional operation and maintenance service (in-house or outsourced) that could include easily the new tasks necessary for the PV management.

4. Determination of the shopping centres PV potential

A novel methodology, illustrated in Fig. 5, has been developed to estimate the PV potential in shopping centres. This new methodology, detailed along this chapter, has been specially designed to be applied in shopping centres. We have used statistical raw data about the characteristics of the buildings to calculate the available roof space in shopping centres, and by means of the definition and determination of reduction ratios, we have finally obtained the PV potential, in terms of power capacity and capacity of electricity generation in a wide world area corresponding with the countries in the top ten list of accumulated PV power in 2014.

4.1. Calculation of the PV roof space

The first step in the application of the methodology is determining the PV roof space. It is defined in this article as the shopping centre roof surface without physical, technical or shading limitations for placing solar panels on it. The first step to calculate the PV roof space is the determination of the available area in shopping centres. The parameter chosen here to quantify this area is the gross leasable area (GLA hereinafter). GLA is widely used in the real state sector and indicates the total floor area designed for tenant occupancy and exclusive use, including any basements, mezzanines, or upper floors. Therefore, using GLA is a way to classify commercial buildings giving a value of the amount of space available for renting.

Table 1 shows the present GLA values for the countries considered in this article. As it can be seen, the total GLA value is about 845 million of square meters, with a special presence in the US housing 72% of the total.

Although Russia allocates presently around 516 shopping centres representing about 17 million of square metres of GLA, has not been included in this study because the lack of both national regulations to promote PV integration and RES implementation targets.

Not all the shopping centres will be able to host a PV facility because they do not have roof or it is inaccessible. In some cases, on the roofs might be located car parks; and others, mainly in those shopping centres located inside cities or populated areas, may be underground or integrated in buildings with other uses, as hotels or households.

For those centres with roof area limitations due to architectural or functional issues (i.e. parking areas located in the roof), the reduction in the available area will be taken into account by means of the application of the availability rate as it will be defined below in this chapter.

Due to the fact that there is not available statistic data about the constructive characteristics of the shopping centres, it is

[1] A prosumer is a consumer and producer of electricity.

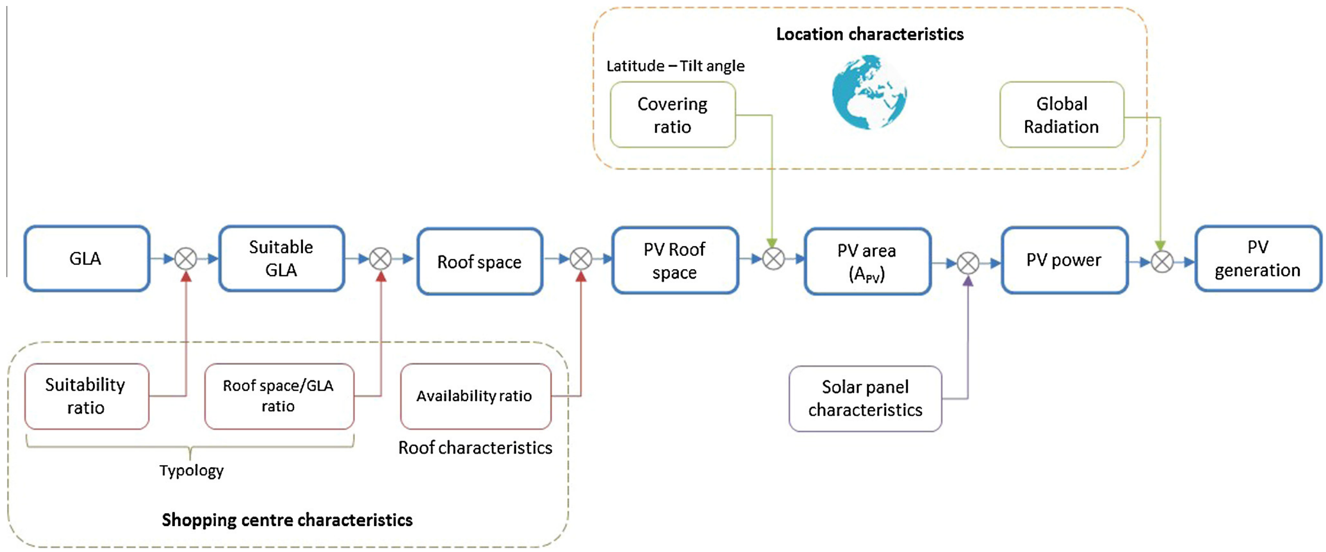

Fig. 5. Methodology to estimate PV capacity and generation potential.

Table 1
GLA values for shopping centres with a size bigger than 5000 m^2. *Sources:* US (International Council of Shopping Centers, 2015b), EU28 (Cushman and Wakefield, 2014; International Council of Shopping Centers, 2015a; RegioData Research, 2013), rest of countries (Cushman and Wakefield, 2014).

Region	Shopping centre type	GLA range		Number of facilities	GLA (m^2)	GLA over total (%)
		m^2	sq ft			
US	Super-Regional Mall	>74,000	>800,000	632	72,449,656	
	Regional Mall	37,000–74,000	400,000–800,000	608	33,289,047	
	Community Centre ("Large Neighbourhood Centre")	11,600–37,000	125,000–400,000	9,642	177,042,603	
	Neighbourhood Centre	2,800–11,600	30,000–125,000	32,422	216,279,091	
	Power Centre	23,200–55,700	250,000–600,000	2,249	91,182,862	
	Lifestyle	13,900–46,400	150,000–500,000	437	13,590,001	
	Factory Outlet	7,400–23,200	50,000–400,000	351	7,821,766	
			Total US	46,341	611,655,026	72
EU28	Traditional	>5,000	>53,800	5,626	118,585,681	
	Retail Park	>5,000	>53,800	2,048	32,479,398	
	Factory Outlet Centre	>5,000	>53,800	162	3,036,653	
			Total EU28	7,836	154,101,732	18
China	All types	>5,000	>53,800	621	53,200,000	
			Total China	621	53,200,000	6
Australia	Regional	46,400–74,000	500,000–800,000	91	7,161,000	
	Sub-regional centres	18,500–46,400	200,000–500,000	313	6,727,000	
	Neighbourhood/Supermarket-based	1,850–18,500	20,000–200,000	840	4,340,000	
	Central business district	>5,000	>53,800	123	1,302,000	
			Total Australia	1,367	19,530,000	2
India	All types	>5,000	>53,800	530	6,500,000	
			Total India	530	6,500,000	1
			Grand total	56,695	844,986,758	

impossible to obtain an accurate estimate of the quantity and volume in terms of GLA of shopping centres without roof or entirely inaccessible. However, it must be taken in consideration that these shopping centres likely will be integrated in population areas and they will be small and that in the scope of application of this study are included only the shopping centres with a GLA above 5000 square metres. Nevertheless, it is possible that some shopping centres included in the scope present a total limitation for the installation of PV due to the lack of roof. To consider this limited likelihood, a reduction in the GLA has been considered by the application of a suitability ratio with a conservative value of 0.8.

Once the suitable GLA space is estimated, the next step is calculating the roof space what we have done by means of determining a Roof space/GLA ratio. This ratio will depend on the individual typology and features of every single shopping centre, nevertheless to be considered in our method an average value was determined by analysing the characteristics of a sample of 500 shopping centres spread across the countries included in this study. The analysis consisted in the location and measurement of the individual roof space with Google earth™ (Google Inc., 2013). As an example of the analysis carried out, Table 2 shows a partial list of the shopping centres included in the sample (the entire list of 500 buildings

Table 2
Roof space/GLA ratio calculation in a sample. *Source:* (DTZ, 2013) and self-elaboration.

Country or region	City	Name	GLA m^2	Roof space m^2	Roof space/GLA ratio
EU28	Brussels	Woluwe SC	42,677	31,685	0.742
EU28	Madrid	La Gavia	86,356	77,382	0.896
EU28	Prague	Tesco Letnany	125,000	71,472	0.572
EU28	Copenhagen	City Two	63,000	47,501	0.754
EU28	Marseille	Grand Vitrolles	61,111	61,408	1.005
EU28	Paris	Rosny 2	111,600	57,282	0.513
EU28	Berlin	Gropius Passagen	90,000	36,153	0.402
EU28	Dublin	Blanchardstown Centre	100,000	81,054	0.811
EU28	Bucharest	AFI Palace Cotroceni	75,000	75,320	1.004
EU28	Leeds	White Rose SC	63,638	47,017	0.739
EU28	Kyiv	Ocean Plaza	72,200	31,719	0.439
US	Washington	Tysons Corner Centre	220,000	95,648	0.435
US	Los Angeles	Lakewood Centre	200,000	135,632	0.678
US	Massachusetts	South Shore Plaza	201,100	110,405	0.549
China	Beijing	Golden Resources	557,000	61,512	0.110
China	Shangai	Super Brand Mall	121,400	21,837	0.180
India	Mumbai	Neptune Magnet Mall	98,100	20,310	0.207
India	Chennai	Gold Souk Grande Chennai	56,000	15,828	0.283
Australia	Sidney	Macquaire Centre	138,500	69,208	0.500
Australia	Robina	Robina Town Centre	125,000	99,447	0.796
				Average	0.580

examined is not included for a matter of space) which average Roof space/GLA ratio is 0.58 equal to the value obtained for the whole sample.

Not all the roof space will be obstacle-free and able to allocate the PV equipment. There might be architectural elements, as skylights or parts with not enough carrying capacity, functional, as heating and air conditioning equipment, and nearby or own constructions shading part of the space. All these elements will reduce the roof space, therefore it is necessary to consider a reduction ratio, named here availability ratio, to obtain the effective PV roof space.

Again, this availability ratio will be particular for every single shopping centre according to its typology and constructive characteristics. Several previous studies have determined average values that may be generally applied. A review of them was carried out by Byrne et al. (2015). For commercial buildings is widely recommended a value of 0.65 in cold climates and 0.6 in warm climates (Denholm and Robert, 2008; Gutschner et al., 2002). Under a conservative approach, the minimum value of 0.6 has been considered in this study.

As a result of applying the reduction ratios aforementioned, an estimate of PV roof space can be obtained from suitable GLA. Table 3 shows the detailed calculation for every single country included in the study. The total value reaches 23.5 Ha (over 235 million of square metres).

4.2. Calculation of PV power capacity and generation potentials

Once the PV roof space is determined, the next step is to calculate the power capacity and the generation estimates. With this aim two aspects are essential, on one hand the location of the shopping centre, which will determine the solar irradiation, the optimal inclination angle and the distance between panel rows; on the other hand, the technical characteristics of the solar panels and the rest of the equipment forming the PV facility.

Roof PV facilities are typically designed in fixed-mounted execution, so that, they do not change the orientation of the tilt angle along the year. In order to maximize the total[2] irradiation received, the solar panel rows are faced south (in the northern hemisphere and north in the southern hemisphere) with an optimal tilt angle.

There are several methods for estimating the global radiation incident on a tilted surface from the horizontal radiation, which is the value typically logged in meteorological observatories, and by means of any of them is possible to obtain the optimal tilt angle in every single day in the year (Hay and Davies, 1980; Hottel and Woertz, 1942; Klucher, 1979; Liu and Jordan, 1960; Perez et al., 1990, 1987, 1988; Reindl et al., 1990). Nevertheless, for fixed-mounted facilities is widely recommended to use an optimal angle value around the site latitude (Gunerhan and Hepbasli, 2007; Lewis, 1987); therefore, it will be the value considered in this study.

The tilt angle has a direct effect in the distance between solar panel rows. The classic method to calculate this distance is to consider that the panels will receive the solar radiation without shadows most of the lower solar zenith angle day. The calculation is illustrated in Fig. 6, and the results are shown in Table 4.

Once the distance between panels is determined, the next step is the calculation of the solar panels area. The relation between the tilt-mounted solar panels area and the sum of the horizontal projection of the panel's surface and the area corresponding with the distance between rows is named the covering ratio (CR hereinafter), which, as illustrated in Fig. 6, can be calculated as:

$$CR = \frac{w}{a+d} \tag{1}$$

Table 4 shows the results obtained for the covering ratio for different latitude angles between 0° and 50°. As can be seen, on the equator the optimum tilt angle is 0° and the covering ratio is one, therefore all the PV roof space can be covered with horizontal-mounted solar panels. The ratio decreases while the latitude increases reaching the minimum for a latitude of 50° where only 0.2 m^2 of solar panels can be installed per every square meter of PV roof space.

An average covering ratio is applied to the PV roof space according to the location to obtain the total solar panels area, called PV Area, for every single location included in the study. The results are shown in Table 5.

The peak power installable in the roof PV facility (P_P) will be determined by the characteristics of the solar panel, that is:

$$P_p = A_{PV} \cdot \frac{P_{SP}}{A_{SP}} \tag{2}$$

where A_{SP} is the solar panel area and P_{SP} the maximum output power under standard conditions. Nowadays there are different

[2] Total radiation is the total sum of the beam, diffuse and reflected or albedo.

Table 3
PV Roof space calculation.

Region	GLA (Ha)		Suitability ratio		Suitable GLA (Ha)		Roof space/GLA ratio		Roof space (Ha)		Availability ratio		PV Roof space (Ha)
US	61,166	×	0.8	=	48,932	×	0.58	=	28,381	×	0.6	=	17,028
EU28	15,410				12,328				7150				4290
China	5320				4256				2468				1481
Australia	1953				1562				906				544
India	650				520				302				181
Total	84,499				67,599				39,207				23,524

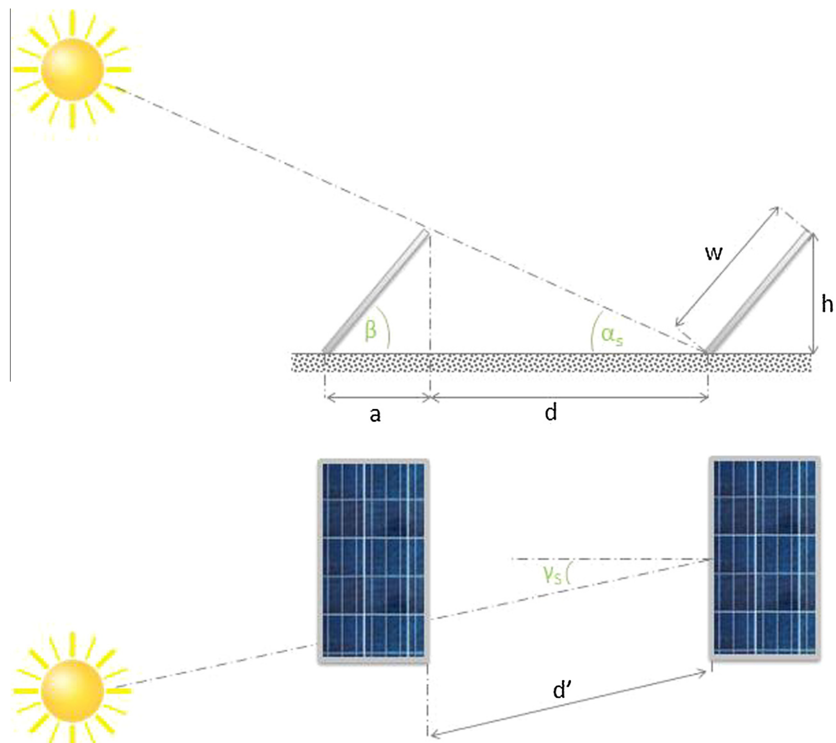

Fig. 6. Diagram for the calculation of the distance between solar panels. Azimuth solar panel angle is 0.

Table 4
Calculation of the distance between panels as a function of the site latitude (the slope of the panel is equal to the latitude).

Latitude (φ) (°)	Solar altitude angle (α_s)[a] (°)	Solar azimuth angle (γ_s)[a] (°)	d' (cm)	d (cm)	a (cm)	$a + d$ (cm)	Covering ratio $w/(a + d)$
50	6.66	40.31	524.46	339.3	51.4	390.7	0.20
40	14.23	41.52	202.77	134.4	61.3	195.7	0.41
30	21.60	43.71	101.03	69.8	69.3	139.1	0.58
20	28.63	47.06	50.11	36.7	75.2	111.9	0.72
10	35.15	51.80	19.73	15.5	78.8	94.3	0.85
0	40.91	58.23	0.0	0.0	80.0	80.0	1.00

[a] α_s and γ_s are the value for the latitude angle and the solar azimuth at nine o'clock on the 21st of December in the location, calculated according to (Duffie and Beckman, 2013) and taking into account that the slope angle β is equal to the location latitude.

Table 5
Calculation of the PV area.

Region	PV roof space (Ha)	Latitude (φ) range (°)	Average covering ratio	PV area (A_{PV}) (Ha)
US	17,028	30–45° N	0.45	7663
EU28	4290	35–60° N	0.36	1544
China	1481	15–45° N	0.76	1126
Australia	544	15–45° S	0.76	413
India	181	0–30° N	0.78	141
Total	23,524			10,887

Table 6
Solar panel characteristics.

Characteristic	Value
Manufacturer	Trina solar
Model	TSM-PC14
Cell type	Si Multicrystalline
Max power (STC conditions)	300 W
Efficiency (ε)	15,5%
Dimensions ($h \times w \times$ d)	1956 × 992 × 40 mm^3

Table 7
PV power potential in shopping centres.

Region	Solar panels area (A_{PV}) (Ha)		$\frac{P_{SP}}{A_{SP}}$		PV power capacity		
					SC potential (GW)	Present installed (GW)	SC potential vs 2014 (%)
US	7663	×	1.55	=	11,848	18,317	65
EU28	1544				2388	86,796	3
China	1126				1740	28,050	6
Australia	413				639	28,050	2
India	141				218	3059	7
Total	10,887				16,833	164,272	10

Table 8
PV generation potential in shopping centres.

Region	Solar panels area (A_{PV}) (Ha)	Average irradiance (G_T) (kW h/m^2/year)	Yearly PV Generation		
			SC potential (GW h/year)	Total in 2014 (GW h/year)	SC potential vs total in 2014 (%)
US	7663	2008	17,306	4,297,300	0.40
EU28	1544	1300	2259	3,108,600	0.07
China	1126	1643	2080	5,649,600	0.04
Australia	413	1825	848	244,500	0.35
India	141	1825	290	1,208,400	0.02
Total	10,887		22,783	14,508,400	0.16

Table 9
Consumption and PV coverage calculation. *Source:* (International Council of Shopping Centers; U.S. Energy Information Administration, 2003) and self-elaboration.

Region	GLA (Ha)		Floor-space/GLA		Floor-space (Ha)		SC consumption intensity (GW h/Ha)		SC consumption (GW h/year)	SC potential (GW h/year)	PV share (%)
US	61,166	×	0.6	=	101,943	×	2.395	=	244,128	17,306	7
EU28	15,410				25,684				61,506	2259	4
China	5320				8867				1234	2080	10
Australia	1953				3255				7795	848	11
India	650				1083				2594	290	11
Total	84,499				140,831				337,257	22,783	7

technologies for the manufacturing of solar panels, the most widely used is made of multi-crystalline silicon cells (International Technology Roadmap for Photovoltaic, 2015; REN21, 2013). These solar panels have recently reached efficiency levels over 20% in laboratory (National Center for Photovoltaics, 2015). For the calculation of the P_P, we have selected a solar panel manufactured with multi-crystalline silicon cells and a certified efficiency of 15.5%. Other characteristics are shown in Table 6.

Therefore, for the solar panel selected:

$$\frac{P_{panel}}{A_{panel}} = \frac{300\ \text{W}}{(1.956 \cdot 0.992)\ \text{m}^2} = 1.55\ \text{MW/Ha} \quad (3)$$

La Table 7 illustrates the calculation of the power capacity. A potential of 16,833 GW is obtained, that is of the same order of magnitude as the total capacity installed in US ending 2014. Taking into consideration that the total power installed at the end of 2104 in the countries included in this article was 164,272 GW, the shopping centres PV potential means 10%.

The yearly electricity generation in the shopping centres can be estimated using the following expression:

$$E = G_T \cdot A_{PV} \cdot PR \cdot \varepsilon \quad (4)$$

where G_T is the total yearly solar irradiation incident on an optimally-tilted solar panel (in this study equal to the site latitude), ε is the solar panel efficiency and PR is the facility performance ratio.

There are many sources to obtain the global radiation in a flat surface tilted at latitude angle. In this study, the data used in the calculations have been extracted from (Australian and New Zealand Solar Energy Society, 2006; Huld et al., 2012; National Renewable Energy Laboratory, 2015), then an average global radiation was estimate for every single country or territory.

The PV facilities present PR values in the 60–90% range (Dierauf et al., 2013; Reich et al., 2012). In this study, an average value of 75% was considered for PR. Finally, for the solar panel efficiency, the value considered is the one included in Table 6.

Other factors might be considered in the calculation of the energy generation. One of them is the degradation of the solar panels, effect that could be limited with an appropriate maintenance of the facilities, including when it is necessary, the replacement of affected units. Other is the dependency of the generation with the environmental conditions; especially the temperature, that affects to the output power of the solar panels in an inversely proportional way. In this matter, due to the general perspective of this research and the wide area covered, it would not be recommendable to set up here specific environmental conditions to be applied to the calculations because they could affect diversely (increasing the generation in some places and decreasing it in others); so that, the real effect should be evaluated for every single facility independently.

Table 8 shows the results obtained for the electricity generation calculated with the Eq. (4). Based on the hypothesis set up in this study, it would be possible a yearly electricity production of 22,783 GW h, that is 0.16% of total electricity consumption in 2014 in the territorial range of this article.

4.3. Shopping centres electricity consumption

According to CBECS (U.S. Energy Information Administration, 2003), the yearly average electricity consumption per square metre

Fig. 7. Shopping Centre La Gavia, IKEA and Carrefour centres (Madrid, Spain). *Source:* Google earth™.

of floor-space[3] in shopping centres larger than 50,000 sq ft (4645 m^2) is 41,5 kW h/m^2. As estimated in (International Council of Shopping Centers), the relation between GLA and floor-space is in the 0.5–0.65 range. In this study it has been considered an average value of 0.6.

Table 9 shows the estimate of the yearly electricity consumption in the shopping centres located in the countries included in the study and the share that could be supply by the PV facility. The results indicate that it would be possible to cover around 7% of the total electricity demand, with special relevance in Australia and India, where the PV share might reach 11%.

4.4. Uncertainty about the results

In the methodology proposed in this paper, three coefficients have been used to reduce the total GLA space available in shopping centres to obtain the PV roof space: the suitability ratio, the roof space/GLA ratio and the availability ratio.

Among these three coefficients, the roof space/GLA ratio was set up by means of the analysis of a wide sample of 500 shopping centres carried out specifically by the authors for this research, and the availability ratio was determined from reliable research carried out for others and widely used in the late technical literature.

As a result of the aforementioned, the major degree of uncertainty over the results obtained in this chapter arises from the determination of the suitability ratio. The application of the methodology shows that the final results obtained in Section 4.2 for PV power capacity and generation potential are linear with the value considered for the suitability ratio. Conscious of the impact of this ratio in the results, it was set up with a conservative value of 0.8.

5. An example of application. La Gavia shopping centre

The research carried out in this paper has included shopping centres located in many countries and different locations, therefore it presents a wide and diversified spectre of application. However, we have considered illustrative applying the methodology with an example that represents the key advantages of these type of commercial buildings for the installation of PV facilities. The shopping centre selected is named La Gavia (Klepierre Management, 2015). It is located in a high populated neighbourhood of Madrid (Spain), far from the nearest electricity generation plants. Enclosed in the same outdoor area there are two accessories buildings: a Carrefour store (Centros Comerciales Carrefour, 2015) and an Ikea store (Inter IKEA Systems B.V., 2015) centres. Fig. 7 shows a Google earth™ (Google Inc., 2013) satellite image of La Gavia shopping centre (bordered in blue[4]) and the two accessory buildings (bordered in red and green). In total, the complex has over 77,000 m^2 of roof space.

Table 10
Application of the methodology to La Gavia shopping centre and the accessory buildings.

Concept	Units	Ikea	Carrefour	Shopping centre
Roof space	(m^2)	16,922	13,470	46,990
Availability ratio		0.6		
PV roof space	(m^2)	10,153	8082	28,194
Latitude (φ)	(°)	40° 22′		
Optimum slope angle	(°)	35°		
Average covering ratio		0.41		
PV area (A_{PV})	(m^2)	4163	3314	11,560
Power potential	(MW)	0.64	0.51	1.79
Total power potential	(MW)	2.94		
Average irradiance (GT)	(kW h/m^2/year)	2029		
Generation potential	(MW h/year)	982	782	2727
Total generation potential	(MW h/year)	4491		
Floor-space	(m^2)	174,319		
Consumption estimate	(MW h/year)	41,745		
PV share		11%		

[3] In CBECS the floor-space is defined as all the area enclosed by the exterior walls of a building, both finished and unfinished, including indoor parking facilities, basements, hallways, lobbies, stairways, and elevator shafts.

[4] For interpretation of color in Fig. 7, the reader is referred to the web version of this article.

The application of our methodology to the Gavia shopping centre gives a PV capacity in the complex of 2.94 MW able to produce 4.291 MW h per year; what means 11% of the estimate shopping centre yearly consumption. The calculation details are included in Table 10.

6. Conclusions

The penetration of PV is still far from the targets set up for this technology to contribute to the mitigation of GHG emissions responsible of climate change.

The installation of PV facilities in building offers the possibility of producing electricity near the consumption point. In terms of building integration, the shopping centres are one the best choices to allocate PV because their typology and constructive characteristics may allow that, under similar conditions, the installable power capacity were triple than in residential buildings. Nevertheless, in order to estimate their own PV potential, other type of buildings, as schools, hospitals and industrial buildings, should be target of further research.

PV facilities integrated in shopping centres could contribute largely to achieve the targets, because the 16,800 GW of power capacity potential obtained is equivalent to 10% of the total PV capacity installed at the end of 2014. In the US, where presently there is only around 325 MW installed in commercial buildings, it could be possible the installation of around 11.8 GW, that is 65% of total power capacity installed in the whole country ending 2014. The PV facilities installable in the territorial scope of this study would be able to produce 22.7 TW h yearly, meaning 0.16% to the total electricity demand or 14% of the PV share in 2014.

If the PV roof facilities were used for self-consumption, they could cover about 7% on average of electricity demand, although in some countries the PV share could reach 11%.

The shopping centres are also an efficient choice if the surplus electricity is fed to the grid. They are typically located near large populated areas with high energy demand, and the generation could reach the consumption points in an efficiently way with low losses.

The installation of the PV potential obtained in this study on shopping centre roofs could avoid the use of over 23,000 Ha of land, a surface larger than the area covered for the cities of New York and Washington together.

References

Arbeitsgemeinschaft Energiebilanzen, 2014. Stromerzeugung nach Energieträgern 1990–2014 <http://www.ag-energiebilanzen.de/4-1-Home.html>.

Australian and New Zealand Solar Energy Society, 2006. Australian Solar Radiation Data Handbook.

Australian Energy Regulator, 2014. State of the Energy Market 2014.

Barth, B., Concas, G., Binda Zane, E., Franz, O., Frías, P., Hermes, R., Lama, R., Loew, H., Mateo, C., Rekinger, M., Michele Sonvilla, P., Vandenbergh, M., 2014. PV GRID. Final Project Report. August 2014 <www.pvgrid.eu>.

British Petroleum, 2015. BP Statistical Review of World Energy. June 2015 <www.bp.com/statisticalreview>.

Byrne, J., Taminiau, J., Kurdgelashvili, L., Kim, K.N., 2015. A review of the solar city concept and methods to assess rooftop solar electric potential, with an illustrative application to the city of Seoul. Renew. Sustain. Energy Rev. 41, 830–844. http://dx.doi.org/10.1016/j.rser.2014.08.023.

Centros Comerciales Carrefour, S.A., 2015. Carrefour La Gavia <http://www.carrefour.es/tiendas-carrefour/hipermercados/carrefour/la_gavia.aspx#cerrar> (accessed 2015).

Colmenar-Santos, A., Campíñez-Romero, S., Pérez-Molina, C., Castro-Gil, M., 2012. Profitability analysis of grid-connected photovoltaic facilities for household electricity self-sufficiency. Energy Policy 51, 749–764. http://dx.doi.org/10.1016/j.enpol.2012.09.023.

Cushman, Wakefield, 2014. Global Shopping Center Development Report. Spring 2014 <www.cushmanwakefield.com>.

Defaix, P.R., van Sark, W.G.J.H.M., Worrell, E., de Visser, E., 2012. Technical potential for photovoltaics on buildings in the EU-27. Sol. Energy 86, 2644–2653. http://dx.doi.org/10.1016/j.solener.2012.06.007.

Denholm, P.M., Robert, 2008. Supply Curves for Rooftop Solar PV-Generated Electricity for the United States. National Renewable Energy Laboratory, Report No.: NREL/TP-6A0-44073.

Dierauf, T., Growitz, A., Kurtz, S., Becerra Cruz, J.L., Riley, E., Hansen, C., 2013. Weather-Corrected Performance Ratio National Renewable Energy Laboratory, SS13.4510, T.N.; April 2013 Report No.: NREL/TP-5200-57991 <http://www.nrel.gov/docs/fy13osti/57991.pdf>.

DTZ, 2013. European Retail Guide Shopping Centres <http://www.dtz.dk/files/other/Markedsrapport/dtz_european_retail_guide_-_shopping_centres_march_2013.pdf>.

Duffie, J.A., Beckman, W.A., 2013. Solar Engineering of Thermal Processes, fourth ed. John Wiley & Sons Inc., Hoboken, New Jersey.

European Climate Foundation, 2010. Roadmap 2050: A Practical Guide to a Prosperous, Low Carbon Europe <http://www.roadmap2050.eu/project/roadmap-2050>.

Feldman, D., Boff, D., Margolis, R., 2015. National Survey Report of PV Power Applications in the United States 2014. International Energy Agency, Paris.

Feldman, D., Margolis, R., Boff, D., 2014. Q2/Q3 '14 Solar Industry Update. U.S. Department of Energy, <energy.gov/sunshot>.

Google Inc., 2013. Google Earth (Version 7.1.2.2041).

Gunerhan, H., Hepbasli, A., 2007. Determination of the optimum tilt angle of solar collectors for building applications. Build. Environ. 42, 779–783. http://dx.doi.org/10.1016/j.buildenv.2005.09.012.

Gutschner, M., Nowak, S., Ruoss, D., Toggweiler, P., Schoen, T., 2002. Potential for Building Integrated Photovoltaics. International Energy Agency, Photovoltaic Power Systems Programme. Task 7, Report No.: PVPS T7-4.

Hay, J.E., Davies, J.A., 1980. Calculation of the solar radiation incident on an inclined surface. In: Proceedings of the First Canadian Solar Radiation Data Workshop, Toronto, Canada, p. 59.

Hernández-Moro, J., Martínez-Duart, J.M., 2013. Analytical model for solar PV and CSP electricity costs: present LCOE values and their future evolution. Renew. Sustain. Energy Rev. 20, 119–132. http://dx.doi.org/10.1016/j.rser.2012.11.082.

Hottel, H.C., Woertz, B.B., 1942. Performance of flat-plate solar heat collectors. Trans. ASME 64, 64–91.

Huld, T., Müller, R., Gambardella, A., 2012. A new solar radiation database for estimating PV performance in Europe and Africa. Sol. Energy 86, 1803–1815. http://dx.doi.org/10.1016/j.solener.2012.03.006.

Inter IKEA Systems B.V., 2015. IKEA Ensanche de Vallecas <http://www.ikea.com/es/es/store/ensanche_de_vallecas/indexPage> (accessed 4/10/2015).

Intergovernmental Panel on Climate Change, 2011. Special Report on Renewable Energy Sources and Climate Change Mitigation. Cambridge University Press, United Kingdom and New York, NY, USA.

Intergovernmental Panel on Climate Change, 2014. Climate Change 2014: Synthesis Report. Contribution of Working Groups I, II and III to the Fifth Assessment Report of the Intergovernmental Panel on Climate Change. Geneva, Switzerland <http://www.ipcc.ch/report/ar5/syr/>.

International Council of Shopping Centers, Asia-Pacific Shopping Centre Classifications. New York.

International Council of Shopping Centers, 2015a. The Socio-Economic Contribution of European Shopping Centres <http://www.icsc.org/uploads/research/general/European-Impact-Study-2015.pdf?utm_source=research-homepage&utm_medium=web&utm_campaign=European-Impact-Study-2015>.

International Council of Shopping Centers, 2015b. U.S. Shopping-Center Classification and Characteristics <http://www.icsc.org/uploads/research/general/US_CENTER_CLASSIFICATION.pdf>.

International Energy Agency, 2014a. IEA Energy Technology Perspectives 2014. Paris, France <http://www.iea.org/etp/etp2014/>.

International Energy Agency, 2014b. Technology Roadmap Solar Photovoltaic Energy. 2014 ed., Paris, France.

International Renewable Energy Agency, 2015. Resource <http://resourceirena.irena.org/gateway/>.

International Technology Roadmap for Photovoltaic, 2015. ITRPV 2014 Results. April 2015.

Izquierdo, S., Rodrigues, M., Fueyo, N., 2008. A method for estimating the geographical distribution of the available roof surface area for large-scale photovoltaic energy-potential evaluations. Sol. Energy 82, 929–939. http://dx.doi.org/10.1016/j.solener.2008.03.007.

Johnston, W., Taeni, C., Egan, R., 2015. National Survey Report of PV Power Applications in Australia 2014. International Energy Agency, Paris.

Karteris, M., Slini, T., Papadopoulos, A.M., 2013. Urban solar energy potential in Greece: a statistical calculation model of suitable built roof areas for photovoltaics. Energy Build. 62, 459–468. http://dx.doi.org/10.1016/j.enbuild.2013.03.033.

Klepierre Management, 2015. Shopping Center La Gavia <http://es.club-onlyou.com/La-Gavia> (accessed 2015).

Klucher, T.M., 1979. Evaluating models to predict insolation on tilted surfaces. Sol. Energy 23.

Lazard, 2014. Levelized Cost of Energy v8 <http://www.lazard.com/perspective/levelized-cost-of-energy-v8-abstract/>.

Lewis, G., 1987. Optimum tilt of a solar collector. Solar Wind Technol. 4, 407–410. http://dx.doi.org/10.1016/0741-983X(87)90073-7.

Li, D., Liu, G., Liao, S., 2015. Solar potential in urban residential buildings. Sol. Energy 111, 225–235. http://dx.doi.org/10.1016/j.solener.2014.10.045.

Liu, B.Y.H., Jordan, R.C., 1960. The interrelationship and characteristic distribution of direct, diffuse and total solar radiation. Sol. Energy 4.

Luthander, R., Widén, J., Nilsson, D., Palm, J., 2015. Photovoltaic self-consumption in buildings: a review. Appl. Energy 142, 80–94. http://dx.doi.org/10.1016/j.apenergy.2014.12.028.

Mai, T., Wiser, R., Sandor, D., Brinkman, G., Heath, G., Denholm, P., Hostick, D.J., Darghouth, N., Schlosser, A., Strzepek, K., 2012. Exploration of High-Penetration Renewable Electricity Futures. Golden, CO <http://www.nrel.gov/docs/fy12osti/52409-2.pdf>, Report No.: NREL/TP-6A20-52409-1.

National Center for Photovoltaics, 2015. Research Cell Efficiency Records. U.S. Department of Energy <http://www.nrel.gov/ncpv/>.

National Renewable Energy Laboratory, 2012. SunShot Vision Study. U.S. Department of Energy <www.energy.gov/sunshot>, Report No.: DOE/GO-102012-3037.

National Renewable Energy Laboratory, 2015. MapSearch. Retrieved 2015 <http://www.nrel.gov/gis/mapsearch/>.

Ondraczek, J., Komendantova, N., Patt, A., 2015. WACC the dog: the effect of financing costs on the levelized cost of solar PV power. Renewable Energy 75, 888–898. http://dx.doi.org/10.1016/j.renene.2014.10.053.

Ordóñez, J., Jadraque, E., Alegre, J., Martínez, G., 2010. Analysis of the photovoltaic solar energy capacity of residential rooftops in Andalusia (Spain). Renew. Sustain. Energy Rev. 14, 2122–2130. http://dx.doi.org/10.1016/j.rser.2010.01.001.

Ossenbrink, H., Huld, T., Jäger Waldau, A., Taylor, N., 2013. Photovoltaic Electricity Cost Maps. Report No.: JRC 83366.

Peng, J., Lu, L., 2013. Investigation on the development potential of rooftop PV system in Hong Kong and its environmental benefits. Renew. Sustain. Energy Rev. 27, 149–162. http://dx.doi.org/10.1016/j.rser.2013.06.030.

Perez, R., Ineichen, P., Seals, R., Michalsky, J., Stewart, R., 1990. Modeling daylight availability and irradiance components from direct and global irradiance. Sol. Energy 44, 271–289. http://dx.doi.org/10.1016/0038-092X(90)90055-H.

Perez, R., Seals, R., Ineichen, P., Stewart, R., Menicucci, D., 1987. A new simplified version of the Perez diffuse irradiance model for tilted surfaces. Sol. Energy 39.

Perez, R., Stewart, R., Seals, R., Guertin, T., 1988. The Development and Verification of the Perez Diffuse Radiation Model. Oct-1988. Report No.: SAND88-7030.

Philipps, S.P., Kost, C., Schlegl, S., 2014. Up-to-Date Levelised Cost of Electricity of Photovoltaics. Fraunhofer Institute for Solar Energy Systems, ISE.

Pillai, I.R., Banerjee, R., 2007. Methodology for estimation of potential for solar water heating in a target area. Sol. Energy 81, 162–172. http://dx.doi.org/10.1016/j.solener.2006.04.009.

Red Eléctrica de España S.A., 2015. Informe del Sistema Eléctrico Español 2014. Madrid <http://www.ree.es/es/publicaciones/sistema-electrico-espanol/informe-anual/informe-del-sistema-electrico-espanol-2014#>.

RegioData Research, 2013. EU Shopping Centers Factsheets. RegioData Research <http://www.retailcenters.eu/factsheets>.

Reich, N.H., Mueller, B., Armbruster, A., van Sark, W.G.J.H.M., Kiefer, K., Reise, C., 2012. Performance ratio revisited: is PR < 90% realistic? Prog. Photovoltaics Res. Appl. 20, 717–726. http://dx.doi.org/10.1002/pip.1219.

Reindl, D.T., Beckman, W.A., Duffie, J.A.D., 1990. Evaluation of hourly tilted surface radiation models. Sol. Energy 45.

REN21, 2013. Renewables Gobal Future Report. Paris. <http://wwwren21.net/future-of-renewables/global-futures-report/>.

REN21, 2015. Renewables 2015 Global Status Report. Paris. <http://wwwren21.net/status-of-renewables/global-status-report/>.

RTE Réseau de transport d'électricité, 2015. 2014 Annual Electricity Report <http://www.rte-france.com/en/news/electricity-report-2014-drop-electricity-demand-and-increase-renewable-energies-which>.

Schallenberg-Rodriguez, J., 2013. Photovoltaic techno-economical potential on roofs in regions and islands: the case of the Canary Islands. Methodological review and methodology proposal. Renew. Sustain. Energy Rev. 20, 219–239. http://dx.doi.org/10.1016/j.rser.2012.11.078.

Singh, R., Banerjee, R., 2015. Estimation of rooftop solar photovoltaic potential of a city. Sol. Energy 115, 589–602. http://dx.doi.org/10.1016/j.solener.2015.03.016.

Solar Energy Industries Association, 2014. Solar Means Business 2014. Top U.S. Commercial Solar Users, Washington, DC.

Stetz, T., Rekinger, M., Theologitis, I., 2014. Transition from uni directional to bi directional distribution grids. Management summary of IEA Task 14 Subtask 2 – Recommendations based on Global Experience. September, 2014. Report No.: IEA PVPS Task 14:03-2014.

The US Department of Energy, 2015. The US Department of Energy <http://www.energy.gov/> (accessed 2015).

The White House. President of the US, 2013. The President's Climate Action Plan. Executive Office of the President.

U.S. Energy Information Administration, 2003. Commercial Buildings Energy Consumption Survey. U.S. Energy Information Administration.

U.S. Energy Information Administration, 2015. Electricity Data Browser <http://www.eia.gov/electricity/data/browser/> (accessed 14/07/2015 2015).

U.S. Environmental Protection Agency, 2015. Carbon Pollution Emission Guidelines for Existing Stationary Sources: Electric Utility Generating Units; Final Rule. U.S. Federal Register, pp. 64661–65120.

UK Government. Department of Energy & Climate Change, 2015. Renewable Energy in 2014 <https://www.gov.uk/government/statistics/energy-trends-june-2015-special-feature-articles-renewable-energy-in-2014>.

Wiginton, L.K., Nguyen, H.T., Pearce, J.M., 2010. Quantifying rooftop solar photovoltaic potential for regional renewable energy policy. Comput. Environ. Urban Syst. 34, 345–357. http://dx.doi.org/10.1016/j.compenvurbsys.2010.01.001.

Yamada, H., Ikki, O., 2015. National Survey Report of PV Power Applications in Japan 2014. Paris.

ANEXO V: "*AN ASSESSMENT OF PHOTOVOLTAIC POTENTIAL IN SHOPPING CENTRES*". CERTIFICADO DE PUBLICACIÓN.

ELSEVIER

Solar Energy

Certificate of publication for the article titled:

"An assessment of photovoltaic potential in shopping centres"

Authored by:

Antonio Colmenar-Santos, Severo Campíñez-Romero
Clara Pérez-Molina, Francisco Mur-Pérez

Published in:

Volume 135C, 2016, Pages 662-673

ANEXO VI: "*AN ASSESSMENT OF PHOTOVOLTAIC POTENTIAL IN SHOPPING CENTRES*". FACTOR DE IMPACTO.

2018 Journal Performance Data for: SOLAR ENERGY

ISSN: 0038-092X
PERGAMON-ELSEVIER SCIENCE LTD
THE BOULEVARD, LANGFORD LANE, KIDLINGTON, OXFORD OX5 1GB, ENGLAND
USA

TITLES
ISO: Sol. Energy
JCR Abbrev: SOL ENERGY

LANGUAGES
English

CATEGORIES
ENERGY & FUELS - SCIE

PUBLICATION FREQUENCY
12 issues/year

The data in the two graphs below and in the Journal Impact Factor calculation panels represent citation activity in 2018 to items published in the journal in the prior two years. They detail the components of the Journal Impact Factor. Use the "All Years" tab to access key metrics and additional data for the current year and all prior years for this journal.

2018 Journal Impact Factor & percentile rank in category for: SOLAR ENERGY

4.674

2018 Journal Impact Factor

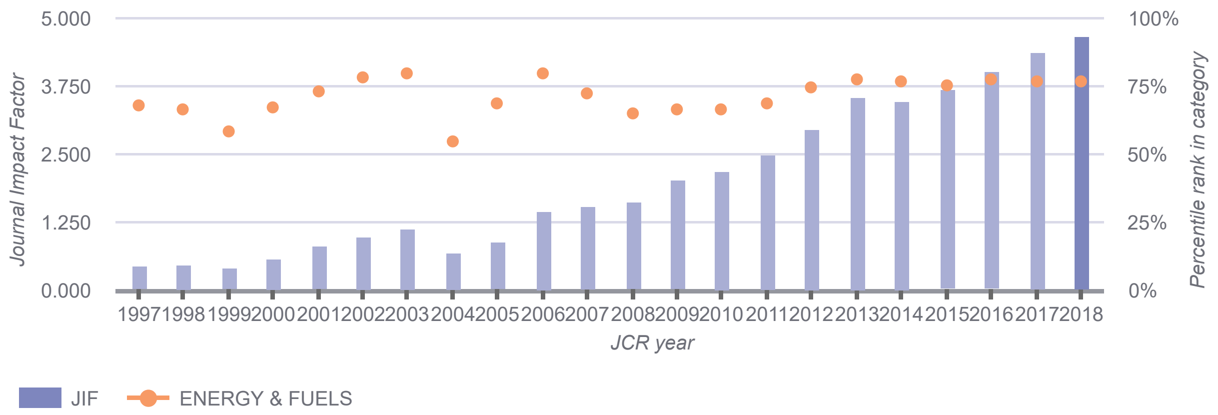

2018 JIF Citation Distribution for: SOLAR ENERGY

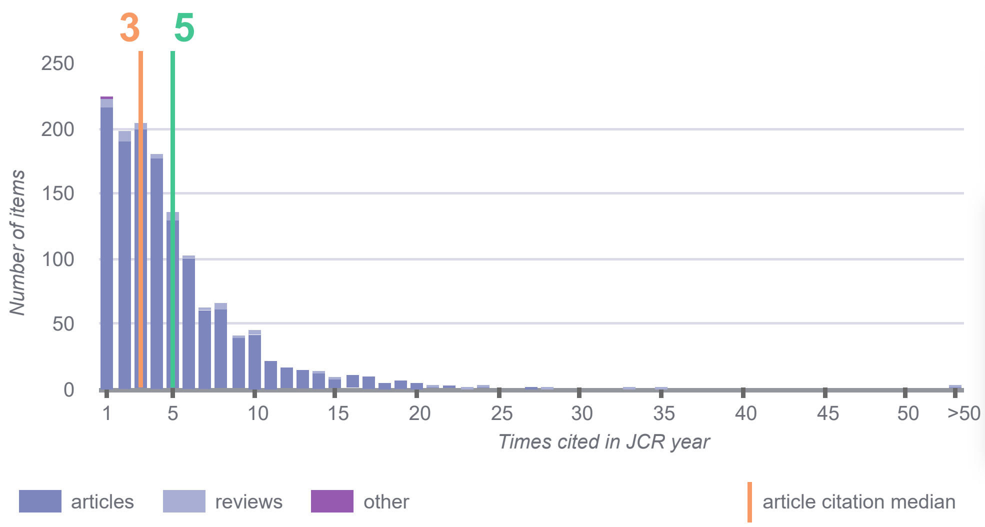

110

Unlinked citations

0

Times Cited

- **149** articles
- **4** reviews
- **23** other

Journal Impact Factor Calculation

2018 Journal Impact Factor $= \frac{7,166}{1,533} = 4.674$

How is Journal Impact Factor Calculated?

$$\text{JIF} = \frac{\text{Citations in 2018 to items published in } \textbf{2016 (3,752) + 2017 (3,414)}}{\text{Number of citable items in } \textbf{2016 (701) + 2017 (832)}} = \frac{7,166}{1,533}$$

Journal Impact Factor contributing items

Citable items in 2017 and 2016 (1,533)

TITLE	CITATIONS COUNTED TOWARDS JIF
Review of photovoltaic power forecasting By: Antonanzas, J.; Osorio, N.; Escobar, R.; Urraca, R.; Martinez-de-Pison, F. J.; et al. **Volume: 136 Page: 78-111 Accession number: WOS:000383004200009** **Document Type: Review**	80
Tabulated values of the Shockley-Queisser limit for single junction solar cells By: Ruhle, Sven **Volume: 130 Page: 139-147 Accession number: WOS:000374426900013** **Document Type: Article**	66
Design of high-performance water-in-glass evacuated tube solar water heaters by a high-throughput screening based on machine learning: A combined modeling and experimental study By: Liu, Zhijian; Li, Hao; Liu, Kejun; Yu, Hancheng; Cheng, Kewei **Volume: 142 Page: 61-67 Accession number: WOS:000392771600007** **Document Type: Article**	65
On recent advances in PV output power forecast By: Raza, Muhammad Qamar; Nadarajah, Mithulananthan; Ekanayake, Chandima **Volume: 136 Page: 125-144 Accession number: WOS:000383004200011** **Document Type: Review**	35
Triphenylamine based dyes for dye sensitized solar cells: A review By: Mahmood, Asif **Volume: 123 Page: 127-144 Accession number: WOS:000368204600012** **Document Type: Review**	33
Integration of storage and renewable energy into district heating systems: A review of modelling and optimization By: Olsthoorn, Dave; Haghighat, Fariborz; Mirzaei, Parham A. **Volume: 136 Page: 49-64 Accession number: WOS:000383004200007** **Document Type: Review**	28
Innovating to zero the building sector in Europe: Minimising the energy consumption, eradication of the energy poverty and mitigating the local climate change By: Santamouris, Mat **Volume: 128 Page: 61-94 Accession number: WOS:000373865000004** **Document Type: Article**	27

Citations in 2018 (7,166)

TITLE	CITATIONS COUNTED TOWARDS JIF
SOLAR ENERGY	1448
RENEWABLE & SUSTAINABLE ENERGY REVIEWS	434
ENERGY CONVERSION AND MANAGEMENT	327
APPLIED ENERGY	286
ENERGY	239
ENERGIES	217
RENEWABLE ENERGY	204
APPLIED THERMAL ENGINEERING	151
SOLAR ENERGY MATERIALS AND SOLAR CELLS	112
JOURNAL OF CLEANER PRODUCTION	97

Key Indicators 2018

IMPACT METRICS		
Total Cites	33,264	✓Trend
Journal Impact Factor	4.674	Trend
5 Year Impact Factor	4.807	Trend
Immediacy Index	1.011	Trend
Impact Factor Without Journal Self Cites	3.729	Trend

INFLUENCE METRICS		
Eigenfactor Score	0.03119	Trend
Article Influence Score	0.785	Trend
Normalized Eigenfactor	3.71116	Trend

SOURCE METRICS		
Citable Items	1,048	Trend
% Articles in Citable Items	94.94	Trend
Average JIF Percentile	77.184	Trend
Cited Half-Life	6.6	Trend
Citing Half-Life	5.6	Trend

Metric Trend

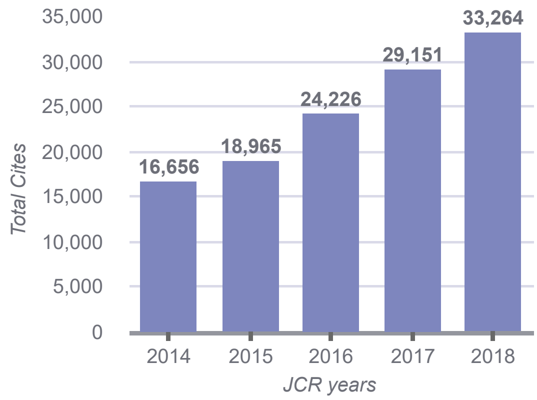

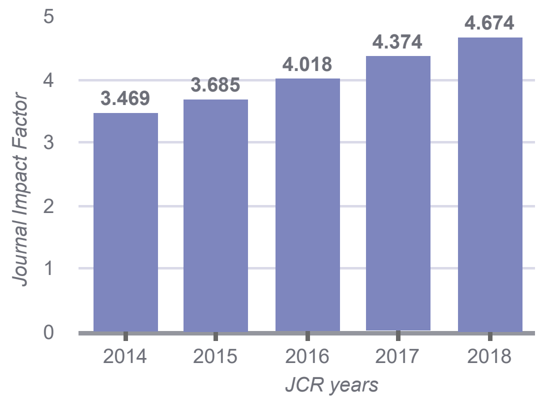

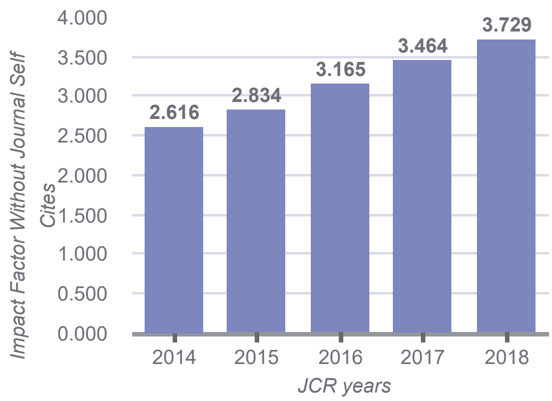

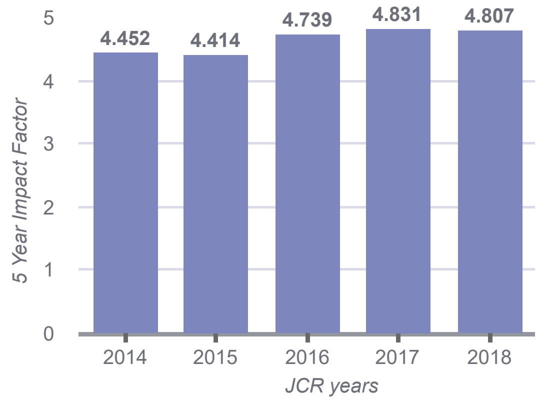

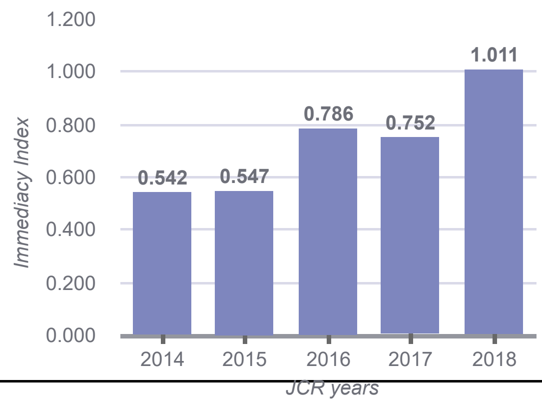

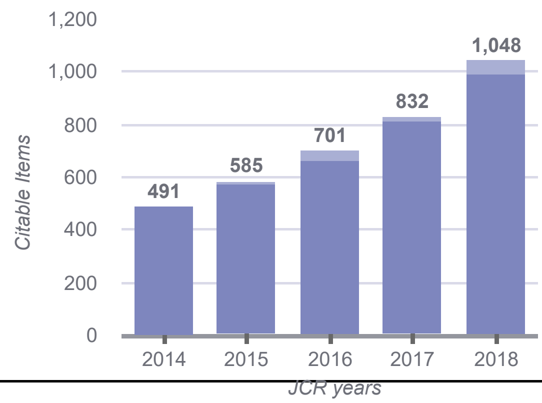

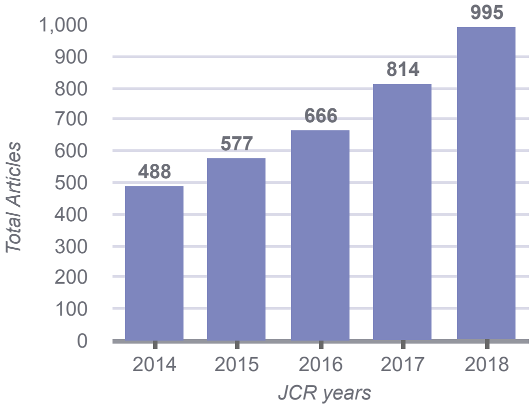
Total Articles
JCR years
2014
2015
2016
2017
2018
488
577
666
814
995

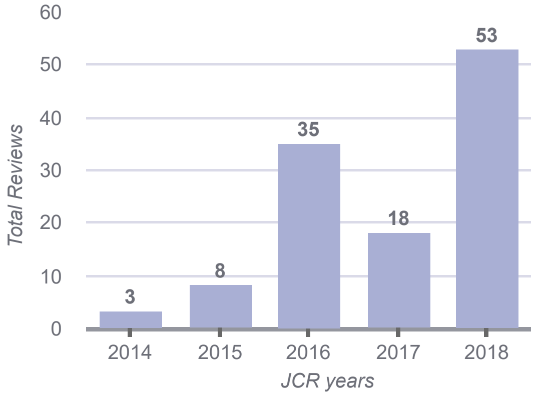
Total Reviews
JCR years
2014
2015
2016
2017
2018
3
8
35
18
53

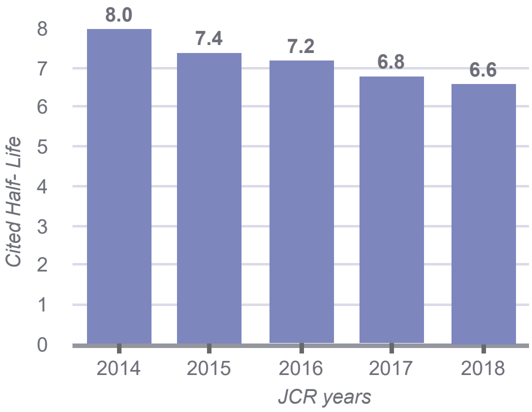
Cited Half- Life
JCR years
2014
2015
2016
2017
2018
8.0
7.4
7.2
6.8
6.6

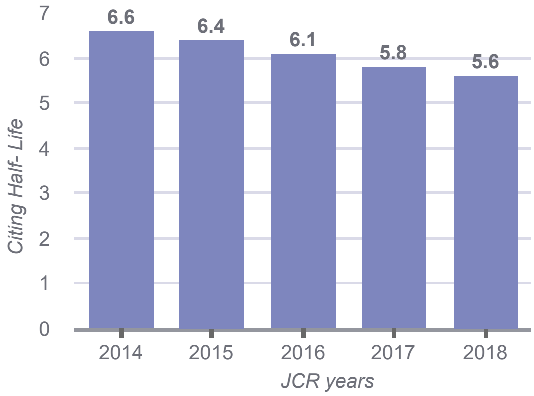
Citing Half- Life
JCR years
2014
2015
2016
2017
2018
6.6
6.4
6.1
5.8
5.6

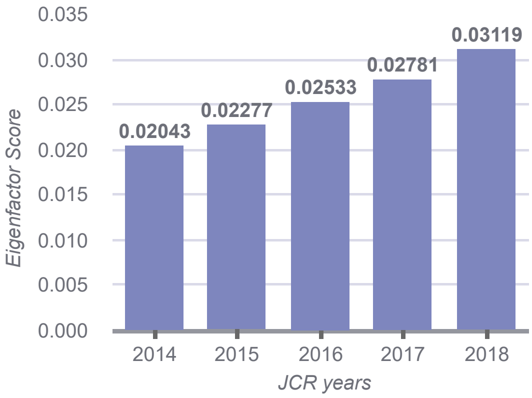
Eigenfactor Score
JCR years
2014
2015
2016
2017
2018
0.02043
0.02277
0.02533
0.02781
0.03119

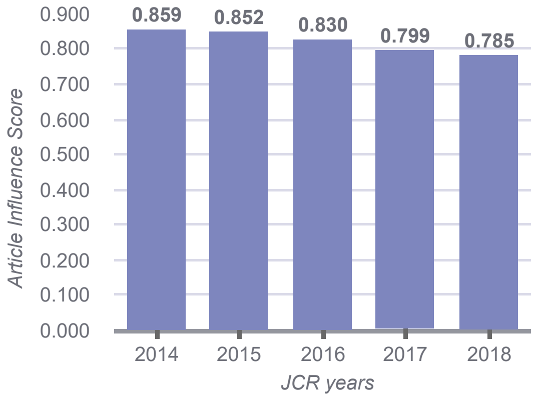
Article Influence Score
JCR years
2014
2015
2016
2017
2018
0.859
0.852
0.830
0.799
0.785

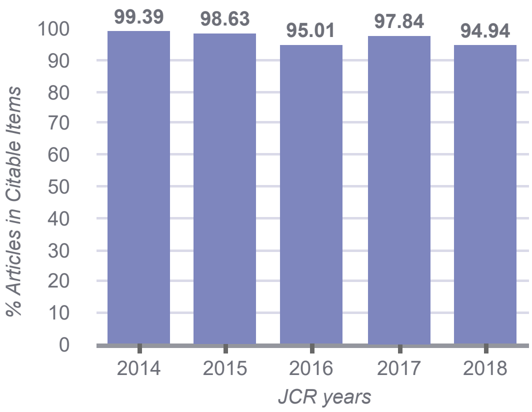
% Articles in Citable Items
JCR years
2014
2015
2016
2017
2018
99.39
98.63
95.01
97.84
94.94

Clarivate Analytics

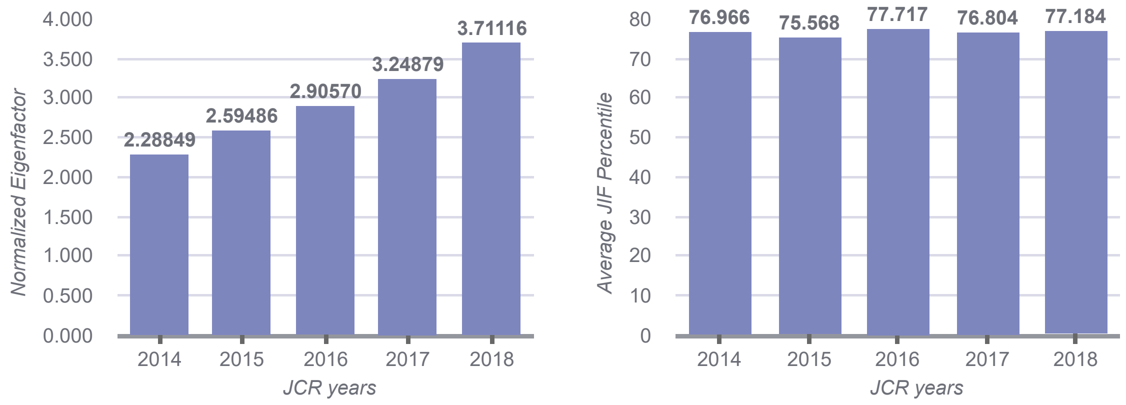

Source data

Journal source data 2018

	Articles	Reviews	Combined(C)	Other(O)	Percentage(C/(C+O))
Number in JCR Year 2018 (A)	995	53	1,048	15	98%
Number of References (B)	40,341	6,015	46,356	28	99%
Ratio (B/A)	40.5	113.5	44.2	1.9	

Box plot

Category Box Plot 2018

Category Box Plot

The category box plot depicts the distribution of Impact Factors for all journals in the category. The horizontal line that forms the top of the box is the 75th percentile (Q1). The horizontal line that forms the bottom is the 25th percentile (Q3). The horizontal line that intersects the box is the median Impact Factor for the category.
Horizontal lines above and below the box, called whiskers, represent maximum and minimum values.
The top whisker is the smaller of the following two values:
the maximum Impact Factor (IF)
Q1 IF + 3.5(Q1 IF - Q3 IF)
The bottom whisker is the larger of the following two values:
the minimum Impact Factor (IF)
Q1 IF - 3.5(Q1 IF - Q3 IF)
Box Plots are provided for the current JCR year for each of the categories in which the journal is indexed.

SOL ENERGY, IF: 4.674

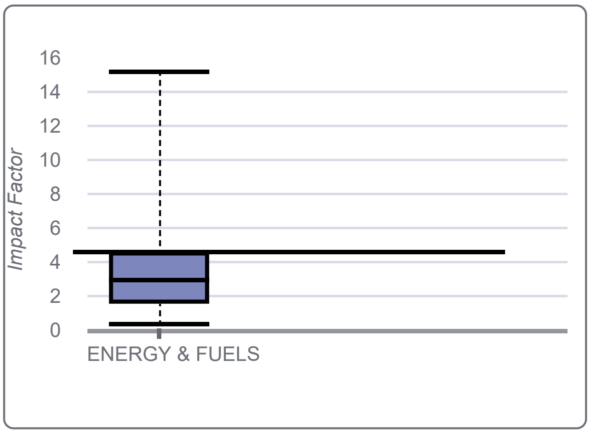

Rank

Rank

JCR Impact Factor

JCR Year	ENERGY & FUELS		
	Rank	Quartile	JIF Percentile
2018	24/103	Q1	77.184
2017	23/97	Q1	76.804
2016	21/92	Q1	77.717
2015	22/88	Q1	75.568
2014	21/89	Q1	76.966
2013	19/83	Q1	77.711
2012	21/81	Q2	74.691
2011	26/81	Q2	68.519
2010	27/79	Q2	66.456
2009	24/71	Q2	66.901
2008	24/67	Q2	64.925
2007	18/64	Q2	72.656
2006	13/62	Q1	79.839
2005	20/63	Q2	69.048
2004	28/61	Q2	54.918
2003	13/62	Q1	79.839
2002	14/63	Q1	78.571
2001	18/66	Q2	73.485
2000	22/66	Q2	67.424
1999	27/64	Q2	58.594
1998	23/67	Q2	66.418
1997	19/58	Q2	68.103

ESI Total Citations

Rank

JCR Year	ENGINEERING
2018	30/893-Q1
2017	31/867-Q1
2016	32/861-Q1
2015	31/850-Q1
2014	30/838-Q1
2013	39/837-Q1

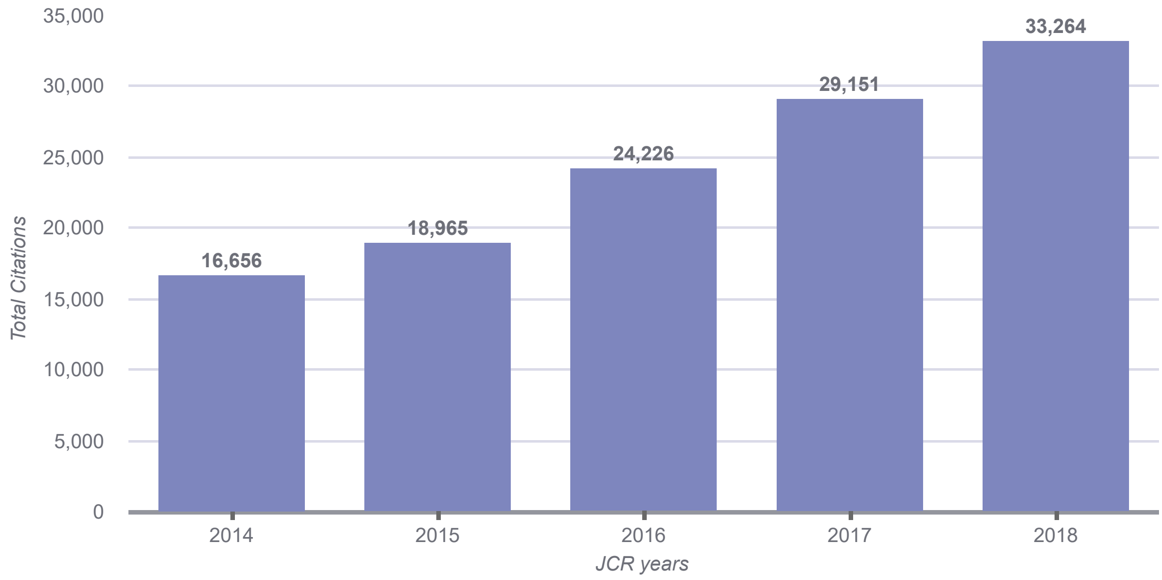

Cited Journal Data

Cited Half-Life Data

Cited Year	2018	2017	2016	2015	2014	2013	2012	2011	2010	2009	2008-All
#Cites from 2018	1,060	3,414	3,752	2,828	2,558	1,921	1,897	2,042	1,232	1,382	11,178
Cumulative %	3.19%	13.45%	24.73%	33.23%	40.92%	46.70%	52.40%	58.54%	62.24%	66.40%	100.00%

Cited Journal Graph 2018

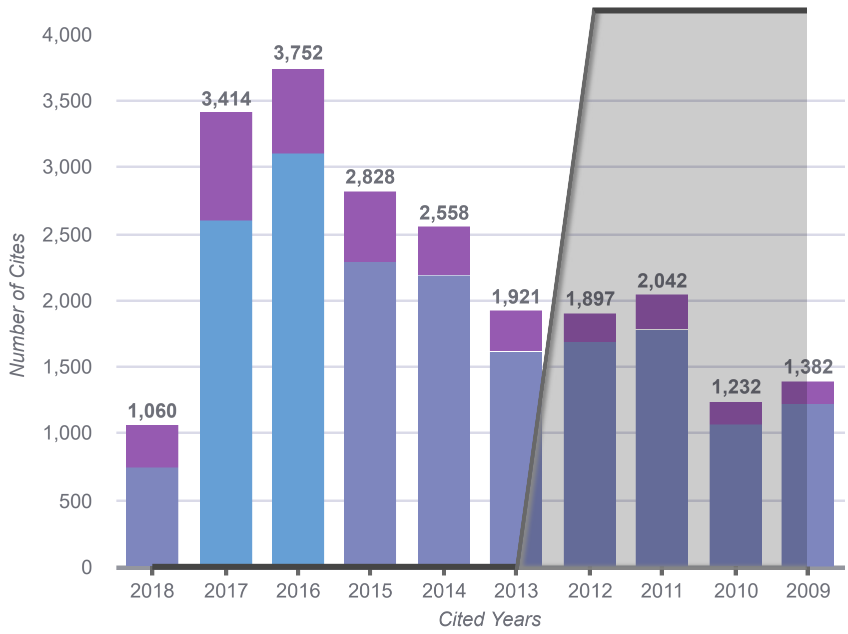

CITED JOURNAL GRAPH

The Cited Journal Graph shows the distribution (by cited year) of citations published in journals during the JCR year to items published in the Journal during the last 10 years.

The white/grey division indicates the cited half-life (if < 10.0). Half of the citations are to items that were published more recently than the cited half-life.

The two light-blue columns indicate citations used to calculate the Impact Factor (always the 2nd and 3rd columns).

Non-self-citations: citations from the journal to articles in other journals.

Journal self - citations: citations from articles in the journal to articles in the same journal.

Cited Journal Data 2018

	Impact	Citing Journal	All Yrs	2018	2017	2016	2015	2014	2013	2012	2011	2010	2009	Rest
		ALL Journals	33,264	1,060	3,414	3,752	2,828	2,558	1,921	1,897	2,042	1,232	1,382	11,178
		ALL OTHERS (667)	667	20	43	62	55	52	38	38	32	23	33	271
1	4.674	SOL ENERGY	5,075	321	810	638	528	369	309	212	263	161	164	1,300
2	10.556	RENEW SUST ENERG REV	2,388	19	155	279	198	173	138	137	146	79	94	970
3	5.439	RENEW ENERG	1,419	8	78	126	128	77	88	98	90	50	64	612
4	8.426	APPL ENERG	1,394	39	149	137	132	132	87	94	85	51	51	437
5	7.181	ENERG CONVERS MANAGE	1,172	45	167	160	105	86	72	98	62	38	51	288
6	5.537	ENERGY	1,115	35	109	130	98	80	61	77	64	42	46	373
7	2.707	ENERGIES	1,062	53	102	115	82	73	74	58	78	55	42	330
8	4.026	APPL THERM ENG	714	14	74	77	49	51	38	39	41	26	26	279
9	4.495	ENERG BUILDINGS	516	4	41	42	32	48	23	21	22	22	29	232
10	6.019	SOL ENERG MAT SOL C	501	23	56	56	42	40	34	26	25	11	30	158
11	6.395	J CLEAN PROD	405	10	46	51	28	44	22	16	28	18	16	126
12	2.592	SUSTAINABILITY-BASEL	242	6	30	26	25	29	7	9	10	11	8	81
13	1.511	J RENEW SUSTAIN ENER	239	11	10	24	15	17	22	9	15	9	11	96
14	3.343	INT J ENERG RES	230	6	19	19	26	18	17	16	17	11	13	68
15	1.190	J SOL ENERG-T ASME	223	0	15	19	20	23	17	12	16	4	16	81
16	3.517	J ENERGY STORAGE	216	6	17	11	19	24	9	15	9	12	12	82
17	4.084	INT J HYDROGEN ENERG	211	8	34	23	12	9	7	7	15	4	5	87
18	4.624	SUSTAIN CITIES SOC	191	8	22	20	7	20	9	11	15	3	5	71
19	4.820	BUILD ENVIRON	190	4	19	9	11	21	5	14	9	8	3	87
20	2.217	APPL SCI-BASEL	177	13	18	16	14	15	11	8	14	12	7	49
21	6.035	DESALINATION	173	1	23	19	18	3	7	9	3	2	11	77
22	4.346	INT J HEAT MASS TRAN	173	2	18	22	12	17	8	13	11	9	9	52
23		GREEN ENERGY TECHNOL	169	0	12	19	13	8	14	16	11	8	7	61
24		INT J RENEW ENERGY R	167	4	14	24	15	13	9	10	12	7	10	49
25	3.398	IEEE J PHOTOVOLT	164	9	26	21	15	15	13	8	10	2	10	35
26	2.195	J MATER SCI-MATER EL	162	11	40	20	15	18	5	11	11	3	5	23

Showing 1 - 28 rows of 1,214 total

Citing Journal Data

Citing Half-Life Data

Citing Year	2018	2017	2016	2015	2014	2013	2012	2011	2010	2009	2008-All
#Cites from 2018	1,565	4,960	5,327	4,954	4,372	3,617	2,835	2,528	1,900	1,630	12,696
Cumulative %	3.37%	14.07%	25.55%	36.23%	45.66%	53.46%	59.57%	65.02%	69.11%	72.63%	100.00%

Citing Journal Graph 2018

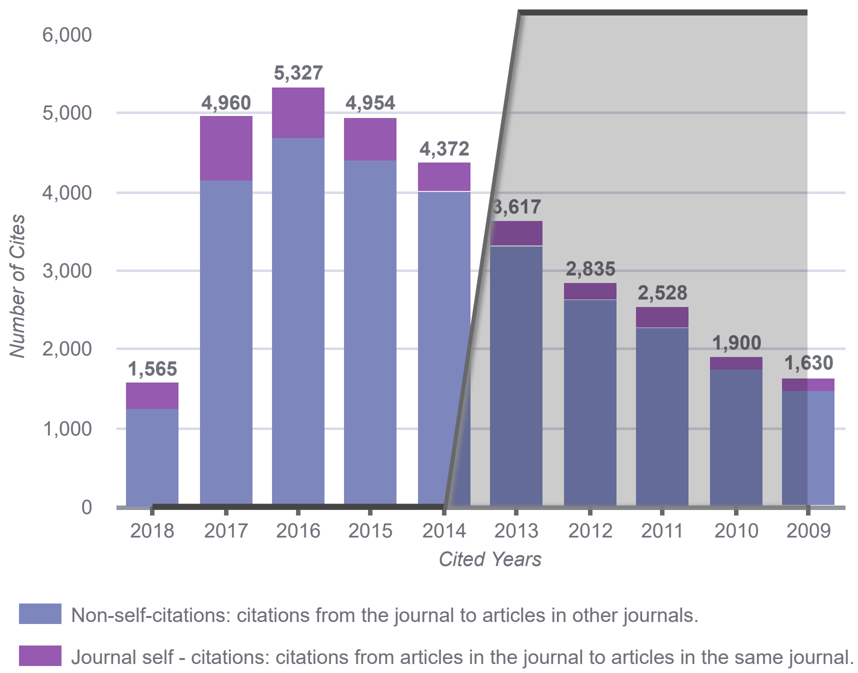

CITING JOURNAL GRAPH

The Citing Journal Graph shows the distribution (by cited year) of citations published in the Journal during the JCR year to items published in journals during the last 10 years.

The white/grey division indicates the citing half-life (if < 10.0). Half of the citations are to items that were published more recently than the citing half-life.

Citing Journal Data 2018

	Impact	Cited Journal	All Yrs	2018	2017	2016	2015	2014	2013	2012	2011	2010	2009	Rest
		ALL Journals	46,384	1,565	4,960	5,327	4,954	4,372	3,617	2,835	2,528	1,900	1,630	12,696
		ALL OTHERS (6172)	6,172	149	524	532	534	453	409	377	345	268	200	2,381
1	4.674	SOL ENERGY	5,075	321	810	638	528	369	309	212	263	161	164	1,300
2	6.019	SOL ENERG MAT SOL C	1,457	53	201	197	120	112	84	98	102	53	56	381
3	10.556	RENEW SUST ENERG REV	1,414	93	253	240	210	133	162	78	73	83	44	45
4	8.426	APPL ENERG	1,058	39	153	143	158	125	129	69	50	74	48	70
5	5.439	RENEW ENERG	1,006	56	137	181	100	82	64	40	53	29	40	224
6	7.181	ENERG CONVERS MANAGE	998	48	145	152	145	118	72	19	25	33	21	220
7	5.537	ENERGY	753	37	95	116	86	84	58	43	37	31	19	147
8	3.521	APPL PHYS LETT	608	2	14	14	42	68	51	42	41	42	45	247
9	4.026	APPL THERM ENG	574	50	112	106	39	51	44	10	35	16	9	102
10	4.495	ENERG BUILDINGS	572	20	55	74	76	57	58	49	24	24	9	126
11	7.776	PROG PHOTOVOLTAICS	530	20	47	51	73	35	61	37	42	17	13	134
12		ENRGY PROCED	495	0	45	59	126	172	24	50	18	1	0	0
13	25.809	ADV MATER	457	18	42	59	51	52	32	33	55	28	17	70
14	2.328	J APPL PHYS	436	5	9	14	17	18	30	19	22	17	24	261
15	1.888	THIN SOLID FILMS	428	5	22	16	20	21	32	12	27	12	33	228
16	10.733	J MATER CHEM A	426	11	87	82	99	81	66	0	0	0	0	0
17	33.250	ENERG ENVIRON SCI	392	11	32	63	65	82	33	46	37	13	9	1
18	14.695	J AM CHEM SOC	364	2	29	32	40	34	19	34	22	13	50	89
19	8.456	ACS APPL MATER INTER	363	4	49	78	74	65	34	29	13	12	5	0
20	4.309	J PHYS CHEM C	358	6	13	36	33	60	45	31	31	34	32	37
21	1.190	J SOL ENERG-T ASME	352	3	7	20	20	23	25	24	24	15	15	176
22	4.346	INT J HEAT MASS TRAN	288	14	31	17	25	30	25	17	18	9	7	95
23	12.279	NANO LETT	276	1	8	11	23	39	37	37	23	20	21	56
24	41.063	SCIENCE	270	2	29	19	30	21	37	21	23	9	8	71
25	6.035	DESALINATION	258	8	21	29	20	18	16	14	17	14	14	87
26	24.884	ADV ENERGY MATER	255	18	37	34	54	60	19	18	15	0	0	0
27		THESIS	249	3	15	25	24	32	12	13	15	11	15	84
28	3.398	IEEE J PHOTOVOLT	237	9	25	39	39	68	31	21	5	0	0	0

Showing 1 - 30 rows of 2,033 total

These data summarize the characteristics of the journal's published content for the most recent three years, that is, 2018 and the two prior years, combined. This information is based on all listed authors and addresses. It is meant to be descriptive rather than comparative.

Contributions by country/region

country		count
1.	CHINA MAINLAND	503
2.	India	332
3.	USA	304
4.	Spain	223
5.	GERMANY (FED REP GER)	145
6.	Italy	127
7.	Australia	122
8.	Iran	115
9.	England	102
10.	France	99

Contributions by organizations

organization		count
1.	INDIAN INSTITUTE OF TECHNOLOGY SYSTEM (IIT SYSTEM)	126
2.	CHINESE ACADEMY OF SCIENCES	87
3.	UNITED STATES DEPARTMENT OF ENERGY (DOE)	58
-	HELMHOLTZ ASSOCIATION	58
5.	CENTRE NATIONAL DE LA RECHERCHE SCIENTIFIQUE (CNRS)	47
6.	UNIVERSITY OF CALIFORNIA SYSTEM	44
7.	COUNCIL OF SCIENTIFIC & INDUSTRIAL RESEARCH (CSIR) - INDIA	33
8.	KING FAHD UNIVERSITY OF PETROLEUM & MINERALS	32
9.	UNIVERSITY OF NEW SOUTH WALES SYDNEY	24
10.	XI'AN JIAOTONG UNIVERSITY	23
-	UNIVERSITI MALAYA	23

Scopus

Source details

Solar Energy

Scopus coverage years: from 1957 to Present

Publisher: Elsevier

ISSN: 0038-092X

Subject area: Materials Science: General Materials Science | Energy: Renewable Energy, Sustainability and the Environment

View all documents > | Set document alert | Save to source list | Journal Homepage

CiteScore 2018
5.24

SJR 2018
1.593

SNIP 2018
1.622

CiteScore | CiteScore rank & trend | CiteScore presets | Scopus content coverage

CiteScore 2018

Calculated using data from 30 April, 2019

5.24 = Citation Count 2018 / Documents 2015 - 2017* = 11.273 Citations > / 2150 Documents >

*CiteScore includes all available document types

View CiteScore methodology > CiteScore FAQ >

CiteScoreTracker 2019

Last updated on *14 October, 2019*
Updated monthly

4.42 = Citation Count 2019 / Documents 2016 - 2018 = 11.595 Citations to date > / 2623 Documents to date>

CiteScore rank

Category	Rank	Percentile
Materials Science — General Materials Science	#49/438	88th
Energy — Renewable Energy, Sustainability and the Environment	#24/153	84th

View CiteScore trends > Add CiteScore to your site

Metrics displaying this icon are compiled according to Snowball Metrics, a collaboration between industry and academia.

About Scopus

What is Scopus
Content coverage
Scopus blog
Scopus API
Privacy matters

Language

日本語に切り替える
切换到简体中文
切換到繁體中文
Русский язык

Customer Service

Help
Contact us

ELSEVIER

Terms and conditions Privacy policy

RELX

Scopus

Compare sources

Select up to 10 sources to compare

Selected sources: ☐ Solar Energy ×

Remove all selections

CiteScore publication by year

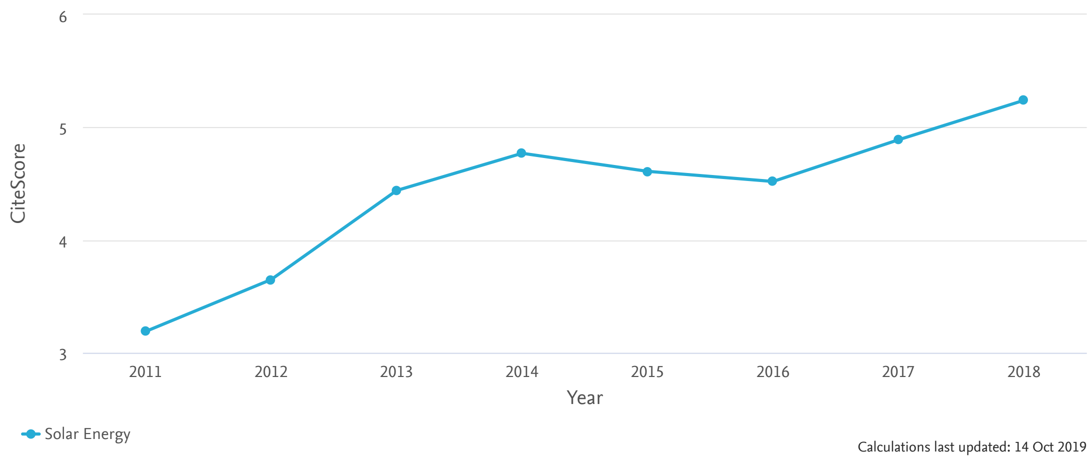

Calculations last updated: 14 Oct 2019

SJR by year

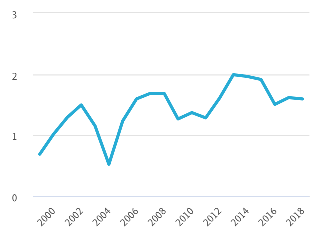

SNIP by year

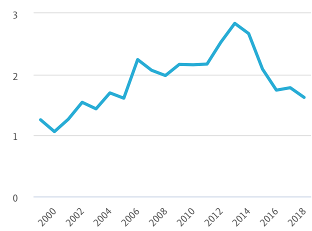

Citations by year

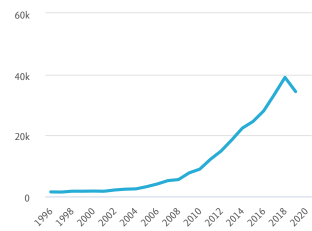

Documents by year

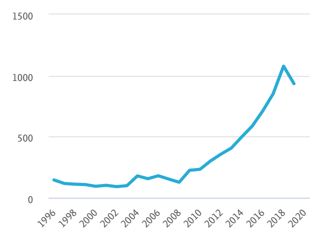

Percent not cited by year

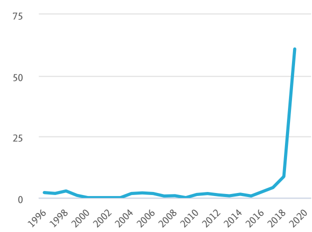

Percentage review articles by year

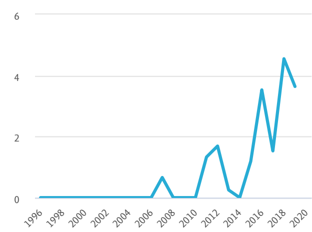

Solar Energy

Country United Kingdom - SIR Ranking of United Kingdom

151

H Index

Subject Area and Category
Energy
- Renewable Energy, Sustainability and the Environment

Materials Science
- Materials Science (miscellaneous)

Publisher Elsevier Ltd.

Publication type Journals

ISSN 0038092X

Coverage 1957-ongoing

Scope Solar Energy, the official journal of the International Solar Energy Society®, is devoted exclusively to the science and technology of solar energy applications. The Society was founded in 1954 and is now incorporated as a non-profit educational and scientific institution. With participation encompassing 100 countries, ISES® serves as a centre for information on research and development in solar energy utilisation. Through its publications and its sponsorship of technical conferences, the Society provides a world forum for the active consideration of solar energy. Solar Energy welcomes manuscripts presenting information not previously published in journals on any aspect of solar energy research, development, application, measurement or policy. The term "solar energy" in this context includes the indirect uses such as wind energy and biomass. Because of the international character of Solar Energy, articles that deal solely with the solar radiation or wind data base of a specific country are not normally considered suitable for Solar Energy. Submitted manuscripts may take the form of reports of original studies or reviews of significant prior work in a given area. All manuscripts are subject to reviews to assure accuracy, clarity, and long-term value.

Homepage

How to publish in this journal

Contact

Join the conversation about this journal

Quartiles

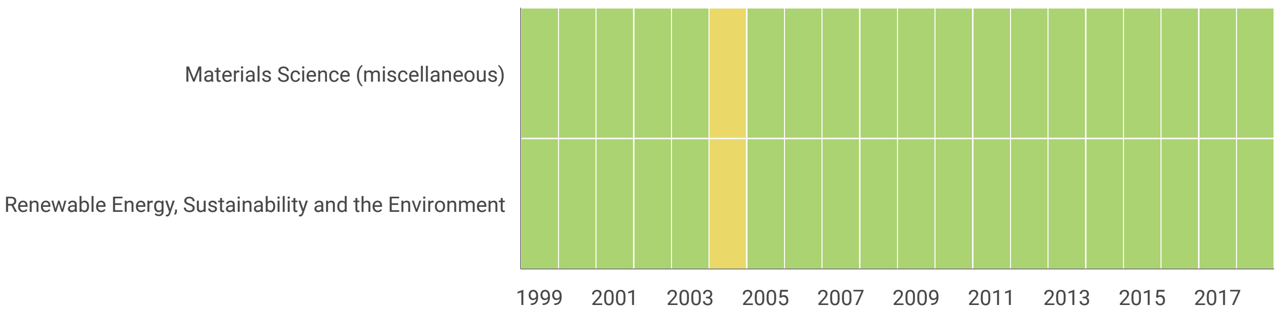

SJR

Citations per document

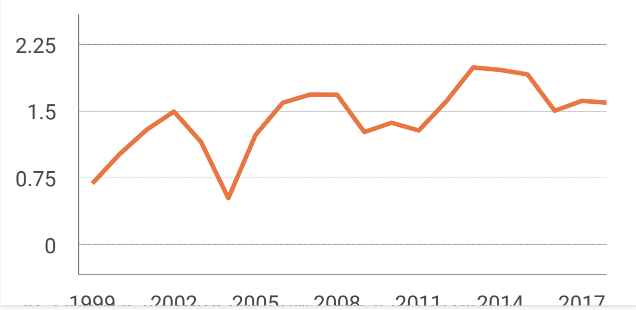

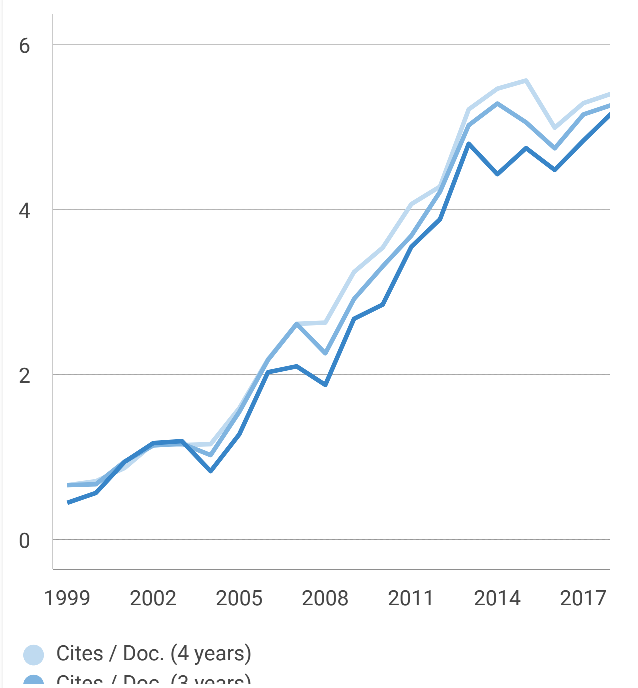

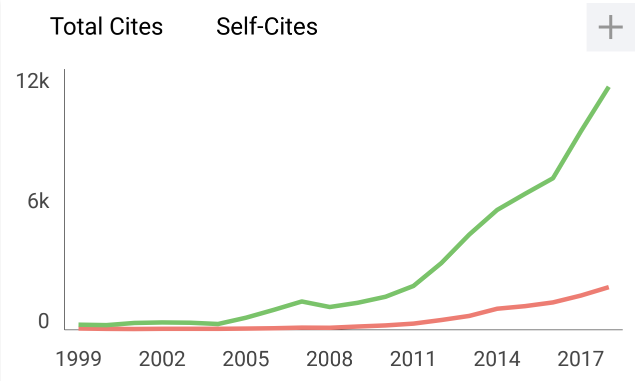

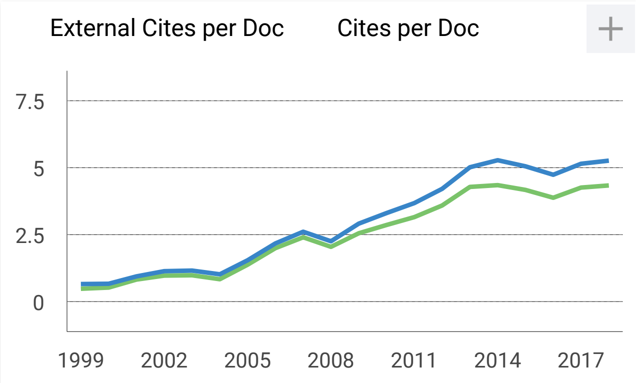

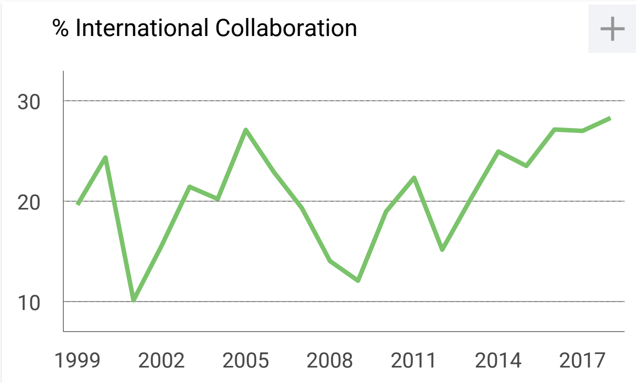

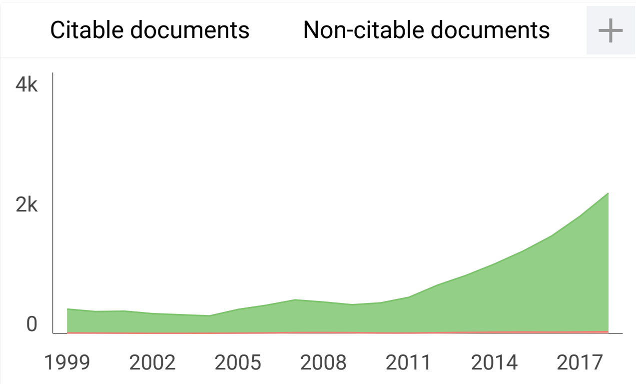

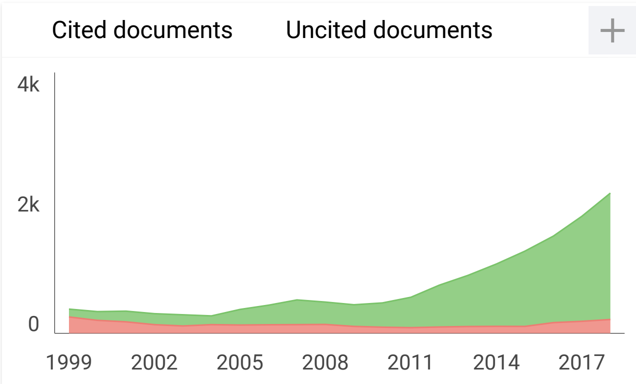

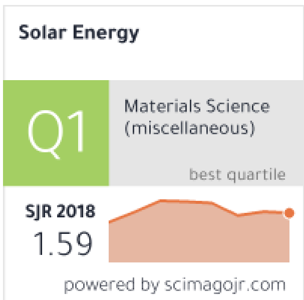

← Show this widget in your own website

Just copy the code below and paste within your html code:

<a href="https://www.scimag

ANEXO VII: "*A HYDROGEN REFUELLING STATIONS INFRASTRUCTURE DEPLOYMENT FOR CITIES SUPPORTED ON FUEL CELL TAXI ROLL-OUT*". COPIA DE LA PUBLICACIÓN.

Energy 148 (2018) 1018–1031

Contents lists available at ScienceDirect

Energy

journal homepage: www.elsevier.com/locate/energy

A hydrogen refuelling stations infrastructure deployment for cities supported on fuel cell taxi roll-out

Severo Campíñez-Romero, Antonio Colmenar-Santos*, Clara Pérez-Molina, Francisco Mur-Pérez

Departamento de Ingeniería Eléctrica, Electrónica y de Control, UNED, Juan del Rosal, 12 — Ciudad Universitaria, 28040 Madrid, Spain

ARTICLE INFO

Article history:
Received 12 June 2017
Received in revised form
18 January 2018
Accepted 4 February 2018
Available online 8 February 2018

Keywords:
Fuel cell vehicles
Hydrogen refuelling stations
Greenhouse gas emissions
Mitigation

ABSTRACT

A shift towards lower-carbon fuels is mandatory to achieve the decarbonisation of the transport sector, which is responsible of 14% of world greenhouse gas emissions. Despite to the fact that fuel cell electric vehicles are zero tail-pipe emissions vehicles, their use is presently residual. A massive integration of fuel cell vehicles faces a “chicken-egg dilemma”: vehicles need a proper refuelling infrastructure to provide a safe and continuous hydrogen supply, but a viable deployment of the refuelling infrastructure needs the support of an initial market of vehicles.

In this article, we design a feasible strategy for overcoming the dilemma, using the local taxi fleet as a stable market of hydrogen consumers to start up a retail hydrogen supply infrastructure in high-populated cities. The design is based on three objectives: ensuring hydrogen supply, having throughout the city a nearby alternative for refuelling and maximizing the infrastructure utilisation rate.

The strategy applied to the city of Madrid show that $415 million of public funds allocated along 25 years would provide in six years a network of 112 hydrogen refuelling stations, able to supply the hydrogen needs of 15,000 new fuel cell electric taxis what would cut the emissions of 300 kt CO_2 yearly.

1. Introduction

In 2010, transport-related GHG emissions reached 7 $GtCO_2eq$, what represents 14% of total. Among them, 72% corresponded to road transport [1]. Without the implementation of mitigation measures, global emissions from transport would reach 12 $GtCO_2eq$ by 2050, but in the scenarios aimed to achieve the 2 °C limit, emissions should be around 6 $GtCO_2eq$, what in fact means lower levels than in 2010 [1].

Most developed countries are the major GHG producers [2]. In 2014, in the US, the transport was responsible of 26% of the total emissions [3]. In the same year the transport sector produced in the EU-28 countries 25.5% of emissions, of which 73% came from road transport and among them 44% were emitted by passenger cars [4].

The practical implementation of mitigation measures is not showing the expected performance. According to the International Energy Agency (IEA) in 2016 several countries were on track, and some of them even exceed, many of the targets set in their particular Paris Agreement pledges [5]; but it would not be nearly enough to limit warming to less than 2 °C [6].

Three main fundamentals lead the GHG emissions mitigations measures focused on transport: increasing the efficiency of the vehicles, changing the transport habits and shifting to lower-carbon fuels [7].

In the ambit of fuel shifting, high-emission fuels can be replaced for electricity and hydrogen, both used in EVs, and for biofuels used in ICEs. Fig. 1 illustrates the main characteristics of EVs and ICEs.

The use of biofuels reached 3% in 2015 and it is foreseen a marginal increase up to 4% by 2021 [8]. Similar advances have been seen in PHEV and BEV integration. In 2015, there were 1.26 million EVs running, meaning 1% of penetration and reaching high shares of 23% in Norway and 10% in the Netherlands [9]. Multiple research is ongoing to boost the penetration levels, favouring the integration [10] and improving the recharging conditions [11].

The integration of hydrogen presents the lower advance. Hydrogen can be used in vehicles equipped with hydrogen internal combustion engines (HICE) or in EVs equipped with hydrogen fuel cells (FCEV), In comparison with the other types of EVs, FCEVs offer a lower GHG emission level than PHEVs and lower recharging time

* Corresponding author.
E-mail address: acolmenar@ieec.uned.es (A. Colmenar-Santos).

https://doi.org/10.1016/j.energy.2018.02.009
0360-5442/

Nomenclature

General	
BEV	Battery electric vehicle
EV	Electric vehicle
FCEV	Fuel cell electric vehicle
FCET	Fuel cell electric taxi
HICE	Hydrogen internal combustion engine
HRS	Hydrogen refuelling station
IEA	International Energy Agency
PHEV	Plug-in Hybrid electric vehicle *SMR* Steam methane reforming
TCO	Total cost of ownership
WE	Water electrolysis
Financial	
IRR	Internal Rate of Return
K	Discount rate for NPV calculation
TDEP	Asset depreciation period
RPI	Retail price index (%)
CF_z	Cash flow for year z
CFA_z	Cumulative cash flow for year z
NPV	Net present value
z	Ordinal indicating the number of years the asset has been operating
FL	Financial Leverage
VAT	Value added tax (%)
TAX	Incomes taxes (%)
ADSCR	Annual debt service coverage ratio

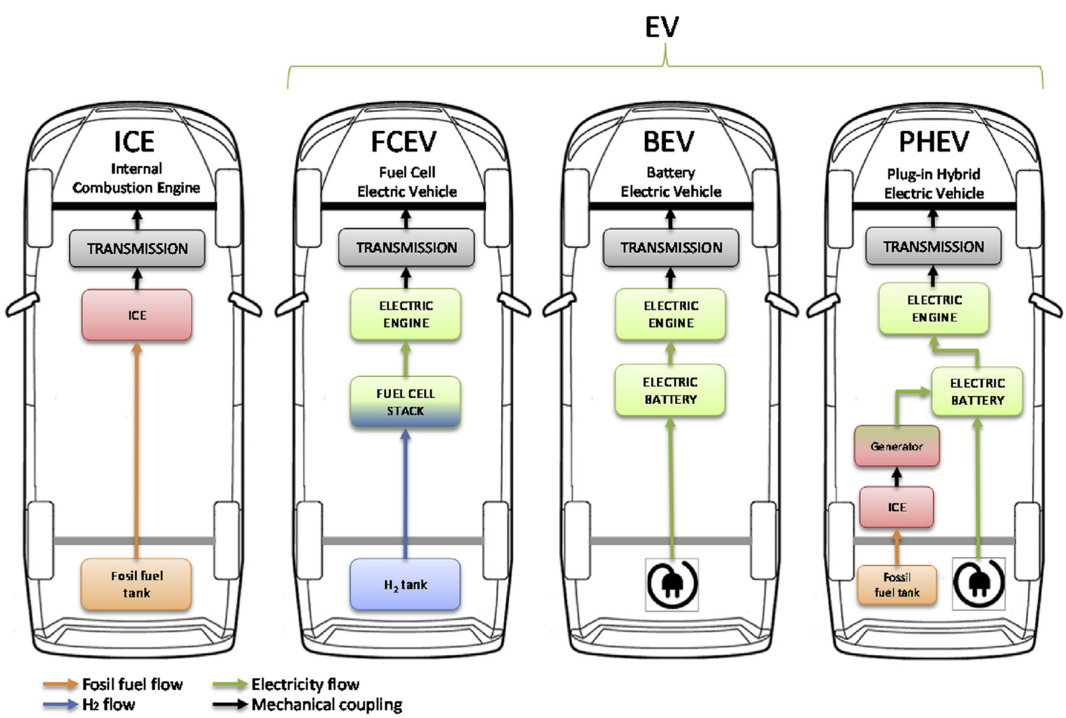

Fig. 1. EVs and ICEs functioning principles.

and greater range of autonomy than BEVs. Therefore, FCEVs present a mobility similar to present conventional ICE vehicles [12].

Well-to-wheel FCEV emissions depend on the hydrogen production mix and the share of RES in the generation of the electricity involved, but generally is well below ICE and PHEV and around BEV levels [12–15]. Recent research focused on taxi life cycle analysis has determined lower energy consumption and CO_2 emissions of FCEV in comparison with BEVs [16].

With regard to fuel prices, though the costs for PHEV and BE are currently lower, in terms of total cost of ownership[1] (TCO), both FCEVs and BEVs show comparable values and slightly higher to PHEV [12,13,17].

All the GHG reduction strategies include the integration of FCEVs in vehicle fleets. The IEA includes in the pathway to achieve 2DS scenario,[2] a 25% share of FCEVs in 2050, which would contribute to get 10% reduction of transport-related emissions [12]. The EU HYWAYS project [18], estimates 2.5 million FCEVs by 2020. In California is projected the integration of 10,500 FCEVs in 2018 and more than 34,000 units by ending 2021 [19]. A minimum of 10 million vehicles and a maximum of 40 million in the best scenario are planned for the US by 2035 [20].

[1] Total Cost of Ownership considers all the costs related with the purchase and use of the vehicle, including fuel cost so that takes into account the vehicle fuel economy.

[2] The IEA 2DS scenario sets up strategies to achieve the goal of limiting the global mean temperature increase to 2 °C.

Several manufactures already include FCEVs in their portfolio and most have plans to include them in the short or medium term [21–25]. Currently, FCEVs and H_2 production and refuelling systems are based on mature technologies that ensure safe and feasible operation at commercial levels for the general public [26,27] and the industry and the scientific community keep on searching solutions for the technical improvement of FCEVs and HRS [28].

Nevertheless, the present status is far from accomplishing the targets. Currently, the world FCEV fleet is around 2000 units with a predominant presence in the state of California (USA), some European counties and Japan. Fig. 2 details the distribution of the FCEV fleet worldwide in 2016.

The HRS deployment is similar; 200 units were in operation in 2016, with California, some European countries and Japan leading the market. The distribution is detailed in Fig. 3.

The main reason behind the slow the FCEV deployment is the lack of a H_2 refuelling network [32]. The car-owner decision for acquiring a FCEV must be supported by the certainty of a safe, nearby and with no restrictions refuelling, whose characteristics were able to give to car-owners a similar comfort level than they already have using traditional hydrocarbon fuelled vehicles. In other words, the FCEV deployment needs to be coordinated with a proper HRS infrastructure roll-out. But for creating this HRS infrastructure is mandatory that the facilities be economically sustainable and preferably fundable. It means that incomes from H_2 sales must be ensured by a sustained, or even growing over time, FCEV market. This is a good example of the situation known as "*the chicken and the egg dilemma*" [18,33,34].

Multiple solutions are being proposed by recent research focused on the development of a distributed hydrogen supply infrastructure, including methodologies for searching the best HRS locations [35,36] and the analysis of the optimal cost-effective hydrogen production, transport and distribution mix [37–39]. But all of them are hardly implementable without the support of a FCEV market. To overcome the *dilemma* a coordinated and simultaneous deployment of FCEV and HRS is mandatory.

Vehicle fleets have been identified as a good initial market for alternative fuels [40,41]. Big fleets could offer a chance to achieve an important FCEV penetration. There are important taxi fleets in most of big and middle-size cities; some examples are shown in Table 1.

The deployment of HRSs in urban centres is a recommended strategy to start a vast hydrogen supply infrastructure [52]. Additionally, due to the high concentration of vehicles, high-populated cities are big polluters.

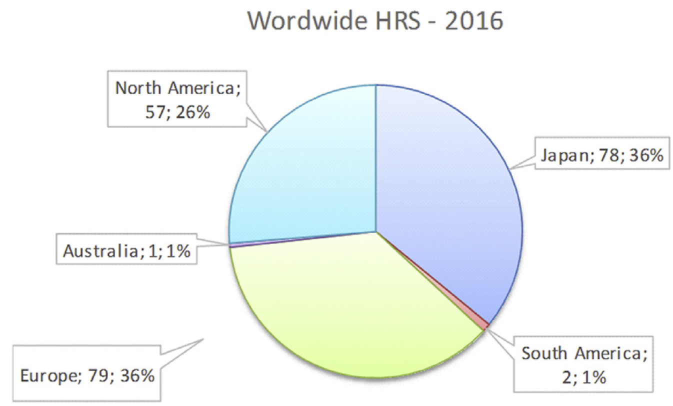

Fig. 3. Number and share of HRS worldwide. Source: [21,30,31].

Table 1
Population, number of taxis and passenger cars in several populated cities.

City	Population (million)	Taxi fleet size	Taxis/ inhabitant	Cars (million)	Taxis/ Cars
London [42–44]	8.50	22,500	2.65	2.60	0.9%
NYC [45–47]	8.55	31,500[a]	3.68	2.10	1.5%
Madrid [48–51]	3.16	15,000[b]	4.75	1.44	1.0%

[a] Includes Yellow cars, Boro taxi and black cars.
[b] Only includes taxi licensed by county. Cars serving for Uber, Cabify or similar companies are not included.

In summary, taxi fleets present important advantages to initiate the FCEV deployment:

- It is a big fleet of vehicles, therefore they offer a strong market for supporting the new HRSs.
- The number of taxis in a city depends generally on its population, but the share is usually under the control of local authorities in an adequate range to assure a reasonable number of clients for every taxi to make the investment in the license feasible.
- The range of operation is basically limited to the city where they are licensed to operate, so that their fuel needs could be supplied by a local HRS network.

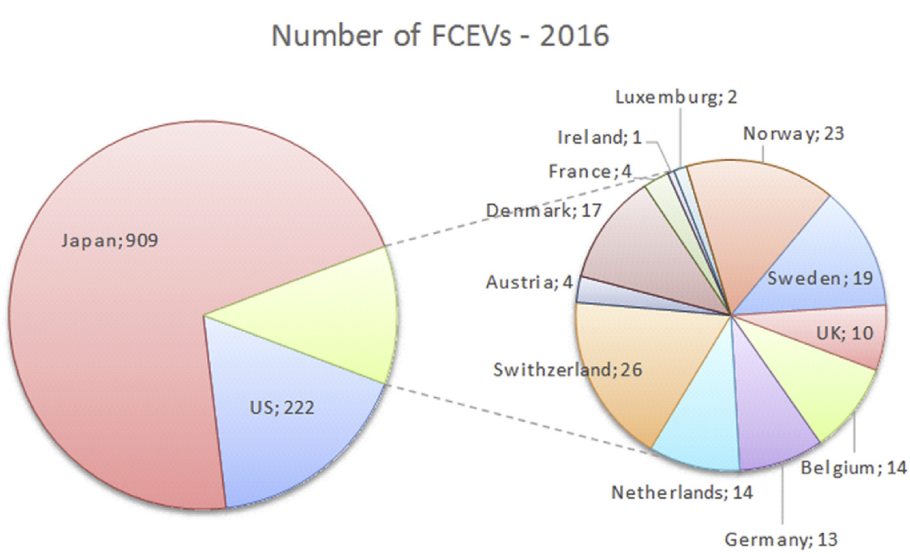

Fig. 2. Main FCEV markets in 2016. Source: [21,29,30].

- Fleets are generally regulated by licencing processes issued by local authorities, so requirements (i.e. fuel) to get the licenses might be specified.
- Taxis have a short replacement period, so that, the whole fleet could be replaced in the short or the medium term.
- Taxis are the more pollutant passenger vehicles in the city because they run every day long distances. Any action focused on them would have a bigger impact than on any other.
- Taxi owners pay taxes in the city where they are licensed to drive, hence it would be possible the allocation of subsidies via tax credits.

With a deployment of fuel cell electric taxis (FCETs) under control, the next step is to carry out coordinately a proper design of the HRS network to ensure the supply of hydrogen needs. Once again, a development coordinated by local authorities might offer advantages because:

- Local authorities generally own lands inside the city limits that can be rented by the HRS owner at a low price to reduce costs.
- Some regulation can be set in order to favouring the development and construction of the facilities.
- Authorities can address grants and subsidies for the construction, financing and operation of HRSs, integrating funds from other national and international governmental sources. As an example, the state of California, by means of the California Energy Commission allocates $20 million yearly for the development of a hydrogen supply network of 100 HRS. Up to 2015 more than $80 million have been used in 49 HRSs and additional $9.9 million funds have been addressed for the direct subsidy of operation and maintenance costs [19].
- Cities would be directly beneficiary of the reduction of pollutant emissions obtaining important savings derived from the improvement in air quality.

This article is aimed at determining a solution, practicable, feasible and fundable to initiate, in high populated cities, a HRS network sufficient to support a massive integration of FCEVs in the urban environment, using as a stable market the city taxi fleets as well as establish the economic framework. In order to obtain results and illustrate the proposed methodology, real data corresponding with the city of Madrid, capital of Spain, has been used. The results are applicable to cities with taxi fleets of similar conditions.

Below in chapter 2 it is defined the methodology developed to determine the details of the HRS base case. In chapter 3, it is designed the HRS and FCEV deployment and their technical characteristics and use the methodology with real data to define the subsidies necessary to support the HRS roll-out. In chapter 4 it is included a sensitivity analyses in relation to the most important parameters to evaluate the effect of their variations in the results. In the chapter 5 the reduction of the GHG emissions resulting from the FCEV integration is calculated. Finally, in the chapter 6 the conclusions of the results obtained in the study are presented.

2. Methodology

The methodology is aimed at determining a *base case*, defined as a business plan, technically viable and financially sustainable, for the construction and operation of a HRS network sufficient to supply the H_2 needs of the FCET fleet of a city. The base case is focused on those HRSs in the worst scenario. They are those put in operation in the first year of the deployment which will have a lower utilisation rate during the first running years and, their construction and operating are expected to be more expensive since they would not be benefited by learning curves and economy of scale.

The technical viability is ensured by analysing present technologies and choosing, among them, the solutions more adequate for the integration in the urban environment of a network with a size according to the FCET roll-out.

The method chosen to quantify feasibility and financial viability of HRS is the valuation of the financial indicators Internal Rate of Return (IRR)[3] and Annual Debt Service Coverage Rate (ADSCR). As the investment can be carried out with or without external financial resources (debt), hence the IRR has been calculated for 25 years in both scenarios named Project IRR and Shareholder IRR correspondingly.

Before obtaining the IRR, the cash flows of the investment in both scenarios are calculated following the methodology described in Table 2.

The Net Present Value (NPV, hereafter) of the investment is calculated from each of the yearly cash flows, discounting back to its present value at the discount rate k, that is

$$\mathrm{NPV} = \sum_{z=1}^{n} \frac{\mathrm{CF_z}}{(1+\mathrm{k})^{z}} - \mathrm{I_o} \quad (1)$$

where I_o is the portion of total cost assumed by the investor, with its value depending on the Financial Leverage (FL hereinafter)[4] is:

$$\mathrm{I_o} = FL\ x\ CAPEX \quad (2)$$

IRR is defined as the interest rate k at which the NPV is zero, that is:

$$0 = \sum_{z=1}^{n} \frac{\mathrm{CF_z}}{(1+\mathrm{IRR})^{z}} - \mathrm{I_o} \quad (3)$$

Table 2
Cash flow calculation methodologies. Self-elaboration.

	Project Cash Flow Without external financing source		Shareholder Cash Flow With external financing source
+	Incomes from H_2 sales H_2 delivery price x sales margin	+	Incomes from H_2 sales H_2 delivery price x sales margin
-	Construction costs (CAPEX)	-	Construction costs (CAPEX x FL)
-	Operating expenses O&M. OPEX. H_2 delivery price	-	Operating expenses O&M. OPEX H_2 delivery price
=	**Gross operating margin (EBITDA)**	=	**Gross operating margin (EBITDA)**
-	Assets depreciation	-	Assets depreciation
=	**Earnings before interests and taxes (EBIT)**	=	**Earnings before interests and taxes (EBIT)**
		-	Loan repayment (capital + interest)
=	**Earnings before taxes**	=	**Earnings before taxes**
-	Taxes	-	Taxes
=	**Earnings after taxes**	=	**Earnings after taxes**
+	Assets depreciation	+	Assets depreciation
=	**Yearly project cash flow (CF_z)**	=	**Yearly shareholder cash flow (CF_z)**
+	Cumulative previous year project cash flow	+	Cumulative previous shareholder year cash flow
=	**Cumulative present year project cash flow (CFA_z)**	=	**Cumulative present year shareholder cash flow (CFA_z)**

[3] IRR determines the interest rate of the monetary resources used in the investment: the higher is the IRR the better is the investment.

[4] The Financial Leverage (FL) is the percentage of the investment cost financed with an external resource or debt.

ADSCR quantifies the capacity of HRS to generate enough incomes to repay the debt got to finance the facility. It is calculated according to the following equation, where the bigger to 1 is ADSCR, the better is the investment from the point of view of its capability to repay the debt:

$$ADSCR_z = \frac{EBIT}{Loan\ repayment\ (capital + interest)} \quad (4)$$

The steps given for determining the base case are the following:

1. Design the FCETs fleet deployment.
2. Set the technical and economic parameters to define the number and performance of the HRSs.
3. Identify and quantify the subsidies and the financial support necessary to ensure the economic sustainability of the facilities.
4. Carry out a sensitivity analysis of the results to find out the base case robustness.

3. Results

To apply and illustrate the methodology proposed in the chapter 2, the city of Madrid was used, whose characteristics are shown in Table 3. The results can be extrapolated to cities with similar taxi fleets.

3.1. The FCET deployment and fuel economy

The share of FCET and the rhythm of replacement of the traditional taxis by new FCET have an important impact in the viability of the HRS. With the aim to design the FCET deployment, a taxi was supposed to run yearly an average distance of 100,000 km. The limit for a commercial vehicle can be around 500,000 km, so that the taxi lifespan was set in 5 years. If it is supposed a similar distribution of vehicles along their lifespan, a replacement rate of 20% is obtained.

With the same objective, it has been considered that only 100 units are replaced in the first year (around 1% of the Madrid taxi fleet). It is a conservative estimate because it is supposed to find a certain barrier to entry at the beginning of the roll-out.

Regarding the FCET fuel economy hydrogen consumption, commercial vehicles offer currently values around 109 km/kg (68 mi/kg), therefore this is the input considered in the study [22,23].

3.2. HRS characterization and infrastructure development

The development of the HRS network must be conducted with three main objectives: (i) ensuring hydrogen supply, (ii) having throughout the city a nearly alternative for refuelling and (iii) maximizing the HRSs utilisation rate.[5] The tools we use to fulfil these objectives are a proper dimensioning in terms of HRS daily capacity of supply, the control of the number of HRS and their location inside the city.

Table 3
Population, number of taxis and passenger cars in several main cities.

City	Extension (Ha)	Population (millions)	Taxi fleet	Cars (millions)
Madrid [48–51]	60,436	3.16	15,000[a]	1.44

[a] Only includes taxi licensed by county. Cars serving for Uber, Cabify or similar companies are not included.

[5] The HRS utilisation rate is defined in a certain period as the hydrogen sold in the period divide by the HRS hydrogen delivery capacity.

From a technological point of view, there are several possible configurations for a HRS and the choice will determine the inputs and the construction and operation costs [26,53,54]. The first choice to make is if the hydrogen is produced in the own HRS (on-site production) or it is produced in other place and delivered to HRS (central production). The second choice is related with the hydrogen production methods. In case of central production, the hydrogen can be delivered to the HRS via trucks as compressed gas (CGH_2 Truck) or liquid (LH_2 Truck) or via pipeline [19,26,53]. The delivery method will depend on the local supply network and the HRSs needs and the choice set HRS characteristics relative to hydrogen download and storage systems. Fig. 4 illustrates the aforementioned hydrogen delivery methods.

There are multiple methods to produce hydrogen in central, therefore the hydrogen delivered to the HRS would be obtained from a mix of all of them [14,56]. When hydrogen is produced on site, two methods are the most widely spread: SMR from natural gas and WE, where the main consumable is the electricity [26,53] that can be generated from renewable sources (photovoltaic or wind) [57], even though in the own HRS.

Table 4 shows a summary compiled from several sources of HRS capital costs for different capacities and technologies, and Fig. 5 summarises the variation of capital costs with the HRS capacity. As can be noticed, there is a great disparity in costs, derived fundamentally of the multiple variables taking part in the HRS definition and the assumptions taken in each source respect of the impact in prices of the economy of scale and learning curves (see Fig. 6).

The technology implemented in the first units of HRSs should be that what imply a lower installation cost and gives, at the same time, the possibility to use the capabilities of present fossil fuels distribution networks. Therefore, our proposal is the use of central-produced hydrogen, delivered to HRSs by CGH_2 or LH_2 trucks depending on the distance from the point of production or temporary storage and the stations [18,26].

In our design, the size of the facilities is also used to control the HRS deployment. The key point is giving to the consumer a place for refuelling located at a reasonable distance while HRS utilisation rates are kept inside limits. The FCET deployment should be constantly supervised by the local authorities and its rhythm of growth will be taking into account to design the HRS roll-out. On one hand, the number of HRSs must be limited to ensure a minimum utilisation rate; on the other hand, bigger stations imply lower costs but longer distances for refuelling while a solution with smaller stations would be more expensive but would offer a shorter refuelling distance. It is essential find a balance between size and number of units. With this aim, the solution adopted in this study was the implementation of a regular distribution throughout the territory. For the city of Madrid, starting the roll-out with 10 units with a capacity of 450 kg/d. it means a place for refuelling at a maximum distance of 5.5 km.

Although the location of the first HRSs must be wisely selected for every single city, the regular distribution here proposed should be kept in the first stages of the deployment to ensure the existence of a refuelling point at a maximum distance and at any point inside the city limits.

It is obvious that taxi refuelling patterns are not homogenous throughout the city as they are led by traffic flow density and origin-destination points [59–61]. Therefore, the capacity of the first HRSs must be carefully adjusted to ensure a minimum utilisation rate and the feasibility of the station.

With this base of design, the choice of the exact locations of HRSs must be object of a detailed analysis for every single city, carried out according to particular urban development plans and taking into consideration the possibility of complementing part of

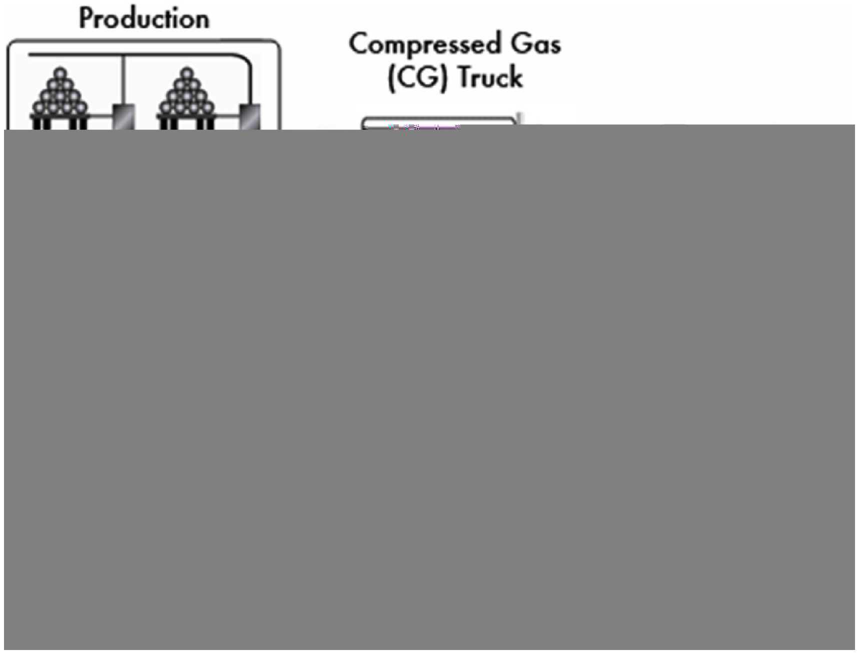

Fig. 4. Hydrogen delivery pathways. Source: [55].

Table 4
HRS capital cost.

Source	Range	Capacity (kg H_2/d)	Capital cost	Capital cost per capacity ($m per kg/d)
HSCC [27,58]	State of the art	160	$2.65 m	16,563
	Early commercial	450	$2.8 m	6222
	More stations	600	$3.09 m	5150
	Larger stations	1500	$5.05 m	3367
UC Davis [33]	Phase 1 years 1–2	100	$1 m	10,000
	from start	250	$1.5 m	6000
	Phase 2 years 3–4	170	$0.9 m	5294
	from start	250	$1.4 m	5600
	Phase 3 years 5 +	170	$0.5 m	2941
	from start	250	$0.9 m	3600
		500	$1.5 m	3000
FCH JU[a] [34]	Baseline	150	$0.99 m	6571
H2FIRST [53]	Delivered gaseous hydrogen	300	$1.26 m	4200
	Delivered gaseous hydrogen	200	$1.17 m	5850
	Delivered gaseous hydrogen	100	$1.09 m	10,900
	Delivered liquid hydrogen	300	$2 m	6667
California Energy Commission [19]	Delivered gaseous hydrogen	180	$2.01 m	11,167
	Delivered liquid hydrogen	350	$2.8 m	8000
	On-site electrolysis	130	$3.21 m	24,692
			Average	6272

[a] When the data source was in € it was converted to $ using the USD/€ = 1,1 exchange rate.

the existing petrol stations with the systems to deliver hydrogen. In these conditions, considering a FCET fuel economy of 109 km/kg and a yearly driven distance around 100,000 km (see chapter 3.2), the 100 first units would need 91,7 tH_2 in their first operation year. With a total capacity of 1642 tH_2, the utilisation factor of the first 10 HRSs would be slightly below 6% in the first year, but would pass 70% in the second and subsequent years.

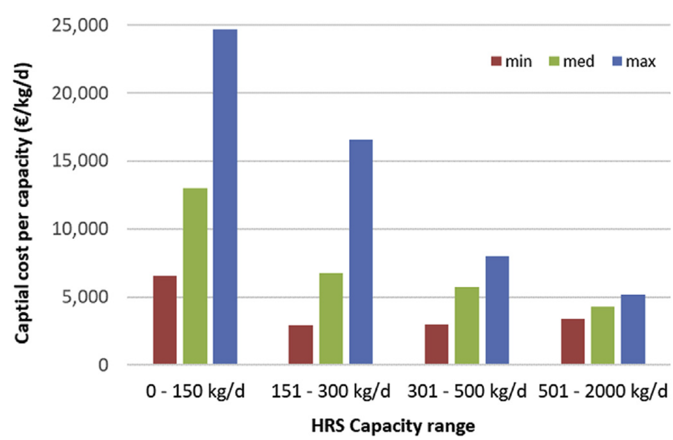

Fig. 5. Distribution of capital costs on the HRS capacity. Source: Table 4.

From the second year onwards, the growth of HRS has been calculated to meet the hydrogen needs of the FCET roll-out defined in the chapter 3.1. with an utilisation factor of 75% Fig. 7 illustrates the deployment of HRS and FCET designed in this study. As can be noticed, from the sixth operating year the whole city taxi fleet would have been replaced by FCETs and the deployment of HRSs would reach 112 units, with a capacity enough to supply the needs of the fleet with a utilisation factor near 75%. With only 100 units of FCET running the city with a yearly hydrogen needs of around 90,000 kg H_2, an initial number 10 HRSs with a capacity of 450 kg H_2/day would be enough to cover the needs with a low utilisation rate (around 6%). Despite it could be possible cover the hydrogen needs with fewer HRSs, it is suggested a number of ten as necessary to cover the territory with an acceptable refuelling distance.

In our assumptions, the total cost for the construction of the HRS was estimated in $2.8 m, corresponding with the average value obtained from Table 4 applied to a capacity of 450 kg/d. This estimate is consistent with the results obtained by applying the tool included in the Hydrogen Refuelling Station Analysis Model

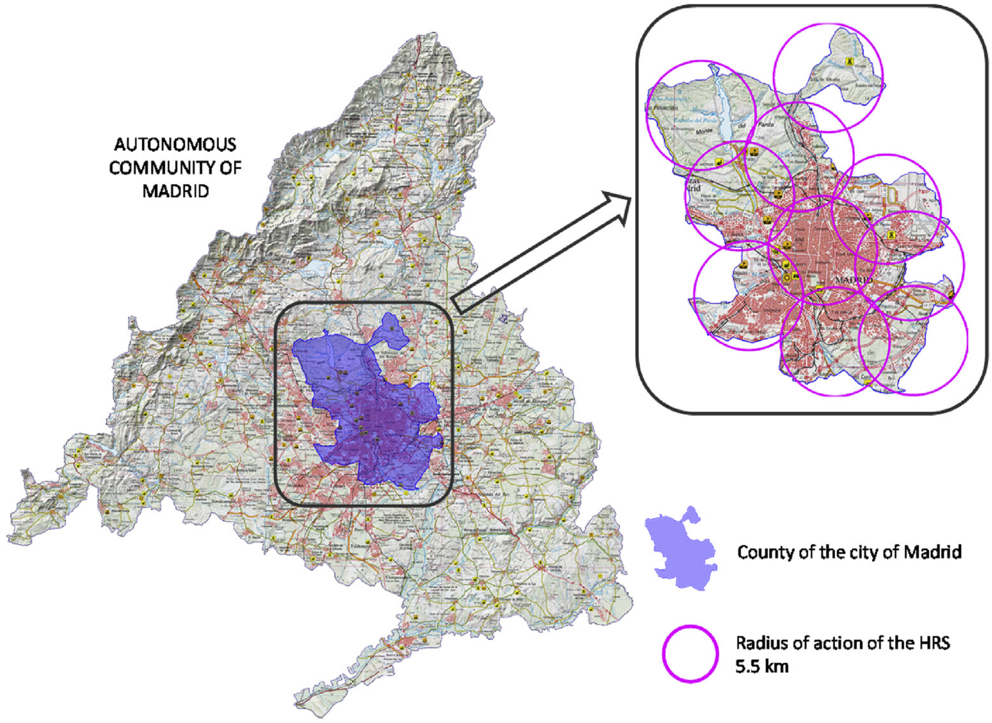

Fig. 6. Proposed location of the first 10 HRSs to cover the total area of the County of the city of Madrid with a maximum refuelling distance of 5.5 km.

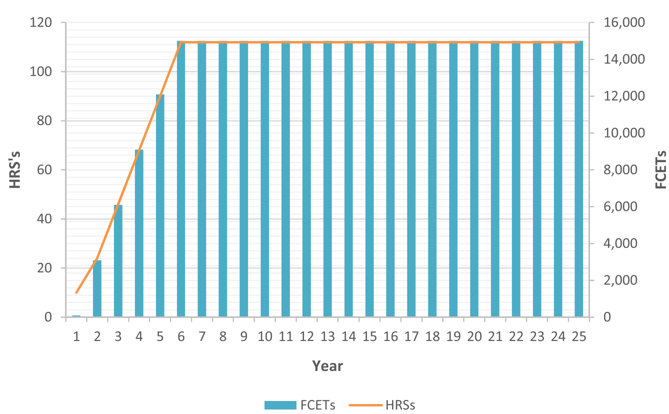

Fig. 7. HRS and FCET roll-out.

(HRSAM), developed by the National Renewable Energy Laboratory [55]. This tool calculates the cost of HRS for several technical configurations and capacities and gives a result of $2.07 m for a HRS with a capacity of 450 k/d of central-produced hydrogen delivered by CGH_2 trucks.

Operating costs arise from the hydrogen delivery cost[6] and operation and maintenance (Opex) of the facility.

Currently the hydrogen production cost is in the range 2–8 $/kg depending on the productive methods [13,14,56,57,62], so that the hydrogen delivery price for the HRS will be determined by the production mix and the costs associated with transport and distribution.

In our proposal, the target was that fuel cost for final user, in this case the FCET owner, comparable with the present petrol retail cost. Due to fuel economy of ICE and FCEV[7] [22,23], a cost of 1.3 $/l of petrol is equivalent to a cost of 10.65 $/kg of hydrogen. Based on this, the hydrogen price included in our assumptions is 9 $/kg. This value is consistent with the present hydrogen retail price of 8 $/kg in the state of California [19], where there is one of the most important HRS networks worldwide. In our methodology, it was not supposed a price reduction from an economy of scale due to the increase in hydrogen consumption, because the needs for 15,000 taxis would be only around 0.14% of the world production or near 7% of the Spanish production in 2016 [63].

HRSs will add a sales margin over the hydrogen delivery price. This sales margin is the origin of the HRS incomes. A sales margin of 20% was assumed, what, over a hydrogen delivery price of 9 $/kg, sets the HRS contribution to the purchase price around 2 $/kg. The final H_2 price for customer will be 11 $/kg. Table 5 shows a comparison between the cost of diesel and H2 for the taxi owner.

Table 6 summarises the assumptions considered in the calculation of the financial parameters to quantify the feasibility of HRSs:

Fig. 8 shows the shareholder and project cash flows of those HRSs operating since the first year of the deployment. The cash flows were obtained by applying the methodology detailed in the chapter 2 with the assumptions of Table 6. As it can be noticed, both cash flows are never positive along the whole period under analysis, therefore, investing in a HRS would not be feasible. Although financing the investment with external debt exposes investors to a less aggressive deficit during the first operating years, the cost of the financing makes finally the cash flow more negative.

Once stated the impossibility to achieve feasibility under normal operating conditions, an analysis was conducted to identify whether under certain conditions the investment would become

[6] The hydrogen delivery cost is the price paid for the hydrogen delivered to the HRS.

[7] ICE fuel economy = 14 km/l. FCEV fuel economy = 109 km/kg.

Table 5
Fuel cost comparative.

Concept	Qty	Unit	Comment
Yearly distance per taxi	100,000	km/year	
ICE Fuel Economy	13.60	km/l	
Diesel cost	1.44	$/l	Retail market value
Yearly Diesel cost	10,586	$/year	
H_2 Fuel Economy	109	km/kg	
H_2 cost	11	$/kg	
Yearly H_2 cost	9871	$/year	
Difference	−715	$/year	

Table 6
Summary of assumptions in IRR and ADSCR calculation.

Assumptions	Name	Value	Unit	Source
HRS Costs	Capital construction cost (CAPEX)	2.80	$m	Estimate from Table 4
	Operating costs (OPEX)	150	$k	Fixed value. Source [27,33]
HRS deployment	Capacity	450	kg/d	
	Utilisation	75%		
	Initial number	10		
FCET	Number of taxis in the city	15,000	cars	Number of taxis in Madrid [48]
	Taxis replaced by FCET the first year	100	cars	Estimate
	Yearly taxi replacement rate	20%		Estimate
	km per year and car	100,000	km/yr	Estimate
	H_2 consumption	109	km/kg	Equivalent to 68 mi/kg [22,23]
H2 sales	Hydrogen delivery price	9	$/kg	
	Sales operating margin	20%		
Taxes	Profit taxes	30%		
	VAT	21%		Current in Spain
Financial terms	Financial leverage	75%		Market value.
	Annual interest rate	5%		Estimate.
	Inflation rate	3%		Annual. Estimate
	Loan repayment period	20	yr	
	Depreciation period	20	yr	

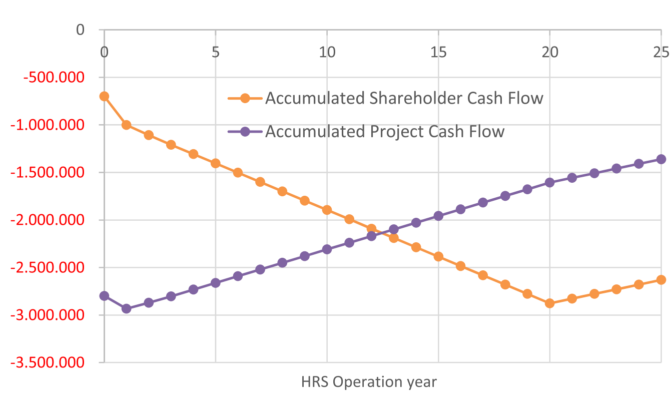

Fig. 8. Accumulated CFs.

viable. The evolution of shareholder and project IRRs was evaluated respect of the variation, in a reasonable range around the assumptions detailed in Table 6, of the parameters with a bigger impact in the feasibility. Fig. 9 illustrates how the reduction in CAPEX is not able by itself to produce a minimum level of feasibility.

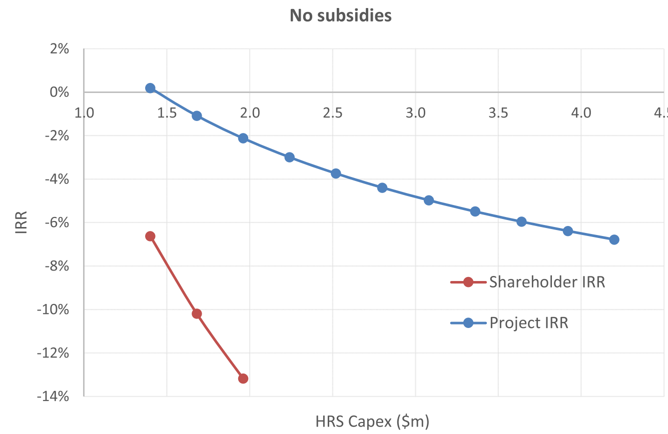

Fig. 9. Variation of the IRR with the HRS Capex.

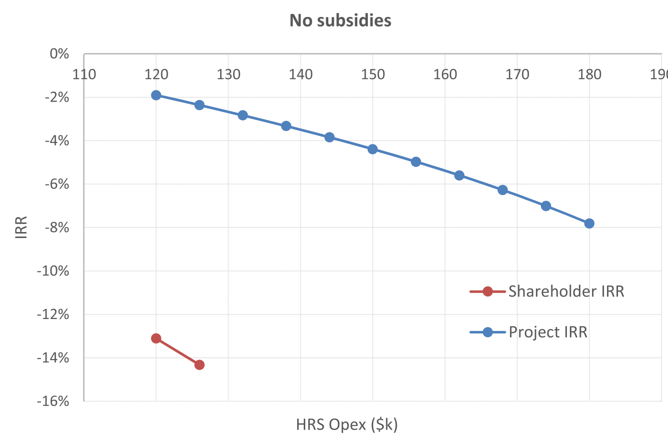

Fig. 10. Variation of the IRR with the HRS Opex.

As it can be seen in Fig. 10, neither the optimization of the operating cost takes IRRs to valid levels.

As it is shown in Fig. 11, the increase of the H_2 delivery price, even up to elevated levels, does not make feasible the facility.

Finally, as it is illustrated in Fig. 12, only a rise in sales margin over 25% would bring a minimal feasibility but at low rates unacceptable for any investor.

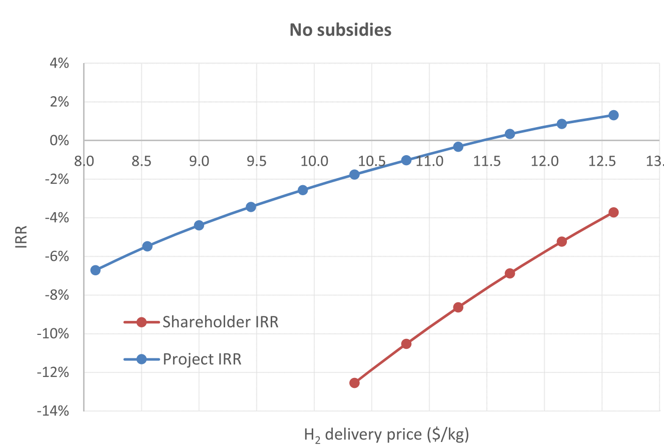

Fig. 11. Variation of the IRR with the H_2 delivery price.

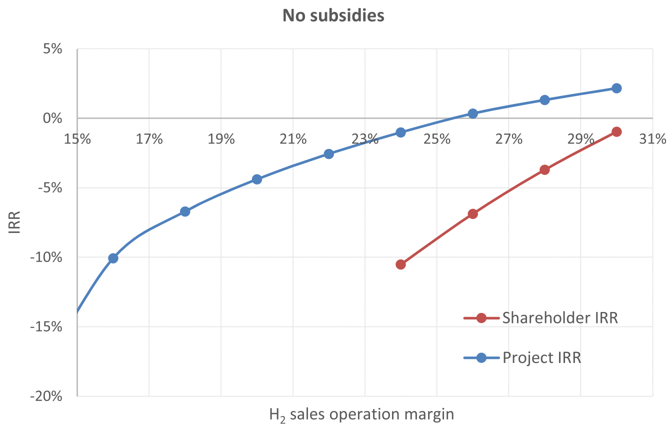

Fig. 12. Variation of the IRR with the H_2 sales operation margin.

Financing the investment does not help to improve feasibility because, as it can be seen in Figs. 9–12, due to the financing costs the shareholder IRR is always worse than the Project IRR.

3.3. Subsidies. The HRS base case

Once it has been stated the impossibility of achieving a minimum level of feasibility for HRSs operating under normal conditions, some kind of subsidies will be necessary. These subsidies may be addressed to:

- Construction costs (Capex), by means of direct non-refundable grants.
- Operating costs (Opex) with the subsidy of the operation and maintenance expenses for a specific period.
- Financing terms, with the subsidy of the interest rates or supporting financial guarantees (i.e. bonds) to improve the financial leverage.
- Tax credits.

With the aim to design the optimal subsidies framework, the following conditions were considered:

1a The subsidies applied to reduce Capex and Opex have the major positive effect on the feasibility. As it is shown in Fig. 13 a subsidy share of 50% in both takes the shareholder IRR around 9%.

2a The reduction in Capex implies an indirect subsidy to financing costs, because the amount to be financed is reduced.

3a The subsidies addressed to Opex during part of the HRS lifespan would allow the control by the funders because mechanisms could be implemented to force the HRS owner to have the facilities fully operational as a condition to receive the funds. Moreover, due to its temporary character, this subsidy offers the possibility to adjust the amount in case of variation of the rest of parameters, and the subsidy could be eliminated it the market conditions were able to ensure the viability of the investment.

4a The subsidies applied to tax credits present an important advantage because the do not imply a disbursement of funds but a decrement of governmental incomes due to a lower fiscal charge. Nevertheless, without the application of other helps simultaneously, partial or total tax exemption does not have an effect in the feasibility because taxes are paid only in case of having benefits and this situation would not be possible without other helps.

5a When is coordinately implemented with other type of subsidies, tax exemption has a moderate effect on the feasibility, as it can be noticed in Fig. 14. So that, the exemption can be used as a complement to adjust the IRR according to the evolution of the rest of the variables.

6a Some countries apply taxes to the use of hydrocarbon fuels. Generally, these are indirect non-fiscal taxes not aimed at collecting but at covering the costs related with the pollution produced by using this type of fuels under the principle “polluter pays”. The objective of this type of taxes is also to promote the reduction on the emissions by discouraging the use of high-emission fuels increasing the purchase price.

The replacement of taxis by FCEVs would imply a reduction of the funds coming from these taxes, but this reduction must not be seen as a subsidy because the source of pollution is eliminated and therefore the costs that the tax is intended to cover (in other words “who does not pollute, does not pay”).

Considering the previous considerations, for a target IRR, the HRS base case would be defined by a subsidies package addressed to Capex, Opex and tax exemptions. The weight of each one in such package will determine the total amount of funds and the schedule of disbursements.

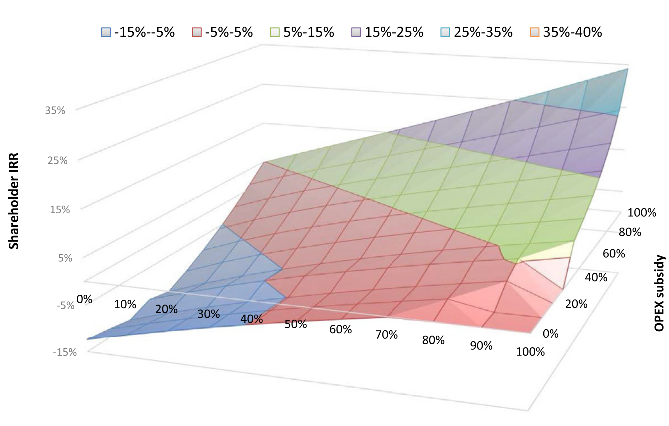

Fig. 13. Variation of Shareholder IRR with Capex and Opex subsidies.

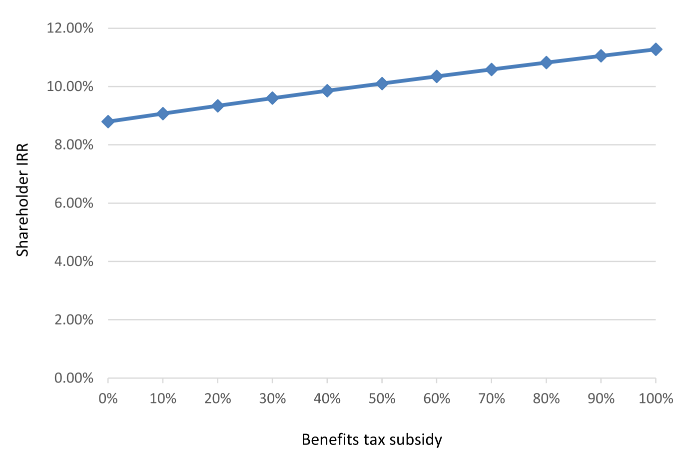

Fig. 14. Variation of Shareholder IRR with benefit tax subsidies.

Table 7
Combination of Capex and Opex subsidies to achieve Shareholder IRR = 10%. Benefit tax subsidy = 50% in all the cases.

Capex subsidy	Opex subsidy	Total Subsidies (m$)
30%	82%	508
40%	66%	462
50%	50%	415
60%	34%	369
70%	18%	322
80%	1%	271

Table 7 shows the net present value[8] of funds that should be allocated in several assumptions of subsidies to Capex and Opex for a target shareholder IRR of 10%; in all the cases tax exemption is set at 50%. As it can be noticed, the total amount decreases when the Capex subsidy increases, so that, a priori, an elevated level of subsidy to Capex should be included in the base case.

Nevertheless, other point to be considered before defining the subsidies scenario is how funds are delivered along the time. Fig. 15 illustrates the schedule of the disbursements in each of the cases of Table 7. As it can be noticed, the subsidies allocated to Capex demand a big amount of funds at the beginning of the roll-out. Once all the HRSs projected are built (in five years as it is shown in Fig. 7), the subsidies to Opex flatten the demand of funds making the schedule disbursements more affordable.

An adequate balance point is found for a subsidy of 50% allocated both for Capex and Opex simultaneously. According to Fig. 14, a 50% of tax credits would be necessary to achieve the target IRR of 10%. Therefore, the subsides package that determines the base case is detailed in Table 8, and implies the allocation of $415 million (net present value) disbursed along 25 years according to

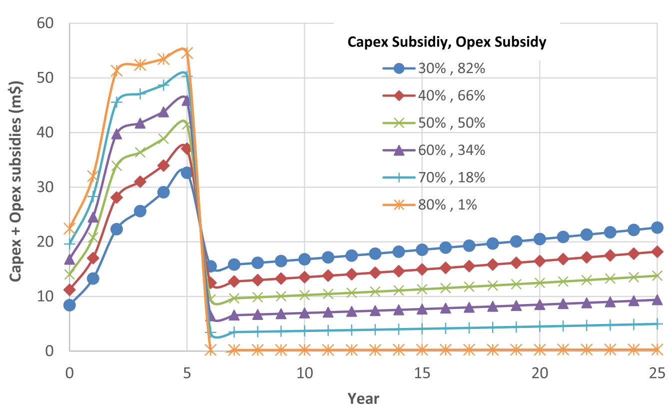

Fig. 15. Subsidies deployment schedule for several combinations of Capex and Opex subsidies to achieve Shareholder IRR = 10%.

Table 8
Subsidies for the HRS base case.

Subsidies	Value	Details
Capex	50%	Discount over the Capex
Opex	50%	Annual subsidy to the Opex
Profit taxes	50%	Annual subsidy to the profit taxes equivalent to 50% tax credit.

[8] The net present value was calculated at a discount rate equal to the inflation rate included in Table 6.

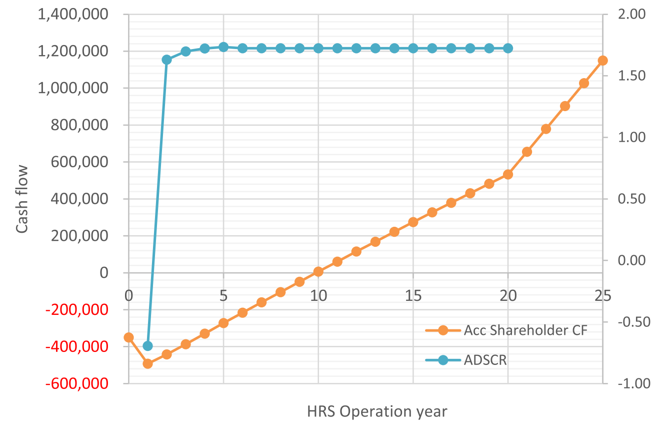

Fig. 16. HRS base case shareholder cash flow (Shareholder IRR = 10%).

the schedule shown in Fig. 15. This amount is equal to 8% of the total budget of the Madrid City Council for the year 2017 [64].

Under this framework, the cash flows would be enough to achieve an acceptable level of feasibility in terms of IRR. As it can be seen in Fig. 16, around the 10th year the cash flow turns positive and, except in the first year, ADSCR is over 1.5 what means a wide margin of incomes to cover debt payments.

4. Sensitivity analysis

To validate the robustness and applicability of the base case, it has been carried out a sensitivity analysis respect of the assumptions (Table 6) with most impact on the HRS incomes and expenses and, consequently, on the results obtained in the chapter 3.

4.1. Respect to the FCET roll-out

Incomes from H_2 sales will depend on FCET market size, so that incomes vary with the initial number of FCETs and the taxi replacement rate. With a conservative approach, in the assumptions (Table 6) a reduced initial number of units has been considered (100 units, barely 1% of the total fleet) because it is supposed to find a certain barrier to entry at the beginning of the roll-out.

Fig. 17 shows the sensitivity of IRR respect variations of the initial number of FCETs and taxi replacement rate. As it can be seen, in both cases the effect is not relevant. A variation in the initial number of FCETs in the range from 50% (50 FCETs) to 300%

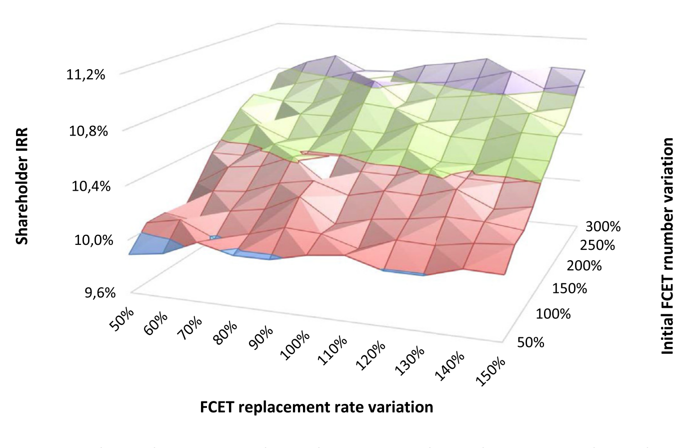

Fig. 17. Shareholder IRR sensitivity versus FCET roll-out variations.

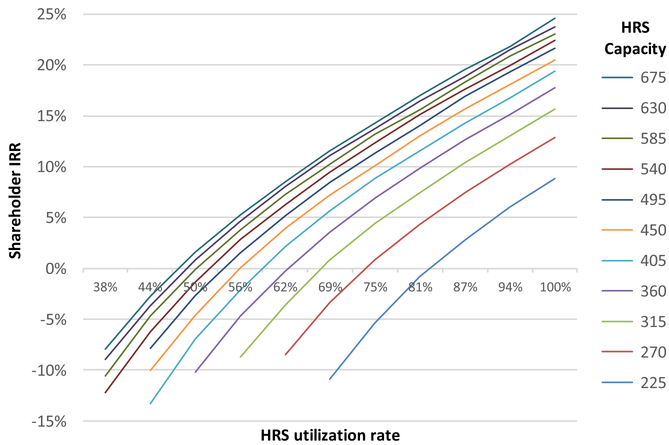

Fig. 18. Shareholder IRR sensitivity versus HRS utilisation rate and capacity.

(300 FCETs) impacts around 1% on IRR because the effect is limited to the first year (see Fig. 18).

On the other hand, the effect of the replacement rate variation is negligible when the HRS deployment is designed to supply the FCET roll-out needs (chapter 3.1) keeping an adequate utilisation rate and so that the number of HRSs grows coordinately with the replacement taxi fleet rate.

4.2. Respect to the utilisation rate and the HRS size

As it is illustrated in Fig. 19, the IRR is very sensitive to H_2 delivery price and sales margin because both have an important effect on HRSs incomes along their lifetime. Due to the fact that the H_2 retail price is the result of the H_2 delivery price increased with the sales margin, sensitivity respect to both factors is equal. Also, variations in the H_2 delivery price, out of the control of the HRS managers, could be balanced with the opposite equivalent in sales margin (as an example, Fig. 19 shows how a 12% drop in the H_2 delivery price is balanced with an identical increase in the sales margin). As a result, with an adequate control of sales margin, the H_2 retail price would not be affected by changes in the H_2 delivery price.

4.3. Respect to the H_2 price and the sales margin

As it is illustrated in Fig. 19, the IRR is very sensitive to the H_2 delivery price and the sales margin because both have an important effect on HRSs incomes along their lifetime. Due to the fact that the H_2 retail price is the result of the H_2 delivery price increased with the sales margin, sensitivity respect to both factors is equal. As a consequence, variations in the H_2 delivery price, out of the control of the HRS managers, could be balanced with the opposite equivalent in sales margin (as an example, Fig. 19 shows how a 12% drop in the H_2 delivery price is balanced with an identical increase in the sales margin). As a result, with an adequate control of sales margin, the H_2 retail price would not be affected by changes in the H_2 delivery price.

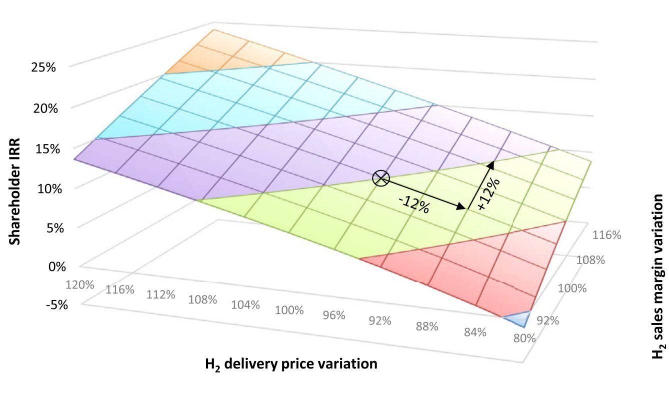

Fig. 19. Shareholder IRR sensitivity versus H_2 delivery price and sales margin.

4.4. Respect to the loan terms

The sensitivity of the IRR respect FL is quite relevant because its value will determine the Capex portion to be supported directly by the capital investor. Nevertheless, the value is fixed in the moment of financial closing and it will not change over time. What is generally variable is the interest rate, usually a value indexed to international reference rates (i.e. Euribor or similar). The variation of IRR respect of the most relevant loan financial terms is shown in Fig. 20, where it can be noticed that, respect of the interest rate, the sensitivity is moderate for low rates of FL and becomes more relevant when FL rises and then a bigger portion of the Capex is financed, increasing the debt cost.

5. GHG emissions cut and abatement cost

The replacement of taxi fleets with FCETs brings environmental benefits that are now quantified. Table 9 shows the calculation of the CO_2 emissions cut. The replacement of around 1% of city passenger cars would reduce emissions about 3.5%.

Fig. 20. Shareholder IRR sensitivity respect of loan financial terms.

Table 9
CO_2 emissions reduction with the FCET roll-out.

Concept	Qty	Unit	Comment
ICE Fuel Economy	14	km/l	Estimated from Ref. [65]
ICE diesel CO_2 emissions	2.65	kg/l	Source [65,66]
Taxi fleet	15,000	cars	See Table 1
Yearly distance per taxi	100,000	km/year	
Total fleet distance	1,500,000,000	km/year	
Total taxi fleet CO_2 emissions	292,204.01	t/year	
Total city passenger cars	1,440,000	cars	See Table 1
% taxi over passenger cars	1.04%		
Total present CO_2 emissions	8,279,900	t/year	Source [67]
% of CO_2 emissions reduction	3.53%		

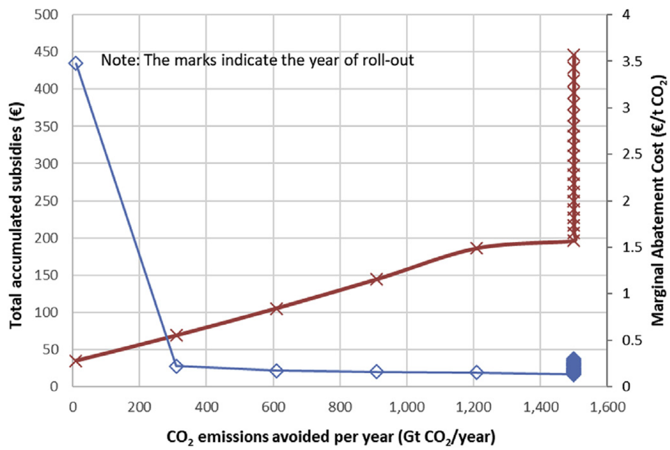

Fig. 21. CO_2 abatement cost curve.

Fig. 21 shows the CO_2 abatement costs corresponding to the HRS and FCET roll-out set in Fig. 7 with the subsidies package fixed in Table 8. As it can be seen the marginal abatement cost is below 0.5 €/t CO_2 once a reduction of 300 Gt is reached in the second year of the deployment.

6. Conclusions

The essential objective of our job was contributing with practical solutions to the implementation of mitigation strategies designed to reduce drastically GHG emission levels and limit the increase in the global average temperature to well below 2 °C above pre-industrial levels.

In this article, it is analysed if the development of a HRS network can be economically supported in terms of feasibility with the replacement by FCEVs of taxi fleets in high-populated cities. The city of Madrid, capital of Spain, with 15,000 taxis was used as an example to illustrate the results.

Our study shows that the development of a HRS network is viable only with the support of governmental authorities by means of politics and subsidies addressed to the promotion and funding of the hydrogen retail infrastructure.

As a result, based on our assumptions, the development of HRS networks would only be possible with a prolonged allocation of funds addressed via subsidies to the construction, the operating costs and to tax exemptions. Once analysed multiple scenarios it is proposed, as an optimal solution, a subsidy package composed of 50% of Capex executed at the beginning of the investment and 50% of operating costs and 50% of tax exemption disbursed along 25 years. This package ensures a reasonable feasibility, around 10% in terms of shareholder IRR along the first 25 operating years. This solution also allows the implementation of mechanisms to control the viability and ensure the target feasibility in case of eventual variations, in a wide range, of the rest of parameters that determine the market conditions.

The total net present cost of the solution applied to the city of Madrid, was estimated in $415 million to be disbursed along 25 years. This amount seems easily coverable by the funds allocated with this purpose by the US or the European Union and many high-populated city councils. As an example, the total budget of the Madrid City Council for the year 2017 is € 5 billion.

As an example of application, in the city of Madrid, with the implementation of our proposal, in six years around 100 HRS would be deployed throughout the city at a maximum refuelling distance of 4 km. This infrastructure would be able to supply over 15 Mkg of H_2 yearly and meet the needs of 15,000 vehicles with a utilisation rate near 75%, what would allow the supply of 25% more hydrogen with the same infrastructure.

In high-populated cities, as Madrid, the replacement of the whole taxi fleet by FCETs, representing around 1% of city passenger cars, would cut 300 kt CO_2 per year, what means above 3% of the total transport-related GHG emissions in the city.

References

[1] Intergovernmental Panel on Climate Change. Climate change 2014: synthesis report. Contribution of working groups I, ii and iii to the fifth assessment report of the intergovernmental panel on climate change. 2014. Geneva, Switzerland, http://www.ipcc.ch/report/ar5/syr/.

[2] International Energy Agency. Energy, climate change and environment 2016 insights. 2016. Paris, France, https://www.iea.org/publications/freepublications/publication/energy-climate-change-and-environment-2016-insights.html.

[3] The United States Environmental Protection Agency. Greenhouse gas inventory data explorer, [online]. 2017. Available, https://www3.epa.gov/climatechange/ghgemissions/inventoryexplorer/ [Accessed 02/02/2017].

[4] European Environmental Agency. Greenhouse gas emissions from transport. 2016 [Online]. Available, http://www.eea.europa.eu/data-and-maps/indicators/transport-emissions-of-greenhouse-gases/transport-emissions-of-greenhouse-gases-6 [Accessed 15/01/2017].

[5] United Nations Treaty Collection. Paris agreement. 2016 [Online]. Available, https://treaties.un.org/pages/ViewDetails.aspx?src=TREATY&mtdsg_no=XXVII-7-d&chapter=27&lang=en [Accessed 9/7/2016].

[6] International Energy Agency. World energy outlook 2016. Executive summary. 2016. Paris, France, http://www.iea.org/publications/freepublications/publication/WorldEnergyOutlook2016ExecutiveSummaryEnglish.pdf.

[7] Sims R, Schaeffer R, Creutzig F, Cruz-Núñez X, D'Agosto M, Dimitriu D, et al. Transport. In: Climate change 2014: mitigation of climate change. Contribution of working group iii to the fifth assessment report of the intergovernmental panel on climate change. NY, USA: Cambridge United Kingdom and New York; 2014. https://www.ipcc.ch/report/ar5/wg3/.

[8] International Energy Agency. Key world energy statistics 2016. 2016. Paris, France, https://www.iea.org/publications/freepublications/publication/key-world-energy-statistics.html.

[9] International Energy Agency. Global EV outlook 2016. 2016. Paris, France, http://www.iea.org/publications/freepublications/publication/Global_EV_Outlook_2016.pdf.

[10] Colmenar-Santos A, Borge-Diez D, Ortega-Cabezas PM, Míguez-Camiña JV. Macro economic impact, reduction of fee deficit and profitability of a sustainable transport model based on electric mobility. Case study: city of León (Spain). Energy 2014;65:303–18. https://doi.org/10.1016/j.energy.2013.11.077.

[11] Colmenar-Santos A, de Palacio C, Borge-Diez D, Monzón-Alejandro O. Planning minimum Interurban fast charging infrastructure for electric vehicles: methodology and application to Spain. Energies 2014;7:1207.

[12] International Energy Agency. Technology roadmap hydrogen and fuel cells. 2013 Edition 2013 Paris, France. https://www.iea.org/publications/freepublications/publication/TechnologyRoadmapHydrogenandFuelCells.pdf.

[13] Fuel Cells and Hydrogen Joint Undertaking. A portfolio of power-trains for europe: a fact-based analysis. The role of battery electric vehicles, plug-in hybrids and fuel cell electric vehicles. 2010. http://www.fch.europa.eu/node/786.

[14] Ramsden T, Ruth M, Diakov V, Laffen M, Timbario TA. Hydrogen pathways: updated cost, well-to-wheels energy use, and emissions for the current technology status of ten hydrogen production, delivery, and distribution scenarios. Golden, CO.: National Renewable Energy Laboratory (NREL); 2013. Report No.: NREL/TP-6A10–60528 United States 10.2172/1107463 NREL English, http://www.osti.gov/scitech/servlets/purl/1107463.

[15] The US Department of Energy Office of Energy Efficiency & Renewable Energy. Hydrogen and fuel cells program plan. 2011. Contract No.: DOE/EE-0651, http://energy.gov/sites/prod/files/2014/03/f12/program_plan2011.pdf.

[16] Baptista P, Ribau J, Bravo J, Silva C, Adcock P, Kells A. Fuel cell hybrid taxi life cycle analysis. Energy Pol 2011;39:4683–91. https://doi.org/10.1016/j.enpol.2011.06.064.

[17] Melaina M, Sun Y, Bush B. Retail infrastructure costs comparison for hydrogen and electricity for light-duty vehicles: preprint. Golden, CO: National Renewable Energy Laboratory (NREL); 2014.

[18] European Commission Directorate-General for Research and Innovation. HyWays. The European hydrogen roadmap. 2008. Luxembourg: Report No.: EUR 23123, http://bookshop.europa.eu/is-bin/INTERSHOP.enfinity/WFS/EU-Bookshop-Site/en_GB/-/EUR/ViewPublication-Start?PublicationKey=KINA23123.

[19] McKinney J, Bond É, Crowell M, Odufuwa E. Joint agency staff report on assembly bill 8: assessment of time and cost needed to attain 100 hydrogen refueling stations in California. California Energy Commission; 2015. Report No.: CEC-600-2015-016.
[20] Bush B, Melaina M. National FCEV and hydrogen fueling station scenarios. Golden, CO (United States)): NREL (National Renewable Energy Laboratory (NREL); 2016.
[21] European Alternative Fuels Observatory. 2016. Available: http://www.eafo.eu/ [Accessed 01/12/2016].
[22] Office of Transportation and Air Quality U.S. Environmental Protection Agency. Compare fuel cell vehicles [online]. 2017. Available, http://www.fueleconomy.gov/feg/fcv_sbs.shtml [Accessed 18/01/2017].
[23] The United States Environmental Protection agency. Model year 2017 fuel economy guide: EPA fuel economy estimates: ; U. S. Department of energy, Washington, D.C.. Washington, D.C: U.S. Environmental Protection Agency; 2016.
[24] Curtin S, Gangi J. Fuel cell technologies market report 2015. Golden, CO (United States)): NREL (National Renewable Energy Laboratory (NREL); 2016. Report No.: DOE/EE1485, http://energy.gov/sites/prod/files/2016/10/f33/fcto_2015_market_report.pdf.
[25] Davis SC, Williams SE, Boundy RG, Moore S. Vehicle technologies market report. Oak Ridge, TN (United States): Oak Ridge National Lab. (ORNL); 2016. p. 2015. Report No.: ORNL/TM–2016/142; Other: VT0505000; VT1202000; CEVT001 United States 10.2172/1255689 Other: VT0505000; VT1202000; CEVT001 ORNL English, http://www.osti.gov/scitech/servlets/purl/1255689.
[26] Parks G, Boyd R, Cornish J, Remick R. hydrogen station compression, storage, and dispensing technical status and costs: systems integration. Golden, CO.: National Renewable Energy Laboratory (NREL); 2014. Report No.: NREL/BK-6A10–58564 United States 10.2172/1130621 NREL English, http://www.osti.gov/scitech/servlets/purl/1130621.
[27] Sprik S, Kurtz J, Ainscough C, Jeffers M, Saur G, Peters M. Hydrogen station data collection and analysis. Golden, CO (United States)): NREL (National Renewable Energy Laboratory (NREL); 2016. Report No.: Project ID TV017.
[28] Colmenar-Santos A, Alberdi-Jiménez L, Nasarre-Cortés L, Mora-Larramona J. Residual heat use generated by a 12 kW fuel cell in an electric vehicle heating system. Energy 2014;68:182–90. https://doi.org/10.1016/j.energy.2014.02.092.
[29] National Renewable Energy Laboratory. Fuel cell and hydrogen technology validation. 2016 [Online]. Available, http://www.nrel.gov/hydrogen/proj_tech_validation.html [Accessed 01/12/2016].
[30] International Partnership for Hydrogen and Fuel Cells in the Economy. IPHE partners. Japan. 2017 [Online]. Available, http://www.iphe.net/partners/japan.html [Accessed 09/02/2017].
[31] netinform. Hydrogen filling stations worldwide. 2017 [Online]. Available, http://www.netinform.net/h2/H2Stations/Default.aspx [Accessed 01-02-2017].
[32] Melendez M. Transitioning to a hydrogen future: learning from the alternative fuels experience. National Renewable Energy Laboratory; 2006. Report No.: NREL/TP-540–39423.
[33] Ogden JM, Yang CA, Nicholas M, Lewis F. NextSTEPS white paper: the hydrogen transition. Davis: Institute of Transportation Studies, University of California; 2014. Report No.: UCD-ITS-RR-14–11, http://steps.ucdavis.edu/files/08-13-2014-08-13-2014-NextSTEPS-White-Paper-Hydrogen-Transition-7.29.2014.pdf.
[34] Roland Berger Strategy Consultants GmbH. A roadmap for financing hydrogen refueling networks – Creating prerequisites for H2-based mobility. Fuel Cells and Hydrogen Joint Undertaking; 2013. http://www.fch.europa.eu/node/784.
[35] Dagdougui H, Ouammi A, Sacile R. Modelling and control of hydrogen and energy flows in a network of green hydrogen refuelling stations powered by mixed renewable energy systems. Int J Hydrogen Energy 2012;37:5360–71. https://doi.org/10.1016/j.ijhydene.2011.07.096.
[36] Kim J-G, Kuby M. The deviation-flow refueling location model for optimizing a network of refueling stations. Int J Hydrogen Energy 2012;37:5406–20. https://doi.org/10.1016/j.ijhydene.2011.08.108.
[37] Agnolucci P. Hydrogen infrastructure for the transport sector. Int J Hydrogen Energy 2007;32:3526–44. https://doi.org/10.1016/j.ijhydene.2007.02.016.
[38] Melaina MW. Initiating hydrogen infrastructures: preliminary analysis of a sufficient number of initial hydrogen stations in the US. Int J Hydrogen Energy 2003;28:743–55. https://doi.org/10.1016/S0360-3199(02)00240-9.
[39] Almansoori A, Betancourt-Torcat A. Design of optimization model for a hydrogen supply chain under emission constraints - A case study of Germany. Energy 2016;111:414–29. https://doi.org/10.1016/j.energy.2016.05.123.
[40] Nesbitt K, Sperling D. Myths regarding alternative fuel vehicle demand by light-duty vehicle fleets. Transport Res Part D 1998;3:259–69. https://doi.org/10.1016/S1361-9209(98)00006-6.
[41] Nesbitt K, Sperling D. Fleet purchase behavior: decision processes and implications for new vehicle technologies and fuels. Transport Res Part C 2001;9:297–318. https://doi.org/10.1016/S0968-090X(00)00035-8.
[42] Government of the United Kingdom. Office for National Statistics. 2017. Overview of the UK population. February 2016 [Online]. Available, https://www.ons.gov.uk/peoplepopulationandcommunity/populationandmigration/populationestimates/articles/overviewoftheukpopulation/february2016 [Accessed 05/02/2017].
[43] Kingdom GotU. Vehicle licensing statistics: 2015. National Statistics; 2016 [Online]. Available, https://www.gov.uk/government/statistics/vehicle-licensing-statistics-2015 [Accessed 05/02/2017].
[44] Kingdom GotU. Taxi and private hire vehicles statistics, England: 2015. National Statistics; 2017 [Online]. Available, https://www.gov.uk/government/statistics/taxi-and-private-hire-vehicles-statistics-england-2015 [Accessed 05/02/2017].
[45] City of New York Department of City Planning. NYC population. 2017 [Online]. Available, https://www1.nyc.gov/site/planning/data-maps/nyc-population/current-future-populations.page [Accessed 09/02/2017].
[46] Comission NYCTL. 2014 taxicab fact book.. 2014. http://www.nyc.gov/html/tlc/downloads/pdf/2014_taxicab_fact_book.pdf.
[47] New York State Department of Motor Vehicles. statistical summaries. 2017 [Online]. Available, https://dmv.ny.gov/about-dmv/statistical-summaries.
[48] Ayuntamiento de Madrid. Portal de datos abiertos. Taxi: situación y Gestión. 2017 [Online]. Available, http://datos.madrid.es/portal/site/egob/menuitem.c05c1f754a33a9fbe4b2e4b284f1a5a0/?vgnextoid=4f16216612d39410VgnVCM2000000c205a0aRCRD&vgnextchannel=374512b9ace9f310VgnVCM100000171f5a0aRCRD [Accessed 01/02/2017].
[49] Instituto de Estadística de la Comunidad de Madrid. Anuario Estadístico de la Comunidad de Madrid. 1985-2017. Transportes y comunicaciones; 2017 [Online]. Available, http://www.madrid.org/iestadis/fijas/estructu/general/anuario/ianucap09.htm [Accessed 01/02/2017].
[50] Instituto de Estadística de la Comunidad de Madrid. Población oficial por Comunidades Autónomas, provincias, capitales y municipios de la Comunidad de Madrid. 2017 [Online]. [Accessed 01/02/2017].
[51] Dirección General de Trafico Ministerio del Interior del Gobierno de España. Seguridad vial. Estadísticas e indicadores. Parque de vehículos; 2017 [Online]. Available, http://www.dgt.es/es/seguridad-vial/estadisticas-e-indicadores/parque-vehiculos/ [Accessed 01/02/2017].
[52] Greene DL, Leiby PN, James B, Perez J, Melendez M, Milbrandt A, et al. Analysis of the transition to hydrogen fuel cell vehicles and the potential hydrogen energy infrastructure requirements. Oak Rigde National Laboratory; 2008. Report No.: ORNL/TM-2008/30.
[53] Pratt J, Terlip D, Ainscough C, Kurtz J, Elgowainy A. H2FIRST reference station design task: project deliverable 2–2. Golden, CO (United States): National Renewable Energy Laboratory (NREL); 2015. Report No.: NREL/TP–5400-64107 United States 10.2172/1215215 NREL English, http://www.osti.gov/scitech/servlets/purl/1215215.
[54] Yang C, Ogden J. Determining the lowest-cost hydrogen delivery mode. Int J Hydrogen Energy 2007;32:268–86. https://doi.org/10.1016/j.ijhydene.2006.05.009.
[55] United States Department of Energy. Hydrogen and fuel cells program. DOE H2A delivery analysis. 2017 [Online]. Available, https://www.hydrogen.energy.gov/h2a_delivery.html [Accessed 13/12/2016].
[56] Alazemi J, Andrews J. Automotive hydrogen fuelling stations: An international review. Renew Sustain Energy Rev 2015;48:483–99. https://doi.org/10.1016/j.rser.2015.03.085.
[57] Siyal SH, Mentis D, Howells M, Energisystemanalys Kth, Energiteknik, et al. Economic analysis of standalone wind-powered hydrogen refueling stations for road transport at selected sites in Sweden. Int J Hydrogen Energy 2015;40:9855–65. https://doi.org/10.1016/j.ijhydene.2015.05.021.
[58] Melaina M, Penev M. Hydrogen station cost estimates: comparing hydrogen station cost calculator results with other recent estimates. Golden, CO (United States): National Renewable Energy Lab. (NREL); 2013. Report No.: NREL/TP–5400–56412 United States 10.2172/1260510 NREL English, http://www.osti.gov/scitech/servlets/purl/1260510.
[59] Jung J, Chow JYJ, Jayakrishnan R, Park JY. Stochastic dynamic itinerary interception refueling location problem with queue delay for electric taxi charging stations. Transport Res Part C 2014;40:123. https://doi.org/10.1016/j.trc.2014.01.008.
[60] Tu W, Li Q, Fang Z, S-l Shaw, Zhou B, Chang X. Optimizing the locations of electric taxi charging stations: A spatial–temporal demand coverage approach. Transport Res C Emerg Technol 2016;65:172–89. https://doi.org/10.1016/j.trc.2015.10.004.
[61] Zhang F, Yuan NJ, Wilkie D, Zheng Y, Xie X. Sensing the Pulse of Urban Refueling Behavior: A Perspective from Taxi Mobility. ACM Transactions on Intelligent Systems and Technology (TIST) 2015;6:1–23. https://doi.org/10.1145/2644828.
[62] Caumon P, Lopez-Botet Zulueta M, Louyrette J, Albou S, Bourasseau C, Mansilla C. Flexible hydrogen production implementation in the French power system: Expected impacts at the French and European levels. Energy 2015;81:556–62. https://doi.org/10.1016/j.energy.2014.12.073.
[63] The US Department of Energy Office of Energy Efficiency & Renewable Energy. Hydrogen analysis resource center. 2017 [Online]. Available, http://hydrogen.pnl.gov/hydrogen-data/hydrogen-production [Accessed 03/03/2017].
[64] Ayuntamiento de Madrid. presupuesto general 2017. 2017 [Online]. Available, http://www.madrid.es/portales/munimadrid/es/Inicio/El-Ayuntamiento/Hacienda/Informacion-financiera-y-presupuestaria/Presupuestos/Presupuestos-generales/Presupuesto-General-2017?vgnextfmt=default&vgnextoid=e23c2af3d8d4a510VgnVCM1000001d4a900aRCRD&vgnextchannel=c73815bdb72f8210VgnVCM2000000c205a0aRCRD [Accessed 06/03/2017].

[65] The United States Environmental Protection Agency. Light-duty automotive technology, carbon dioxide emissions, and fuel economy trends: 1975 through 2016. 2016. Report No.: EPA-420-R-16–1010, https://www.epa.gov/fuel-economy/download-co2-and-fuel-economy-trends-report-1975-2016.
[66] Intergovernmental Panel on Climate Change. 2006 IPCC guidelines for national greenhouse gas inventories, vol. 2. Energy Japan: National Greenhouse Gas Inventories Programme; 2006. http://www.ipcc-nggip.iges.or.jp/public/2006gl/vol2.html.
[67] Comunidad de Madrid. Inventario de emisiones a la atmósfera de la Comunidad de Madrid - gases de efecto invernadero. 2017 [Online]. Available, http://www.madrid.org/cs/Satellite?c=CM_InfPractica_FA&cid=1114186137241&language=es&pagename=ComunidadMadrid%2FEstructura&pv=1114189280882 [Accessed 15/12/2016].

ANEXO VIII: *"A HYDROGEN REFUELLING STATIONS INFRASTRUCTURE DEPLOYMENT FOR CITIES SUPPORTED ON FUEL CELL TAXI ROLL-OUT"*. CERTIFICADO DE PUBLICACIÓN.

ELSEVIER

Energy

Certificate of publication for the article titled:

"A hydrogen refuelling stations infrastructure deployment for cities supported on fuel cell taxi roll-out"

Authored by:

Severo Campíñez-Romero, Antonio Colmenar-Santos
Clara Pérez-Molina

Published in:

Volume 148C, 2018, Pages 1018-1031

ANEXO IX: *"A HYDROGEN REFUELLING STATIONS INFRASTRUCTURE DEPLOYMENT FOR CITIES SUPPORTED ON FUEL CELL TAXI ROLL-OUT"*. DEL FACTOR DE IMPACTO.

2018 Journal Performance Data for: ENERGY

ISSN: 0360-5442
eISSN: 1873-6785
PERGAMON-ELSEVIER SCIENCE LTD
THE BOULEVARD, LANGFORD LANE, KIDLINGTON, OXFORD OX5 1GB, ENGLAND
ENGLAND

TITLES
ISO: Energy
JCR Abbrev: ENERGY

LANGUAGES
English

CATEGORIES
THERMODYNAMICS - SCIE

ENERGY & FUELS - SCIE

PUBLICATION FREQUENCY
11 issues/year

The data in the two graphs below and in the Journal Impact Factor calculation panels represent citation activity in 2018 to items published in the journal in the prior two years. They detail the components of the Journal Impact Factor. Use the "All Years" tab to access key metrics and additional data for the current year and all prior years for this journal.

2018 Journal Impact Factor & percentile rank in category for: ENERGY

5.537
2018 Journal Impact Factor

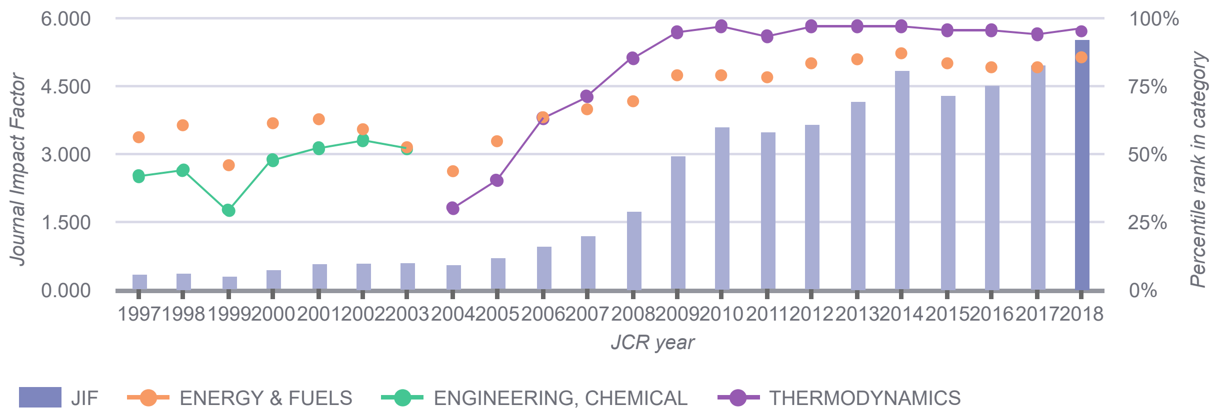

2018 JIF Citation Distribution for: ENERGY

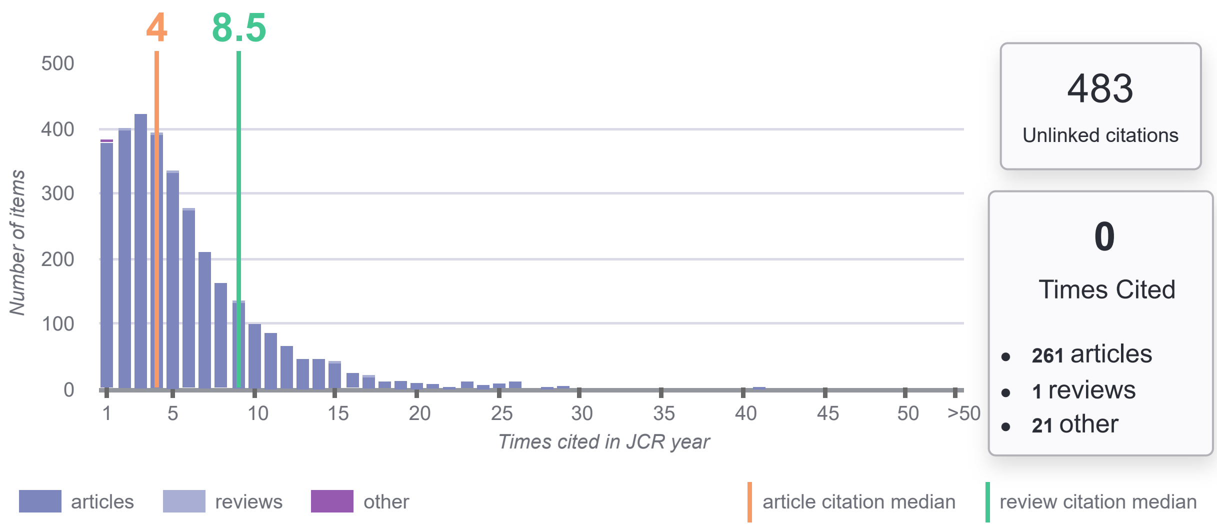

483
Unlinked citations

0
Times Cited

- **261** articles
- **1** reviews
- **21** other

Journal Impact Factor Calculation

$$\text{2018 Journal Impact Factor} = \frac{19{,}391}{3{,}502} = 5.537$$

How is Journal Impact Factor Calculated?

$$\text{JIF} = \frac{\text{Citations in 2018 to items published in } \mathbf{2016\ (9{,}786) + 2017\ (9{,}605)}}{\text{Number of citable items in } \mathbf{2016\ (1{,}575) + 2017\ (1{,}927)}} = \frac{19{,}391}{3{,}502}$$

Journal Impact Factor contributing items

Citable items in 2017 and 2016 (3,502)

TITLE	CITATIONS COUNTED TOWARDS JIF
Using bias-corrected reanalysis to simulate current and future wind power output By: Staffell, Iain; Pfenninger, Stefan **Volume: 114 Page: 1224-1239 Accession number: WOS:000387194800100** **Document Type: Article**	50
Smart energy and smart energy systems By: Lund, Henrik; Ostergaard, Poul Alberg; Connolly, David; Mathiesen, Brian Vad **Volume: 137 Page: 556-565 Accession number: WOS:000414879400050** **Document Type: Article**	45
Long-term patterns of European PV output using 30 years of validated hourly reanalysis and satellite data By: Pfenninger, Stefan; Staffell, Iain **Volume: 114 Page: 1251-1265 Accession number: WOS:000387194800102** **Document Type: Article**	41
Performance analysis of superheated steam injection for heavy oil recovery and modeling of wellbore heat efficiency By: Sun, Fengrui; Yao, Yuedong; Chen, Mingqiang; Li, Xiangfang; Zhao, Lin; et al. **Volume: 125 Page: 795-804 Accession number: WOS:000401202300068** **Document Type: Article**	41
International review of district heating and cooling By: Werner, Sven **Volume: 137 Page: 617-631 Accession number: WOS:000414879400056** **Document Type: Article**	38
Electrothermal dynamics-conscious lithium-ion battery cell-level charging management via state-monitored predictive control By: Zou, Changfu; Hu, Xiaosong; Wei, Zhongbao; Tang, Xiaolin **Volume: 141 Page: 250-259 Accession number: WOS:000426335600024** **Document Type: Article**	37
Morphology controlled preparation of ZnCo2O4 nanostructures for asymmetric supercapacitor with ultrahigh energy density By: Xu, Le; Li, Huaming; Zhao, Yan; Lian, Jiabiao; Xu, Yuanguo; et al. **Volume: 123 Page: 296-304 Accession number: WOS:000399510900025** **Document Type: Article**	36

Citations in 2018 (19,391)

TITLE	CITATIONS COUNTED TOWARDS JIF
ENERGY	4369
ENERGY CONVERSION AND MANAGEMENT	1155
APPLIED ENERGY	1066
ENERGIES	844
JOURNAL OF CLEANER PRODUCTION	626
APPLIED THERMAL ENGINEERING	549
RENEWABLE & SUSTAINABLE ENERGY REVIEWS	544
RENEWABLE ENERGY	328
INTERNATIONAL JOURNAL OF HYDROGEN ENERGY	295
FUEL	249

Key Indicators 2018

IMPACT METRICS		
Total Cites	64,992	✓Trend
Journal Impact Factor	5.537	Trend
5 Year Impact Factor	5.747	Trend
Immediacy Index	1.308	Trend
Impact Factor Without Journal Self Cites	4.289	Trend

INFLUENCE METRICS		
Eigenfactor Score	0.08919	Trend
Article Influence Score	0.966	Trend
Normalized Eigenfactor	10.61112	Trend

SOURCE METRICS		
Citable Items	2,175	Trend
% Articles in Citable Items	99.22	Trend
Average JIF Percentile	90.878	Trend
Cited Half-Life	4.3	Trend
Citing Half-Life	5.4	Trend

Metric Trend

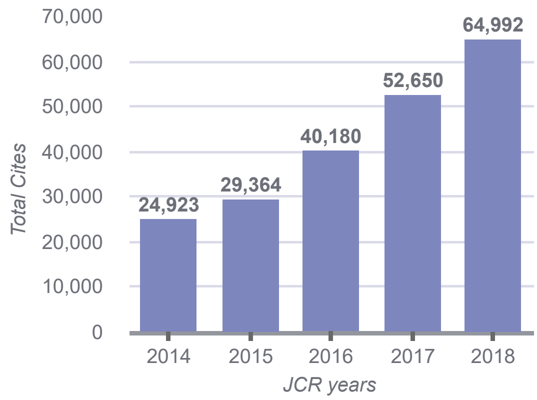

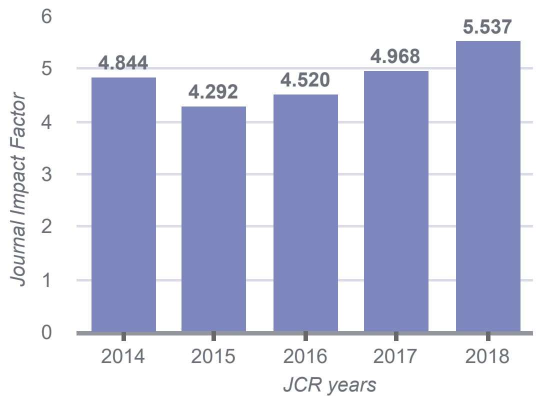

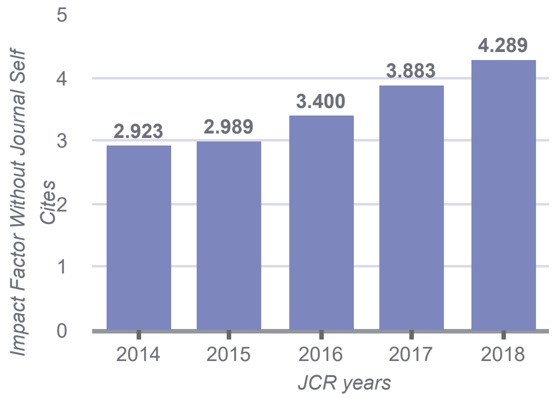

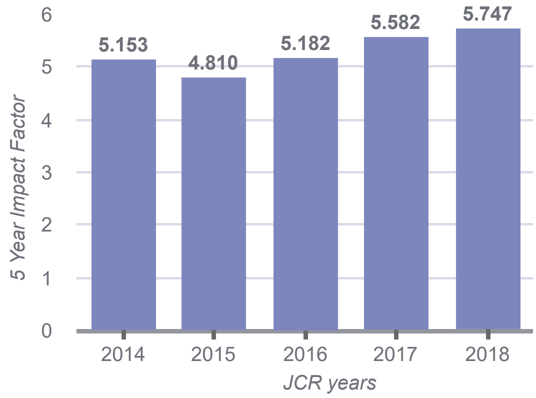

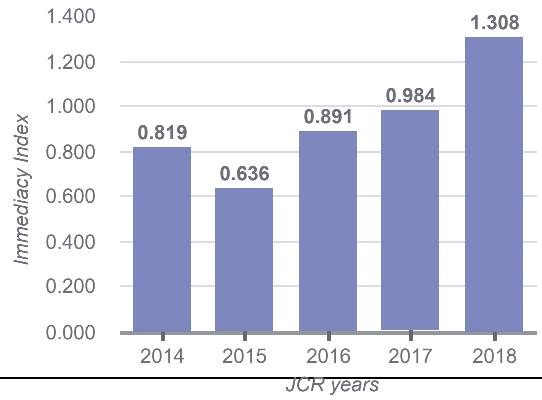

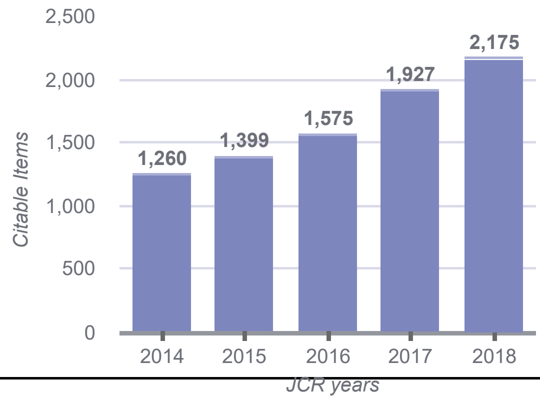

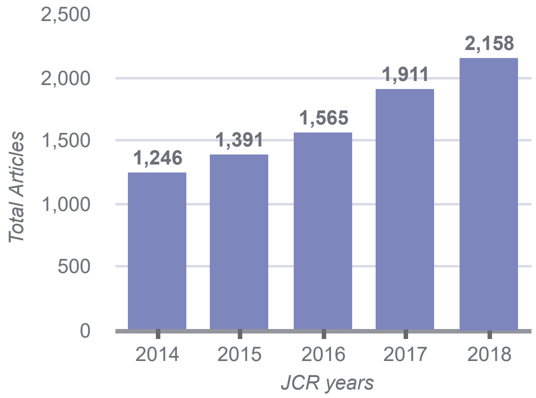
2,500
2,000
1,500
1,000
500
0
Total Articles
1,246
1,391
1,565
1,911
2,158
2014
2015
2016
2017
2018
JCR years

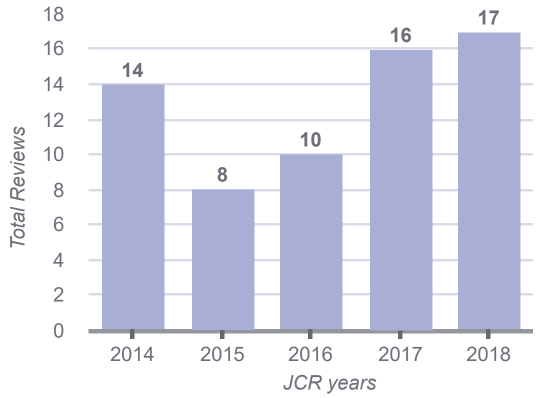
18
16
14
12
10
8
6
4
2
0
Total Reviews
14
8
10
16
17
2014
2015
2016
2017
2018
JCR years

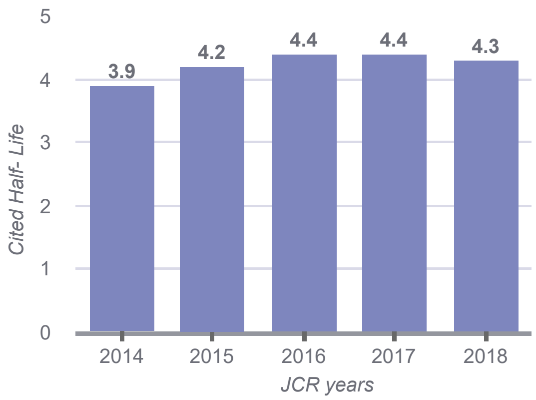
5
4
3
2
1
0
Cited Half- Life
3.9
4.2
4.4
4.4
4.3
2014
2015
2016
2017
2018
JCR years

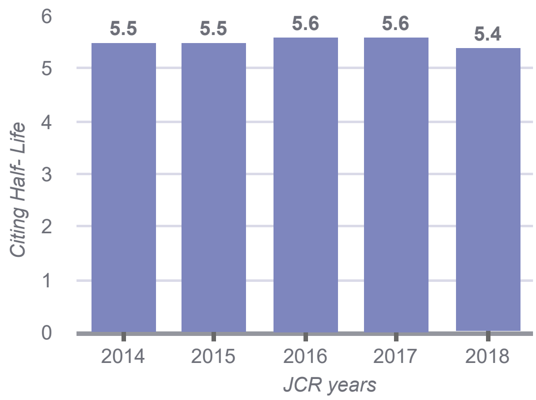
6
5
4
3
2
1
0
Citing Half- Life
5.5
5.5
5.6
5.6
5.4
2014
2015
2016
2017
2018
JCR years

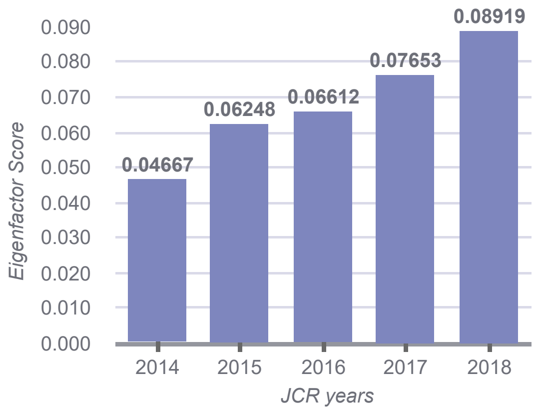
0.090
0.080
0.070
0.060
0.050
0.040
0.030
0.020
0.010
0.000
Eigenfactor Score
0.04667
0.06248
0.06612
0.07653
0.08919
2014
2015
2016
2017
2018
JCR years

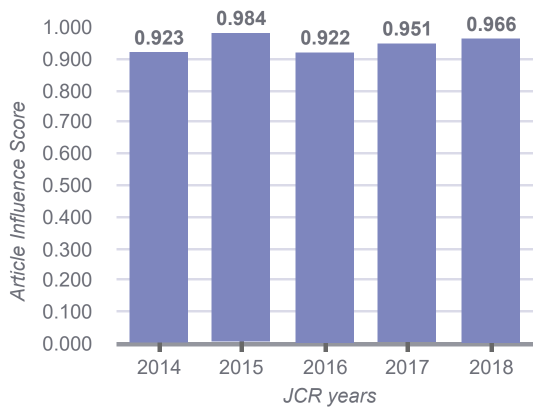
1.000
0.900
0.800
0.700
0.600
0.500
0.400
0.300
0.200
0.100
0.000
Article Influence Score
0.923
0.984
0.922
0.951
0.966
2014
2015
2016
2017
2018
JCR years

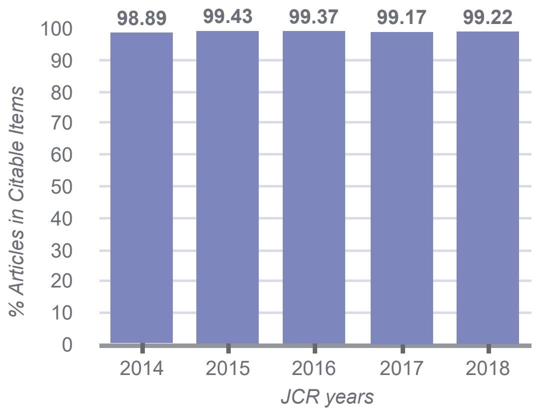
100
90
80
70
60
50
40
30
20
10
0
% Articles in Citable Items
98.89
99.43
99.37
99.17
99.22
2014
2015
2016
2017
2018
JCR years

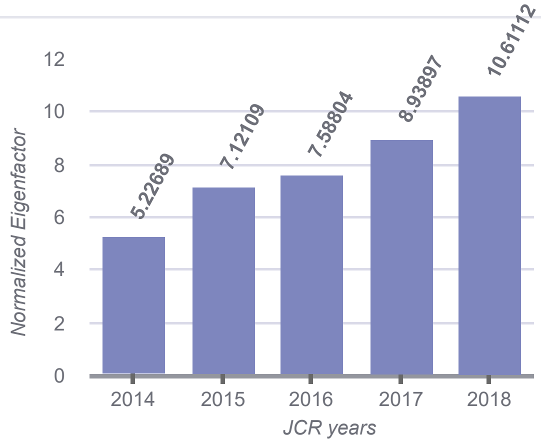
Normalized Eigenfactor
12
10
8
6
4
2
0
5.22689
7.12109
7.58804
8.93897
10.61112
2014
2015
2016
2017
2018
JCR years

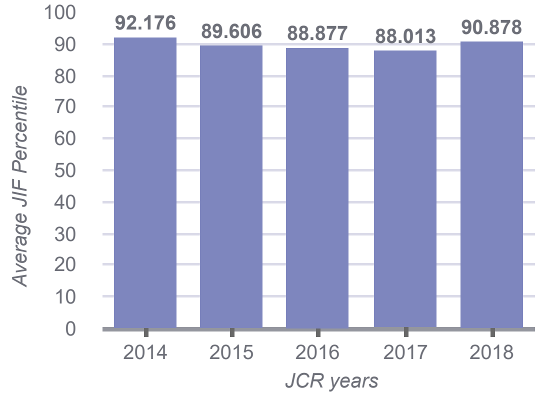
Average JIF Percentile
100
90
80
70
60
50
40
30
20
10
0
92.176
89.606
88.877
88.013
90.878
2014
2015
2016
2017
2018
JCR years

Source data

Journal source data 2018

	Articles	Reviews	Combined(C)	Other(O)	Percentage(C/(C+O))
Number in JCR Year 2018 (A)	2,158	17	2,175	21	99%
Number of References (B)	94,467	1,780	96,247	260	99%
Ratio (B/A)	43.8	104.7	44.3	12.4	

Box plot

Category Box Plot 2018

Category Box Plot

The category box plot depicts the distribution of Impact Factors for all journals in the category. The horizontal line that forms the top of the box is the 75th percentile (Q1). The horizontal line that forms the bottom is the 25th percentile (Q3). The horizontal line that intersects the box is the median Impact Factor for the category.
Horizontal lines above and below the box, called whiskers, represent maximum and minimum values.
The top whisker is the smaller of the following two values:
the maximum Impact Factor (IF)
Q1 IF + 3.5(Q1 IF - Q3 IF)
The bottom whisker is the larger of the following two values:
the minimum Impact Factor (IF)
Q1 IF - 3.5(Q1 IF - Q3 IF)
Box Plots are provided for the current JCR year for each of the categories in which the journal is indexed.

ENERGY, IF: 5.537

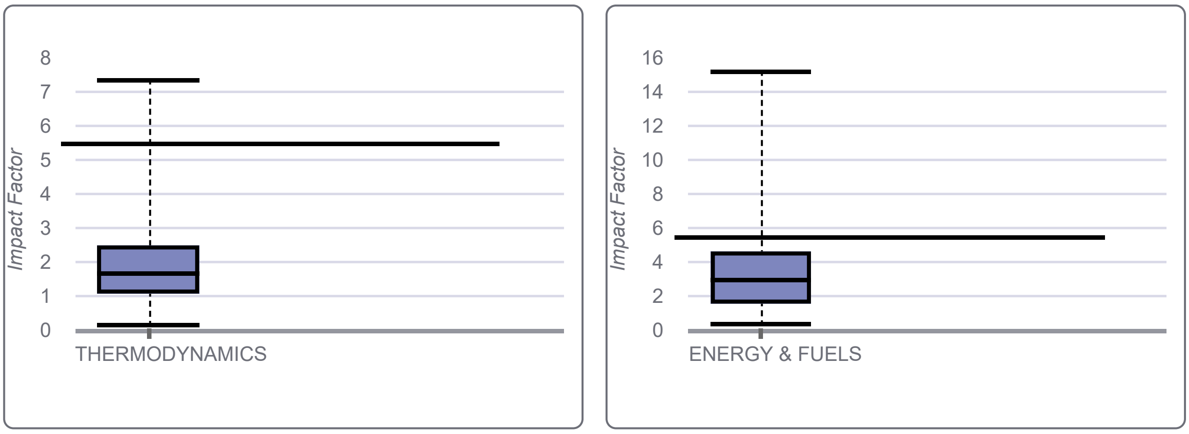

Rank

Rank

JCR Impact Factor

JCR Year	THERMODYNAMICS			ENERGY & FUELS			ENGINEERING, CHEMICAL		
	Rank	Quartile	JIF Percentile	Rank	Quartile	JIF Percentile	Rank	Quartile	JIF Percentile
2018	3/60	Q1	95.833	15/103	Q1	85.922	N/A	N/A	N/A
2017	4/59	Q1	94.068	18/97	Q1	81.959	N/A	N/A	N/A
2016	3/58	Q1	95.690	17/92	Q1	82.065	N/A	N/A	N/A
2015	3/58	Q1	95.690	15/88	Q1	83.523	N/A	N/A	N/A
2014	2/55	Q1	97.273	12/89	Q1	87.079	N/A	N/A	N/A
2013	2/55	Q1	97.273	13/83	Q1	84.940	N/A	N/A	N/A
2012	2/55	Q1	97.273	14/81	Q1	83.333	N/A	N/A	N/A
2011	4/52	Q1	93.269	18/81	Q1	78.395	N/A	N/A	N/A
2010	2/51	Q1	97.059	17/79	Q1	79.114	N/A	N/A	N/A
2009	3/49	Q1	94.898	15/71	Q1	79.577	N/A	N/A	N/A
2008	7/44	Q1	85.227	21/67	Q2	69.403	N/A	N/A	N/A
2007	13/43	Q2	70.930	22/64	Q2	66.406	N/A	N/A	N/A
2006	16/42	Q2	63.095	23/62	Q2	63.710	N/A	N/A	N/A
2005	25/41	Q3	40.244	29/63	Q2	54.762	N/A	N/A	N/A
2004	28/39	Q3	29.487	35/61	Q3	43.443	N/A	N/A	N/A
2003	N/A	N/A	N/A	30/62	Q2	52.419	58/119	Q2	51.681
2002	N/A	N/A	N/A	26/63	Q2	59.524	57/126	Q2	55.159
2001	N/A	N/A	N/A	25/66	Q2	62.879	60/123	Q2	51.626
2000	N/A	N/A	N/A	26/66	Q2	61.364	62/117	Q3	47.436
1999	N/A	N/A	N/A	35/64	Q3	46.094	79/110	Q3	28.636
1998	N/A	N/A	N/A	27/67	Q2	60.448	64/113	Q3	43.805
1997	N/A	N/A	N/A	26/58	Q2	56.034	62/105	Q3	41.429

ESI Total Citations

Rank

JCR Year	ENGINEERING
2018	7/893-Q1
2017	10/867-Q1
2016	13/861-Q1
2015	13/850-Q1
2014	15/838-Q1
2013	22/837-Q1

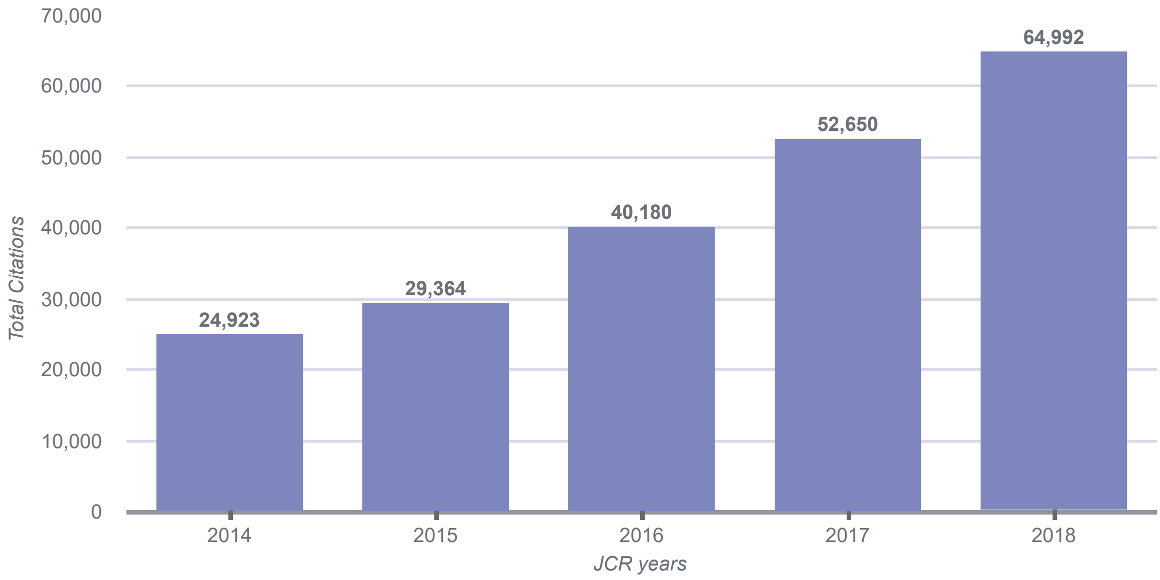

Cited Journal Data

Cited Half-Life Data

Cited Year	2018	2017	2016	2015	2014	2013	2012	2011	2010	2009	2008-All
#Cites from 2018	2,845	9,605	9,786	8,039	7,729	5,027	4,705	4,348	3,521	1,409	7,978
Cumulative %	4.38%	19.16%	34.21%	46.58%	58.47%	66.21%	73.45%	80.14%	85.56%	87.72%	100.00%

Cited Journal Graph 2018

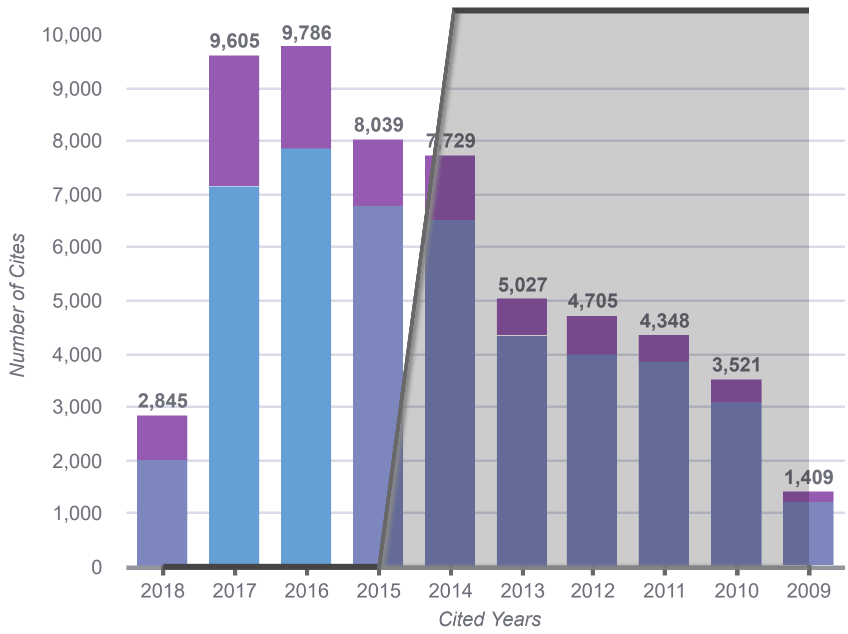

CITED JOURNAL GRAPH

The Cited Journal Graph shows the distribution (by cited year) of citations published in journals during the JCR year to items published in the Journal during the last 10 years.

The white/grey division indicates the cited half-life (if < 10.0). Half of the citations are to items that were published more recently than the cited half-life.

The two light-blue columns indicate citations used to calculate the Impact Factor (always the 2nd and 3rd columns).

Non-self-citations: citations from the journal to articles in other journals.

Journal self - citations: citations from articles in the journal to articles in the same journal.

Cited Journal Data 2018

	Impact	Citing Journal	All Yrs	2018	2017	2016	2015	2014	2013	2012	2011	2010	2009	Rest
		ALL Journals	64,992	2,845	9,605	9,786	8,039	7,729	5,027	4,705	4,348	3,521	1,409	7,978
		ALL OTHERS (1116)	1,116	24	120	123	116	128	81	88	88	77	33	238
1	5.537	ENERGY	10,894	834	2,454	1,915	1,243	1,205	698	710	501	415	186	733
2	7.181	ENERG CONVERS MANAGE	3,264	209	614	541	432	385	251	203	178	125	57	269
3	8.426	APPL ENERG	3,167	142	536	530	423	413	222	239	157	171	38	296
4	2.707	ENERGIES	2,762	212	462	382	335	325	186	184	174	160	49	293
5	10.556	RENEW SUST ENERG REV	2,678	34	199	345	382	369	252	257	216	167	71	386
6	6.395	J CLEAN PROD	2,279	67	337	289	280	224	173	183	177	147	62	340
7	4.026	APPL THERM ENG	2,024	51	239	310	300	252	199	152	166	102	32	221
8	5.439	RENEW ENERG	1,228	10	126	202	172	147	121	96	95	65	37	157
9	5.128	FUEL	895	20	125	124	98	108	85	77	61	62	22	113
10	4.084	INT J HYDROGEN ENERG	883	33	158	137	118	111	65	38	37	53	21	112
11	2.592	SUSTAINABILITY-BASEL	869	61	137	105	76	100	58	77	63	37	20	135
12	4.674	SOL ENERGY	753	37	95	116	86	84	58	43	37	31	19	147
13	4.495	ENERG BUILDINGS	736	16	85	114	99	78	53	39	51	43	19	139
14	4.880	ENERG POLICY	609	15	76	71	73	92	48	42	42	43	17	90
15	3.021	ENERG FUEL	557	32	96	71	64	64	43	42	55	30	7	53
16	4.346	INT J HEAT MASS TRAN	468	10	60	71	83	68	39	29	30	19	11	48
17	2.914	ENVIRON SCI POLLUT R	393	17	72	36	43	42	34	32	46	30	11	30
18	6.669	BIORESOURCE TECHNOL	359	18	93	57	36	33	24	25	29	20	3	21
19	3.343	INT J ENERG RES	352	7	48	46	46	41	32	30	22	15	3	62
20	1.511	J RENEW SUSTAIN ENER	326	16	60	47	38	41	18	24	23	14	9	36
21	3.375	IND ENG CHEM RES	317	14	41	32	39	38	33	29	20	17	7	47
22	4.624	SUSTAIN CITIES SOC	282	10	44	63	28	35	28	20	9	13	6	26
23	2.217	APPL SCI-BASEL	277	42	61	44	33	24	13	14	5	12	8	21
24		ENERG ECON	272	8	26	31	29	35	28	19	20	12	8	56
25	3.177	INT J REFRIG	268	7	32	38	38	28	27	18	20	13	4	43
26	4.098	IEEE ACCESS	258	16	45	57	30	35	14	21	15	15	3	7
27	7.044	RESOUR CONSERV RECY	226	3	14	20	35	34	17	20	19	13	5	46

Showing 1 - 29 rows of 1,931 total

Citing Journal Data

Citing Half-Life Data

Citing Year	2018	2017	2016	2015	2014	2013	2012	2011	2010	2009	2008-All
#Cites from 2018	3,254	11,742	11,663	9,900	8,772	6,869	5,896	5,368	4,341	3,703	24,999
Cumulative %	3.37%	15.54%	27.62%	37.88%	46.97%	54.09%	60.20%	65.76%	70.26%	74.10%	100.00%

Citing Journal Graph 2018

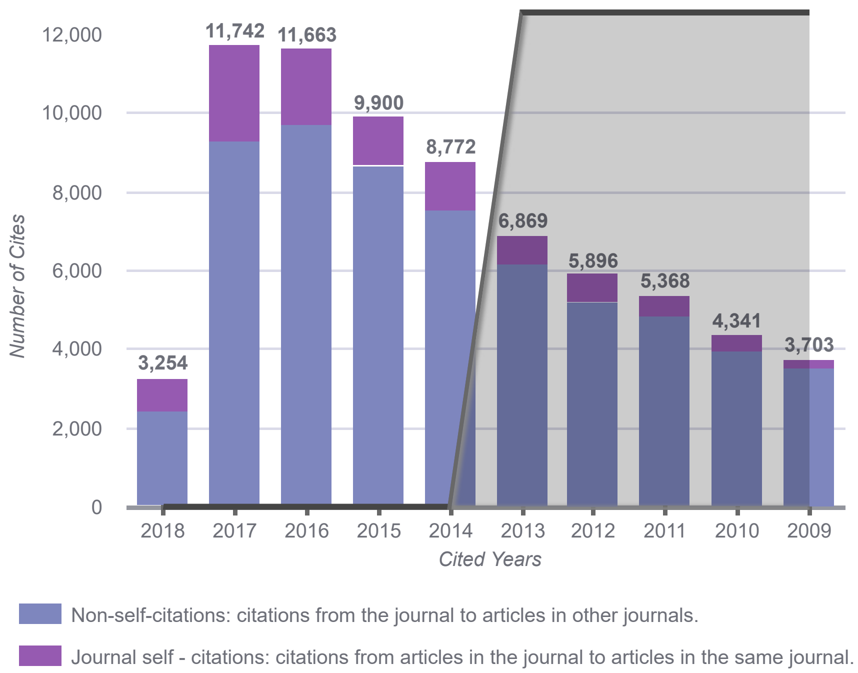

CITING JOURNAL GRAPH

The Citing Journal Graph shows the distribution (by cited year) of citations published in the Journal during the JCR year to items published in journals during the last 10 years.

The white/grey division indicates the citing half-life (if < 10.0). Half of the citations are to items that were published more recently than the citing half-life.

Citing Journal Data 2018

	Impact	Cited Journal	All Yrs	2018	2017	2016	2015	2014	2013	2012	2011	2010	2009	Rest
		ALL Journals	96,507	3,254	11,742	11,663	9,900	8,772	6,869	5,896	5,368	4,341	3,703	24,999
		ALL OTHERS (15928)	15,928	213	1,343	1,517	1,360	1,154	994	888	862	748	612	6,237
1	5.537	ENERGY	10,894	834	2,454	1,915	1,243	1,205	698	710	501	415	186	733
2	8.426	APPL ENERG	4,928	223	848	974	666	629	412	307	299	234	167	169
3	10.556	RENEW SUST ENERG REV	3,292	156	583	582	478	365	268	251	173	129	125	182
4	7.181	ENERG CONVERS MANAGE	3,196	145	524	471	528	392	222	97	116	73	108	520
5	4.026	APPL THERM ENG	2,426	119	455	416	209	226	211	109	126	75	90	390
6	4.880	ENERG POLICY	1,988	43	158	149	89	205	201	212	181	184	151	415
7	5.439	RENEW ENERG	1,948	120	255	309	241	177	127	122	103	112	95	287
8	5.128	FUEL	1,443	55	165	154	177	148	127	104	61	78	49	325
9	4.084	INT J HYDROGEN ENERG	1,324	16	228	169	135	116	111	99	98	88	67	197
10	4.495	ENERG BUILDINGS	1,218	50	137	191	146	132	89	99	81	58	37	198
11	4.674	SOL ENERGY	1,115	35	109	130	98	80	61	77	64	42	46	373
12	6.669	BIORESOURCE TECHNOL	969	36	69	105	112	86	102	82	107	92	44	134
13	7.467	J POWER SOURCES	969	5	55	86	92	121	74	49	75	58	33	321
14		ENERG ECON	821	15	91	69	65	63	102	77	45	47	36	211
15	6.807	IEEE T POWER SYST	813	17	45	59	77	48	90	50	55	29	34	309
16	3.177	INT J REFRIG	789	21	86	102	93	94	33	40	44	15	42	219
17		ENRGY PROCED	783	1	227	96	149	164	35	44	41	0	25	1
18	3.021	ENERG FUEL	750	14	54	49	47	61	76	71	50	87	71	170
19	6.395	J CLEAN PROD	737	119	228	187	69	48	22	16	10	6	9	23
20		THESIS	552	4	26	42	50	56	49	36	34	23	26	206
21	4.346	INT J HEAT MASS TRAN	543	20	67	44	54	38	48	16	17	23	22	194
22	4.418	INT J ELEC POWER	495	26	14	79	94	85	66	37	24	18	4	48
23	3.375	IND ENG CHEM RES	481	4	18	30	28	71	51	44	35	15	30	155
24	2.707	ENERGIES	449	25	135	90	55	41	35	32	15	5	12	4
25	4.120	COMBUST FLAME	443	9	18	37	36	21	23	30	28	27	33	181
26	4.507	FUEL PROCESS TECHNOL	414	8	36	35	53	35	45	20	29	28	27	98

Showing 1 - 28 rows of 3,992 total

These data summarize the characteristics of the journal's published content for the most recent three years, that is, 2018 and the two prior years, combined. This information is based on all listed authors and addresses. It is meant to be descriptive rather than comparative.

Contributions by country/region

country	count
1. CHINA MAINLAND	1,874
2. USA	508
3. Iran	476
4. England	309
5. India	300
6. Italy	299
7. Spain	286
8. South Korea	265
9. GERMANY (FED REP GER)	191
10. Canada	173

Contributions by organizations

organization	count
1. CHINESE ACADEMY OF SCIENCES	165
2. TSINGHUA UNIVERSITY	162
3. SHANGHAI JIAO TONG UNIVERSITY	126
4. NORTH CHINA ELECTRIC POWER UNIVERSITY	113
5. INDIAN INSTITUTE OF TECHNOLOGY SYSTEM (IIT SYSTEM)	91
6. TIANJIN UNIVERSITY	83
- HUAZHONG UNIVERSITY OF SCIENCE & TECHNOLOGY	83
8. XI'AN JIAOTONG UNIVERSITY	82
9. CHINA UNIVERSITY OF PETROLEUM	80
10. TECHNICAL UNIVERSITY OF DENMARK	77

Scopus

Source details

Energy

Scopus coverage years: from 1976 to Present

Publisher: Elsevier

ISSN: 0360-5442 E-ISSN: 1873-6785

Subject area: Engineering: Civil and Structural Engineering | Engineering: Building and Construction | Engineering: Mechanical Engineering | Engineering: Industrial and Manufacturing Engineering | Environmental Science: Pollution | Engineering: Electrical and Electronic Engineering

View all documents > | Set document alert | Save to source list | Journal Homepage

CiteScore 2018
6.20

SJR 2018
2.048

SNIP 2018
1.822

CiteScore | CiteScore rank & trend | CiteScore presets | Scopus content coverage

CiteScore 2018

Calculated using data from 30 April, 2019

6.20 = Citation Count 2018 / Documents 2015 - 2017* = 30.731 Citations > / 4954 Documents >

*CiteScore includes all available document types

View CiteScore methodology > CiteScore FAQ >

CiteScoreTracker 2019

Last updated on *14 October, 2019*
Updated monthly

5.79 = Citation Count 2019 / Documents 2016 - 2018 = 33.138 Citations to date > / 5728 Documents to date>

CiteScore rank

Category	Rank	Percentile
Engineering — Civil and Structural Engineering	#3/287	99th
Engineering — Building and Construction	#5/167	97th
Engineering — Mechanical Engineering	#20/583	96th

View CiteScore trends > Add CiteScore to your site

Metrics displaying this icon are compiled according to Snowball Metrics ↗, a collaboration between industry and academia.

Scopus

Source details

Energy

Scopus coverage years: from 1976 to Present

Publisher: Elsevier

ISSN: 0360-5442 E-ISSN: 1873-6785

Subject area: Engineering: Civil and Structural Engineering | Engineering: Building and Construction | Engineering: Mechanical Engineering | Engineering: Industrial and Manufacturing Engineering | Environmental Science: Pollution | Engineering: Electrical and Electronic Engineering

View all documents > | Set document alert | Save to source list | Journal Homepage

CiteScore 2018
6.20

SJR 2018
2.048

SNIP 2018
1.822

CiteScore | CiteScore rank & trend | CiteScore presets | Scopus content coverage

CiteScore 2018

Calculated using data from 30 April, 2019

6.20 = Citation Count 2018 / Documents 2015 - 2017* = 30.731 Citations > / 4954 Documents >

*CiteScore includes all available document types

View CiteScore methodology > CiteScore FAQ >

CiteScoreTracker 2019

Last updated on *14 October, 2019*
Updated monthly

5.79 = Citation Count 2019 / Documents 2016 - 2018 = 33.138 Citations to date > / 5728 Documents to date>

CiteScore rank

Category	Rank	Percentile
Industrial and Manufacturing Engineering		
Environmental Science — Pollution	#7/109	94th
Engineering — Electrical and Electronic Engineering	#45/658	93rd

View CiteScore trends > Add CiteScore to your site

Metrics displaying this icon are compiled according to Snowball Metrics, a collaboration between industry and academia.

About Scopus

What is Scopus
Content coverage
Scopus blog
Scopus API
Privacy matters

Language

日本語に切り替える
切换到简体中文
切換到繁體中文
Русский язык

Customer Service

Help
Contact us

ELSEVIER

Terms and conditions Privacy policy

RELX

Scopus

Compare sources

Select up to 10 sources to compare

Selected sources: ☐ Energy ×

Remove all selections

CiteScore publication by year

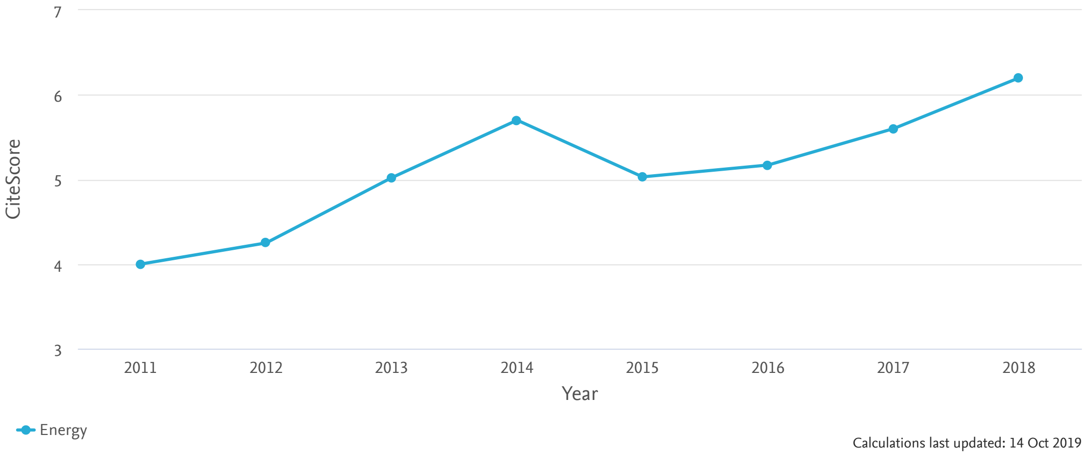

Calculations last updated: 14 Oct 2019

SJR by year

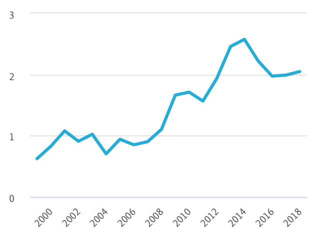

SNIP by year

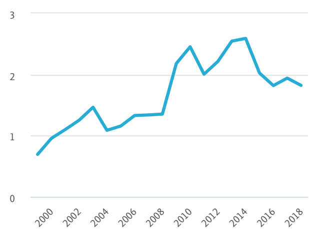

Citations by year

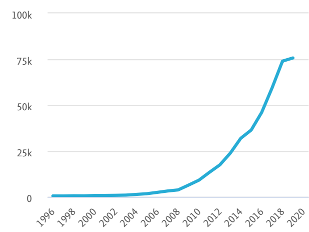

Documents by year

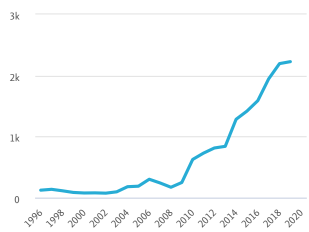

Percent not cited by year

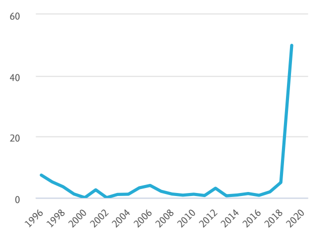

Percentage review articles by year

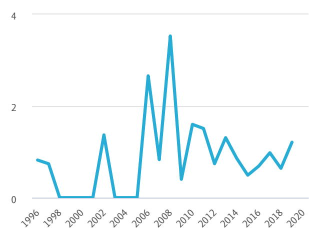

Energy

Country	United Kingdom - SIR Ranking of United Kingdom
Subject Area and Category	Energy Energy (miscellaneous) Engineering Building and Construction Civil and Structural Engineering Electrical and Electronic Engineering Industrial and Manufacturing Engineering Mechanical Engineering Environmental Science Pollution
Publisher	Elsevier Ltd.
Publication type	Journals
ISSN	03605442
Coverage	1976-ongoing
Scope	This journal is a multi-disciplinary focus for activities relating to the development, assessment and management of energy-related programs. It is hoped that this publication will prove to be an important factor in raising the standards of discussions, analyses, and evaluations relating to energy programs. The following are among the topical areas on which important contributions are solicited: input-output analyses relating to energy-consuming systems, careful resource or reserve assessments of all types, energy-conservation measures and their implementations, incisive evaluation of energy-systems managements, environmental-impact assessments, and policy alternatives stressing economic implications.

158

H Index

Homepage

How to publish in this journal

Contact

Join the conversation about this journal

Quartiles

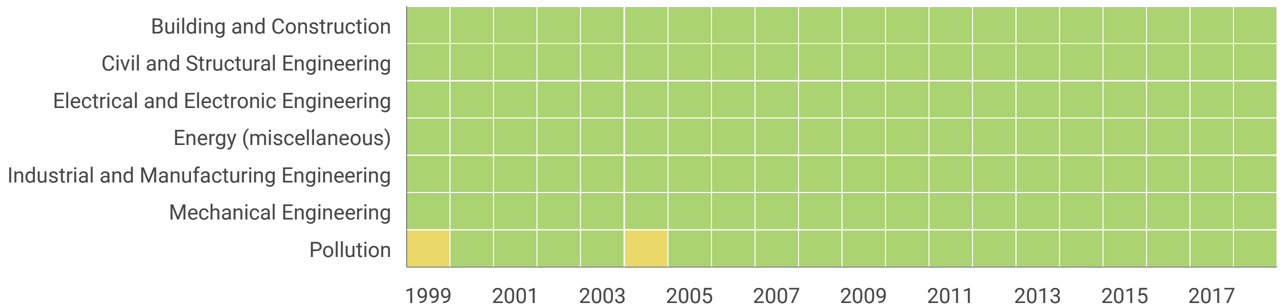

SJR

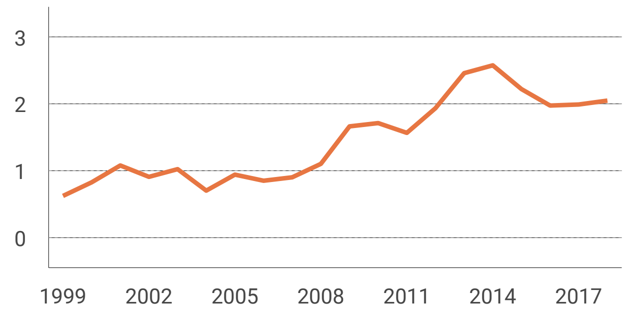

Citations per document

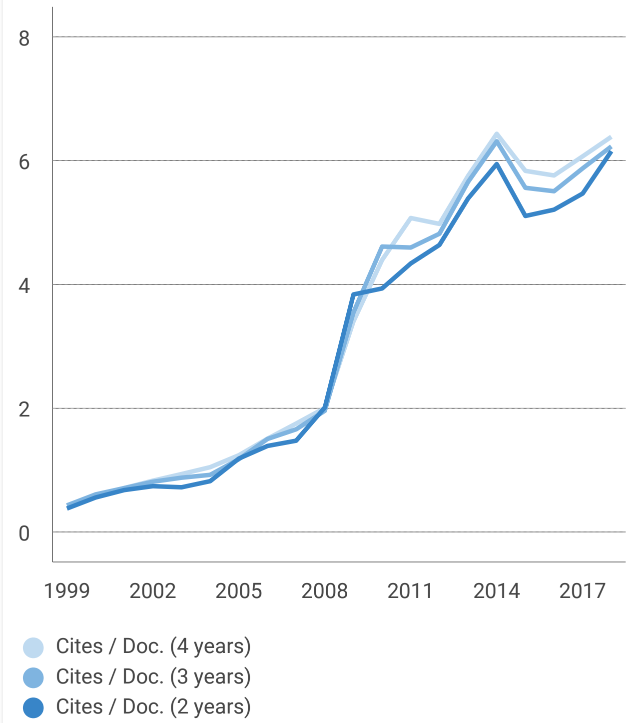

Total Cites Self-Cites

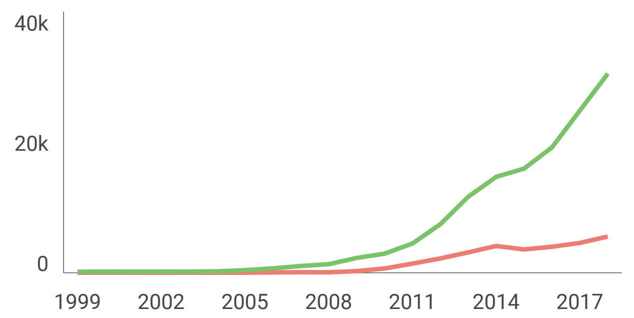

External Cites per Doc Cites per Doc

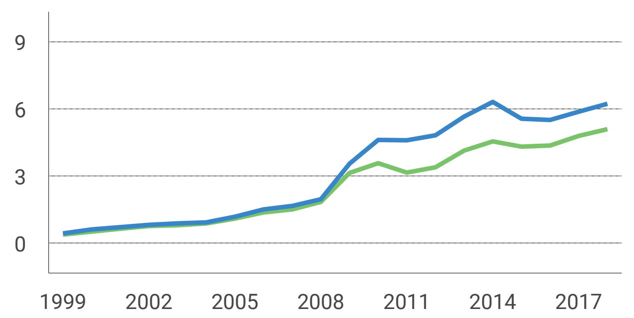

% International Collaboration

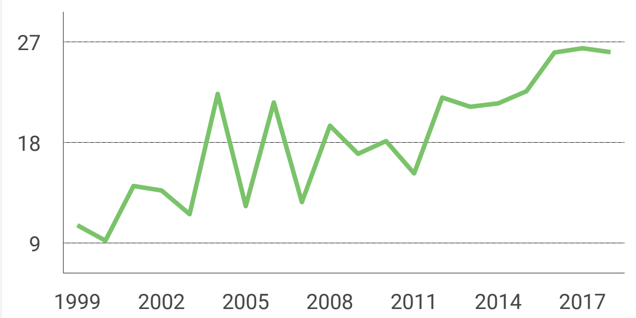

Citable documents Non-citable documents

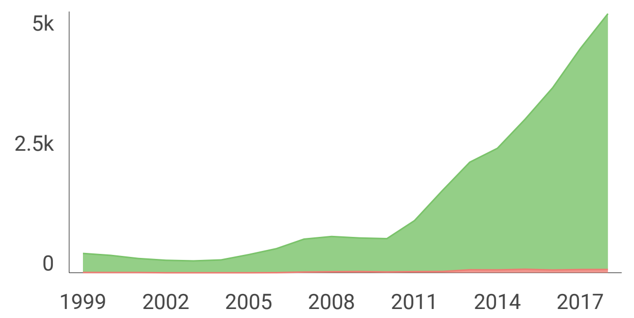

Cited documents Uncited documents

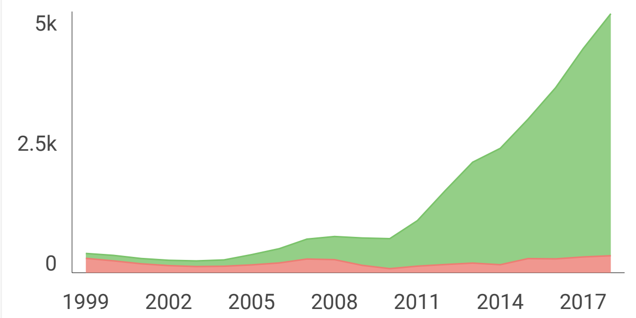

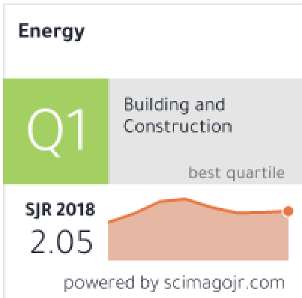

← Show this widget in your own website

Just copy the code below and paste within your html code:

<a href="https://www.scimag

ANEXO X: "*SIMPLIFIED ANALYSIS OF THE ELECTRIC POWER LOSSES FOR ON-SHORE WIND FARMS CONSIDERING WEIBULL DISTRIBUTION PARAMETERS*" COPIA DE LA PUBLICACIÓN.

Energies **2014**, *7*, 6856-6885; doi:10.3390/en7116856

OPEN ACCESS

energies

ISSN 1996-1073

www.mdpi.com/journal/energies

Article

Simplified Analysis of the Electric Power Losses for On-Shore Wind Farms Considering Weibull Distribution Parameters

Antonio Colmenar-Santos [1,*], Severo Campíñez-Romero [1], Lorenzo Alfredo Enríquez-Garcia [2] and Clara Pérez-Molina [1]

[1] Industrial Engineering Higher Technical School, Spanish University for Distance Education, Juan del Rosal St., 12, Madrid 28040, Spain; E-Mails: scampinez1@alumno.uned.es (S.C.-R.); clarapm@ieec.uned.es (C.P.-M.)

[2] Escuela Superior Politécnica de Chimborazo, Riobamba-Chimborazo, EC060103, Ecuador; E-Mail: lorenzenriquez@yahoo.com

* Author to whom correspondence should be addressed; E-Mail: acolmenar@ieec.uned.es; Tel.: +34-913-987-788; Fax: +34-913-986-028.

External Editor: Frede Blaabjerg

Received: 14 July 2014; in revised form: 20 August 2014 / Accepted: 17 October 2014 / Published: 28 October 2014

Abstract: Electric power losses are constantly present during the service life of wind farms and must be considered in the calculation of the income arising from selling the produced electricity. It is typical to estimate the electrical losses in the design stage as those occurring when the wind farm operates at rated power, nevertheless, it is necessary to determine a method for checking if the actual losses meet the design requirements during the operation period. In this paper, we prove that the electric losses at rated power should not be considered as a reference level and a simple methodology will be developed to analyse and foresee the actual losses in a set period as a function of the wind resource in such period, defined according to the Weibull distribution, and the characteristics of the wind farm electrical infrastructure. This methodology facilitates a simple way, to determine in the design phase and to check during operation, the actual electricity losses.

Keywords: wind farm; electric losses; Weibull distribution

1. Introduction

Electric losses do not have an important effect on the net electricity production of a wind farm (WF), but due to the fact that they are constantly present for the entire service life of the WF, it is necessary to implement technical measures to limit them. Nevertheless, yearly losses around 2%–3% of the energy generated occur [1,2].

Usually the electric losses in onshore and offshore WFs are calculated from the estimated yearly capacity factor (The capacity factor, CF is defined, in a yearly period, as the percentage of the year during which the WF should have been working at nominal power to generate the entire production obtained in the year. The gross value, Gross CF, does not include the wake losses, the electric losses up to the point where the electricity fed into the grid is measured, and the production losses due to the mechanical availability of the WTG. The net value, Net CF, includes the effect of all the aforementioned losses expressed as a percentage) corresponding with long-term wind conditions [3,4] and the rated power of the WF [5–7]. These estimated electric losses at rated power are used in the design of the WF for setting technical requirements and to determine the foreseen net generation. The use of this method, considering the non-linear dependency of the electric losses with respect to the power flow, as well as the influence of the WF topology and the distribution of the wind in the set period, can introduce an important error in the business plan if the estimate of the losses at rated power is used as a reference to reduce the generation in the WF and the associated incomes for selling the net electricity fed into the system [6,8], principally because the error in such estimates will affect the cash flows during the whole service life of the WF.

Lately, feed-in-tariffs have been drastically reduced [9,10], the prices in power purchase agreements have been decreasing [11–13] and some competitive mechanisms have been included by public administrations in the processes for awarding WF licenses [14,15], so it is necessary to take to the extreme measures to improve the efficiency as well as implement systems and procedures to confirm the operation under the right conditions. For all of these reasons, the WF owners and their technical advisors include in the request for construction proposals and the subsequent contracts, the definition of methods to check if the electric infrastructures are working properly and producing losses in the guaranteed range. Once again it is practically unfeasible trying to compare the actual measured value with the one used in the design when its calculation is based in the CF and the operation at rated power [6].

The issue, although easy to deal with from a technical point of view, presents a friction point between the owner, the contractor, as designer of the WF, and the operator, perhaps due to the fact that the analysis and the subsequent result is not quite intuitive because the more energy is produced by the WF, the less electrical losses result, as a percentage, and in any case they are always different from those obtained with the classical method of calculation based in the operation at rated power. The study can be done with power flow analysis software, but this approach needs the creation of a complex model of the WF and the wind resource for every WTG and every set period.

The aim of this article is to develop a simple methodology to determine a range for the foreseen electric losses and to confirm, at any time, if the actual losses are in the right range and, therefore, if the WF is working properly. The methodology takes into account the characteristics of the wind resource, modelled according to a standard probability function in the wind sector: the Weibull distribution [16,17]. The method also is intended to be a practical tool for the owner, to put a cap on the reduction in the incomes result of the electrical losses and, together with the constructor and the operator of the WF, to establish requirements for design and construction and to implement appropriate working tests. In brief, the method has a practical approach, and it is focused on helping to the definition and later confirmation of the electricity losses.

The approach to define the wind resource in order to be used in the losses calculation is presented in Section 2. In Section 3, two methods for calculating the electric losses are given, as well as the results for its application in a WTG, in a cluster or circuit of WTGs and in the entire WF. The financial impact in the cash flows and the net value of the WF is shown in Section 4, and finally, the conclusions are presented in Section 5.

2. Characterization and Variability of the Wind Resource

The Weibull distribution is the most suitable probability function to represent the wind resource in a specific site along a specific period of time [16,17]. The equation for the density function is [18,19]:

$$f(s) = \frac{k}{\lambda}\left(\frac{s}{\lambda}\right)^{k-1} e^{-\left(\frac{s}{\lambda}\right)^{k}} \quad (1)$$

where k and λ, are, respectively, the shape and scale parameters, and together define the wind resource. The variable s represents the wind speed. Nevertheless, the wind resource at a given site is variable with time and the period considered and so, the Weibull distribution parameters vary as well even though this period represents the same time (*i.e.*, a specific month in the year).

With the aim to illustrate this wind resource variability, actual data from a meteorological station equipped with anemometers and wind vanes, both calibrated, located at a height of 80 m on the west coast of the Republic of South Africa have been used (nowadays there is an ongoing process of request for proposals for the construction, operation and maintenance of a WF at the selected location; the exact location is not given because this information is under a non-disclosure agreement with the owner of the data). Figure 1 shows the graphic representation of the Weibull density function for the real wind resource in the year 2012 and within each one of the months of 2012 and the Table 1 presents the variation of the Weibull parameters and the mean wind speed in the same periods.

Figure 1. Weibull distribution functions corresponding with the year 2012.

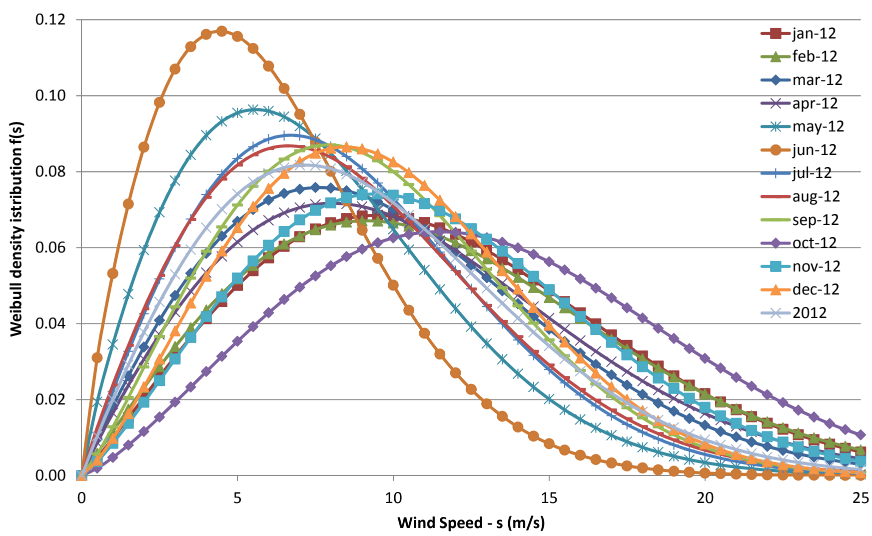

Table 1. Variation of the Weibull parameters and the mean wind speed in 2012.

Weibull parameters	Period												
	Jan.	**Feb.**	**Mar.**	**Apr.**	**May**	**Jun.**	**Jul.**	**Aug.**	**Sep.**	**Oct.**	**Nov.**	**Dec.**	**Year**
Shape—k	2.09	2.02	1.94	1.93	1.85	1.81	1.99	1.93	2.19	2.30	2.21	2.28	1.96
Scale—λ (m/s)	12.92	12.86	11.09	11.72	8.50	6.90	9.54	9.67	10.48	14.73	12.40	10.89	10.35
Mean wind speed	11.44	11.39	9.83	10.39	7.54	6.14	8.45	8.57	9.28	13.05	10.98	9.64	9.17

Figure 2 shows the power density (wind power density is defined in a specific period of time as the mean power available per square meter of swept area of a wind turbine) for the wind conditions included in Table 1. As it may be noticed, the energetic content of the wind resource is not constant, and hence, due to the fact that the electricity losses in the WF depend on the power generated by every WTG, it is essential to analyse the electrical losses in a specific period of time, in which the wind resource will be modelled with the corresponding Weibull parameters, in general different in every period.

Figure 2. Wind power density in 2012.

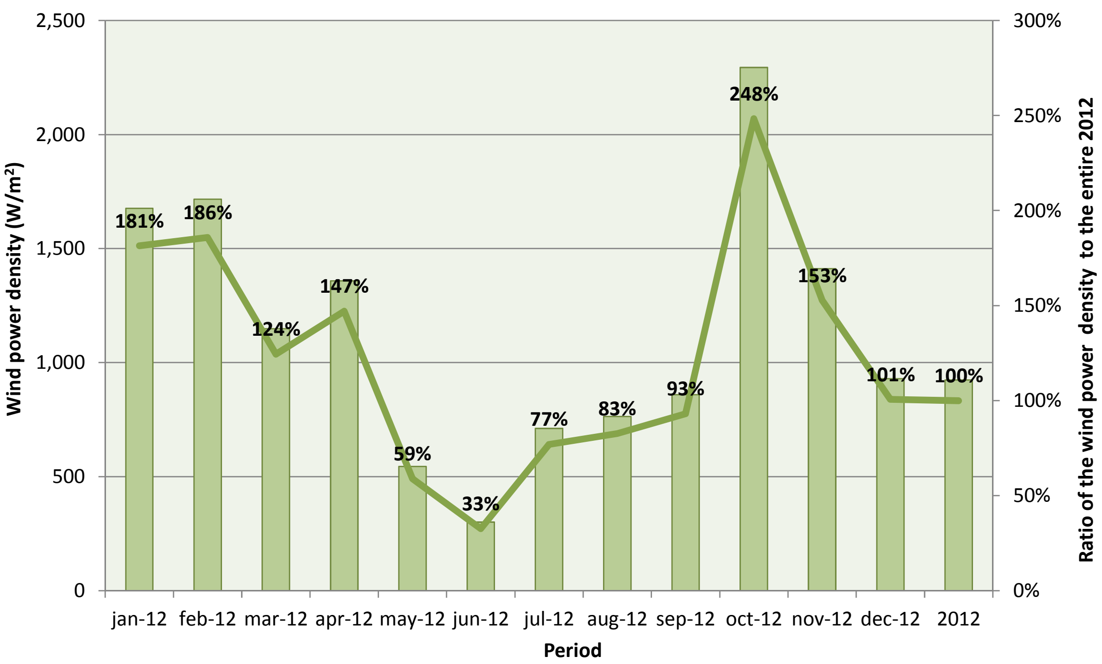

3. Calculation of the Electrical Losses

In general, the WF, including the systems to connect it to the electric grid, implies a simple electrical circuit to be solved with the traditional tools of power flow analysis, but even so, a reduced number of WTGs gives a high number of buses (every WTG adds two buses and four equations to the problem: the connection of the generator to the step-up transformer and the connection of the latter to the collector system) and the analysis requires the use of expert software and therefore to make a model for the entire WF including all the electrical infrastructures.

Most of the WTGs include systems to allow the regulation of the voltage in the PCC by means of controlling the reactive power interchanged with the grid [20]. Thanks to this capacity, the WFs contribute actively to keep the voltage levels within the targets set up by the grid operators independently of the flows of active power. Under normal conditions of operation, the flows of reactive power are small (the power factor is close to one) and the voltage magnitudes in the buses of the WF are very close to the nominal value. In this article, we study the active power losses, and hence, considering the aforementioned statements, a simplification in the calculation can be implemented with the application of the flow analysis in direct current to the study of the active power flows. This simplification implies a certain error that will not affect the comparison between the traditional method to calculate the electric losses and the methodology introduced in this article (to check the validity of the assumptions made to use the power flow analysis in direct current the WF studied was simulated running for several wind conditions the classical power flow analysis in alternating current, in all the simulations the results validated the assumptions, giving minimal differences less than 6° between the angles in adjacent buses and less than the 1.35% respect to the nominal value in the voltage magnitude).

Therefore, all the cases analysed in this article have been carried out by means of the application of the analysis of power flow in direct current according to the basics indicated in [21].

3.1. Application to One WTG

The Figure 3 shows the single line diagram of a WTG connected to the electric grid in the BUS_{PCC}.

Figure 3. Single line diagram of one WTG.

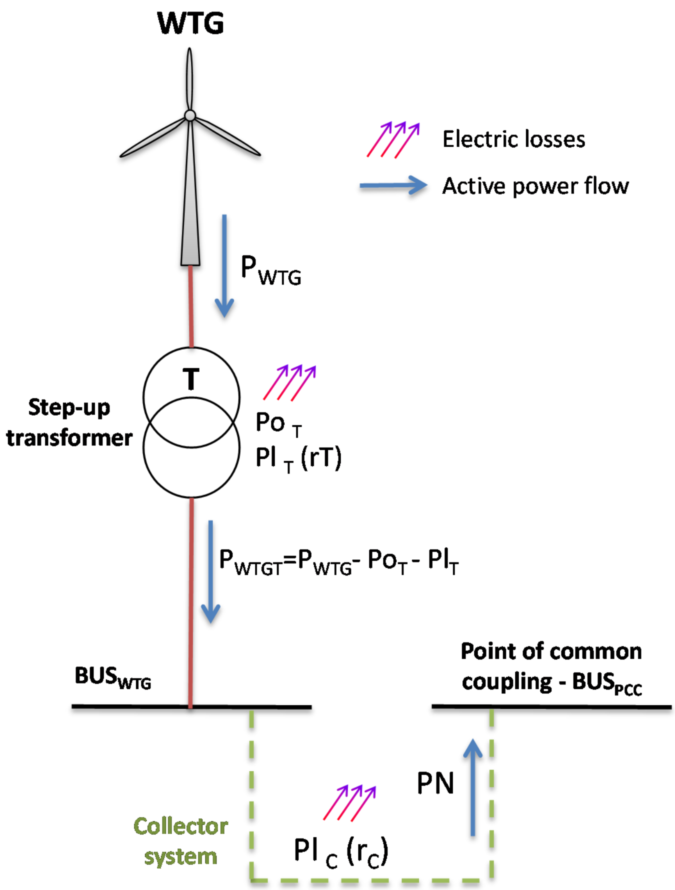

The active power injected in the BUS_{WTG} is the active power generated by the WTG reduced by the power losses in the step-up transformer, both load and no-load. This power is designated as P_{WTGT} (all the powers are dependent on the instantaneous speed of the wind at the hub elevation, so they should be represented with g(s)-type functions, to simplify the equations, the reference to the wind dependence has not been included except in those cases in which it has been considered necessary to understand the right meaning. Hence in the rest of the article $P_{ANY}(s) = P_{ANY}$), and its formula is:

$$P_{WTGT} = P_{WTG} - (Po_T + Pl_T) \tag{2}$$

The no-load power losses Po_T will be constant while the voltage remains constant, a premise for using the power flow analysis in direct current. The load losses in the step-up transformer Pl_T will depend on the power flow, therefore, these will be calculated as follows:

$$Pl_T = \left(\frac{P_{WTG} - Po_T}{V_{GRID}}\right)^2 r_T = (P_{WTG} - Po_T)^2 \frac{r_T}{V_{GRID}{}^2} \tag{3}$$

In the cable that connects the BUS_{WTG} to the BUS_{PCC}, there will be an active power losses Pl_C. The active power injected in the BUS_{PCC}:

$$PN = [P_{WTG} - (Po_T + Pl_T)] - Pl_C \tag{4}$$

$$PN = P_{WTG} - Po_T - (P_{WTG} - Po_T)^2 \frac{r_T}{V_{GRID}{}^2} - Pl_C \tag{5}$$

According to [21] the electric losses in the collector system cable are:

$$Pl_C = \left[P_{WTG} - Po_T - (P_{WTG} - Po_T)^2 \frac{r_T}{V_{GRID}{}^2}\right]^2 \frac{r_C}{V_{GRID}{}^2} \tag{6}$$

The expression for the active power injected in the BUS_{PCC} can be:

$$\begin{aligned} PN = {} & P_{WTG} - Po_T - (P_{WTG} - Po_T)^2 \frac{r_T}{V_{GRID}{}^2} \\ & - \left[P_{WTG} - Po_T - (P_{WTG} - Po_T)^2 \frac{r_T}{V_{GRID}{}^2}\right]^2 \frac{r_C}{V_{GRID}{}^2} \end{aligned} \tag{7}$$

Defining P_{WTGT} as the power generated by the group WTG reduced by the losses in the step-up transformer as:

$$P_{WTGT} = P_{WTG} - Po_T - (P_{WTG} - Po_T)^2 \frac{r_T}{V_{GRID}{}^2} \tag{8}$$

The net power delivered to the coupling point is:

$$PN = P_{WTGT} - P_{WTGT}^2 \frac{r_C}{V_{GRID}{}^2} \tag{9}$$

Therefore, the total losses will be:

$$Pl = P_{WTG} - \left(P_{WTGT} - P_{WTGT}^2 \frac{r_C}{V_{GRID}{}^2}\right) \tag{10}$$

The losses at rated power can be calculated with the following expression:

$$El_{FP} = \frac{Pl_{rated}}{P_{rated}} \tag{11}$$

3.1.1. Energy Losses

Once calculated the total losses Pl, the energy lost in the set period T is:

$$El = \int_0^T Pl(t)\,dt = T\int_0^\infty Pl(s)\,f(s)\,ds \tag{12}$$

where $f(s)$ is the Weibull density function shown in Equation (1) and $Pl(s)$ is the function that links the electric losses with the instantaneous wind speed at WTG hub elevation. As shown in Figure 4, the WTG power curve can be divided in four sections, in which is possible to formulate an analytical expression linking the wind speed at hub height and the power generated and therefore with the electric losses.

Figure 4. WTG power curve with and without the internal transformer. Both divided into sections.

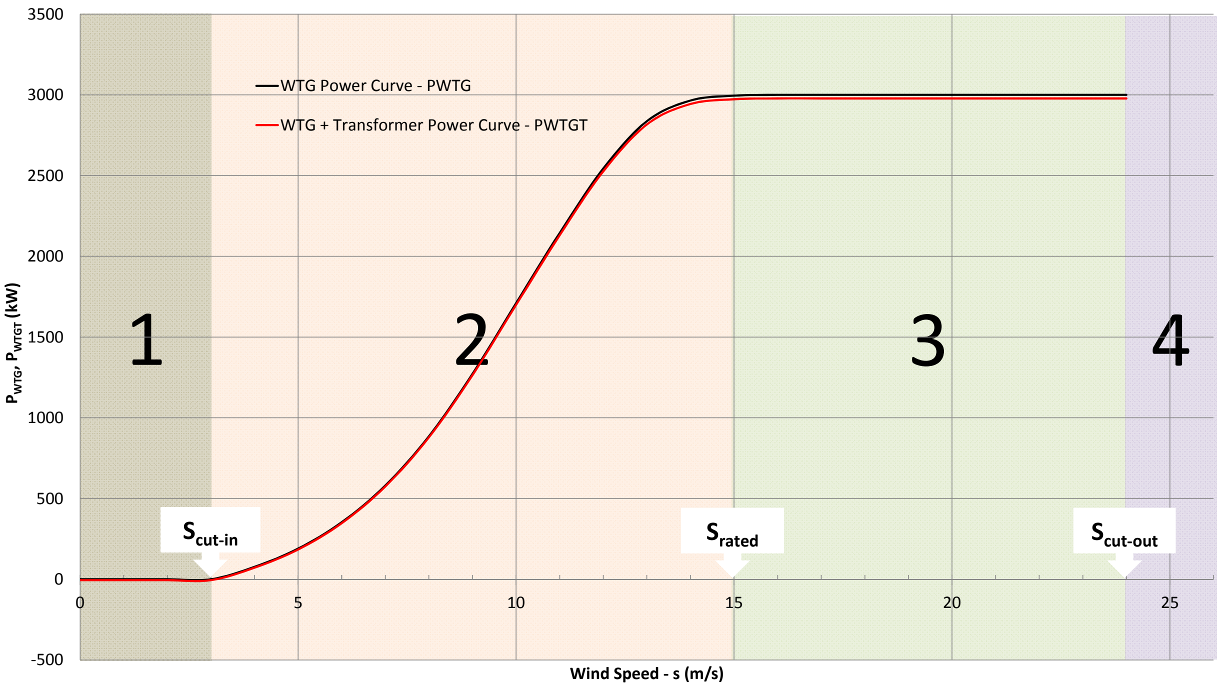

In Section 1, $s \in [0, s_{cut-in}]$ and 4, $s \in [s_{cut-in}, \infty]$, the power generated by the WTG is zero, therefore:

$$P_{WTG}^{(1} = P_{WTG}^{(4} = 0 \tag{13}$$

$$P_{WTGT}^{(1} = P_{WTGT}^{(4} = -Po_T - (-Po_T)^2 \frac{r_T}{V_{GRID}{}^2} \tag{14}$$

$$Pl^{(1} = Pl^{(4} = Pl_o = Po_T + (-Po_T)^2 \frac{r_T}{V_{GRID}{}^2} + \left[-Po_T - (-Po_T)^2 \frac{r_T}{V_{GRID}{}^2}\right]^2 \frac{r_C}{V_{GRID}{}^2} \tag{15}$$

In Section 3, $s \in [s_{rated}, s_{cut-out}]$, the WTG operates at rated power for all the wind speed range, then:

$$P_{WTG}^{(3} = P_{rated} \tag{16}$$

$$P_{WTGT}^{(3} = P_{rated} - Po_T - (P_{rated} - Po_T)^2 \frac{r_T}{V_{GRID}{}^2} \tag{17}$$

$$\begin{aligned} Pl^{(3} = Pl_{rated} = Po_T + (P_{rated} - Po_T)^2 \frac{r_T}{V_{GRID}{}^2} \\ + \left[P_{rated} - Po_T - (P_{rated} - Po_T)^2 \frac{r_T}{V_{GRID}{}^2}\right]^2 \frac{r_C}{V_{GRID}{}^2} \end{aligned} \tag{18}$$

In Section 2, $s \in [s_{cut-in}, s_{rated}]$, the power curve can be modelled using a polynomial expression [22–24] as given below (the fitting of $P_{WTG}^{(2}$, $P_{WTGT}^{(2}$ and $(P_{WTGT}^2)^{(2}$ with fourth degree polynomials, considering the power curve shown in Figure 4, gives coefficients of correlation R^2 above 0.99):

$$P_{WTG}^{(2} = \sum_{m=1}^{4} a_m\, s^m \tag{19}$$

$$P_{WTGT}^{(2} = \sum_{n=1}^{4} b_n\, s^n \tag{20}$$

$$(\, P_{WTGT}^2)^{(2} = \sum_{p=1}^{4} c_p\, s^p \tag{21}$$

$$Pl^{(2} = \sum_{m=1}^{4} a_m\, s^m - \left(\sum_{n=1}^{4} b_n\, s^n - \frac{r_C}{V_{GRID}{}^2} \sum_{p=1}^{4} c_p\, s^p\right) \tag{22}$$

Considering these polynomial expressions, the Equation (12) can be re-written as follows:

$$\begin{aligned} \frac{El}{T} = \int_0^{s_{cut-in}} Pl^{(1}(s)\, f(s) ds + \int_{s_{cut-in}}^{s_{rated}} Pl^{(2}(s)\, f(s) ds + \int_{s_{rated}}^{s_{cut-out}} Pl^{(3}(s)\, f(s) ds \\ + \int_{s_{cut-out}}^{\infty} Pl^{(4}(s)\, f(s) ds \end{aligned} \tag{23}$$

Because the losses in Sections 1, 3 and 4 are constant, and taking into account the relation between the Weibull density function $f(s)$ and the distribution function $F(s)$:

$$\int_{s_1}^{s_2} f(s)\, ds = F(s_2) - F(s_1) \tag{24}$$

where $F(s)$, for a Weibull distribution has the following expression:

$$F(s) = 1 - e^{-\left(\frac{s}{\lambda}\right)^k} \tag{25}$$

$$\begin{aligned} \frac{El}{T} = Pl_o\, F(s_{cut-in}) + \int_{s_{cut-in}}^{s_{rated}} Pl^{(2}(s)\, f(s) ds + Pl_{rated}\, [F(s_{cut-out}) - F(s_{rated})] \\ + Pl_o\, [1 - F(s_{cut-out})] \end{aligned} \tag{26}$$

$$Pl^{(2} = \sum_{m=1}^{4} a_m\, s^m - \left(\sum_{n=1}^{4} b_n\, s^n - \frac{r_C}{V_{GRID}{}^2} \sum_{p=1}^{4} c_p\, s^p\right) \tag{27}$$

$$\frac{El^{(2}}{T} = \int_{s_{cut-in}}^{s_{rated}} \left[\sum_{m=1}^{4} a_m \, s^m - \left(\sum_{n=1}^{4} b_n \, s^n - \frac{r_C}{V_{GRID}{}^2} \sum_{p=1}^{4} c_p \, s^p \right) \right] f(s) ds \quad (28)$$

Considering the Appendix A, the solution for this integral is:

$$\frac{El^{(2}}{T} = \sum_{m=1}^{4} \left(a_m - b_m + \frac{r_C}{V_{GRID}{}^2} \, c_m \right) \lambda^m \left\{ \gamma \left[\left(\frac{m}{k} + 1 \right), \left(\frac{s_{rated}}{\lambda} \right)^k \right] - \gamma \left[\left(\frac{m}{k} + 1 \right), \left(\frac{s_{cut-in}}{\lambda} \right)^k \right] \right\} \quad (29)$$

Therefore, the expression for the total energy losses in the set period T is:

$$\frac{El}{T} = Pl_o \, [1 + F(s_{cut-in}) - F(s_{cut-out})] + \sum_{m=1}^{4} \left(a_m - b_m + \frac{r_C}{V_{GRID}{}^2} \, c_m \right) \lambda^{m-1} \left\{ \gamma \left[\left(\frac{m}{k} + 1 \right), \left(\frac{s_{rated}}{\lambda} \right)^k \right] - \gamma \left[\left(\frac{m}{k} + 1 \right), \left(\frac{s_{cut-in}}{\lambda} \right)^k \right] \right\} + Pl_{rated} \, [F(s_{cut-out}) - F(s_{rated})] \quad (30)$$

3.1.2. Energy Generated

Considering again the division of the WTG power curve into four sections, the expression for the electricity generated is given by:

$$\frac{Eg}{T} = \int_{0}^{s_{cut-in}} P_{WTG}{}^{(1}(s) \, f(s) ds + \int_{s_{cut-in}}^{s_{rated}} P_{WTG}{}^{(2}(s) \, f(s) ds + \int_{s_{rated}}^{s_{cut-out}} P_{WTG}{}^{(3}(s) \, f(s) ds + \int_{s_{cut-out}}^{\infty} P_{WTG}{}^{(4}(s) \, f(s) ds \quad (31)$$

Taking into account the Expressions (13), (16) and (19), the electricity generated can be formulated as follows:

$$\frac{Eg}{T} = \int_{s_{cut-in}}^{s_{rated}} \left[\sum_{m=1}^{4} a_m \, s^m f(s) \right] ds + P_{rated} \, [F(s_{cut-out}) - F(s_{rated})] \quad (32)$$

And according to the Appendix A, the final solution is:

$$\frac{Eg}{T} = \sum_{m=1}^{4} a_m \, \lambda^m \left\{ \gamma \left[\left(\frac{m}{k} + 1 \right), \left(\frac{s_{rated}}{\lambda} \right)^k \right] - \gamma \left[\left(\frac{m}{k} + 1 \right), \left(\frac{s_{cut-in}}{\lambda} \right)^k \right] \right\} + P_{rated} \, [F(s_{cut-out}) - F(s_{rated})] \quad (33)$$

3.1.3. Characterization of the Electrical Infrastructures

For the analyses of the losses, the equipment was modelled with the following parameters and variables (the equivalent circuit is shown in Figure 5)

- The WTG as an ideal generator of which instantaneous power output is obtained from the power curve corresponding with the wind speed at the hub height. This representation does not introduce error in the calculations because the power curve gives the net power output for all the wide range of operating voltage of the WTG.

- The WTG step-up transformer by means of a parallel resistance for the non-load losses Po_T and a serial resistance r_T for the load losses.
- The collector system cable between the BUSWTG and the BUSPCC with a serial resistance r_C.

Figure 5. Equivalent electric circuit for the simulation.

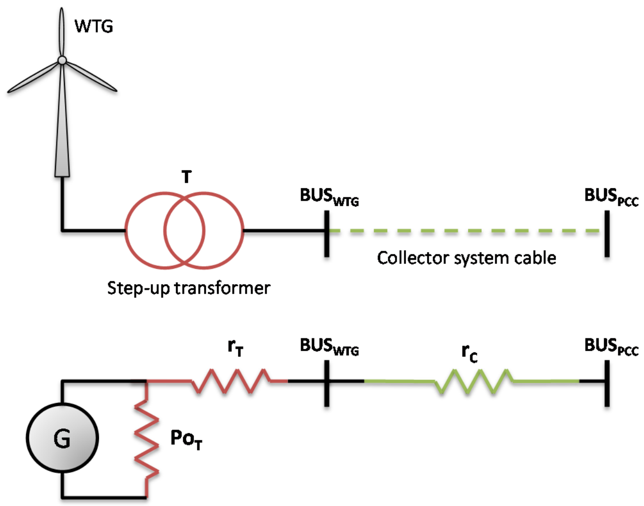

To run the simulations, representative values based on actual data from commercial equipment widely used in the construction of the WFs have been assigned to the variables of the equivalent circuit. Regarding the WTG, the one selected was the V112 of Vestas [25], with 3 MW of rated power and 112 m of rotor diameter. The power curve for this WTG is shown in Figure 4. The main characteristics are similar to those of the WTGs of other manufacturers (Siemens [26], Alstom [27], Gamesa [28], *etc.*). The values considered for the non-load and load losses of the step-up transformer correspond with standard transformer supplied by Vestas along with the WTG.

The connections of the WTGs to the collector system are usually done with isolated aluminium cables buried in trenches. The size of the cables is calculated according to the requirements of ampacity, short-circuit withstand and drop voltage. The main manufacturers offer sizes ranging between 10 mm^2 and 500 mm^2, but due to a matter of economy of scale, a maximum of two or three different sizes are usually used in the collector system. In the simulations, a mean size was supposed for the collector system. The insulation of the cable affects its electric resistance. Currently, three different technologies are predominant in the market: polyvinyl chloride (PVC); cross-linked polyethylene (XLPE) and ethylene propylene. The most used insulation materials are XLPE and EPR and in both cases the effect on the resistance presented by the cable are equal [29].

Respect to the length of the collector system, it will be directly conditioned by the WTG layout. Obviously, the best positions should be selected in terms of wind resource. With the objective of maximizing the generation at a minimum cost, several methods have been suggested to optimize WF layouts [30–33]. However, very often, especially at sites where the wind resource is homogenous over all the area available and for the purpose of minimising losses caused by the wake effect [31,34,35] the WTGs are located within a distance in the range of two or three times the length of the WTG rotor diameter in the line perpendicular to the prevailing wind direction [18,36]. In our case, according to these basic rules, the distance should be between 224 m and 366 m, therefore a mean length of 350 was selected.

To define the voltage magnitude of the collector system, it is important to consider on the one hand that the size of the switchgears and the step-up transformers increase with the magnitude and that these elements are usually installed inside the WTGs with space limitations. On the other hand, using a low voltage level implies higher currents in the collector system and the use of bigger sizes in the cables. The market offer nowadays equipment with nominal voltages values up to 40 kV [37–39] therefore a typical standard voltage level of 36 kV was selected.

A summary with of characteristics of the infrastructure elements used in the simulations is included in Table 2.

Table 2. Characteristics of the infrastructure elements used in the simulation of a WTG.

Element	**Name**	**Value**	**Unit**	**Comment**
WTG	Manufacturer and type	Vestas V112-3 MW	–	Class I WTG [40] 112 m of rotor diameter
	Power curve	Figure 4	–	Vestas standard
Step-up transformer	Manufacturer and type	Standard for V112-3 MW	–	–
	Po_T	5.3	kW	Manufacturer data for the WTG selected
	r_T	2.42	Ω	Manufacturer data for the WTG selected. Corresponds with a 0.7% of positive sequence short-circuit resistance at the transformer rated power
Collector system	V_{GRID}	36	kV	Typical
Interconnection cable to the collector system	Length (L)	350	m	The selected WTG has a 112 m rotor diameter. To reduce weak losses the separation between neighbour WTGs should be in the range of 2 or 3 times the length of the rotor diameter
	Material	Al		Typical
	Size	120	mm^2	Medium value
	Insulation material	XLPE/EPR		Typical
	r_C per km	0.3226	Ω/km	–
	r_C	0.1129	Ω	–

3.1.4. Calculation and Simulation Results

The expression for the relative energy losses is:

$$El(\%) = \frac{El}{Eg} \times 100 \tag{34}$$

The calculation of the electricity generation and losses for a wide range of values of the Weibull parameters was done using MATLAB [41] The behaviour of the WTG and the associated electric infrastructures detailed in the Table 2 was simulated to calculate the electricity generation by applying Equation (30) and the electricity losses by applying Equations (33) and (34). The results, illustrated in Figure 6, show that, in relation with the losses calculated when the WTG operates at rated power and for any wind regime considered, the actual electric losses are always higher, reaching even the double.

Figure 6. Electric losses of the energy generated for a WTG as a function of the Weibull parameters representatives of the period considered.

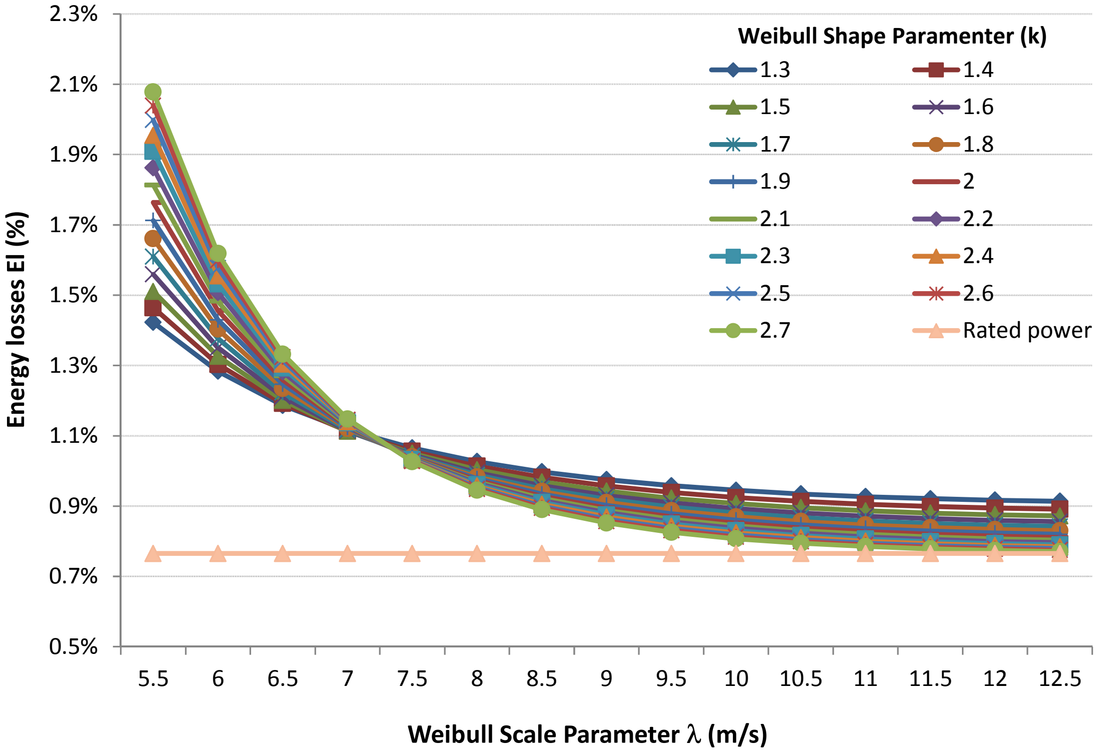

3.2. Application to a WF

Generally, WFs are made up of several WTGs. In the design stage, the WTGs are grouped in evacuation circuits under criteria for making best use of the capacity of the equipment and for optimizing the total cost of the cable needed to form the collector system.

The number of WTGs for every single circuit depends on several factors: the relative location of the WTG among themselves and in relation to the substation; the WTG rated power; the collector system voltage magnitude and the capacity of the switchgears because the total current of the circuit flow through the last WTG. Typically, the switchgears supplied with the WTGs have a rated current of 630 A [37–39], thus for a WTG rated power of 3 MW, a nominal voltage of 36 kV in the collector system and a minimum load factor of 0.8, the maximum number of WTGs per circuit should be:

$$n_i < \frac{630\ A}{\dfrac{0.8 \times 3{,}000\ \text{kW}}{\sqrt{3} \times 36\ \text{kV}}} \sim 10\ \text{WTGs} \tag{35}$$

Nevertheless, taking into account reliability criteria, it is very common to do the design in groups of less WTGs per circuit, with the criterion of facilitating the operation of the WF and minimizing the losses of generation in case of trip or failure of the switchgear that connects the circuit to the substation. However, it is not reasonable to have a small number of WTGs per circuit, because it would imply a high number of circuits and an increase of the length of the collector system cables and the number of switchgears in the substation. An optimization, taking into account the aforementioned factors, gives a typical number of 3 circuits with 5 or 6 WTGs per circuit for a WF around 50 MW [7,42,43].

Figure 7 shows the single line diagram of a 6 WTG circuit as well as the electric infrastructure to connect it to the PCC.

Figure 7. Single line diagram of a circuit and the power evacuation infrastructure up to the PCC.

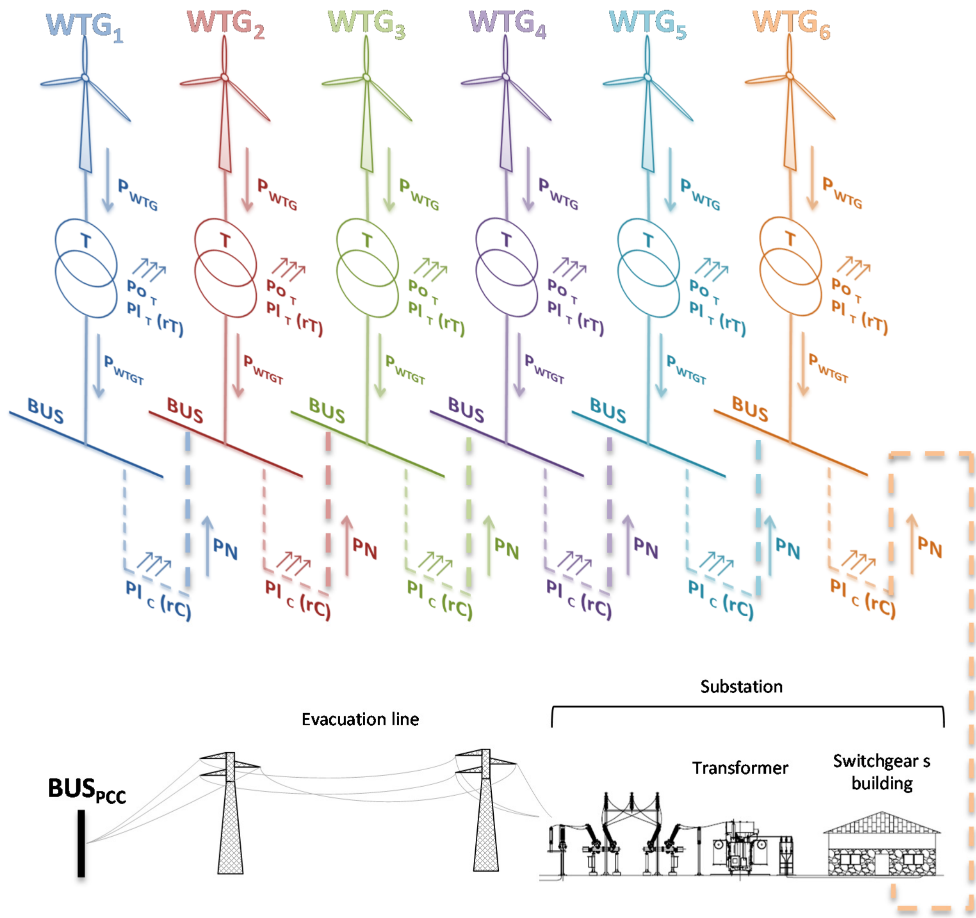

3.2.1. Energy Losses

In the general case, which single line diagram and electric equivalent circuit are shown in Figure 8, the active power injected in a generic bus named *i* + 1 coming from the previous bus *i* through the collector system cable is the result of:

1. The active power generated by the WTG, P_{WTGi}, reduced by the losses of the step-up transformer $(Po_{Ti} + Pl_{Ti})$.
2. The addition of the net active power coming from the previous bus, PN_{i-1}.
3. The subtraction of the electric losses in the cable between both cables, Pl_{Ci}.

Figure 8. WF single line and electric equivalent diagrams.

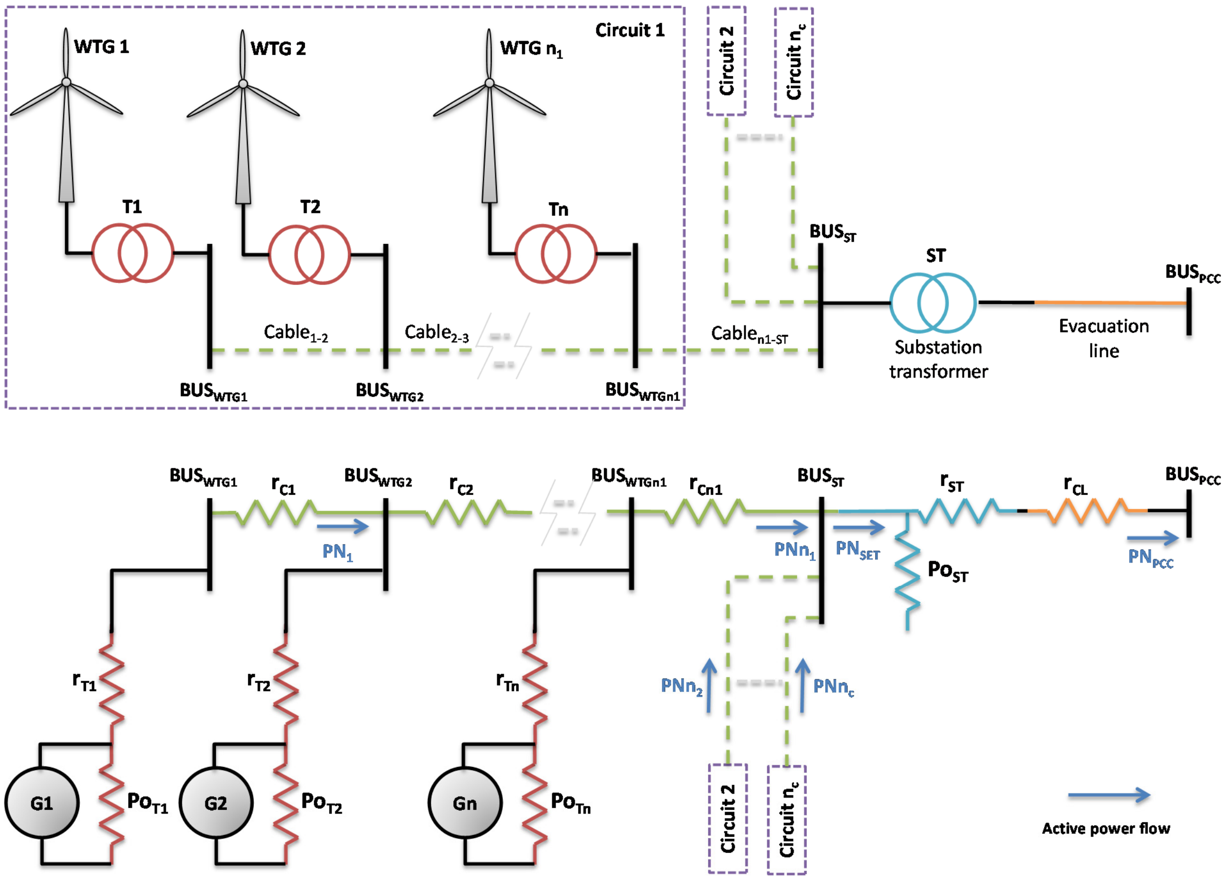

Considering Equations (3) and (6), corresponding to the losses in the step-up transformer and in the collector system cable, the expression for the net power injected in the BUSST is:

$$PN_i = PN_{i-1} + P_{WTGi} - Po_{Ti} - (P_{WTGi} - Po_{Ti})^2 \frac{r_{Ti}}{V_{GRID}{}^2} - \left[PN_{i-1} + P_{WTGi} - Po_{Ti} - (P_{WTGi} - Po_{Ti})^2 \frac{r_{Ti}}{V_{GRID}{}^2}\right]^2 \frac{r_{Ci}}{V_{GRID}{}^2} \quad (36)$$

In general, the wind of each WTG hub will be different, but it does not present important differences that affect qualitatively the objectives of the simulation. In fact, the effect would be similar to supposing a different scale parameter for the Weibull representation of the wind resource for each turbine. As can be seen in Figure 6, for a WTG a variation of 5% in the scale parameter representative of the period considered in the calculations has a limited impact in the losses exceeding 10% only for very low resource periods. This assumption is applicable except in special conditions depending on the complexity of the land orography, the layout of the WTG and the wind direction. In those cases different Weibull functions should be considered. Therefore, in the calculations it was supposed that the wind in every single WTG hub is the same and accordingly to the power generated is also the same and equal to P_{WTG}.

Likewise, the step-up transformers installed in each WTG will have the same characteristics, so that the no-load losses as well as the short-circuit resistance can be supposed the same for all of them.

Considering the aforementioned, for each one of the n_C circuits forming the WF, the net active power injected in the BUSST would be the result of Equation (36) particularized for the last WTG, so that, for a generic circuit *j*:

$$\begin{aligned} PN_{n_j} &= PN_{n_j-1} + P_{WTG} - Po_T - (P_{WTG} - Po_T)^2 \frac{r_T}{V_{GRID}{}^2} \\ &- \left[PN_{n_j-1} + P_{WTG} - Po_T - (P_{WTG} - Po_T)^2 \frac{r_T}{V_{GRID}{}^2} \right]^2 \frac{r_{Ci}}{V_{GRID}{}^2} \end{aligned} \quad (37)$$

The total net active power injected in the BUS_{ST} is the sum of the net power coming from all the circuits, so that:

$$PN_{SET} = \sum_{j=1}^{c} PN_{nj} \quad (38)$$

Finally, the active power delivered in the BUS_{PCC}, results reducing PN_{SET} by the step-up transformer losses (no-load and load) and the power losses in the evacuation line:

$$\begin{aligned} PN_{PCC} &= PN_{SET} + (PN_{SET} - Po_{ST})^2 \frac{r_{ST}}{V_{PCC}{}^2} \\ &+ \left[PN_{SET} - Po_{ST} - (PN_{SET} - Po_{ST})^2 \frac{r_{ST}}{V_{PCC}{}^2} \right]^2 \frac{r_{CL}}{V_{PCC}{}^2} \end{aligned} \quad (39)$$

Taking into account that the number of WTGs in the WF is n_{WF}, the total active power generated is given by:

$$PG_{WF} = n_{WF}\, P_{WTG} \quad (40)$$

And therefore, the total active power losses in the WF are:

$$Pl_{\mathrm{WF}} = PG_{\mathrm{WF}} - PN_{PCC} \quad (41)$$

The electricity lost in the set period *T* is the result of the integration of the previous Equation (41) in such a period:

$$El_{WF} = \int_0^T Pl_{WF}(t)\, dt = T \int_0^\infty Pl_{WF}(s)\, f(s) ds \quad (42)$$

But now, the Equation (41) for $Pl_{WF}(s)$ does not allow a direct integration to obtain an analytic equation as it was done for a sole WTG. The fact that the losses in every part of the collector system depend recursively on the previous losses, and the simplification implemented by means of the substitution of the WTG power curve by a polynomial fitting, turn unmanageable the defined integral Equation (42).

In this case, instead of an analytical solution, the integral was solved in a discrete way. The Weibull wind distribution can be indicated in discrete intervals of the wind speed. In addition, WTG manufacturers give usually the power curve in a tabulated serial values relating the intervals of the wind speed at hub height with the power output. This way introduces a certain error dependent on the width of the interval, such that the wider the interval is, the higher the error is. At the limit, so that the interval was equal to zero, the solution would correspond with the analytical solution and the error would be zero. Anyway, considering the usual intervals given by manufacturers, 0.5 or 1 m/s, the error is not very relevant for the qualitative results of the simulations, due to the fact that both curves, power output and wind distribution, present smooth outlines and slopes, and therefore there will not be important variations in each interval (in order to delimit the margin error, a comparison between the results obtained with

Equation (30) and the discrete method developed in this section applied for one WTG was carried out, the differences were, for all the range of the Weibull parameters, lower than 4%).

From these discrete values for the wind resource and the power generated by each WTG it is possible to calculate for every single interval of the wind speed, the losses in all the collector system sections, all the circuits and finally the total losses for the entire WF. An example of the result obtained in the application of this method is shown in Figure 9, where the histograms for a wind resource with Weibull parameters k = 1.9 and λ = 10 m/s and a WF made up of three circuits with six WTGs in each one of the circuits (total WF power 3 × 6 × 3 = 54 MW) are illustrated.

Figure 9. Histograms for the wind density distribution and the power losses.

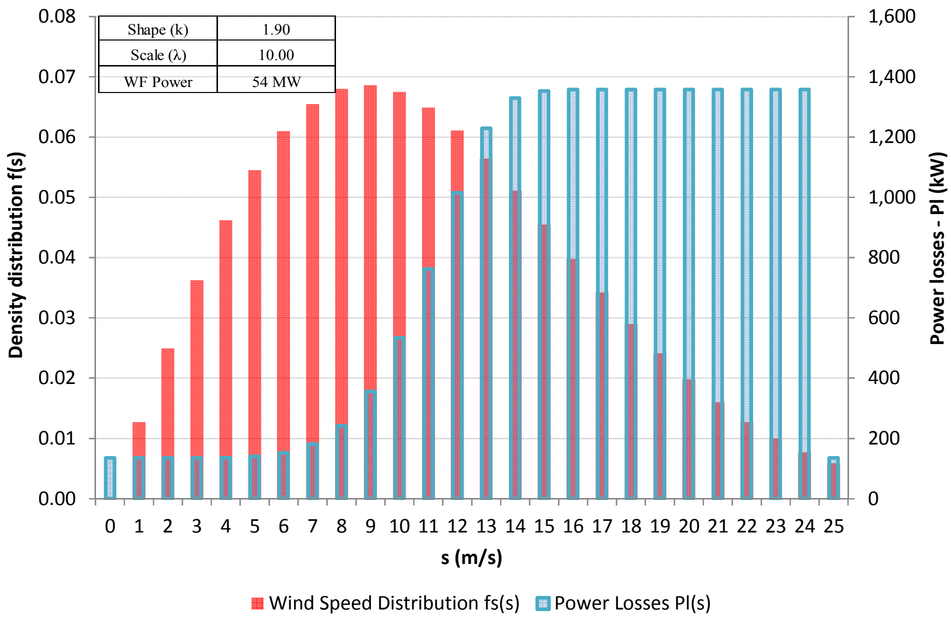

Finally, once the value of losses in each interval is obtained, the total electricity lost in the set period T, is given by:

$$El_{WF} = T \sum_{s=0}^{s_{cut-out}} Pl_{WF}(s)\, f(s) \Delta s \tag{43}$$

3.2.2. Energy Generated

Considering that the number of WTGs in the WF is n_{WF}, the total electricity generated by the WF is given by:

$$Eg_{WF} = n_{WF} \times Eg \tag{44}$$

where E_g is the electricity generated by every WTG calculated in Equation (33).

3.2.3. Characterization of the WF and the Electric Infrastructures

For the simulation of the WF, it is necessary to extend the modelling of the equipment developed in the Section 3.1.3., to the elements that connect the WTGs to the PCC: the substation transformer and the evacuation line. The equivalent electric circuit is drawn in Figure 8. In the simulations these elements were represented by the following parameters:

- The substation transformer by means of a parallel resistance for the non-load losses Po_{ST} and a serial resistance r_{ST} for the load losses. Both parameters are obtained from the standard short-circuit and losses test carried out for every single transformer.
- The evacuation line between the substation (BUS_{ST}) and the BUS_{PCC} with a serial resistance r_C.
- The evacuation voltage magnitude is, in general, different and higher than the collector system voltage magnitude.

In the same way as the case of a sole WTG, to run the simulations, representative values based on actual data from commercial equipment widely used in the construction of the WFs [44–46] have been assigned to the variables of the equivalent circuit. The installed power of the WF was assumed to be a medium value of 54 MW, corresponding to 18 WTGs of 3 MW, distributed in three circuits with six WTGs each one. The PCC voltage magnitude was initially set in 132 kV, valid to evacuate the power capacity of the WF, and lately, as shown in Section 3.2.4., a sensitivity analysis respect to the voltage magnitude was carried out.

To define the parameters of the evacuation line, three different sizes of aluminium conductor steel reinforced (ACSR) were considered. This type of cable is very widely used for a wide range of power capacity and voltage magnitudes values [47,48]. First the simulation was made for a size of the conductor in accordance with the rest of the assumptions (WF power installed and voltage magnitude of the PCC) and then a sensitivity analysis respect to the variation of the size of the cable was carried out. The power transmission limits and the value of the resistance are shown in Table 3.

Table 3. Power transmission limits and resistance for some ACSR cables. Designation according to standard UNE-EN 50 182 [49] (the Spanish standard equivalent to IEC 61089 [44]).

Voltage (kV)	**147-AL1/34-ST1A** [a]	**242-AL1/39-ST1A**	**402-AL1/52-ST1A**
	Power limit (cos φ = 0.8) (MVA)		
45	26.95	36.11	50.38
66	39.53	52.96	73.89
132	79.05	105.91	147.79
220	Not used	Not used	246.31
–	147-AL1/34-ST1A	242-AL1/39-ST1A	402-AL1/52-ST1A
–	Resistance at 85 °C		
r_{CL} (Ω/km)	0.2483	0.1195	0.0719

[a] According to UNE—EN 50 182 [49] the first number indicates the area (in mm^2) of aluminium and the second one the area (in mm^2) of steel.

Regarding the substation transformer, for the chosen power of 54 MW, the nameplate power should be around 60 MVA. For a power transformer of this nominal power, the short circuit impedance must be upper than 11% according to what is establish in the standard IEC 60076-5 [50].

Table 4 shows a summary of the parameters included in the simulations to model the WF and the rest of the electrical equipment necessary for the connection to the PCC.

Table 4. Characteristics of the new infrastructure elements used in the simulation of the entire WF.

Element	Name	Value	Unit	Comment
Wind Farm	Power	54	MW	18 × 3 MW
	Composition	3 circuits 6 WTG per circuit	–	–
Substation transformer	Nominal Power	60	MVA	–
	Po_{ST}	40	kW	Manufacturer data
	Ucc	11.00	%	According to standard IEC 60076 [50]
–	x/r	35	–	IEEE Transformers Committee recommendations [51]
PCC Voltage	V_{GRID}	132	kV	Typical
Evacuation line	Length (L)	15	km	–
	Material	147-AL1/34-ST1A	–	Designation according to standard UNE-EN 50 182 (Spanish standard equivalent to IEC 61089). See Table 3
	r_{CL} per km	3.7251	Ω/km	Value for the cable selected. Source [49]

3.2.4. Simulation Results and Sensitivity Analysis

First of all the losses of a circuit made up of 6 WTGs up to the BUS_{ST} were calculated The simulation was done by applying Equation (33) to only one circuit, so that:

$$El_{n_j} = T \sum_{s=0}^{s_{cut-out}} PN_{n_j}(s)\, f(s) \Delta s \tag{45}$$

And therefore:

$$El_{n_j}(\%) = \frac{El_{n_j}}{6 \times Eg} \times 100 \tag{46}$$

The results of the simulation are shown in Figure 10. Unlike the results for one WTG, now the losses calculated at rated power cannot be considered as a minimum because for several values of the Weibull parameters the actual losses go below it.

In the simulation represented in Figure 10, the size of the collector system cable was saaumed to be as indicated in Table 2. Generally the dimensioning of the collector system will depend on the characteristics of the WF as well as on the requirements of drop voltage and ampacity, so that it is important to analyse the sensitivity of the losses respect to the cable size. With this objective the simulation of the sensitivity of the ratio of the actual losses to the losses at rated power with the wind resource and the cable size was carried out The variation of the wind resource was implemented by maintaining fixed the shape parameter k = 2 (Rayleigh distribution) and modifying the scale parameter (λ) and the variation of the cable size modifying the value of the resistance r_C. The results are presented in Figure 11. As it can be noted, generally, except in the case of both high wind resource (high scale parameter) and high cable resistance the losses at rated power are an upper limit for the actual losses.

Figure 10. Electric losses of the energy generated for a circuit of six WTGs as a function of the Weibull parameters representative of the period considered.

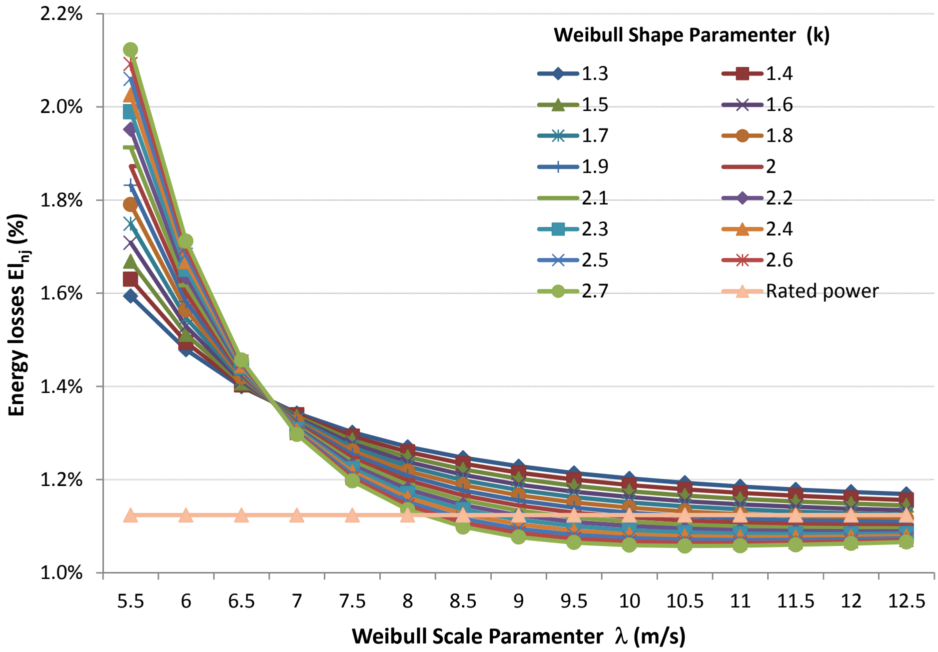

Figure 11. Sensitivity of the electric losses of the energy generated for a circuit of six WTGs with the value of the resistance of the collector system cable and with the scale Weibull parameter representative of the period considered considering the Weibull shape parameter equal to 2.

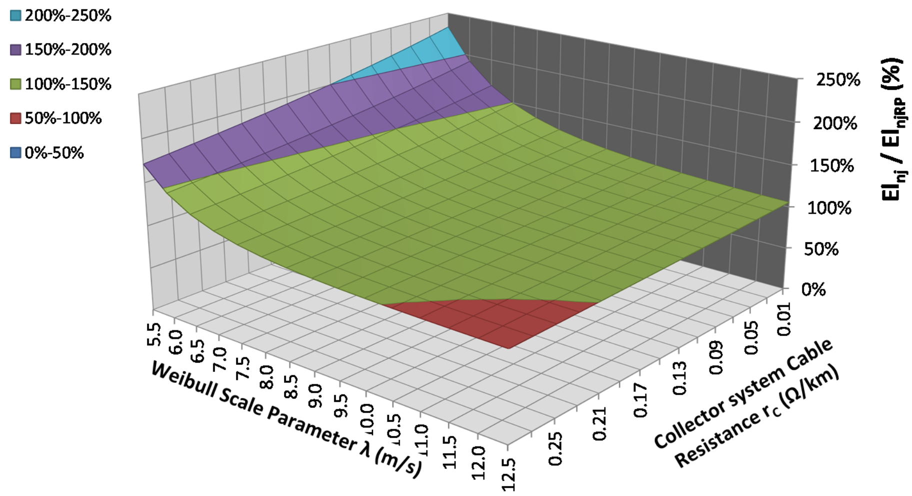

For the entire WF, considering Equation (43), the electricity losses as a percentage of the generation are:

$$El_{WF}(\%) = \frac{El_{WF}}{Eg_{WF}} \times 100 \tag{47}$$

The electricity losses at rated power are a particular case when the wind speed is equal or higher to s_{rated}, and can be obtained with the following expression:

$$El_{WF_{FP}}(\%) = 100 \times \left.\frac{PN_{SET}}{PG_{WF}}\right|_{s=s_{rated}} \tag{48}$$

The result of the simulation is illustrated in Figure 12. Unlike the results obtained for one WTG or a group, when the entire WF is considered, the actual losses are, practically in all the wind range, under the losses calculated when the WF operates at rated power which could be considered as a upper limit.

Figure 12. Electric losses of the energy generated for the WF as a function of the Weibull parameters representatives of the period considered.

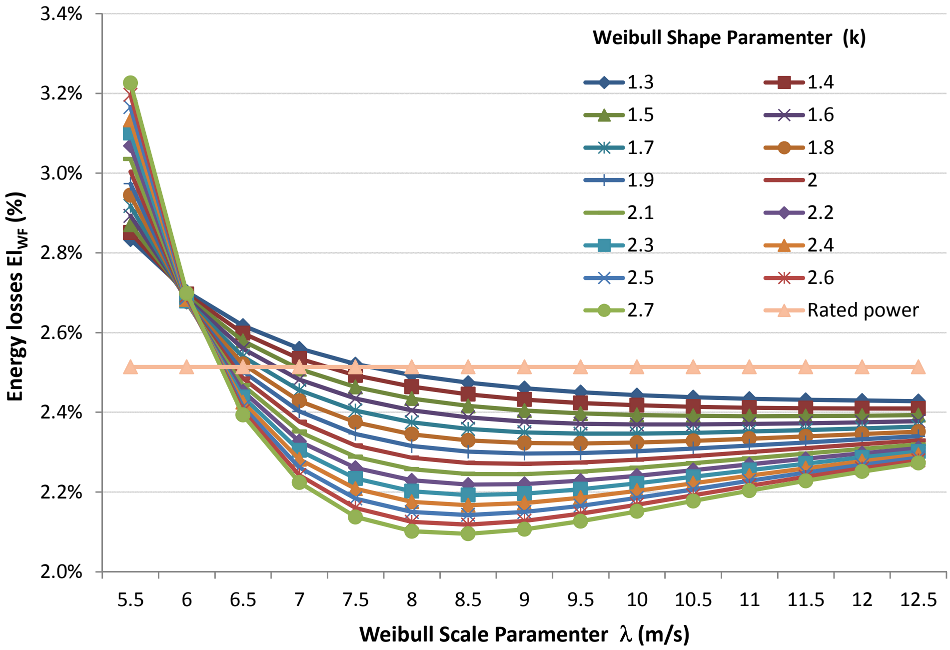

The length and the design of the evacuation line, as well as the PCC voltage level have a significant effect in the total losses, because by the line flows the total power and the losses are directly proportional to square of the active power flowing and are inversely proportional to the PCC voltage level.

With the aim of evaluating the effect the variation of these parameters on the electric losses, a sensitivity analysis was carried out with respect to them, by calculating the sensitivity of the ratio of the actual losses to the losses at rated power, with the wind resource and the type of conductor of the evacuation line. Once again, the variation of the wind resource was implemented by maintaining fixed the shape parameter k = 2 (Rayleigh distribution) and modifying the scale parameter (λ) and the variation of the conductor modifying the value of the resistance r_{CL}, in a range enough to cover all the types included in Table 3. Due to the effect of the PCC voltage magnitude in the losses, simulations were made for two different values widely used. The results are illustrated in Figure 13, where is shown how the actual losses for a particular infrastructure can be lower or higher than the losses at rated power, which is evidence that the latter should not be considered as a reference value in any case.

Figure 13. Sensitivity of the electric losses of the WF with the value of the resistance of the evacuation line cable and with the scale Weibull parameter representative of the period considered (Weibull shape parameter equal to 2) for two PCC voltage level. (**a**) 45 kV and (**b**) 132 kV.

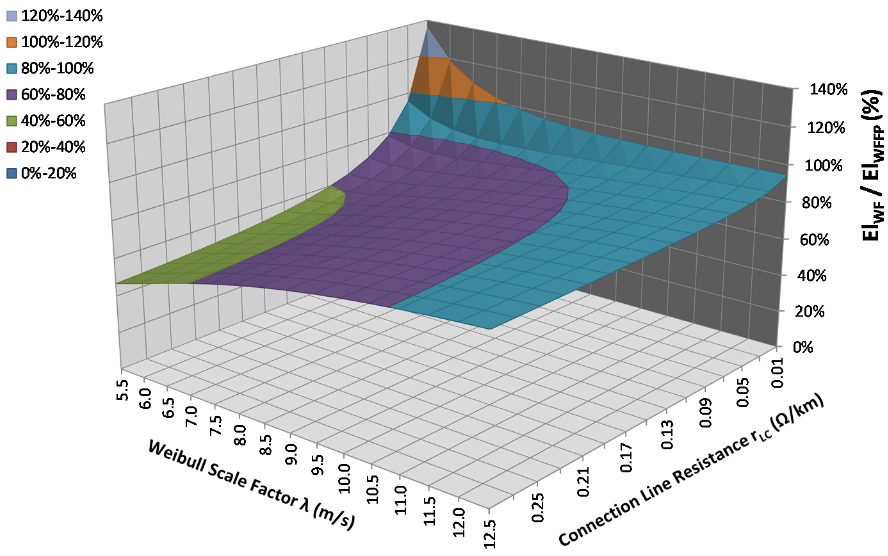

(a) 45 kV

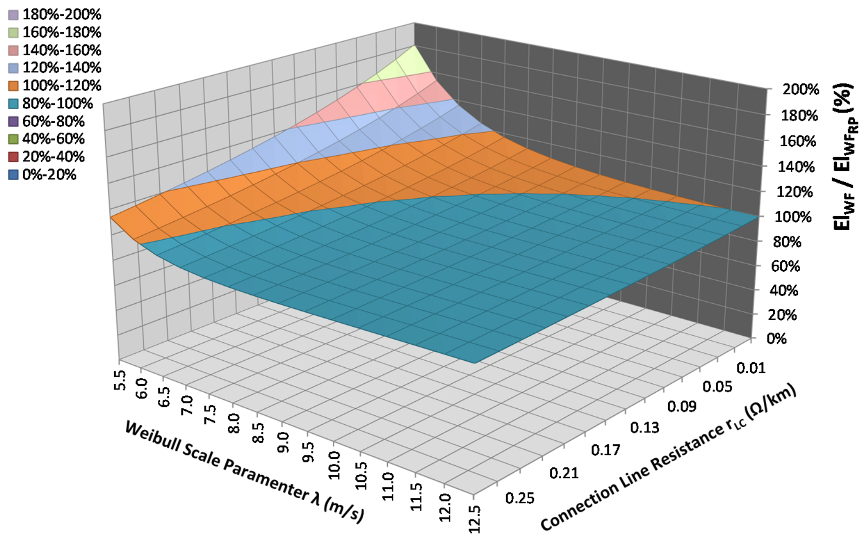

(b) 132 kV

3.3. Comparative of the Behaviour of the Electric Losses

As can be noticed in Figures 6 and 12 there is a clear difference in the behaviour of the electric losses with respect of those calculated at rated power for each one of the both cases analysed: whereas for a single WTG the losses at rated power mean a minimum, for the entire WF the losses at rated power implies a maximum for almost all the range of the Weibull parameters except for periods with low wind resource (low scale parameter).

This distinct behaviour arises mainly from the different weight of the non-load losses (not depending on the wind resource) with respect to the total. For a single WTG and a circuit of several, due to the presence of the step-up transformers, the non-load losses represent a higher ratio than in the case of the entire WF because the addition of the load losses from the evacuation line and the substation transformer.

In case of a circuit of six WTG, the behaviour is similar to a single WTG except for periods with high wind resource, in which the load losses in the collector system increases (Figure 10).

3.4. Validity of the Proposed Method

To check the validity of the proposed method, it was applied to two real wind farms sited in different locations: Spain (25.2 MW with nine wind turbines of 1.8 MW and three of 3 MW and Argentina (51 MW with wind turbines of 3 MW). The method was applied for several periods during 2013 and 2014, with different wind conditions and in which the functioning of the wind farms were not affected by any unusual conditions (*i.e.*, big corrective maintenance). In all the cases the results obtained by the application of the simplified method proposed in this paper were in a gap of ±6% of real data for the electric losses.

4. Impact of the Losses in the Financial Value of the WF

The electric losses reduce the income resulting from selling the electricity generated by the WF. These incomes are the only source to repay the financing obtained to develop and build the WF. Although the reduction is not a very important percentage with respect to the income, the recurrence during the WF service life has an impact in the net value of the WF as an investment that must be considered.

The Net Present Value (NPV) is a classical way to state how much an investment is worth. It is defined as the sum of the present values of the individual cash flows updated to the construction year at a set up discount rate, reduced by the investment costs. It is calculated according to the following Equation [52]:

$$NPV = \sum_{z=1}^{n} \frac{CF_z}{(1+r)^z} - I \tag{49}$$

Where the yearly cash flows are calculated as it is detailed in Table 5.

Table 5. Cash flow calculation methods Self-elaboration.

Cash Flow	
+	Incomes from electricity remuneration
−	Operating expenses
=	Gross operating margin (EBITDA)
−	Depreciation
=	Earnings before interests and taxes (EBIT)
−	Financial expenses
=	Earnings before taxes
−	Taxes
=	Earnings after taxes
+	Depreciation
=	Yearly cash flow (CF_z)

As can be noticed in Equation (49), the variation of the NPV is linear with respect to the incomes and subsequently to the losses. As a practical example to establish the range of this variation, the effect in the expected NPV was calculated for a WF with the characteristics detailed in Section 3.2.3., in function of the difference between the losses calculated following the method proposed in this article and the losses calculated at rated power. In the calculations were taken into account the assumptions included in the Table 6, which are all currently applicable to the WF studied.

Table 6. Assumptions for NPV calculation.

Breakdown	Name	Value	Unit	Comment
Prices	Wind Farm Construction	1,100	€/kW	Sources [13,30,53,54]
	Wind Farm O&M	20.00	€/MWh	Source [8,53]
	Land easements	3,000	€/(MW × year)	Includes assembly areas
	Insurance	0.50	% Incomes	All risk and Civil Liability. Typically calculated over incomes
	Administration	0.02	% Incomes	Typically calculated over incomes
	Yearly prices increase	2	%	Typically indexed to inflation. Estimate based on the trend in the inflation forecast [55,56]
Power purchase agreement	Initial PPA price	80.00	€/MWh	Estimated from [10]
	Yearly increase	2	%	Typically indexed to inflation. Estimate based on the trend in the inflation forecast [55,56]
Electricity generation	Gross capacity factor	30	%	–
	Wake losses	5	%	–
	Losses factor	1	%	Includes up to grid connection point
	WTG Mechanical Availability	97	%	WTG Mechanical availability is defined typically in a yearly period, as the percentage of time (year) in which the WTG is ready to roduce electricity Current market value. Source: WTG Manufacturers
Taxes	Profit taxes	30	%	–
	Income taxes	2	%	The final value depends on council and the incomes level. Mean value has been taken into consideration
Financial terms	Depreciation period	10	years	Typical

Figure 14 shows the reduction of the NPV, calculated for an estimated discount rate of 3% (value around the current inflation level in the euro zone), as a function of the ratio of the actual losses to the losses at rated power. In the example, the calculations give a reduction in the NPV around a 0.08% for every 5% of increase of the losses ratio, even reaching to a reduction close to 1.6% if the actual losses double the estimate at rated power.

With the aim to have an order of magnitude of this reduction, Figure 14 includes the loss of NPV in monetary terms for a WF with the characteristics of the Table 4. The important reduction, exceeding 2.3 M€ in case of double losses than estimated can be noticed.

Figure 14. Variation of the NPV with the energy losses.

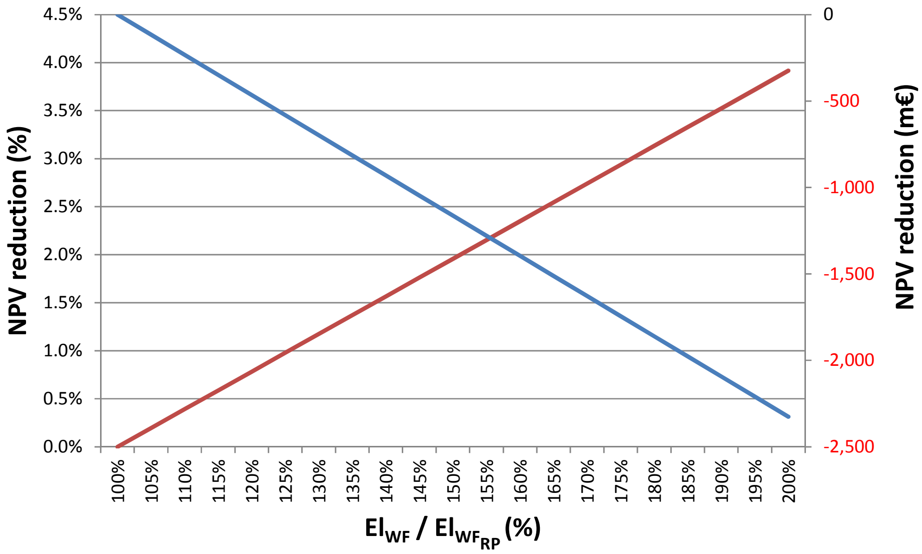

5. Conclusions

The electric losses calculated when all the WTGs in the WF operate at rated power cannot be used as a reference to define or guarantee the losses produced in the WF under actual operating conditions. Depending on the characteristics of the electrical infrastructures of the WF, as well as the real wind resource, the differences could be very important, even doubling or halving the expected value.

It is not possible to set a fixed value to define the expected losses. It is necessary to build a model of the WF, capable considering the actual wind conditions in the set period, to prove if the behaviour of the WF was according to the requirements. Besides, with this method it would be possible to detect, even in the short term, variations in the electric parameters considered in the model and it could be a complementary tool to prevent problems in the electrical infrastructure.

The method used for the analytical fit of the WTG power curve, together with the methodology for the simplified calculation of the actual electric losses established in Section 3.2.1., can be used as a simple tool to define *a priori*, in the design stage, the expected losses and to verify, considering the actual wind resource during, the correct behaviour of the WF. This methodology, with certain tolerances appropriate to the simplifications made, offers the possibility to do the verifications at any time and for any period of time.

The lack of definition produces an uncertainty, minor but perceptible, concerning the cash flows of the WF and therefore implies a relevant impact in its net value as investment.

Nomenclature

Weibull distribution	
$f(s)$	Probability density function for the wind speed Weibull distribution
λ	Scale parameter of the Weibull distribution (m/s)
k	Shape parameter of the Weibull distribution
$F(s)$	Cumulative distribution function for the wind speed Weibull distribution.
s	Wind speed (m/s)

Wind turbine and wind farm characteristics

BUS_{PCC}	Point of common coupling bus
BUS_{ST}	Bus of connection to all the collector system circuits with the evacuation line. Represents the wind farm substation.
BUS_{WTG}	Bus in which the wind turbine is connected to the collector system.
n_C	Number of electric circuits in the wind farm
n_{WF}	Number of wind turbines in the wind farm
PCC	Point of common coupling
r_C	Resistance of the interconnection cable to the collector system
r_{CL}	Resistance of the interconnection line
r_{ST}	Resistance representative of load active power losses in the substation transformer
r_T	Resistance representative of load active power losses in the internal wind turbine step-up transformer
V_{PCC}	Voltage magnitude in the point of common coupling
V_{GRID}	Voltage magnitude of the collector system
WF	Wind Farm
WTG	Wind turbine generator

Power flow analysis

b_{pij}	Parallel susceptance between buses i and j
B_{ij}	Serial susceptance between buses i and j
G_{ij}	Serial conductance between buses i and j
P_{ij}	Active power flow from bus i to bus j
Q_{ij}	Reactive power flow from bus i to bus j
V_i	Voltage magnitude in the bus i.
$\overline{Y_{ij}}$	Admittance between buses i and j.
θ_{ij}	Difference between the voltage angles in buses i and j.

Financial

NPV	Net present value
CF_z	Project cash flow in the year z
z	Ordinal indicating the number of years the PV system has been in service.
I	Investment value
r	Discount rate for NPV calculation

Wind turbine generator power curve

a, b, c	Coefficients of the polynom power curve adjust
P_{WTG}	Power output of the wind turbine
P_{WTGT}	Power output of the wind turbine minus the electric losses in the step-up transformer
P_{rated}	Rated power of the wind turbine
s_{cut-in}	Minimum wind speed at which the wind turbine will generate usable power
$s_{cut-out}$	Wind speed at which wind turbine cease power generation and shut down
s_{rated}	Minimum wind speed at which the wind turbine produces the rated power

Energy and power flow

CF	Capacity factor
Eg	Electricity generated by a wind turbine in the period T
Eg_{WF}	Electricity generated by the entire wind farm
El	Electricity losses in the period T

El_{RP}	Electricity losses when the wind turbine operates at rated power
El_{n_j}	Energy losses in the circuit n_j
$El_{n_{j}{}_{RP}}$	Energy losses in the circuit n_j when all the wind turbines in the circuit operate at rated power
El_{WF}	Energy losses for the entire wind farm
$El_{WF_{RP}}$	Energy losses for the entire wind farm when all the wind turbines operate at rated power
PG_{WF}	Active power generated
Pl	Active power losses
Pl_C	Active power losses in the collector system cable
Pl_o	Active power losses when the wind turbine is not generating power
Pl_{rated}	Active power losses when the wind turbine operates at rated power
Pl_T	Load active power losses in the internal wind turbine step-up transformer
Pl_{WF}	Active power losses for the entire wind farm
PN_{ANY}	Net active power injected in the bus indicated (any)
Po_{ST}	No-load active power losses in the substation transformer
Po_T	No-load active power losses in the internal wind turbine step-up transformer
T	Period of time for energy calculations

Appendix A: Solution for the Integral

The integral to be solved is:

$$\begin{aligned}\int_{s_1}^{s_2}\sum_{i=0}^{n} a_i s^i f(s)ds &= \int_{s_1}^{s_2}\sum_{i=0}^{n} a_i s^i \frac{k}{\lambda}\left(\frac{s}{\lambda}\right)^{k-1} e^{-\left(\frac{s}{\lambda}\right)^k} ds \\ &= \frac{k}{\lambda^k}\sum_{i=0}^{n} a_i \int_{s_1}^{s_2} s^{(k-1+i)} e^{-\left(\frac{s}{\lambda}\right)^k} ds\end{aligned} \tag{A1}$$

The incomplete gamma function γ is defined as:

$$\int_u^v x^{(\alpha-1)} e^{-x} dx = \int_0^v x^{(\alpha-1)} e^{-x} dx - \int_0^u x^{(\alpha-1)} e^{-x} dx = \gamma(\alpha, v) - \gamma(\alpha, u) \tag{A2}$$

Doing the following change of variable:

$$x = \left(\frac{s}{\lambda}\right)^k; s = \lambda x^{\frac{1}{k}};\ dx = \frac{k}{\lambda}\left(\frac{s}{\lambda}\right)^{k-1} ds = \frac{k}{\lambda}\left(x^{\frac{1}{k}}\right)^{k-1} ds = \frac{k}{\lambda} x^{\left(\frac{k-1}{k}\right)};\ ds = \frac{\lambda}{\mathrm{k}} \frac{dx}{x^{\left(\frac{k-1}{k}\right)}} \tag{A3}$$

The integral is given now by:

$$\begin{aligned}\frac{k}{\lambda^k}\sum_{i=0}^{n} a_i \int_{s_1}^{s_2} s^{(k-1+i)} e^{-\left(\frac{s}{\lambda}\right)^k} ds &= \frac{k}{\lambda^k}\sum_{i=0}^{n} a_i \int_{\left(\frac{s_1}{\lambda}\right)^k}^{\left(\frac{s_2}{\lambda}\right)^k} \left(\lambda x^{\frac{1}{k}}\right)^{(k-1+i)} e^{-x} \frac{\lambda}{k} \frac{dx}{x^{\left(\frac{k-1}{k}\right)}} \\ &= \sum_{i=0}^{n} a_i \lambda^i \int_{\left(\frac{s_1}{\lambda}\right)^k}^{\left(\frac{s_2}{\lambda}\right)^k} x^{\frac{i}{k}} e^{-x} dx\end{aligned} \tag{A4}$$

Identifying the parameter α of the incomplete gamma function:

$$\alpha - 1 = \frac{i}{k}; \alpha = \frac{i}{k} + 1 \tag{A5}$$

Finally, the solution of the integral is:

$$\int_{s_1}^{s_2} \sum_{i=0}^{n} a_i\, s^i\, f(s) ds = \sum_{i=0}^{n} a_i\, \lambda^i \left\{ \gamma\left[\left(\frac{i}{k}+1\right), \left(\frac{s_2}{\lambda}\right)^k\right] - \gamma\left[\left(\frac{i}{k}+1\right), \left(\frac{s_1}{\lambda}\right)^k\right] \right\} \tag{A6}$$

Author Contributions

All the authors equally contributed during the writing and the critical revision of the paper, according to the reviewers' comments.

Conflicts of Interest

The authors declare no conflict of interest.

References

1. Díaz-Dorado, E.; Carrillo, C.; Cidrás, J.; Albo, E. Estimation of Energy Losses in a Wind Park. In Proceedings of the 9th International Conference Electrical Power Quality and Utilisation, Barcelona, Spain, 9–11 October 2007.
2. González, J.S.; Gonzalez Rodriguez, A.G.; Mora, J.C.; Santos, J.R.; Payan, M.B. Optimization of wind farm turbines layout using an evolutive algorithm. *Renew. Energy* **2010**, *35*, 1671–1681.
3. Inaba, N.; Takahashi, R.; Tamura, J.; Kimura, M.; Komura, A.; Takeda, K. A Consideration on Loss Characteristics and Annual Capacity Factor of Offshore Wind Farm. In Proceedings of the 2012 XXth International Conference on Electrical Machines (ICEM), Marseille, France, 2–5 September 2012; IEEE: New York, NY, USA, 2012; pp. 2022–2027.
4. Takahashi, R.; Ichita, H.; Tamura, J.; Kimura, M.; Ichinose, M.; Futami, M.; Ide, K. Efficiency Calculation of Wind Turbine Generation System with Doubly-Fed Induction Generator. In Proceedings of the 2012 XXth International Conference on Electrical Machines (ICEM), Rome, Italy, 6–8 September 2010; IEEE: New York, NY, USA, 2010; pp. 1–4.
5. Camm, E.H.; Behnke, M.R.; Bolado, O.; Bollen, M.; Bradt, M.; Brooks, C.; Dilling, W.; Edds, M.; Hejdak, W.J.; Houseman, D.; *et al.* Wind Power Plant Collector System Design Considerations: IEEE PES Wind Plant Collector System Design Working Group. In Proceedings of the 2009. PES '09. IEEE Power & Energy Society General Meeting, Calgary, AB, Canada, 26–30 July 2009; IEEE: New York, NY, USA, 2010; pp. 1–7.
6. Camm, E.H.; Behnke, M.R.; Bolado, O.; Bollen, M.; Bradt, M.; Brooks, C.; Dilling, W.; Edds, M.; Hejdak, W.J.; Houseman, D.; *et al.* Wind Power Plant Substation and Collector System Redundancy, Reliability, and Economics. In Proceedings of the 2009. PES '09. IEEE Power & Energy Society General Meeting ; Power & Energy Society General Meeting, Calgary, AB, Canada, 26–30 July 2009; IEEE: New York, NY, USA, 2010; pp. 1–6.
7. Steimer, P.K.; Apeldoorn, O. Medium voltage power conversion technology for efficient windpark power collection grids. In Proceedings of the 2010 2nd IEEE International Symposium on Power Electronics for Distributed Generation Systems (PEDG), Hefei, China, 16–18 June 2010; IEEE: New York, NY, USA, 2010; pp. 12–18.
8. Blanco, M.I. The economics of wind energy. *Renew. Sustain. Energy Rev.* **2009**, *13*, 1372–1382.

9. The European Wind Energy Association. Wind in Power 2013. Available online: http://www.ewea.org/fileadmin/files/library/publications/statistics/EWEA_Annual_Statistics_2013.pdf (accessed on 21 September 2014).
10. Asociación Empresarial Eólica. *Eólica 2014*; Asociación Empresarial Eólica: Madrid, Spain, 2014. (In Spanish)
11. U.S. Department of Energy. *Wind Technologies Market Report 2012*; U.S. Department of Energy: Oak Ridge, TN, USA, 2013.
12. Kalamova, M.; Kaminker, C.; Johnstone, N. *Source of Finance, Investment Policies and Plant Entry in the Renewable Energy Sector*; OECD Publishing: Paris, France, 2011.
13. U.S. Department of Energy. *Wind Technologies Market Report 2012*; Lawrence Berkeley National Laboratory: Berkeley, CA, USA, 2013.
14. Department of Energy Republic of South Africa Renewable Energy. Independent Power Producer Procurement Programme. Available online: http://www.ipprenewables.co.za/ (accessed on 25 June 2014).
15. McGovern, M. Analysis—Uruguay, the next big South American market. In *Wind Power Monthly*; Haymarket Media Group Ltd.: London, UK, 2013.
16. Carrillo, C.; Cidrás, J.; Díaz-Dorado, E.; Obando-Montaño, A.F. An Approach to Determine the Weibull Parameters for Wind Energy Analysis: The Case of Galicia (Spain). *Energies* **2014**, *7*, 2676–2700.
17. Villanueva, D.; Feijó, A.; Pazos, J.L. Multivariate Weibull distribution for wind speed and wind power behavior assessment. *Resources* **2013**, *2*, 370–384.
18. Amenedo Rodríguez, J.L.; Burgos Díaz, J.C.; Arnalte Gómez, S. *Sistemas Eólicos de Producción de Energía Eléctrica*; Rueda: Madrid, Spain, 2003; p. 439. (In Spanish)
19. Carta González, J.A.; Calero Pérez, R.; Colmenar Santos, A.; Castro Gil, M.-A. *Centrales de Energías Renovables: Generación Eléctrica con Energías Renovables*; Pearson Educación, S.A.: Madrid, Spain, 2009; p. 703. (In Spanish)
20. Margaris, I.D.; Hansen, A.D.; Sorensen, P.; Hatziargyriou, N.D. Illustration of modern wind turbine ancillary services. *Energies* **2010**, *3*, 1290–1302.
21. Gómez Expósito, A.; Abur, A.; Alvarado, F.L.; Alvarez Bel, C.; Pérez Arriaga, J.I.; Rivier Abad, M. Flujo de cargas. In *Análisis y Operación de Sistemas de Energía Eléctrica*; McGraw-Hill Interamericana de España: Madrid, Spain, 2002; p. 769. (In Spanish)
22. Carrillo, C.; Obando Montaño, A.F.; Cidrás, J.; Diaz-Dorado, E. Review of power curve modelling for wind turbines. *Renew. Sustain. Energy Rev.* **2013**, *21*, 572–581.
23. Kusiak, A.; Zheng, H.; Song, Z. On-line monitoring of power curves. *Renew. Energy* **2009**, *34*, 1487–1493.
24. Lydia, M.; Kumar, S.S.; Selvakumar, A.I.; Prem Kumar, G.E. A comprehensive review on wind turbine power curve modeling techniques. *Renew. Sustain. Energy Rev.* **2014**, *30*, 452–460.
25. Vestas Vestas. Available online: http://www.vestas.com (accessed on 25 May 2014).
26. Siemens Wind Power. Available online: http://www.energy.siemens.com/hq/en/renewable-energy/wind-power/ (accessed on 2 June 2014).
27. Alstom Wind Power. Available online: http://www.alstom.com/power/renewables/wind/ (accessed on 25 June 2014).

28. Gamesa Corporation Gamesa. Available online: http://www.gamesacorp.com/en/ (accessed on 25 June 2014).
29. Prysmian Group. *Medium Voltage Cables Catalogue*; Prysmian Group: Milan, Italy, 2013.
30. Serrano González, J.; Burgos Payán, M.; Santos, J.M.R.; González-Longatt, F. A review and recent developments in the optimal wind-turbine micro-siting problem. *Renew. Sustain. Energy Rev.* **2014**, *30*, 133–144.
31. Shamsoddin, S.; Porté-Agel, F. Large eddy simulation of vertical axis wind turbine wakes. *Energies* **2014**, *7*, 890–912.
32. Son, E.; Lee, S.; Hwang, B.; Lee, S. Characteristics of turbine spacing in a wind farm using an optimal design process. *Renew. Energy* **2014**, *65*, 245–249.
33. Turner, S.D.O.; Romero, D.A.; Zhang, P.Y.; Amon, C.H.; Chan, T.C.Y. A new mathematical programming approach to optimize wind farm layouts. *Renew. Energy* **2014**, *63*, 674–680.
34. González-Longatt, F.; Wall, P.; Terzija, V. Wake effect in wind farm performance: Steady-state and dynamic behavior. *Renew. Energy* **2012**, *39*, 329–338.
35. Hasager, C.B.; Rasmussen, L.; Peña, A.; Jensen, L.E.; Réthoré, P.-E. Wind farm wake: the horns rev photo case. *Energies* **2013**, *6*, 696–716.
36. Porté-Agel, F.; Wu, Y.-T.; Chen, C.-H. A numerical study of the effects of wind direction on turbine wakes and power losses in a large wind farm. *Energies* **2013**, *6*, 5297–5313.
37. ABB Super-slim Switchgear for Wind Turbines. Available online: http://www.abb.com/cawp/seitp202/6bca779c32011d61c125770b003f7ee0.aspx (accessed on 25 June 2014).
38. Ormazabal Gas-insulated switchgear for secondary distribution systems. Available online: http://www.ormazabal.com/es/tu-negocio/productos/cgm3–36-kv-iec-630–21-ka?refer=1300 (accessed on 20 June 2014).
39. Siemens Gas-insulated Switchgear for Secondary Distribution Systems. Available online: http://w3.siemens.com/powerdistribution/global/EN/mv/medium-voltage-switchgear/gis-secondary-distribution-systems/Pages/gas-insulated-switchgear-for-secondary-distribution-systems.aspx (accessed on 28 May 2014).
40. International Electrotechnical Commission. *Wind Turbines. Part 1: Design Requirements*; International Electrotechnical Commissio: Geneva, Switzerland, 2005; Volume IEC 61400-1.
41. Mathworks. *Matlab*, R2012a; Mathworks: Natick, MA, USA.
42. Dutta, S.; Overbye, T.J. A Clustering Based Wind Farm Collector System Cable Layout Design. In Proceedings of the Power and Energy Conference, Urbana, IL, USA, 25–26 February 2011; IEEE: New York, NY, USA, 2011; pp. 1–6.
43. Feltes, J.W.; Fernandes, B.S.; Keung, P.K. Case Studies of Wind Park Modeling. In Proceedings of the Power and Energy Society General Meeting, Detroit, MI, USA, 24–29 July 2011; pp. 1–7.
44. International Electrotechnical Commission. *Round Wire Concentric Lay Overhead Electrical Stranded Conductors*; International Electrotechnical Commissio: Geneve, 1991; Volume IEC 614089.
45. General Electric Industrial Transformers—Power. Available online: http://www.geindustrial.com/products/transformers/power-0 (accessed on 25 June 2014).
46. Siemens Power Transformers. Available online: http://www.energy.siemens.com/hq/en/power-transmission/transformers/power-transformers/medium-power-transformers.htm (accessed on 25 June 2014).

47. General Cable Technologies Corporation General Cable Cables. Available online: http://es.generalcable.com/dgeneralcable/GeneralCable/ (accessed on 25 June 2014).
48. Southwire Southwire Product Catalogue. Available online: http://www.southwire.com/products/ProductCatalog.htm (accessed on 30 May 2014).
49. Spanish Association for Standardisation and Certification. *Conductores Para Líneas Eléctricas. Conductores de Alambres Redondos Cableados en Capas Concéntricas*; AENOR: Madrid, Spain, 2002; Volume UNE-EN 50182.
50. International Electrotechnical Commission. *Power Transformers. Part 5: Ability to Withstand Short Circuit*; International Electrotechnical Commissio: Geneve, Spain, 2000; Volume IEC 60076–5.
51. IEEE Transformers Committee, Performance Characteristics Subcommittee. x/r Discussion. In 2003. Available online: http://grouper.ieee.org/groups/transformers/subcommittees/performance/WG_C57_12_00/XoverRdiscussion.pdf (accessed on 25 June 2014).
52. Pérez Gorostegui, E. *Introducción a la Economía de la Empresa*; Editorial Centro de Estudios Ramón Areces: Madrid, Spain, 2007. (In Spanish)
53. International Renewable Energy Agency. *Renewable Energy Technologies: Cost Analysis Series. Volume 1: Power Sector. Issue 5/5. Wind Power*; International Renewable Energy Agency (IRENA): Abu Dhabi, United Arab Emirates, 2012.
54. IDAE Ministerio de Industria Turismo y Comercio. *Plan de Energías Renovables 2011–2020*; Gobierno de España: Madrid, Spain, 2011. (In Spanish)
55. European Commission Economic Financial Affairs Economic Forecasts. Available online: http://ec.europa.eu/economy_finance/eu/forecasts/index_en.htm (accessed on 25 June 2014).
56. PWC Economic Projections. Available online: http://www.pwc.com/gx/en/issues/economy/global-economy-watch/projections/june-2014.jhtml (accessed on 15 June 2014).

ANEXO XI: "*EVALUATION OF SUPPLY–DEMAND ADAPTATION OF PHOTOVOLTAIC–WIND HYBRID PLANTS INTEGRATED INTO AN URBAN ENVIRONMENT*". COPIA DE LA PUBLICACIÓN.

energies

MDPI

Article

Evaluation of Supply–Demand Adaptation of Photovoltaic–Wind Hybrid Plants Integrated into an Urban Environment

Africa Lopez-Rey *, Severo Campinez-Romero, Rosario Gil-Ortego and Antonio Colmenar-Santos

Department of Electric, Electronic and Control Engineering, UNED, Juan del Rosal, 12-Ciudad Universitaria, 28040 Madrid, Spain; scampinez1@alumno.uned.es (S.C.-R.); rgil@ieec.uned.es (R.G.-O.); acolmenar@ieec.uned.es (A.C.-S.)

* Correspondence: alopez@ieec.uned.es; Tel.: +34-913-987-798

Received: 8 April 2019; Accepted: 6 May 2019; Published: 10 May 2019

check for updates

Abstract: A massive integration of renewable energy sources is imperative to comply with the greenhouse emissions reduction targets fixed to achieve the limitation of global warming. Nevertheless, the present integration levels are still far from the targets. The main reason being the technical barriers arising from their non-manageable features. Photovoltaic and wind sources are the widest spread, as their maturity allows generation with a high-efficiency degree. A deep understanding of facilities' performance and how they can match the energy demand is mandatory to reduce costs and extend the technical limits and facilitate their penetration. In this paper, we present a novel methodology to evaluate how photovoltaic–wind hybrid facilities, placed in an urban environment can give generation patterns which will be able to match the demand profiles better than facilities installed individually. This methodology has been applied to a broad number of locations spread over the whole planet. The results show that with high homogeneity in terms of site weather characteristics, the hybrid facilities improve the matching up to 15% over photovoltaic plants and up to 35% over wind.

Keywords: wind energy; photovoltaic; complementarity; grid integration

1. Introduction

On 12 December 2015, the 195 countries participating in 21st Conference of the Parties (Paris Climate Change Conference) [1], organised by the United Nations Framework Convention on Climate Change (UNFCCC) [2], signed the Paris Agreement [3]. This agreement aims to achieve, as soon as possible, a reduction on the carbon emissions to hold the increase in the global average temperature to well below 2 °C above pre-industrial levels. The generation and use of energy are the main contributors to climate change, with 60% of the total greenhouse gases (GHG) emissions. The reduction in energy sector emissions is mandatory to achieve the global warming objectives. Hence, the Paris Agreement determines by 2030 there will be a substantial increase in the use of renewable energy sources (RES) in the world energy mix.

This important agreement is one more step given in the fight against climate change, which has been developed by the international community in the last decades. For this purpose, governments and international organisations and institutions have designed scenarios, strategies and commitments focused on the mitigation and reduction of the present emission levels. In all of them, high RES penetration shares are mandatory, and, with this aim, ambitious plans have been determined.

Along these lines, the United States of America developed the SunShot Initiative [4], focused on the solar photovoltaic renewable source (PV), favouring its integration by means of being competitive with the traditional generation forms before 2020, and the Wind Program [5], designed to speed up the development and integration of wind energy. Likewise, the member countries of the European Union established the Roadmap 2050 [6] to set up the paths to achieve the European commitment to reach in 2050 GHG emissions below 80% of 1990 levels.

Nowadays, the RES technologies with higher integration level are wind and photovoltaic. Figure 1 shows the time evolution of wind and PV installed power worldwide. At the end of 2017, the installed power capacity was 384 GW in PV facilities and 494 GW in wind farms.

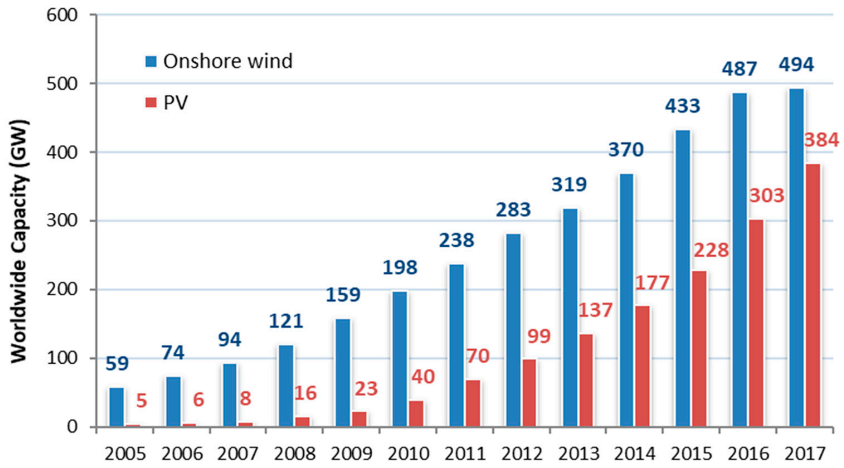

Figure 1. Wind and photovoltaic (PV) installed power worldwide. Source: [7,8].

Wind and PV electricity generation technologies presently offer technical and economic maturity levels. They allow high-efficiency generation almost everywhere at such a low cost compared with the traditional generation based on conventional thermal methods [9–15]. Moreover, among the renewable energy sources, wind and PV electricity generation technologies present high degrees of sustainability under multi-criteria analysis [16–18].

The International Energy Agency (IEA) remarks in its Energy Technology Perspectives 2017 (ETP2017) [19] that, the implementation of PV and onshore wind technologies are on-track to achieve their integration targets. Nevertheless, penetration shares for these technologies are still far from the targets fixed to contribute to the mitigation of GHG emissions. According to the IEA hi-Ren scenario (the high-renewables scenario—hi-Ren scenario—sees energy systems radically transformed to achieve the goal of limiting the global mean temperature increase to 2 °C target with a large share of renewables, which requires fast and strong deployment of photovoltaic and wind power and solar thermal electricity), the installed worldwide power capacity should reach 4674 GW by 2050 for PV and 2700 GW for onshore wind in the same period [20,21]. Innovative technical solutions and regulatory measurements are required to boost a massive RES integration to close the huge gap between the present status and the fixed targets in the next coming years.

The achievement of RES penetration targets is only feasible with actions addressed to facilitate their use in three fields with massive energy consumption: transport, buildings and industry. Among them, building integration shows the biggest potential to increase the share of RES in the energetic mix [22,23].

The widest field for RES building integration is found in the urban environment. Considerable research has been carried out to determine the PV [24–32] and wind potential [33–36] in urban areas and buildings.

PV presents a characteristic that favours its massive penetration in the urban environment: the dispersion degree. Solar radiation is received everywhere with such intensity levels that make possible the production of electricity. In addition, PV building integration offers environmental advantages as against its implementation on rural lands as the former gives a new value to the building roofs and facades.

In regard of wind energy, the installation of wind turbines in urban areas is not widely spread yet, but there are technical solutions to efficiently take advantage of the urban wind stream with its special characteristics of turbulence and direction variability [33,37–41].

In relation to PV–wind hybrid plants (PV+W hybrid hereinafter), extensive research has been developed to quantify the synergies between solar and wind sources. A non-exhaustive list of references is shown in Table 1.

Table 1. Literature review reference list.

Topic	Reference
Smoothing resource and the correlation between the wind and solar PV resource	[42]
Variability and determination of regional or local wind solar complementarity or synergy	[43–47]
Determination of flexibility requirements of large-scale wind and PV penetration	[48]
Impact of wind solar complementarities on storage sizing and use	[49]
Effect of solar and wind resources complementarity in micro-hybrid system reliability	[50]

Cities are big electricity consumers. Therefore, RES integration in urban areas would also offer an important technical advantage because the generation would be placed near to the consumption point. This solution would improve the whole electric system efficiency by reducing the transport and distribution of electricity losses. Moreover, it is a clear example of distributed generation with advantages associated with the control and management of the electric network [51–53].

But the integration of a massive share of variable RES (VRES) in the electric power grid implies technical challenges and extra-costs. The electricity generated in PV and wind facilities have a non-manageable character; which means that it is not possible to control the supply instantaneously (except to reduce it) to match the demand. A high VRES penetration requires the application of measures focused on planning, operation and flexibility of the whole system to respond to the uncertainty and variability in the supply–demand balance in short timescales [54–56]. These measures present estimable costs for the system that could reach 25–35 €/MWh in high penetration scenarios [57,58].

Extensive research has been recently carried out showing that, with the use of adequate coordination control algorithms, large-scale systems made up of multiple individual subsystems can together contribute efficiently in the achievement of global quantities of interest, even in the case that some of the sub-systems became adversarial or non-cooperative due to bad functioning [59]. This resilient performance is fully applicable to a massive integration of VRES based on the implementation of individual small facilities.

Due to the aforementioned, a deep knowledge of the performance of the facilities and their generation patterns becomes relevant. It is essential to understand how they could match the electricity demand, with the aim to offer better control and management of the electricity fed into the grid and, consequently, collaborate to reduce the technical barriers and to decrease the integration cost.

With this target as the main objective of our work, we have carried out a study under the novel perspective to evaluate the supply–demand balance adaptation of PV+W hybrid plants integrated into an urban environment. To have results applicable on a global scale, we have considered hundreds of locations spread all over the world and multiple load profiles for the characterisation of demand. This article first analyses if PV+W hybrid facilities present generation patterns that adapt better to the demand profiles than if the facilities were installed individually, and second, determines a novel methodology to quantify the adaptation degree.

The novelty of our work is fundamentally based on three main grounds:

- The evaluation of supply–demand balance adaptation of PV+W hybrid plants
- The hybrid plants are integrated into an urban environment
- The results are applicable on a global scale as we have considered real weather data from hundreds of locations spread all over the world and multiple profiles for the characterisation of the demand.

The main technical challenge arises from our requirement to obtain results applicable on a global scale. With that aim, we have considered only real weather data from hundreds of meteorological stations and multiple electricity load profiles for the characterisation of the demand in different seasons and days. These requirements have obliged the authors to carry out extensive work to obtain and validate the input data and get it homogeneous.

Below in Section 2, we introduce the methodology developed to evaluate and quantify the level of adaptation of generation patterns to demand profiles. In Section 3, we present the results of applying this methodology to a wide number of locations worldwide and carry out a sensitivity analysis of the results. Finally, in Section 4, the conclusions of our study are discussed.

2. Methodology

Our work aims to analyse if the generation patterns of PV+W hybrid facilities match better with the demand profiles than if the facilities were considered separately. We will not determine what would be the absolute coverage of electricity that the facilities could provide to the whole electric demand. This approach is like evaluating to what extent the generation and demand curves have the same "shape".

We propose the evaluation of the adaptation level by the determination of the matching factor (ε). It will be calculated as the average quadratic error between the electric generation patterns and the demand profiles, previously normalised and particularised for every single location under study, as will be detailed below. In this way, ε would be zero when the adjustment is perfect; it means, when the generation and demand curves have the same shape, and ε would rise to one when the difference becomes higher. The proposed methodology to calculate ε is illustrated in Figure 2.

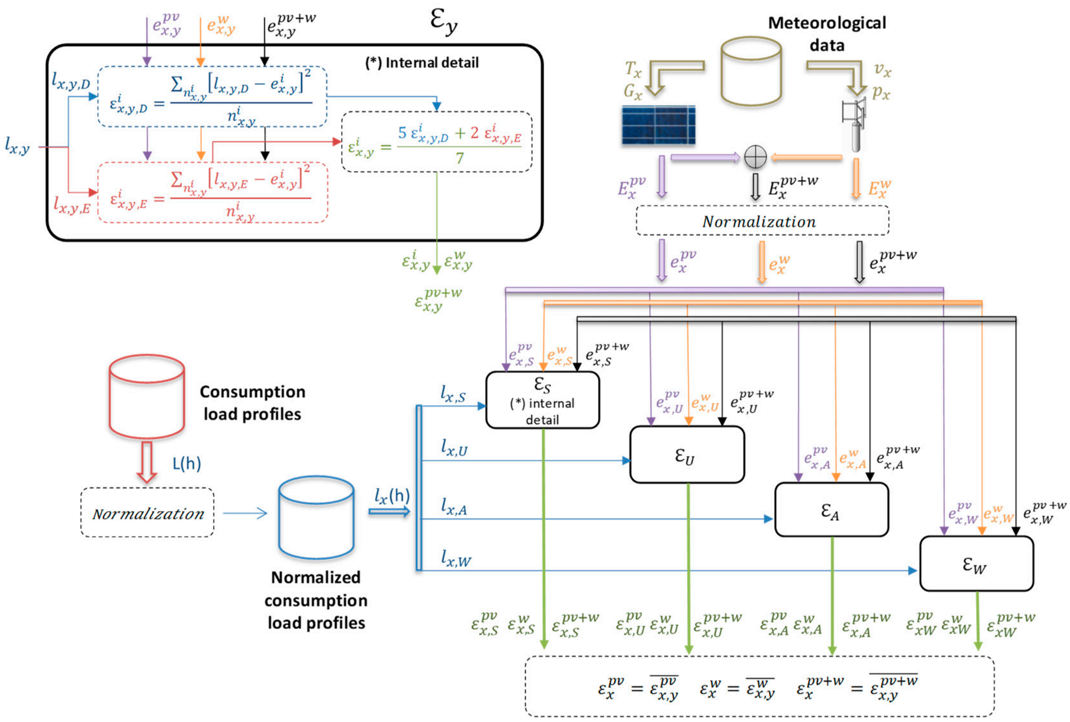

Figure 2. Methodology for obtaining the matching factor (ε) at a single location.

The calculation starts with the collection of hourly climate data representative of an average year in every single location included in the analysis. The data collected have been pressure p, temperature T, wind speed v and irradiation G. To generalise the results, it is essential to count on climatologic data for multiple locations spread around the Earth. With this data, together with the dimensioning and characterisation of a PV+W hybrid facility, we obtain yearly patterns of the foreseen generation for every type of facility E_x^{pv}, E_x^{p} y E_x^{pv+w}.

Second, electricity demand profiles are required. To select the appropriate load profiles to be utilised in the calculation of the matching factor, it is required to quantify to what extent the hybrid facilities' generation would contribute to the country-level aggregated load. With this aim, first we have done a rough estimation of the amount of electricity that could be generated by hybrid facilities placed in an urban environment (buildings) in a scenario of high penetration, and, second, we have calculated the aggregated demand coverage on hourly basis. The hourly aggregated demand coverage was calculated by using Equation (1):

$$Hourly\ aggregated\ demand\ coverage = \frac{NB \times AB \times CF \times AHIC}{RHAD} \quad (1)$$

where:

- *NB* is the number of buildings in the relevant country or region
- *AB* is the share of available buildings in the relevant country or region, defined as those buildings where the installation of a PV+W hybrid facility would be feasible.
- *CF* is the capacity factor of the PV+W hybrid facility, defined for one specific period as the electricity generated by the hybrid facility in one hour divided into its installed capacity.
- *AHIC* is an average PV+W hybrid installed capacity.
- *RHAD* is the hourly aggregated demand representative for the country or area under analysis.

To have an estimate in different scenarios, the calculation of the hourly aggregated demand coverage was done for two regions (Europe and the United States) and a European country (Spain) Table 2 shows the specifics of each region or country considered in the calculations.

Table 2. Region and country specifics for hourly aggregated demand coverage calculation.

Variable	Spain (SP)	Europe EU28 Countries (EU)	US
NB	10,000,000 [60,61]	130,000,000 [62]	142,500,000 [63,64]
CF		50%	
RHAD (MWh)	30,000 [65]	400,000 [66,67]	430,000 [68]

Table 3 shows the hourly aggregate demand coverage of the hybrid facilities for different values of (i) *AHIC* and (ii) *AB*. To obtain conservative values, it was set up 50% of *CF* and limits of 15% for *AB* and 10 kW for the *AHIC*. The results show that shares around 10% of hourly aggregated demand coverage could be reached with moderated values of *AB* and *AHIC*. The hourly coverage might reach levels over 20% in more optimistic scenarios.

Table 3. Hourly aggregated demand coverage.

		AHIC (kW)											
		2			5			7.5			10		
Country/Region		**SP**	**EU**	**US**	**SP**	**EU**	**US**	**SP**	**EU**	**US**	**SP**	**EU**	**US**
AB (% share out of total)	**5.0%**	1.7%	1.6%	1.7%	4.2%	4.1%	4.1%	6.3%	6.1%	6.2%	8.3%	8.1%	8.3%
	7.5%	2.5%	2.4%	2.5%	6.3%	6.1%	6.2%	9.4%	9.1%	9.3%	12.5%	12.2%	12.4%
	10.0%	3.3%	3.3%	3.3%	8.3%	8.1%	8.3%	12.5%	12.2%	12.4%	16.7%	16.3%	16.6%
	12.5%	4.2%	4.1%	4.1%	10.4%	10.2%	10.4%	15.6%	15.2%	15.5%	20.8%	20.3%	20.7%
	15.0%	5.0%	4.9%	5.0%	12.5%	12.2%	12.4%	18.8%	18.3%	18.6%	25.0%	24.4%	24.9%

The level of coverage obtained should be considered in the management of ancillary services and market operations. Based on the above, aggregated load profiles have been selected in the calculation of the matching factor.

The demand evolution presents a high dependency on the climate, the distribution of the working days and the consumer´s habits. One of the objectives of this study is to obtain results applicable globally. Hence, we have utilised multiple profiles to characterise the electricity consumption everywhere. The methodology here proposed includes the determination of 16 different hourly demand curve profiles, as shown in Table 4, distinguishing between (i) the Northern or Southern hemisphere, (ii) the year season and (iii) weekdays and weekends (bank holidays are included in the weekend day category). Based on the above, the demand profiles used in the calculation for every location will be the eight corresponding to the hemisphere where the location is placed.

Table 4. Hourly demand profiles.

Hemisphere	**Day**	**Season**			
		Spring (S)	**Summer (U)**	**Autumn (A)**	**Winter (W)**
Northern (N)	Weekday (D)	L_{NSD}	L_{NUD}	L_{NAD}	L_{NWD}
	Weekend (E)	L_{NSE}	L_{NUE}	L_{NAE}	L_{NWE}
Southern (S)	Weekday (D)	L_{SSD}	L_{SUD}	L_{SAD}	L_{SWD}
	Weekend (E)	L_{SSE}	L_{SUE}	L_{SAE}	L_{SWE}

As has been discussed before, our methodology is applied to quantify the adaptation degree of the generation to the aggregate demand (i.e., for a country) and not only to local demand where the facility is placed (household, garage, shopping centre, etc.). However, the absolute generation level of every facility, even the aggregation of a high number of them cannot be compared to the global, regional or national demand. We are, therefore, obliged to include in the methodology a mechanism to eliminate the scale effect from ε calculation. The way we propose here is to determine normalised patterns for both generation and demand profiles as follows:

1. Both demand profiles and generation patterns are considered on an hourly basis.
2. The normalisation period for generation and demand is daily.
3. The normalised demand profiles are obtained by dividing each hourly data into the respective daily maximum.
4. The individual normalised PV and wind daily generation profiles are obtained by dividing each hourly data into the respective daily maximum.
5. Three normalised generation profiles for the hybrid facility are obtained as per the following methods:

- Method 1: By adding the individual PV and W (wind) normalised profiles:

$$e_x^{pv+w} = e_x^{pv} + e_x^{w} \quad (2)$$

- Method 2: By dividing every hourly data into the maximum value of both facilities.

$$e_x^{pv+w} = \frac{E_x^{pv+w}}{max\left(E_x^{pv}, E_x^{w}\right)} \quad (3)$$

- Method 3: By dividing every hourly data into the daily maximum value of the hybrid facility.

$$e_x^{pv+w} = \frac{E_x^{pv+w}}{max\left(E_x^{pv+w}\right)} \quad (4)$$

These three methods to normalise the values of the hourly hybrid generation profiles do not pretend to have a physical sense by themselves. Our methodology is oriented to find out how the matching factor ε changes when the PV and wind facilities are considered together in a hybrid plant. With this aim, what is relevant to quantify this change is to evaluate it by using the results obtained with the same normalisation method.

Figure 3 shows, as an example, the normalised curves for one day in the period under analysis, where it can be seen:

- The normalised demand hourly profiles for a weekday $l_{x,y,D}$ and for a weekend day $l_{x,y,E}$.
- The normalised generation hourly patterns for the PV facility e_x^{pv} and the wind one e_x^{w}.
- Three hourly generation patterns of the hybrid facility e_x^{pv+w}, each one normalised according to the corresponding method.

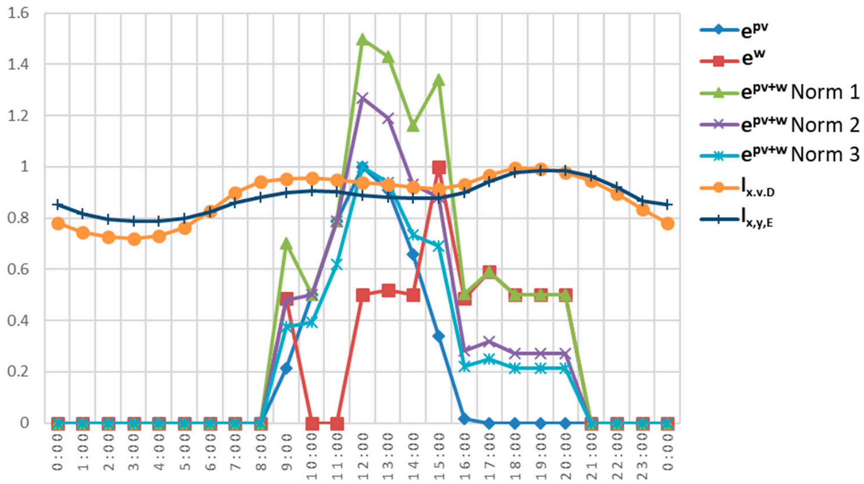

Figure 3. One-day-example of the normalised generation and load profile evolution.

Once the normalised hourly patterns are determined, ε is calculated for every single location by following the next steps:

1. The relevant eight normalised demand profiles are selected according to the site location in the Northern or the Southern hemisphere (Table 4).
2. For every annual season, ε is calculated for weekdays (5) and for weekend days (6). The weighted average value is calculated using (7):

$$\varepsilon^i_{x,y,D} = \frac{\sum_{n^i_{x,y}} \left[l_{x,y,D} - e^i_{x,y} \right]^2}{n^i_{x,y}} \tag{5}$$

$$\varepsilon^i_{x,y,E} = \frac{\sum_{n^i_{x,y}} \left[l_{x,y,E} - e^i_{x,y} \right]^2}{n^i_{x,y}} \tag{6}$$

$$\varepsilon^i_{x,y} = \frac{5\ \varepsilon^i_{x,y,D} + 2\ \varepsilon^i_{x,y,E}}{7} \tag{7}$$

where:

- $\varepsilon^i_{x,y,D}$ and $\varepsilon^i_{x,y,E}$ are the matching factors in weekdays D and weekend days E, respectively, for the facility type i, placed at the location x, during the season y.
- $n^i_{x,y}$ is the number of hours in the season y at the location x.

- $l_{x,y,D}$ and $l_{x,y,E}$ are the normalised demand profiles in weekdays D and weekend days E, respectively, at the hemisphere where is placed the location x, during the season y.
- $e^i_{x,y}$ is the generation pattern for the facility type i, placed at the location x, during the season y.
- $\varepsilon^i_{x,y}$ is the matching factor of the generation facility type i, placed at the location x, during the season y.

3. Finally, the yearly matching factor for each type of facility and location is obtained by averaging the factors calculated for every season as per (8):

$$\varepsilon^i_x = \overline{\varepsilon^i_{xy}} = \frac{\varepsilon^i_{x.S} + \varepsilon^i_{x,U} + \varepsilon^i_{x,A} + \varepsilon^i_{x,W}}{4} \quad (8)$$

2.1. Climatic Data

The climate raw data used in this article has been obtained from the Meteonorm database [69]. This commercial software provides, for an average climatic year, among other variables: hourly data of pressure, temperature, superficial wind speed and solar irradiation incident on an optimally tilted solar panel.

Meteonorm provides weather data everywhere on the planet by means of the interpolation of registered variables in specific points. However, we have only used those locations where the meteorological stations are placed and are logging the climatic variables directly. With this criterion, 844 locations spread over the whole planet were selected.

With the objective to generalise the results of the application of the methodology, the selected locations have been classified following the Köppen–Geiger climatic regions, which divides the Earth into regions according to their weather conditions [70,71]. Figure 4 shows the location of the meteorological stations used in this study and their correspondence with the Köppen–Geiger regions.

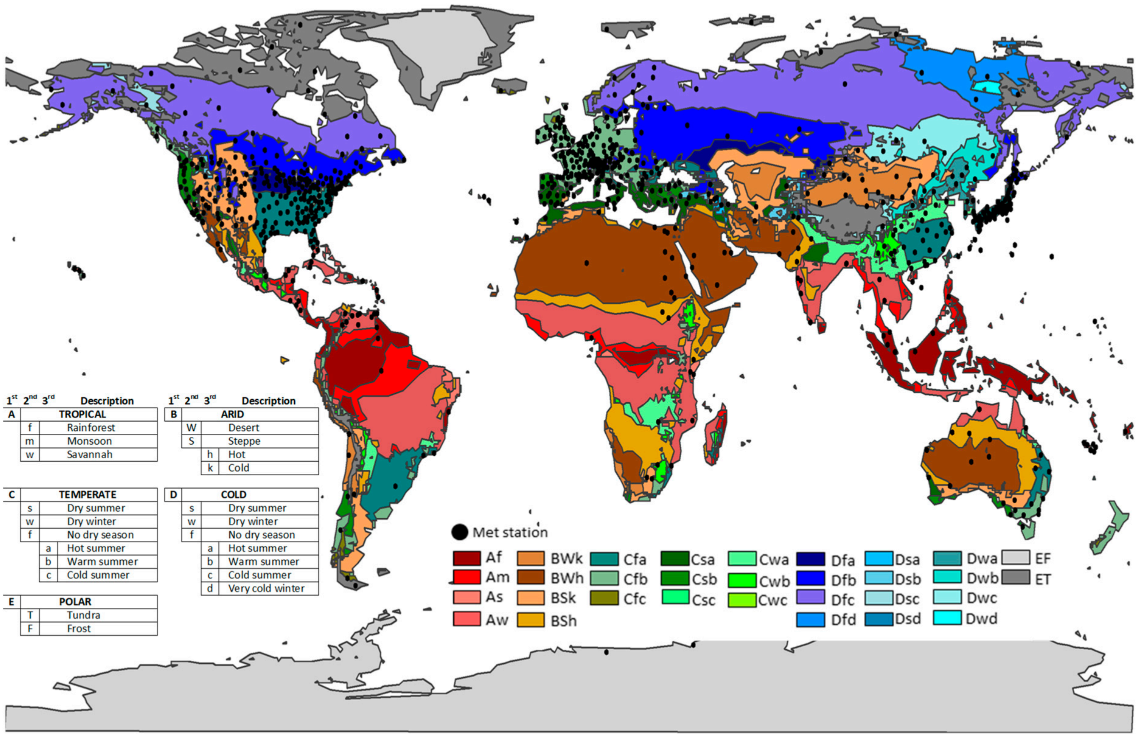

Figure 4. Location of the meteorological stations in the Köppen–Geiger climate classification areas. Source: [72] and self-elaboration.

2.2. Solar PV and Wind Generation Patterns

To estimate the electricity generation, a PV+W hybrid facility prototype has been designed according to the simplified diagram shown in Figure 5.

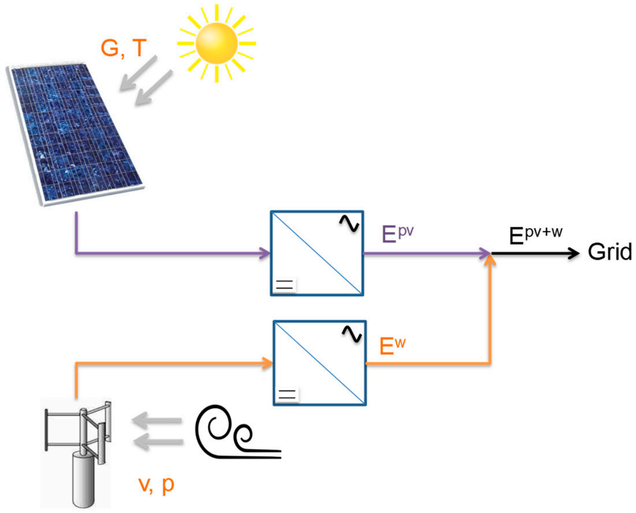

Figure 5. Single line diagram of the photovoltaic+wind hybrid (PV+W hybrid) facility.

The electricity produced by the PV facility placed at the location x is calculated with the following expression, adapted from [73]:

$$E_x^{pv} = G_x \cdot A_{PV} \cdot PR \cdot \eta \cdot [1 + \alpha(T_x - 293)] \quad (9)$$

where:

- G_x is the total solar irradiation incident on an optimally tilted solar panel.
- A_{PV} the surface covered by solar panels.
- η is the solar PV panel efficiency.
- PR is the facility performance ratio.
- α is the maximum power temperature coefficient.
- T_x is the ambient temperature (the temperature coefficient should be applied to the difference between the solar panel temperature and the standard value of 293 K. Nevertheless, as the solar temperature is not available, the correction has been applied considering the ambient temperature).

Nowadays there are different technologies used in the manufacturing of solar panels; the most widely used is multi-crystalline silicon cells [74]. For the calculation of the electricity generation, it was selected a commercial solar panel manufactured with multi-crystalline silicon cells and an efficiency η of 15.5%. The rest of the solar panel characteristics are shown in Table 5.

Table 5. Solar panel characteristics [75].

Characteristic	Value
Manufacturer	Trina Solar
Model	TSM-PC14
Cell type	Si Multicrystalline
Maximum Power (STC conditions)	300 W
Efficiency (η)	15.5%
Dimensions (h × w × d)	1956 × 992 × 40 mm^3
Temperature Coefficient of maximum power (α)	−0.41%/K

The PV facilities present current *PR* values in the 60 to 90% range [76,77], therefore, in this study, a mean value of 75% was considered for *PR*.

The area for solar panels was set up in 23.2 m^2 because it is a medium size surface suitable to be placed on every roof, pergola, etc. According to the characteristics of the solar panel selected, this area means 12 solar panels giving a power capacity of 3.6 kW.

For the wind facility, a vertical-axis wind turbine generator (VAWT) was selected. These types of wind turbines are more efficient in locations where the wind stream presents both high turbulence and continuous variations in the direction, such as in the urban environment [33,37,41]. The VAWT considered in the calculations has a nameplate power of 3.5 kW, similar to the PV installed capacity. Figure 6 shows the VAWT power curve for standard density (ρ_{std} = 1.225 kg/cm^2).

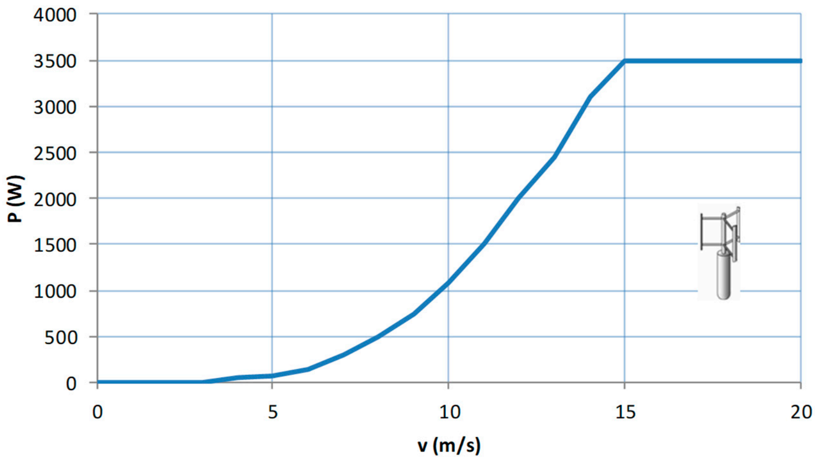

Figure 6. Vertical-axis wind turbine generator (VAWT) power curve for the standard air density ρ_{std} = 1.225 kg/cm^2. Source [78].

The electricity produced by the wind facility is calculated according to the following equation (adapted from [79]):

$$E_x^w = \rho \cdot \frac{P_x}{\rho_{std}} \cdot t \tag{10}$$

where:

- *P* is the output power from the power curve corresponding with the wind speed incident on the el VAWT (Figure 6).
- ρ is the air density.
- *t* is the time.

Finally, the electricity produced by the PV+W hybrid facility is:

$$E_x^{pv+w} = E_x^{pv} + E_x^w \tag{11}$$

The energy produced was calculated for each type of facility (PV, wind and PV+W hybrid) in all locations, obtaining the evolution in an average year with climatic conditions characterised for the variables defined in Chapter 2.1. Figure 7 shows, as an example, the generation curves of the PV, wind and hybrid facilities in an average month of May at one of the locations considered in this study.

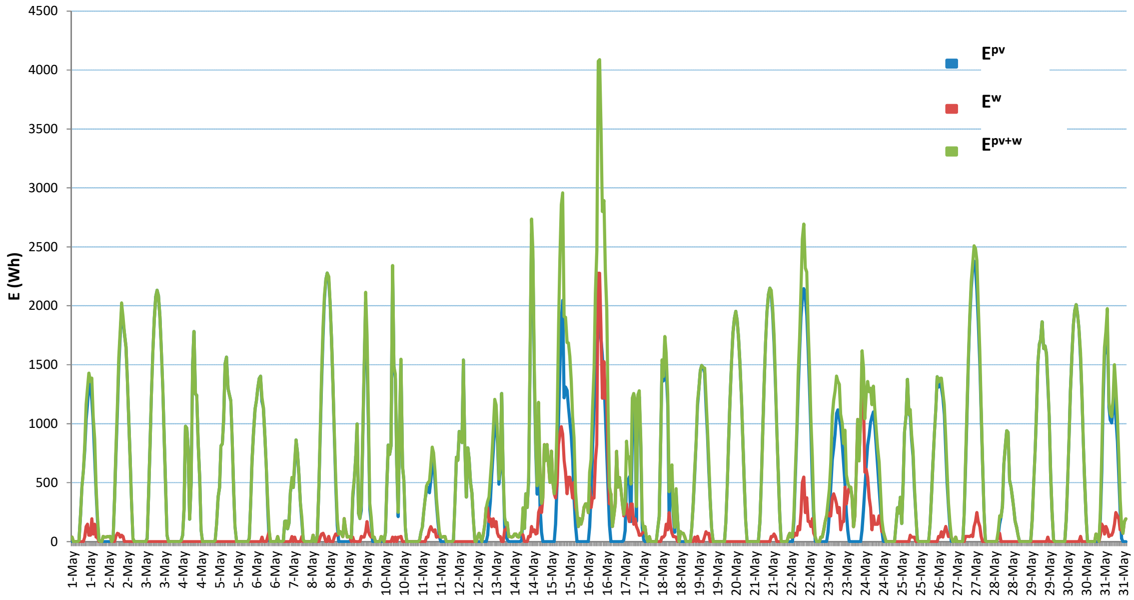

Figure 7. Time evolution of the generation in May.

One interesting result of this first step of the calculation is the contribution of the electricity sources, PV and wind, to the total hybrid facility production. Table 6 shows the PV Facility contribution to the total generation in the group of different climatic regions. Despite the PV and wind capacity being similar, the contribution of PV is a majority with 84% on average; going from 71% in polar climate zones to 91% in tropical areas. This predominance of PV is justified because the facility locations were not chosen with the criterion of having a relevant wind resource.

Table 6. PV contribution to the PV+W hybrid-facility generation. (See Figure 4 for climate zone codification).

Climate Zone	n° Stations	$\frac{E_x^{pv}}{E_x^{pv+w}}$	Climate Zone	n° Stations	$\frac{E_x^{pv}}{E_x^{pv+w}}$
Arid	***109***	0.89	***Tropical***	***66***	0.91
BSh	16	0.90	**Af**	21	0.89
BSk	46	0.86	**Am**	8	0.93
BWh	27	0.90	**As**	4	0.87
BWk	20	0.92	**Aw**	33	0.92
Cold	**188**	0.83	***Temperate***	***459***	0.84
Dfa	29	0.78	**Cfa**	192	0.87
Dfb	90	0.83	**Cfb**	162	0.78
Dfc	40	0.81	**Cfc**	4	0.68
Dfd	4	0.93	**Csa**	45	0.85
Dsa	1	1.00	**Csb**	34	0.87
Dsb	3	0.93	**Cwa**	17	0.91
Dsc	1	0.82	**Cwb**	5	0.96
Dwa	10	0.88			
Dwb	5	0.88	***Polar***	***32***	0.71
Dwc	5	0.95	**EF**	2	0.33
			ET	30	0.74
Global				***854***	0.84842

2.3. Demand Load Profiles

The demand profiles were defined using real data provided from the commercial companies and distributor and transport system operators detailed in Table 7.

Table 7. Demand load profiles data source [65,80–84].

Hemisphere	Distributor/Operator	Country
North	Red Eléctrica de España	Spain
	PJM	USA–Northeast
	Midcontinent Independent System Operator	USA–West
	Northwest PowerPool	USA–Northwest
South	National Electricity Coordinator	Chile
	Australian Energy Market Operation	Western Australia

From all the sources, real hourly demand curves for the 365 days of 2015 were obtained. Then, to determine the sixteen standard demand profiles used in ε calculation (Table 4), the next steps were followed:

1. The curves from every load profile were normalised dividing each hourly data into its respective daily maximum.
2. Once normalised, the curves were separated out from the season and from weekday and weekend days.
3. It was obtained average normalised curves for both hemispheres.

The normalised demand profiles obtained are shown in Figures 8–11.

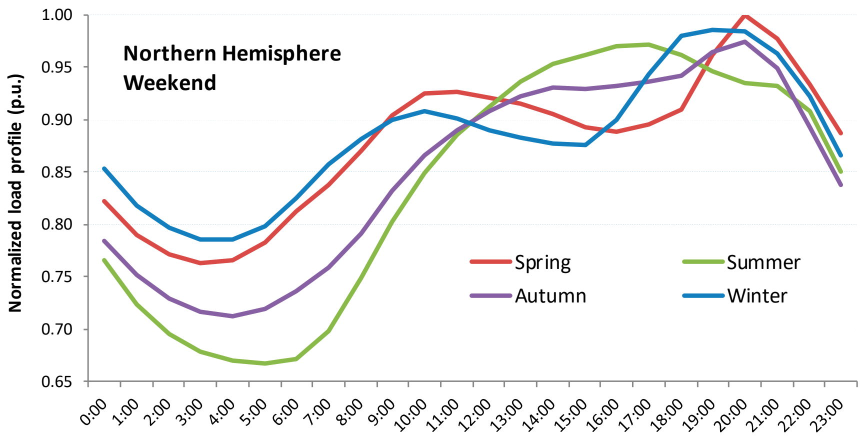

Figure 8. Standard normalised demand profiles for weekend days in the Northern Hemisphere. Source: [65,80–82] and self-elaboration.

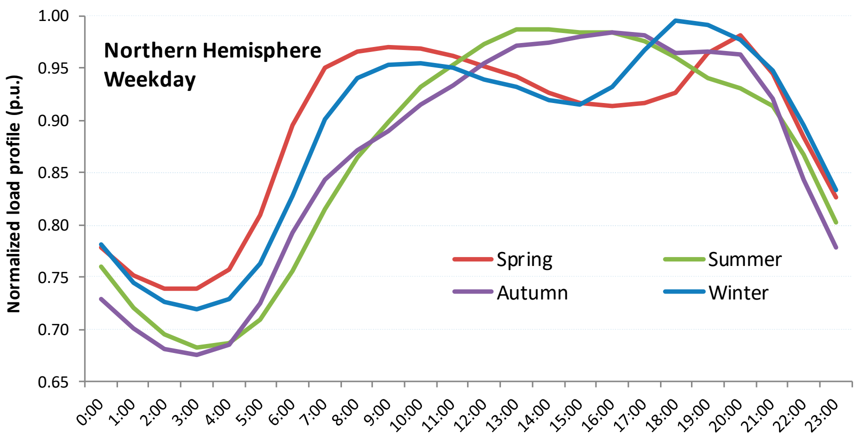

Figure 9. Standard normalised demand profiles for weekdays in the Northern Hemisphere. Source: [65,80–82] and self-elaboration.

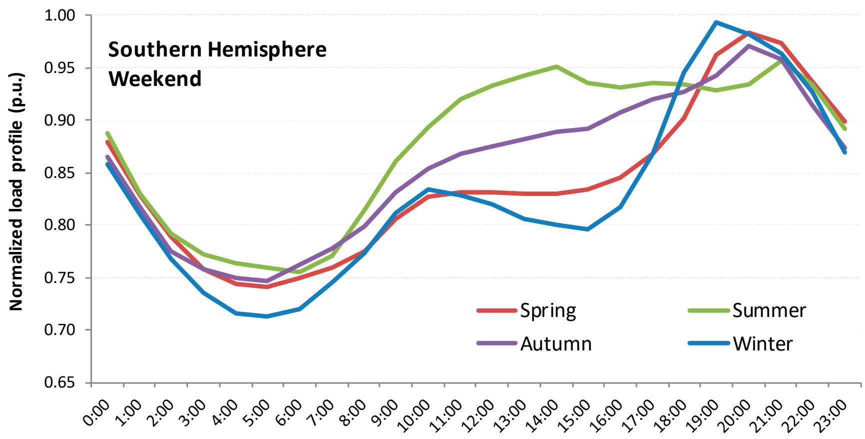

Figure 10. Standard normalised demand profiles for weekend days in the Southern Hemisphere. Source: [83,84] and self-elaboration.

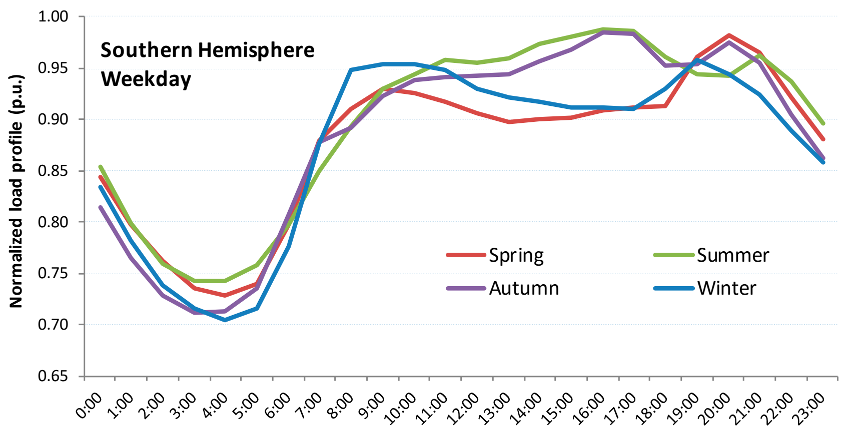

Figure 11. Standard normalised demand profiles for weekdays in the Southern Hemisphere. Source: [83,84] and self-elaboration.

3. Results

Once the normalised generation patterns and demand profiles have been determined, it is possible to obtain ε by applying Equations (5)–(8). The calculation was made individually for the 844 locations defined in Section 2.1 by using a Microsoft VBA macro programme in Excel.

The results, sorted by the Köppen–Geiger climate areas, are shown in Table 8.

The global matching factor obtained for PV facilities ε^{PV} is 0.46. As it can be noted, this value is quite homogeneous in all the climatic regions.

The global matching factor for the wind facilities ε^{W} is 0.6, that means 30% worse adaptation to demand profiles than PV plants. The results present a low dispersion degree with respect to the climatic areas. The minimum value of 0.56 is obtained for polar climates (−5% out of global value), while the maximum, 0.63, is found for tropical climates (+7% out of global).

For PV+W hybrid plants, depending on the normalisation method, the results obtained for ε^{PV+W} go from 0.4 if the method 1 is used, to 0.42 if the method 2 is used and 0.43 if the method 3 is used. Once again, the minimum factor is obtained for sites located in polar climates and the maximum for tropical areas. The degree of dispersion is also very negligible.

Figure 12 illustrates the comparison of the matching factor for the PV+W hybrid plants ε^{PV+W} versus PV facilities ε^{PV}. As it can be noted, in a global context, the adaptation of the hybrid facility is 15% higher for the method 1, 9% higher for the method 2 and 7.7% for the method 3. The highest improvement is given for polar climate areas and the lowest for arid and tropical areas.

Table 8. ε^{pv}, ε^{w} and ε^{pv+w} for every single individual Köeppen–Geiger climatic regions (See Figure 4 for climate zone codification).

Climate Zone	n° Stations	ε^{pv}	ε^{w}	Method 1 $e^{pv+w}=e^{pv}+e^{w}$			Method 2 $e^{pv+w}=\frac{E^{pv+w}}{max(E^{pv},E^{w})}$			Method 3 $e^{pv+w}=\frac{E^{pv+w}}{max(E^{pv+w})}$		
				ε^{pv+w}	$\frac{\varepsilon^{pv+w}}{\varepsilon^{pv}}$	$\frac{\varepsilon^{pv+w}}{\varepsilon^{w}}$	ε^{pv+w}	$\frac{\varepsilon^{pv+w}}{\varepsilon^{pv}}$	$\frac{\varepsilon^{pv+w}}{\varepsilon^{w}}$	ε^{pv+w}	$\frac{\varepsilon^{pv+w}}{\varepsilon^{pv}}$	$\frac{\varepsilon^{pv+w}}{\varepsilon^{w}}$
Arid	***109***	***0.46***	***0.60***	0.40	−12%	−33%	0.43	−6%	−28%	0.43	−5%	−27%
BSh	16	0.46	0.59	0.40	−12%	−32%	0.43	−6%	−27%	0.43	−5%	−26%
BSk	46	0.46	0.59	0.39	−14%	−33%	0.42	−8%	−28%	0.43	−6%	−27%
BWh	27	0.45	0.58	0.40	−12%	−31%	0.43	−6%	−26%	0.43	−5%	−25%
BWk	20	0.45	0.65	0.42	−6%	−35%	0.44	−3%	−32%	0.44	−3%	−32%
Cold	**188**	***0.47***	***0.61***	0.40	−6%	−35%	0.42	−9%	−30%	0.43	−8%	−29%
Dfa	29	0.47	0.55	0.37	−20%	−33%	0.41	−12%	−26%	0.42	−11%	−25%
Dfb	90	0.47	0.60	0.39	−16%	−35%	0.42	−10%	−30%	0.43	−8%	−29%
Dfc	40	0.47	0.62	0.40	−16%	−36%	0.42	−11%	−32%	0.43	−10%	−31%
Dfd	4	0.47	0.71	0.46	−4%	−37%	0.47	−2%	−35%	0.47	−1%	−35%
Dsa	1	0.46	0.76	0.46	0%	−40%	0.46	0%	−40%	0.46	0%	−40%
Dsb	3	0.46	0.65	0.42	−9%	−36%	0.44	−4%	−32%	0.45	−3%	−32%
Dsc	1	0.47	0.60	0.37	−20%	−38%	0.41	−13%	−32%	0.41	−11%	−31%
Dwa	10	0.47	0.64	0.42	−10%	−35%	0.44	−6%	−31%	0.44	−5%	−31%
Dwb	5	0.46	0.64	0.41	−11%	-36%	0.44	−6%	−32%	0.44	−5%	−31%
Dwc	5	0.45	0.68	0.43	−5%	−37%	0.44	−2%	−35%	0.45	−2%	−35%
Polar	***32***	***0.47***	***0.56***	0.37	−22%	−34%	0.38	−19%	−31%	0.39	−17%	−30%
EF	2	0.49	0.34	0.26	−48%	−24%	0.25	−49%	−27%	0.26	−48%	−25%
ET	30	0.47	0.57	0.37	−20%	−34%	0.39	−16%	−31%	0.40	−15%	−30%
Temperate	***459***	***0.47***	***0.61***	0.39	−15%	−35%	0.42	−9%	−30%	0.43	−8%	−29%
Cfa	192	0.47	0.60	0.40	−15%	−34%	0.43	−8%	−29%	0.43	−7%	−28%
Cfb	162	0.47	0.59	0.38	−19%	−36%	0.41	−13%	−31%	0.42	−11%	−29%
Cfc	4	0.47	0.54	0.35	−25%	−35%	0.39	−18%	−29%	0.39	−16%	−28%
Csa	45	0.46	0.62	0.41	−11%	−35%	0.43	−7%	−31%	0.43	−6%	−30%
Csb	34	0.46	0.63	0.41	−12%	−36%	0.43	−6%	−32%	0.44	−5%	−31%
Cwa	17	0.46	0.64	0.42	−10%	−35%	0.44	−5%	−31%	0.44	−4%	−30%
Cwb	5	0.45	0.67	0.43	−5%	−36%	0.44	−2%	−34%	0.45	−2%	−33%
Tropical	***66***	***0.46***	***0.63***	0.41	−10%	−34%	0.44	−5%	−30%	0.44	−4%	−29%
Af	21	0.46	0.62	0.41	−11%	−34%	0.43	−6%	−29%	0.44	−5%	−29%
Am	8	0.46	0.64	0.42	−9%	−35%	0.44	−4%	−31%	0.45	−3%	−30%
As	4	0.46	0.55	0.39	−16%	−30%	0.42	−8%	−23%	0.43	−6%	−22%
Aw	33	0.46	0.64	0.42	−9%	−35%	0.44	−5%	−31%	0.44	−4%	−30%
Global	***854***	***0.46***	***0.60***	0.4	−15%	−35%	0.42	−8.9%	−30%	0.43	−7.7%	−29%

The comparison of the matching factor for the PV+W hybrid facility ε^{PV+W} versus wind ε^{W} is shown in Figure 13. The adaptation is much higher in this case than when it is compared with the PV facility; as it has obtained an improvement of 35% for the method 1, 30% for the method 2 and 29% for the method 3. The values are quite similar in all the climate areas.

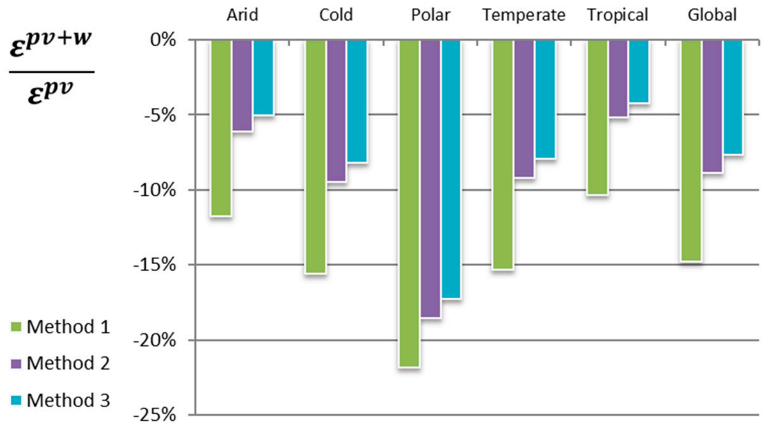

Figure 12. Improvement of the matching factor: ε^{pv+w} (hybrid) over ε^{pv} (solar PV) facilities.

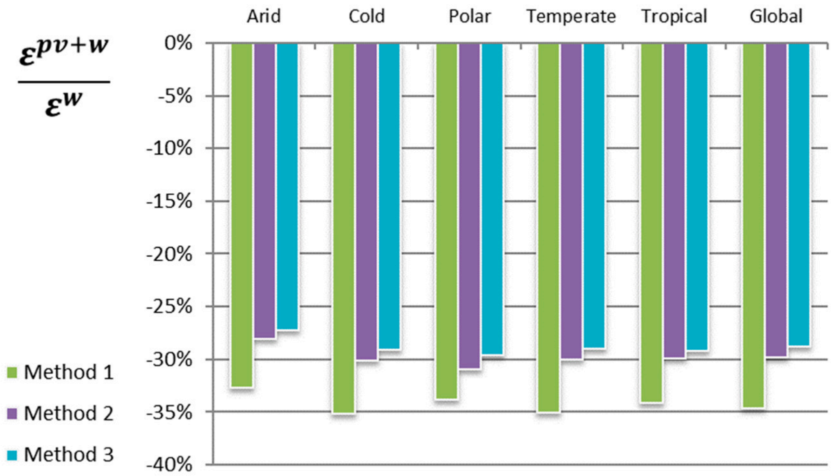

Figure 13. Improvement of the matching factor: ε^{pv+w} (hybrid) over ε^{w} (wind) facilities.

3.1. Sensitivity Analysis

It is mandatory to check if the methodology here proposed would give stable results in case of the variation of the relevant variables considered in the calculations. The technical characteristics of the facilities, as well as the performance parameters of the equipment, are quite steady and will be under control with adequate maintenance. The more relevant variations can arise from (i) deviations or errors in the evaluation of the solar and wind resource at the location or the use of non-optimised facilities (i.e., tilt or azimuth angles of the PV facility different from the ideal) and (ii) different power capacity of the facilities. In this way, to determine the robustness of the methodology two sensitivity analyses were carried out with respect to those variables.

3.1.1. Sensitivity Related to Errors in the Resource Valuation

To evaluate the variations in the valuation of the resource produced by errors, spatial smoothing effector the installation of the facilities (non-optimisation), the electricity generated is calculated by means of a modification of the Formulas (9) and (10) to include the multiplying factors f_{pv} and f_w to simulate the variation of the solar irradiance and wind resource. The methodology was applied for a wide variation range of the multiplying factors between 0.7 to 1.3 which represents a variation of ±30% in the renewable resources.

$$E_x^{pv}\left(f_{pv}\right) = f_{pv} \cdot G_x \cdot A_{PV} \cdot PR \cdot \eta \cdot [1 + \alpha(T_x - 293)] \tag{12}$$

$$E_x^w(f_w) = \rho \cdot \frac{P_x(f_w)}{\rho_{std}} \cdot t \quad (13)$$

The variation of ε^{PV+W} with the multiplication factors is illustrated in the Figure 14. As it can be shown, the methodology is robust because:

1. ε^{PV+W} hardly varies with changes of the irradiation for the three normalisation methods.
2. The effect of variations in wind resource is quite limited. For increases in the mean wind speed of 30% (f_w = 1.3) ε^{PV+W} rises about 5%, while a decrement of 30% (f_w = 0.7) produces a variation range from −5%, (normalisation method 3) to −8% (normalisation method 1).

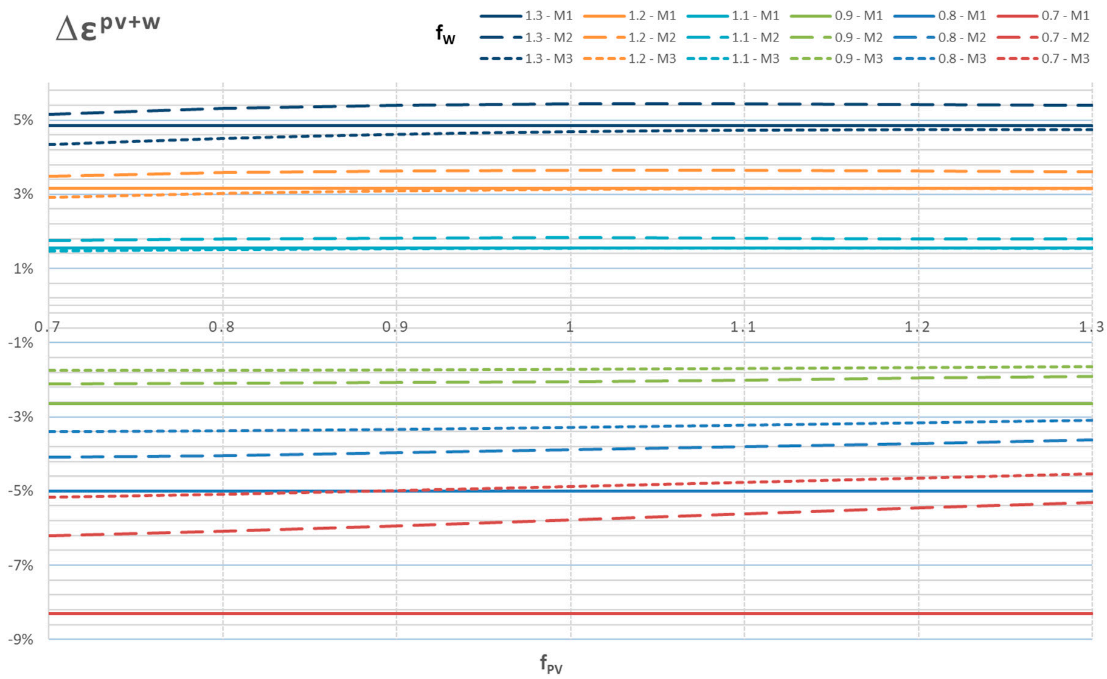

Figure 14. Variation of ε^{PV+W} with the multiplication factors f_{pv} and f_w. (M1, M2 and M3 represent the results obtained by means of application of the normalisation methods 1, 2 and 3, respectively).

3.1.2. Sensitivity Related to the Power Capacity of the Facilities

We applied the methodology considering generation patterns of a PV+W hybrid facility with twice the power capacity of the facility previously considered to evaluate the potential variations in the results produced by changes on the installed power capacity of the wind and PV facilities. The solar panel and VAWT used now have the following characteristics:

1. A commercial solar panel manufactured with multi-crystalline silicon cells and an efficiency η of 17.5%. The rest of the solar panel characteristics are shown in the Table 9.

Table 9. Solar panel characteristics [85].

Characteristic	Value
Manufacturer	Trina Solar
Model	TSM-PD14
Cell type	Si Multicrystalline
Maximum Power (STC conditions)	320 W
Efficiency (η)	17.5%
Dimensions (h × w × d)	1960 × 992 × 40 mm^3
Temperature Coefficient of maximum power (α)	−0.41%/K

2. For the wind facility, a vertical-axis wind turbine generator was selected with a nameplate power capacity of 6 kW (similar to the PV facility capacity). Figure 15 shows the VAWT power curve for standard density (ρ_{std} = 1.225 kg/cm^2).

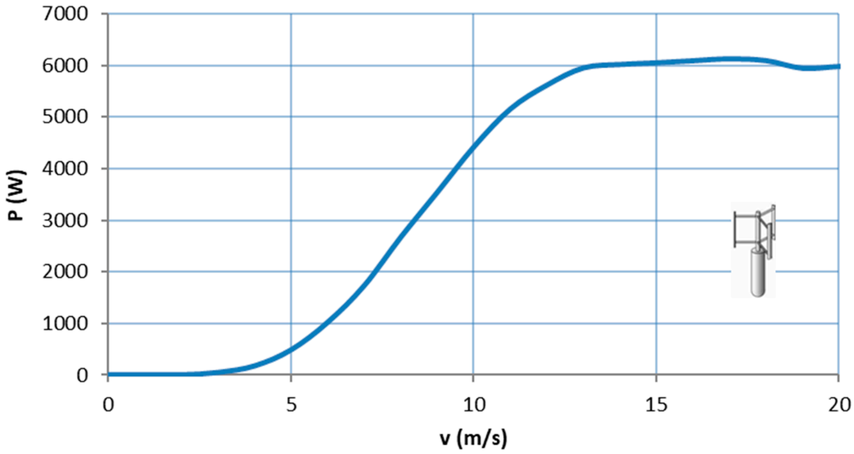

Figure 15. Power curve for the standard air density ρ_{std} = 1.225 kg/cm^2. Source [86].

Figure 16 illustrates the comparison of the matching factor for PV+W hybrid plants ε^{PV+W} versus PV ε^{PV} obtained for facilities with a power capacity of 3.6 kW and 6 kW. In a global context, the adaptation obtained for the 6 kW facility is 19% higher for the method 1, 15% higher for the method 2 and 13% for the method 3. When it is compared with the 3.6 kW, the improvement of the 6 kW facility is higher in all the climate areas.

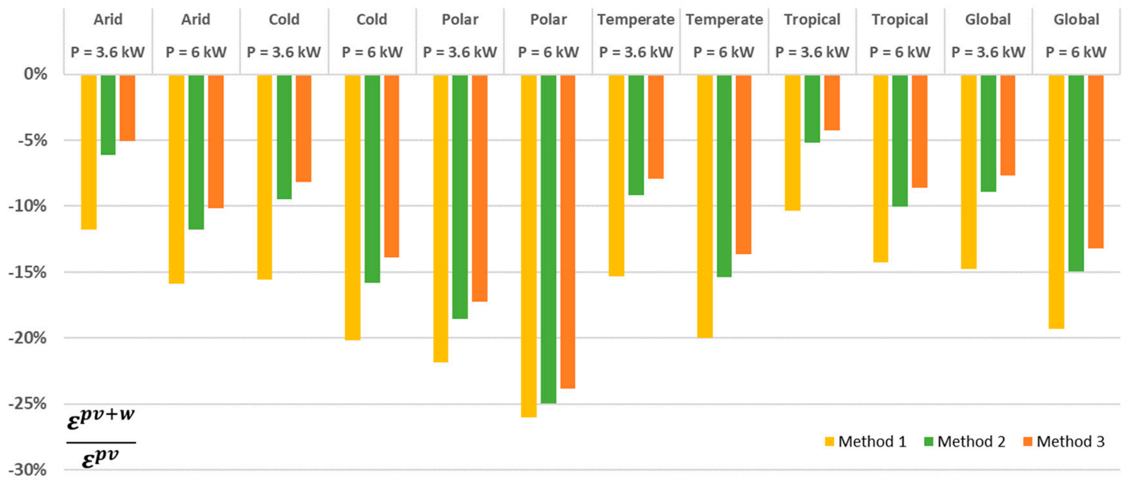

Figure 16. Improvement of the matching factor: ε^{pv+w} (hybrid) over ε^{pv} (PV) facilities for different installed power capacity.

The matching factor for the PV+W hybrid ε^{PV+W} versus wind facilities ε^{W} obtained for the facilities of 3.6 kW and 6 kW is compared in Figure 17. As was obtained for the 3.6 kW facility, the improvement of the matching factor obtained for the 6 kW facility is better when it is compared with the wind facility than when it is compared with the PV facility. The improvement now reaches 32% for method 1, 28% for method 2 and 27% for method 3. The values maintain quite similar ranges in all the climate areas.

The variation of ε^{PV+W} with the multiplication factors introduced in the Chapter 3.1.1. for the 6 kW PV+W hybrid facility is illustrated in the Figure 18. As it can be shown, for the new capacity the methodology also presents a robust performance because the results hardly vary with changes of the irradiation for the three normalisation methods. Once again, the effect of variations in the wind resource is quite limited.

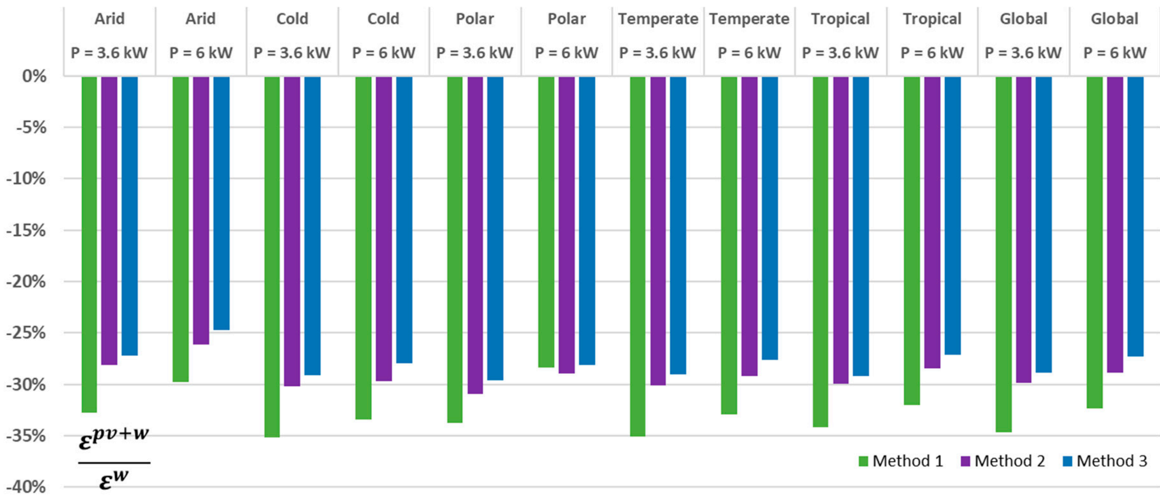

Figure 17. Improvement of the matching factor: ε^{pv+w} (hybrid) over ε^{w} (wind) facilities for different installed power capacity.

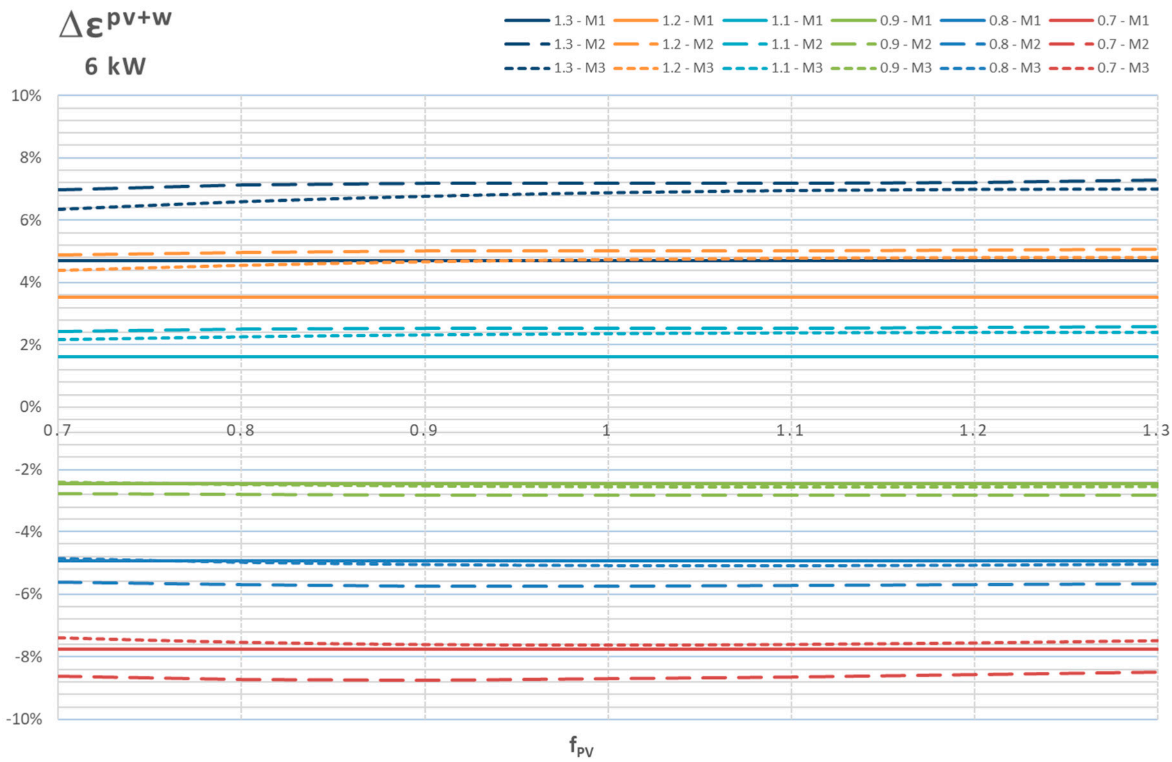

Figure 18. Variation of ε^{PV+W} with the multiplication factors f_{pv} and f_{w}. in a 6 kW power capacity facility (M1, M2 and M3 represent the results obtained by means of application of the normalisation methods 1, 2 and 3, respectively).

4. Discussion

In this paper, we have analysed the behaviour of PV+W hybrid facilities placed in urban areas from the point of view of the adaptability of their generation patterns to the aggregate demand profiles. With this aim, we have designed a novel methodology that includes the definition and calculation of the matching factor (ε) to evaluate and quantify the adaptation level. The novelty of our work is based on three main grounds: (i) the evaluation of supply–demand balance adaptation of PV+W hybrid plants, (ii) the integration of the hybrid plants into an urban environment and (iii) the applicability of the results on a global scale.

The analysis of the generation patterns shows that, in a PV+W hybrid plant where the PV and wind facilities have similar installed power capacity, the PV is always the main contributor in the total energy production in all climate conditions, presenting a global value of 84%, varying from 71% in polar areas to 91% in tropical zones. The main reason for this performance is that the facilities are not placed following a criterion of high-wind-resource location which is common in urban areas.

The results show that PV facilities match demand profiles better than wind energy. The global matching factor obtained for PV ε^{PV} is 0.46 while for wind ε^{W} is 0.6, which means 30% worse adaptation level. The difference, once again, is homogeneous in all climate conditions.

Likewise, hybrid plants adapt better to the demand than when the facilities are independently evaluated. The hybrid plants present ε^{PV+W} in the 0.4 to 0.43 range, depending on the normalisation method used, which means an improvement between 7.7% and 15% in comparison with the adaptation of PV facilities and between 29% and 35% in comparison with wind plants. Once again, the results are homogeneous for all the climate zones.

The proposed methodology has been found robust because the results obtained do not vary substantially with respect to the variation of the solar irradiation or the mean wind speed at the location under study. The methodology also gives comparable results for facilities with different power capacity.

5. Conclusions

An important technical challenge for a massive RES integration is the lack of manageability of the generation to match the demand. A high RES penetration requires the application of measures focused on planning, operation and flexibility of the whole system to respond to the uncertainty and variability in the supply–demand balance in short timescales. These measures present tangible costs to the system.

The results of this study lead us to state that the implementation of PV+W hybrid plants in urban areas would widen the RES integration limits and reduce the cost of high RES penetration because of the improvement of the manageability derived of a better adaptation to the demand profiles.

Additionally, our work gives valuable and quantifiable support to decision-makers to favour RES penetration into the urban environment, which constitutes a perfect example of distributed generation, with the advantages that this type of generation presents for the electric system.

As a result, a massive installation of PV+W hybrid plants would bring benefits for the whole electric system. Therefore, the author's workgroup of the Department of Electrical, Electronic and Control Engineering [87] propose and recommend the implementation of PV+W hybrid plants.

A massive integration into the urban environment presents financial, technical and regulatory barriers. The adequation of existing buildings could require the evaluation of subsidies to avoid financial constraints that could slow down the integration. Moreover, the facilities integrated into the urban environment will be likely owned by consumers (i.e., particulars or small/medium size companies) that could use part of the generation for self-consumption. This situation will require specific legislation to regulate the energy trading and implement technical requirements to avoid negative impact on the distribution networks.

Author Contributions: Conceptualisation: S.C.-R.; methodology: S.C.-R.; software: S.C.-R.; validation: S.C.-R.; formal analysis: S.C.-R.; investigation, S.C.-R.; resources: S.C.-R.; writing—original draft preparation: S.C.-R.; writing—review and editing: A.L.-R., S.C.-R., R.G.-O. and A.C.-S.; supervision: A.C.-S.

Funding: This research received no external funding.

Acknowledgments: The authors would like to thank Laj Cheenikkaparambil Abdullah for his contribution in making this article more readable.

Conflicts of Interest: The authors declare no conflict of interest.

Nomenclature

General

APV	PV area
E	Energy generated (Wh)
e	Normalised energy generated
G	Yearly solar irradiation (insolation) in Wh/m^2 incident on an optimally tilted solar panel
i	Facility type: PV (Photovoltaic), W (Wind) or PV+W (Hybrid)
L	Load electricity demand profile (Wh)
l	Normalised load electricity demand profile
P	Power (W)
PR	Performance ratio of the PV facility
PV	Photovoltaic electricity source
RES	Renewable Energy Source
Subscripts	
x	Location
y	Season: S (spring), U (summer), A (autumn), W (winter).
z	Day type: D (weekday), E (weekend).
Greeks	
α	Temperature coefficient of maximum power
ε	Matching factor
η	Solar panel efficiency
ρ	Air density

References

1. United Nations. UN Climate Change Conference Paris 2015. Available online: http://www.un.org/sustainabledevelopment/cop21/ (accessed on 9 July 2016).
2. United Nations Framework Convention on Climate Change. Available online: http://unfccc.int/2860.php (accessed on 5 July 2016).
3. United Nations Treaty Collection. Paris Agreement. Available online: https://treaties.un.org/pages/ViewDetails.aspx?src=TREATY&mtdsg_no=XXVII-7-d&chapter=27&lang=en (accessed on 9 July 2016).
4. The US Department of Energy; Office of Energy Efficiency & Renewable Energy. The U.S. Department of Energy (DOE) SunShot Initiative. Available online: http://energy.gov/eere/sunshot/sunshot-initiative (accessed on 25 June 2016).
5. The US Department of Energy; Office of Energy Efficiency & Renewable Energy. The U.S. Department of Energy (DOE) Wind Program. Available online: http://energy.gov/eere/wind/about-doe-wind-program (accessed on 25 June 2016).
6. European Climate Foundation. *Roadmap 2050: A Practical Guide to a Prosperous, Low Carbon Europe*; European Climate Foundation: The Hague, The Netherlands, 2010.
7. International Renewable Energy Agency. RESOURCE. 2018. Available online: http://resourceirena.irena.org/gateway/dashboard/ (accessed on 22 April 2018).
8. REN21. *Renewables 2018 Global Status Report*; REN21 Secretariat: Paris, France, 2018; p. 325.
9. Philipps, S.P.; Kost, C.; Schlegl, S. *Up-to-Date Levelised Cost of Electricity of Photovoltaics*; Fraunhofer Institute for Solar Energy Systems ISE: Freiburg, Germany, 2014.
10. Energy Technology Systems Analysis Programme; International Renewable Energy Agency. *Wind Power. Technology Brief*; International Renewable Energy Agency: Abu Dhabi, UAE, 2016; p. 28.
11. Lazard. In *Levelized Cost of Energy v11*; Lazard: New York, NY, USA, 2017; p. 22.
12. Feldman, D.; Margolis, R.; Boff, D. *Q4 2016/Q1 2017 Solar Industry Update*; U.S. Department of Energy: Oak Ridge, TN, USA, 2017; p. 83.
13. Huld, T.; Jäger Waldau, A.; Ossenbrink, H.; Szabo, S.; Dunlop, E.; Taylor, N. *Cost Maps for Unsubsidised Photovoltaic Electricity*; JRC 91937 Joint Research Centre of the European Commission: Brussels, Belgium, 2014; p. 22.

14. Moné, C.; Hand, M.; Bolinger, M.; Rand, J.; Heimiller, D.; Ho, J. *2015 Cost of Wind Energy Review*; NREL/TP-6A20-66861; National Renewable Energy Laboratory: Golden, CO, USA, 2017; p. 115.
15. International Renewable Energy Agency. *Renewable Power Generation Costs in 2017*; International Renewable Energy Agency: Abu Dhabi, UAE, 2018; p. 160.
16. Cayir Ervural, B.; Evren, R.; Delen, D. A multi-objective decision-making approach for sustainable energy investment planning. *Renew. Energy* **2018**, *126*, 387–402. [CrossRef]
17. Patlitzianas, K.D.; Doukas, H.; Kagiannas, A.G.; Psarras, J. Sustainable energy policy indicators: Review and recommendations. *Renew. Energy* **2008**, *33*, 966–973. [CrossRef]
18. Liu, G.; Li, M.; Zhou, B.; Chen, Y.; Liao, S. General indicator for techno-economic assessment of renewable energy resources. *Energy Convers. Manag.* **2018**, *156*, 416–426. [CrossRef]
19. International Energy Agency. *IEA Energy Technology Perspectives 2017*; International Energy Agency: Paris, France, 2017.
20. International Energy Agency. *Technology Roadmap Wind Energy. 2013 Edition*; International Energy Agency: Paris, France, 2013; p. 63.
21. International Energy Agency. *Technology Roadmap Solar Photovoltaic Energy. 2014 Edition*; International Energy Agency: Paris, France, 2014; p. 20.
22. International Renewable Energy Agency. *REmap: Roadmap for a Renewable Energy Future*; International Renewable Energy Agency: Abu Dhabi, UAE, 2016; p. 172.
23. International Renewable Energy Agency. *Renewable Energy in Cities*; International Renewable Energy Agency: Abu Dhabi, UAE, 2016; p. 64.
24. Karteris, M.; Slini, T.; Papadopoulos, A.M. Urban solar energy potential in Greece: A statistical calculation model of suitable built roof areas for photovoltaics. *Energy Build.* **2013**, *62*, 459–468. [CrossRef]
25. Defaix, P.R.; van Sark, W.G.J.H.M.; Worrell, E.; de Visser, E. Technical potential for photovoltaics on buildings in the EU-27. *Sol. Energy* **2012**, *86*, 2644–2653. [CrossRef]
26. Singh, R.; Banerjee, R. Estimation of rooftop solar photovoltaic potential of a city. *Sol. Energy* **2015**, *115*, 589–602. [CrossRef]
27. Wiginton, L.K.; Nguyen, H.T.; Pearce, J.M. Quantifying rooftop solar photovoltaic potential for regional renewable energy policy. *Comput. Environ. Urban Syst.* **2010**, *34*, 345–357. [CrossRef]
28. Colmenar-Santos, A.; Campíñez-Romero, S.; Pérez-Molina, C.; Mur-Pérez, F. An assessment of photovoltaic potential in shopping centres. *Sol. Energy* **2016**, *135*, 662–673. [CrossRef]
29. Mohajeri, N.; Upadhyay, G.; Gudmundsson, A.; Assouline, D.; Kämpf, J.; Scartezzini, J.-L. Effects of urban compactness on solar energy potential. *Renew. Energy* **2016**, *93*, 469–482. [CrossRef]
30. Song, X.; Huang, Y.; Zhao, C.; Liu, Y.; Lu, Y.; Chang, Y.; Yang, J. An Approach for Estimating Solar Photovoltaic Potential Based on Rooftop Retrieval from Remote Sensing Images. *Energies* **2018**, *11*, 3172. [CrossRef]
31. Polo, M.-E.; Pozo, M.; Quirós, E. Circular Statistics Applied to the Study of the Solar Radiation Potential of Rooftops in a Medium-Sized City. *Energies* **2018**, *11*, 2813. [CrossRef]
32. Moraitis, P.; Kausika, B.; Nortier, N.; van Sark, W. Urban Environment and Solar PV Performance: The Case of the Netherlands. *Energies* **2018**, *11*, 1333. [CrossRef]
33. Toja-Silva, F.; Colmenar-Santos, A.; Castro-Gil, M. Urban wind energy exploitation systems: Behaviour under multidirectional flow conditions—Opportunities and challenges. *Renew. Sustain. Energy Rev.* **2013**, *24*, 364–378. [CrossRef]
34. Araújo, A.M.; de Alencar Valença, D.A.; Asibor, A.I.; Rosas, P.A.C. An approach to simulate wind fields around an urban environment for wind energy application. *Environ. Fluid Mech.* **2013**, *13*, 33–50. [CrossRef]
35. Grant, A.; Johnstone, C.; Kelly, N. Urban wind energy conversion: The potential of ducted turbines. *Renew. Energy* **2008**, *33*, 1157–1163. [CrossRef]
36. Grieser, B.; Sunak, Y.; Madlener, R. Economics of small wind turbines in urban settings: An empirical investigation for Germany. *Renew. Energy* **2015**, *78*, 334–350. [CrossRef]
37. Pagnini, L.C.; Burlando, M.; Repetto, M.P. Experimental power curve of small-size wind turbines in turbulent urban environment. *Appl. Energy* **2015**, *154*, 112–121. [CrossRef]
38. Alexandru-Mihai, C.; Alexandru, B.; Ionut-Cosmin, O.; Florin, F. New Urban Vertical Axis Wind Turbine Design. *INCAS Bull.* **2015**, *7*, 67–76. [CrossRef]

39. Carcangiu, S.; Montisci, A. A building-integrated eolic system for the exploitation of wind energy in urban areas. In Proceedings of the 2012 IEEE International Energy Conference and Exhibition (ENERGYCON), Florence, Italy, 9–12 September 2012; pp. 172–177.
40. Pagnini, L.; Piccardo, G.; Repetto, M.P. Full scale behavior of a small size vertical axis wind turbine. *Renew. Energy* **2018**, *127*, 41–55. [CrossRef]
41. Micallef, D.; van Bussel, G. A Review of Urban Wind Energy Research: Aerodynamics and Other Challenges. *Energies* **2018**, *11*, 2204. [CrossRef]
42. Klima, K.; Apt, J. Geographic smoothing of solar PV: Results from Gujarat. *Environ. Res. Lett.* **2015**, *10*, 104001. [CrossRef]
43. Monforti, F.; Huld, T.; Bódis, K.; Vitali, L.; D'Isidoro, M.; Lacal Arantegui, R. Assessing complementarity of wind and solar resources for energy production in Italy. *A Monte Carlo approach.* **2014**, *63*, 576–586. [CrossRef]
44. Santos-Alamillos, F.J.; Pozo-Vázquez, D.; Ruiz-Arias, J.A.; Lara-Fanego, V.; Tovar-Pescador, J. Analysis of Spatiotemporal Balancing between Wind and Solar Energy Resources in the Southern Iberian Peninsula. *J. Appl. Meteorol. Climatol.* **2012**, *51*, 2005–2024. [CrossRef]
45. Widen, J. Correlations Between Large-Scale Solar and Wind Power in a Future Scenario for Sweden. *IEEE Trans. Sustain. Energy* **2011**, *2*, 177–184. [CrossRef]
46. Zhang, H.; Cao, Y.; Zhang, Y.; Terzija, V. Quantitative synergy assessment of regional wind-solar energy resources based on MERRA reanalysis data. *Appl. Energy* **2018**, *216*, 172–182. [CrossRef]
47. Prasad, A.A.; Taylor, R.A.; Kay, M. Assessment of solar and wind resource synergy in Australia. *Appl. Energy* **2017**, *190*, 354–367. [CrossRef]
48. Huber, M.; Dimkova, D.; Hamacher, T. Integration of wind and solar power in Europe: Assessment of flexibility requirements. *Energy* **2014**, *69*, 236–246. [CrossRef]
49. Solomon, A.A.; Kammen, D.M.; Callaway, D. Investigating the impact of wind–solar complementarities on energy storage requirement and the corresponding supply reliability criteria. *Appl. Energy* **2016**, *168*, 130–145. [CrossRef]
50. Jurasz, J.; Beluco, A.; Canales, F.A. The impact of complementarity on power supply reliability of small scale hybrid energy systems. *Energy* **2018**, *161*, 737–743. [CrossRef]
51. The US Department of Energy, Office of Electricity Delivery & Energy Reliability. *The Potential Benefits of Distributed Generation and the Rate-Related Issues That May Impede Its Expansion*; U.S. Department of Energy: Oak Ridge, TN, USA, 2015.
52. Abdmouleh, Z.; Gastli, A.; Ben-Brahim, L.; Haouari, M.; Al-Emadi, N.A. Review of optimization techniques applied for the integration of distributed generation from renewable energy sources. *Renew. Energy* **2017**, *113*, 266–280. [CrossRef]
53. Ruiz-Romero, S.; Colmenar-Santos, A.; Gil-Ortego, R.; Molina-Bonilla, A. Distributed generation: The definitive boost for renewable energy in Spain. *Renew. Energy* **2013**, *53*, 354–364. [CrossRef]
54. Mai, T.; Wiser, R.; Sandor, D.; Brinkman, G.; Heath, G.; Denholm, P.; Hostick, D.J.; Darghouth, N.; Schlosser, A.; Strzepek, K. *Exploration of High-Penetration Renewable Electricity Futures*; NREL/TP-6A20-52409-1; National Renewable Energy Laboratory: Golden, CO, USA, 2012.
55. International Energy Agency. *System Integration of Renewables. An update on Best Practice*; International Energy Agency: Paris, France, 2018.
56. Batalla-Bejerano, J.; Trujillo-Baute, E. Impacts of intermittent renewable generation on electricity system costs. *Energy Policy* **2016**, *94*, 411–420. [CrossRef]
57. Delarue, E.; Van Hertem, D.; Bruninx, K.; Ergun, H.; May, K.; Van den Bergh, K. *Determining the Impact of Renewable Energy on Balancing Costs, Back Up Costs, Grid Costs and Subsidies*; Report for Adviesraad Gas en Elektriciteit—CREG; CREG: Brussels, Belgium, 2016.
58. Hirth, L.; Ueckerdt, F.; Edenhofer, O. Integration costs revisited—An economic framework for wind and solar variability. *Renew. Energy* **2015**, *74*, 925–939. [CrossRef]
59. Shang, Y. Resilient Multiscale Coordination Control against Adversarial Nodes. *Energies* **2018**, *11*, 1844. [CrossRef]
60. Spanish National Statistics Centre. *Buildings and Population Census*; Spanish National Statistics Centre: Madrid, Spain, 2019.
61. Spanish Ministry of Development. *Buildings Construction Licences*; Spanish Ministry of Development: Madrid, Spain, 2019.

62. Eurostat. CensusHub2. 2019. Available online: https://ec.europa.eu/CensusHub2/query.do?step=selectHyperCube&qhc=false (accessed on 20 March 2019).
63. U.S. Census Bureau. American FactFinder. Annual Estimates of Housing Units for the United States, Regions, Divisions, States, and Counties: April 1, 2010 to July 1, 2017. 2017 Population Estimates. Available online: https://factfinder.census.gov/faces/tableservices/jsf/pages/productview.xhtml?pid=PEP_2018_PEPANNRES&src=pt (accessed on 20 March 2019).
64. U.S. Energy Information Administration. *Commercial Buildings Energy Consumption Survey (CBECS)*; U.S. Energy Information Administration: Washington, DC, USA, 2016.
65. Red Eléctrica de España, S.A. Esios. System Operator Information System. Available online: https://www.esios.ree.es/en/analysis/10004?vis=1&start_date=31-03-2016T00%3A00&end_date=31-03-2016T23%3A50&compare_start_date=30-03-2016T00%3A00&groupby=minutes10&compare_indicators=545,544 (accessed on 2 April 2018).
66. ENTSO-E. *Electricity in Europe 2017. Synthetic Overview of Electric System Consumption, Generation and Exchanges in 34 European Countries*; ENTSO-E: Brussels, Belgium, 2018; p. 20.
67. ENTSO-E. *Monthly Hourly Load Values*; ENTSO-E: Brussels, Belgium, 2019.
68. U.S. Energy Information Administration. *U.S. Electric System Operating Data*; U.S. Energy Information Administration: Washington, DC, USA, 2019.
69. *Meteotest Genossenchaff Meteonorm*, 7th ed. Available online: https://meteonorm.com/t (accessed on 10 January 2018).
70. Köppen, W.; Geiger, R. Das geographische System der Klimate. In *Handbuch der Klimatologie*; Köppen, W., Geiger, R., Eds.; Verlag von Gebrüder Borntraeger: Berlin, Germany, 1936; Volume I, p. 44.
71. Kottek, M.; Grieser, J.; Beck, C.; Rudolf, B.; Rubel, F. World Map of the Köppen-Geiger climate classification updated. *Meteorol. Z.* **2006**, *15*, 259–263. [CrossRef]
72. University of Veterinary Medicine Vienna. Institute for Veterinary Public Health. World Maps of Köppen-Geiger Climate Classification. Available online: http://koeppen-geiger.vu-wien.ac.at/ (accessed on 20 June 2016).
73. Duffie, J.A.; Beckman, W.A.; Worek, W.M. *Solar Engineering of Thermal Processes*, 4th ed.; John Wiley & Sons, Inc.: Hoboken, NJ, USA, 2013; p. 928.
74. International Technology Roadmap for Photovoltaic. *ITRPV 2017 Results*; VDMA: Francfurt, Germany, 2018; p. 71.
75. Trina Solar. Products. PC14. 72-Cell Utility Module. Available online: http://www.trinasolar.com/uk/product/PC14.html (accessed on 15 May 2016).
76. Reich, N.H.; Mueller, B.; Armbruster, A.; van Sark, W.G.J.H.M.; Kiefer, K.; Reise, C. Performance ratio revisited: Is PR > 90% realistic? *Prog. Photovolt. Res. Appl.* **2012**, *20*, 717–726. [CrossRef]
77. Dierauf, T.; Growitz, A.; Kurtz, S.; Becerra Cruz, J.L.; Riley, E.; Hansen, C. *Weather-Corrected Performance Ratio*; NREL/TP-5200-57991; National Renewable Energy Laboratory: Golden, CO, USA, 2013.
78. V-AIR. Vertical Axis Wind Turbine VisionAir5. Available online: http://www.visionairwind.com/wp-content/uploads/2018/08/VisionAIR5.pdf (accessed on 6 April 2019).
79. Carta González, J.A.; Calero Pérez, R.; Colmenar-Santos, A.; Castro Gil, M.-A. *Centrales de Energías Renovables: Generación Eléctrica con Energías Renovables*; Pearson Educación, S.A.: Madrid, Spain, 2009; p. 728.
80. PJM. Data Viewer. Load. Available online: https://dataviewer.pjm.com/dataviewer/pages/public/load.jsf (accessed on 2 April 2018).
81. Northwest Power Pool. Geographic NWPP Aggregated Wind Generation and Load Data. Available online: http://www.nwpp.org/our-resources/NWPP-Reserve-Sharing-Group/Geographic-NWPP-Aggregated-Wind-Generation-and-Load-Data (accessed on 2 April 2018).
82. Midcontinent Independent System Operator. I. Market Reports. Available online: https://www.misoenergy.org/markets-and-operations/market-reports/#nt=%2FMarketReportType%3ASummary%2FMarketReportName%3ADaily%20Regional%20Forecast%20and%20Actual%20Load%20(xls)&t=10&p=0&s=MarketReportPublished&sd=desc (accessed on 2 April 2018).
83. Coordinador Eléctrico Nacional. Operación Real. Available online: https://sic.coordinador.cl/informes-y-documentos/fichas/operacion-real/ (accessed on 1 April 2018).

84. Australian Energy Market Operation. Electricity Load Profiles—Aggregated Price and Demand Data—Historical. Available online: https://www.aemo.com.au/Electricity/National-Electricity-Market-NEM/Data-dashboard#aggregated-data (accessed on 1 April 2018).
85. Trina Solar. Products. PD14. 72-Cell Utility Module. Available online: http://static.trinasolar.com/sites/default/files/ES_TSM_PD14_datasheet_B_2017_web.pdf (accessed on 21 April 2018).
86. Kingspan Renewable Technologies. KW6 Wind Turbine. Available online: https://www.kingspan.com/gb/en-gb/products/renewable-technologies/wind-energy/kw6-wind-turbine (accessed on 21 April 2018).
87. National Distance Education University. Department of Electrical, Electronic and Control Engineering. Available online: http://www2.uned.es/personal/antoniocolmenar/publicaciones.htm (accessed on 1 May 2016).